which starts flowing with making of the transition contact of the closing side (here $T_B$). The circulating current $\bar{I}_C$ is determined by the step voltage and the transition resistors:

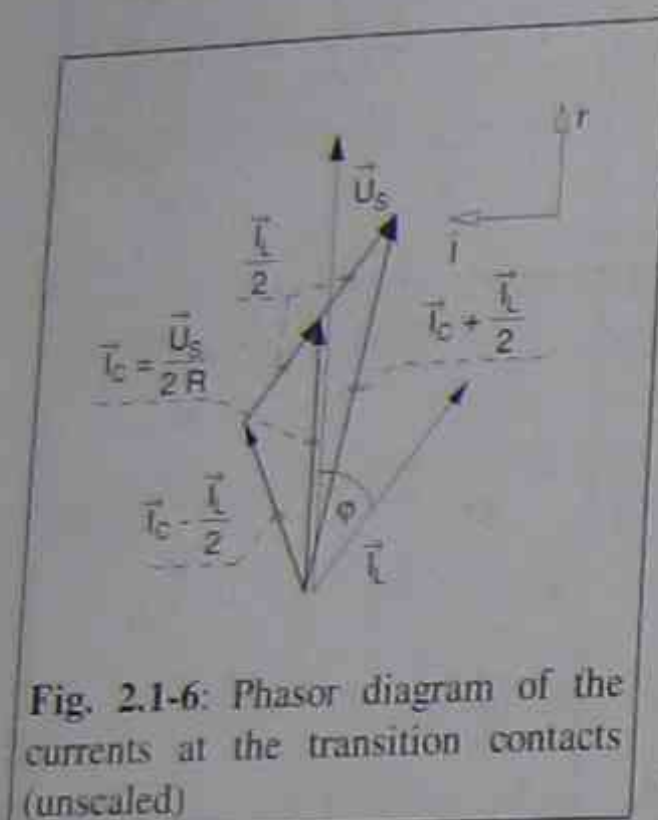$$\bar{I}_C = \frac{\bar{U}_S}{2 \cdot R} \qquad (2.1\_4)$$



**Fig. 2.1-6**: Phasor diagram of the currents at the transition contacts (unscaled)

Now the transition contact of the opening side (here $T_A$) opens and breaks one half of the through-current and the circulating current. The value of this vectorial sum of the currents depends on the switching direction (adding or subtracting turns).

The transition contacts have to break the circulating current plus one half of the through-current in one direction ("heavy"), whereas in the other switching direction ("light") the transition contacts have to break the circulating current minus one half of the through-current. These relationships are shown in Fig. 2.1-6. The currents which have to be switched by the transition contacts follow with $\bar{I}_L = \left|\bar{I}_L\right|(\cos\varphi - j\sin\varphi)$:

for "heavy" direction:

$$\left|\bar{I}_T\right| = \left|\bar{I}_C + \frac{\bar{I}_L}{2}\right| = \sqrt{\left(\frac{\left|\bar{U}_S\right|}{2 \cdot R} + \frac{\left|\bar{I}_L\right|}{2} \cdot \cos\varphi\right)^2 + \left(-\frac{\left|\bar{I}_L\right|}{2} \cdot \sin\varphi\right)^2} \qquad (2.1\_5a)$$

for "light" direction:

$$\left|\bar{I}_T\right| = \left|\bar{I}_C - \frac{\bar{I}_L}{2}\right| = \sqrt{\left(\frac{\left|\bar{U}_S\right|}{2 \cdot R} - \frac{\left|\bar{I}_L\right|}{2} \cdot \cos\varphi\right)^2 + \left(-\frac{\left|\bar{I}_L\right|}{2} \cdot \sin\varphi\right)^2} \qquad (2.1\_5b)$$

From these equations we can derive that the switched current at the transition contacts $\bar{I}_T$ becomes maximal in the "heavy" switching direction at the phase angle $\varphi = 0°$, which means a power factor of 1. The power factor only affects the magnitude of the switched current and recovery voltage, but the phase angle between switched current and recovery voltage is at every power factor 0 degree. This will be shown in paragraph 4.2.1. The main switching contacts have to break the through-current in every direction.

The recovery voltage at the opening transition contact of the opening side (here $T_A$) is the vectorial sum of the step voltage and the voltage drop across the transition resistor R caused by the through-current. This value also depends on the switching direction and becomes:

$$\bar{U}_{rT} = \bar{U}_S \pm \bar{I}_L \cdot R \qquad (2.1\_6)$$

By closing the main switching contact of the closing side the diverter switch operation is completed (neglecting the operation of the main contacts).

For the next tap-change operation in the same direction the above-mentioned sequence will be repeated, but now the side B of the diverter switch becomes the opening side and side A becomes the closing side (compare Table 2.1-2). Consequently the two sides of the diverter switch alternate operation during consecutive tap-changes. The arising stresses on the contacts are the same for both sides of the diverter switch and only differ with the switching direction (adding or subtracting turns).
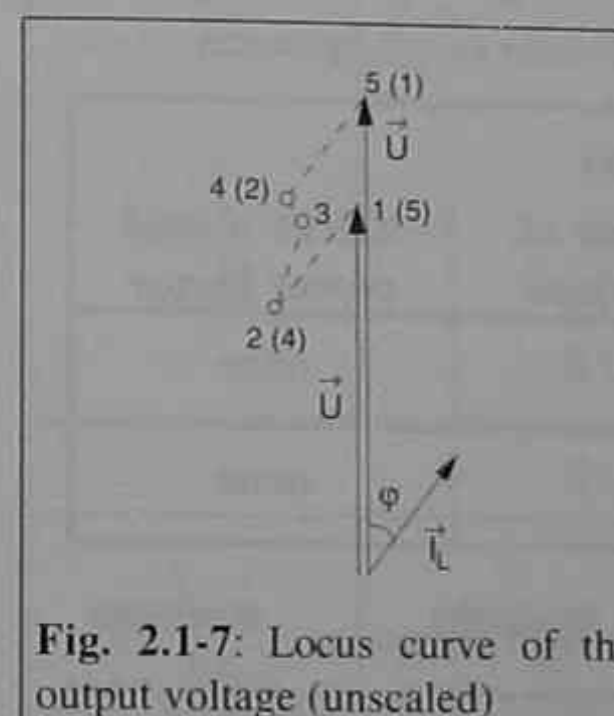


**Fig. 2.1-7**: Locus curve of the output voltage (unscaled)

Fig. 2.1-7 shows the locus curve of the output voltage $\bar{U}$ of the transformer when moving from one tapping to the adjacent one, derived from the phasor diagrams listed in Table 2.1-1. The shape of this curve is similar to a flag. This is the background for the name of this method used to perform the tap-change operation.

Table 2.1-2 shows the operating order of the contacts of the diverter switch for some consecutive switching operations of the OLTC in both directions (adding and subtracting turns). The duties on the main switching contacts and on the transition contacts are given in the Tables 2.1-3 and 2.1-4. In these tables also the number of operations of every set of contacts is given in relationship to the total number N of operations of the diverter switch.

The number of operations of the main switching contacts of the two sides of the diverter switch can be determined simply as one half of the total number of the operations of the OLTC, since the two sides of the diverter switch alternate operation.

In case of the transition contacts the same is valid. In addition it has to be considered that not every operation is a heavy operation. It can be assumed as a mean value that the operations of one side (N/2) are distributed evenly into heavy (N/4) and light (N/4) operations.

From the phasor diagrams we can derive that the power factor only affects the duty on the transition contacts.

Table 2.1-2: Operating order of contacts of a diverter switch for some consecutive switching operations (flag cycle)

| Switching operation from | Operating order of contacts | | | |
|---|---|---|---|---|
| tap (m) to tap (m+1) | $MS_A$ breaks | $T_B$ makes | $T_A$ breaks | $MS_B$ makes |
| tap (m+1) to tap (m+2) | $MS_B$ breaks | $T_A$ makes | $T_B$ breaks | $MS_A$ makes |
| tap (m+2) to tap (m+3) | $MS_A$ breaks | $T_B$ makes | $T_A$ breaks | $MS_B$ makes |
| ... | and so on | and so on | and so on | and so on |
| tap (n) to tap (n-1) | $MS_B$ breaks | $T_A$ makes | $T_B$ breaks | $MS_A$ makes |
| tap (n-1) to tap (n-2) | $MS_A$ breaks | $T_B$ makes | $T_A$ breaks | $MS_B$ makes |
| tap (n-2) to tap (n-3) | $MS_B$ breaks | $T_A$ makes | $T_B$ breaks | $MS_A$ makes |
| ... | and so on | and so on | and so on | and so on |

Table 2.1-3: Main switching contact duty of a flag cycle diverter switch operation

| Contact | Switched current | recovery voltage | Number of operations | Effect of load power factor |
|---|---|---|---|---|
| $MS_A$ | $\bar{I}_L$ | $\bar{I}_L \cdot R$ | N / 2 | none |
| $MS_B$ | $\bar{I}_L$ | $\bar{I}_L \cdot R$ | N / 2 | none |

Table 2.1-4: Transition contact duty of a flag cycle diverter switch operation

| Contact | Switched current | recovery voltage | Number of operations | Effect of load power factor |
|---|---|---|---|---|
| $T_A$ | $(\bar{U}_S + \bar{I}_L \cdot R) \cdot \dfrac{1}{2 \cdot R}$ | $\bar{U}_S + \bar{I}_L \cdot R$ | N / 4 | maximum duty at p.f. = 1.0 |
| | $(\bar{U}_S - \bar{I}_L \cdot R) \cdot \dfrac{1}{2 \cdot R}$ | $\bar{U}_S - \bar{I}_L \cdot R$ | N / 4 | |
| $T_B$ | $(\bar{U}_S + \bar{I}_L \cdot R) \cdot \dfrac{1}{2 \cdot R}$ | $\bar{U}_S + \bar{I}_L \cdot R$ | N / 4 | maximum duty at p.f. = 1.0 |
| | $(\bar{U}_S - \bar{I}_L \cdot R) \cdot \dfrac{1}{2 \cdot R}$ | $\bar{U}_S - \bar{I}_L \cdot R$ | N / 4 | |

## 2.1.2.2 FLAG CYCLE OPERATION (SELECTOR SWITCH)

Table 2.1-5: Connection diagrams, operating order of contacts and phasor diagrams of a flag cycle selector switch operation

Typical of the flag cycle method used to perform a tap-change operation is - as mentioned in the foregoing paragraph - that the through-current is diverted from the main contacts before the circulating current starts flowing. The transition resistors of both sides of the diverter switch were assumed to be equal.

Table 2.1-5 shows the different operating steps of a flag cycle selector switch operation and the relevant phasor diagrams for "light" and "heavy" switching direction (comp. 2.1.2.1).

The resulting phasor diagrams and the locus curve of the output voltage $\bar{U}$ of the transformer when moving from one tapping to the adjacent one (Fig. 2.1-7) are identical in case of a flag cycle diverter switch and a selector switch operation.

Contrary to the diverter switch operation it is typical for the selector switch operation that the two transition contacts do not alternate in consecutive switching operations (see Table 2.1-6). One transition contact is actuated only in operations when turns are added and the other one only when turns will be subtracted. It follows that one transition contact has to break in every operation the circulating current plus one half of the through-current ("heavy"), whereas the other transition contact has to break in every operation the circulating current minus one half of the through-current ("light"). The main switching contact has to break the through-current in every direction.

The duties on the main switching contact and the transition contacts are given in Tables 2.1-7 and 2.1-8. In these tables also the number of operations of every set of contacts is given in relationship to the total number N of operations of the selector switch.

Table 2.1-6: Operating order of contacts of a selector switch for some consecutive switching operations (flag cycle)

| Switching operation from | Operating order of contacts | | | |
|---|---|---|---|---|
| tap (m) to tap (m+1) | MS breaks | $T_B$ makes | $T_A$ breaks | MS makes |
| tap (m+1) to tap (m+2) | MS breaks | $T_B$ makes | $T_A$ breaks | MS makes |
| tap (m+2) to tap (m+3) | MS breaks | $T_B$ makes | $T_A$ breaks | MS makes |
| ... | and so on | and so on | and so on | and so on |
| tap (n) to tap (n-1) | MS breaks | $T_A$ makes | $T_B$ breaks | MS makes |
| tap (n-1) to tap (n-2) | MS breaks | $T_A$ makes | $T_B$ breaks | MS makes |
| tap (n-2) to tap (n-3) | MS breaks | $T_A$ makes | $T_B$ breaks | MS makes |
| ... | and so on | and so on | and so on | and so on |

Table 2.1-7: Main switching contact duty of a flag cycle selector switch operation

| | Main switching contact duty | | | |
|---|---|---|---|---|
| Contact | Switched current | recovery voltage | Number of operations | Effect of load power factor |
| MS | $\bar{I}_L$ | $\bar{I}_L \cdot R$ | N | none |

Table 2.1-8: Transition contact duty of a flag cycle selector switch operation

| | Transition contact duty | | | |
|---|---|---|---|---|
| Contact | Switched current | recovery voltage | Number of operations | Effect of load power factor |
| $T_A$ | $\left(\bar{U}_S + \bar{I}_L \cdot R\right) \cdot \dfrac{1}{2 \cdot R}$ | $\bar{U}_S + \bar{I}_L \cdot R$ | $N/2$ | maximum duty at p.f. = 1.0 |
| $T_B$ | $\left(\bar{U}_S - \bar{I}_L \cdot R\right) \cdot \dfrac{1}{2 \cdot R}$ | $\bar{U}_S - \bar{I}_L \cdot R$ | $N/2$ | |

The different numbers of operations compared to the diverter switch results are due to the different mode of operation as described before.

### 2.1.2.3 SYMMETRICAL PENNANT CYCLE OPERATION (DIVERTER SWITCH)

Typical of this method used to perform a tap-change operation is that the circulating current starts to flow before the through-current is diverted from the main contacts. The transition resistors of both sides of the diverter switch are assumed to be equal.

Table 2.1-9 shows the different operating steps of a symmetrical pennant cycle diverter switch operation and the relevant phasor diagrams for the "light" and "heavy" switching directions (adding or subtracting turns). The principle effect of the power factor to the currents and the designations "light" and "heavy" of the main switching contacts are similar to that of the transition contacts of the flag cycle operation and are given in paragraph 2.1.2.1.

The main switching contact of the opening side (here $MS_A$) has to break the circulating current $\bar{I}_{C1}$, determined by the step voltage $\bar{U}_S$ and one transition resistor R, and the through-current. The value of this vectorial sum of the currents depends on the switching direction.

$$\bar{I}_{C1} = \frac{\bar{U}_S}{R} \qquad (2.1\_7)$$

$$\bar{I}_{MS} = \bar{I}_{C1} \pm \bar{I}_L = \frac{\bar{U}_S}{R} \pm \bar{I}_L \qquad (2.1\_8)$$

The recovery voltage at the opening contacts is determined by the voltage drop across one transition resistor caused by one half of the through-current (the through-current is shared between the two transition resistors in this position) and by the circulating current $\bar{I}_{C2}$, which is determined by the step voltage and both transition resistors. The recovery voltage also depends on the switching direction and is calculated as follows:

$$\bar{I}_{C2} = \frac{\bar{U}_S}{2 \cdot R} \qquad (2.1\_9)$$

$$\bar{U}_{rMS} = \bar{I}_{C2} \cdot R \pm \frac{\bar{I}_L}{2} \cdot R = \frac{\bar{U}_S}{2 \cdot R} \cdot R \pm \frac{\bar{I}_L}{2} \cdot R = \frac{1}{2} \cdot (\bar{U}_S + \bar{I}_L \cdot R) \qquad (2.1\_10)$$

Before the opening of the transition contact of the opening side (here $T_A$) the main switching contact of the closing side (here $MS_B$) closes and bypasses the transition contact. The transition contact of the opening side (here $T_A$) only has to break the circulating current $\bar{I}_{C1}$. The arising recovery voltage is the step voltage. These conditions are valid for both switching directions.

For the next tap-change operation in the same direction the above-mentioned sequence will be repeated, but now the side B of the diverter switch becomes the opening side and side A becomes the closing side (comp. Table 2.1-10). Consequently the two sides of the diverter switch alternate operation during consecutive tap-changes. The arising stresses on the contacts are the same for both sides of the diverter switch and only differ with the switching direction (adding or subtracting turns).
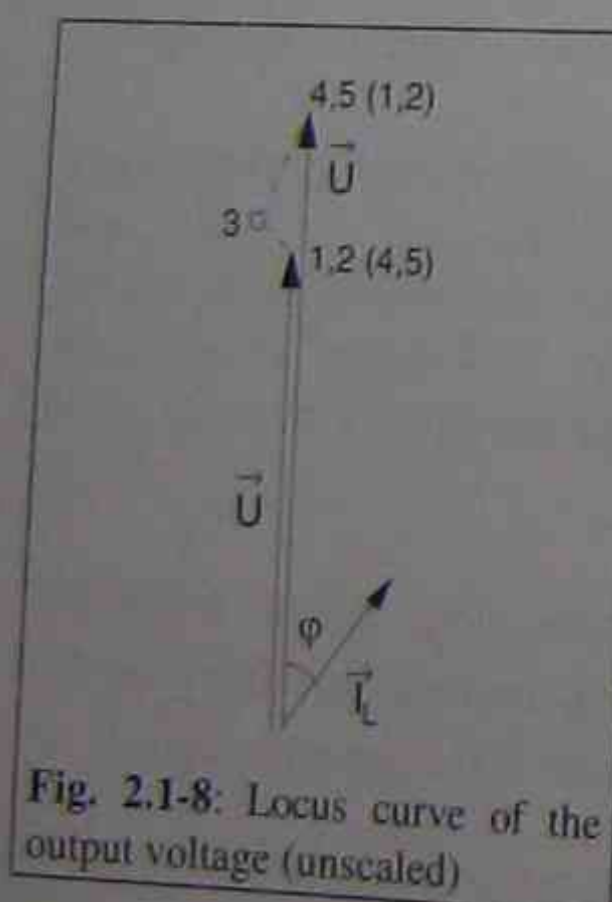


**Fig. 2.1-8:** Locus curve of the output voltage (unscaled)

Fig. 2.1-8 shows the locus curve of the output voltage $\bar{U}$ of the transformer when moving from one tapping to the adjacent one, derived from the phasor diagrams listed in Table 2.1-9. The shape of this curve is similar to a pennant. This is the background for the name of this method used to perform a tap-change operation.

Table 2.1-10 shows the operating order of contacts of the diverter switch for some consecutive switching operations of the OLTC in both directions (adding and substracting turns).

The duties on the main switching contacts and on the transition contacts are given in Tables 2.1-11 and 2.1-12. In these tables also the number of operations of every set of contacts is given in relationship to the total number N of operations of the diverter switch.

**Table 2.1-9:** Connection diagrams, operating order of contacts and phasor diagrams of a symmetrical pennant cycle diverter switch operation

The number of operations of the transition contacts of the two sides of the diverter switch can be determined simply as one half of the total number of operations of the OLTC, since the two sides of the diverter switch alternate operation.

In case of the main switching contacts the same is valid. In addition it has to be considered that not every operation is a heavy operation. It can be assumed as a mean value that the operations of one side (N/2) are distributed evenly into heavy (N/4) and light (N/4) operations.

From the phasor diagrams we can derive that the power factor only affects the duty on the main switching contacts.

Table 2.1-10: Operating order of contacts of a diverter switch for some consecutive switching operations (symmetrical pennant cycle)

| Switching operation from | Operating order of contacts | | | |
|---|---|---|---|---|
| tap (m) to tap (m+1) | $T_B$ makes | $MS_A$ breaks | $MS_B$ makes | $T_A$ breaks |
| tap (m+1) to tap (m+2) | $T_A$ makes | $MS_B$ breaks | $MS_A$ makes | $T_B$ breaks |
| tap (m+2) to tap (m+3) | $T_B$ makes | $MS_A$ breaks | $MS_B$ makes | $T_A$ breaks |
| ... | and so on | and so on | and so on | and so on |
| tap (n) to tap (n-1) | $T_A$ makes | $MS_B$ breaks | $MS_A$ makes | $T_B$ breaks |
| tap (n-1) to tap (n-2) | $T_B$ makes | $MS_A$ breaks | $MS_B$ makes | $T_A$ breaks |
| tap (n-2) to tap (n-3) | $T_A$ makes | $MS_B$ breaks | $MS_A$ makes | $T_B$ breaks |
| ... | and so on | and so on | and so on | and so on |

Table 2.1-11: Main contact duty of a symmetrical pennant cycle diverter switch operation

| Contact | Switched current | recovery voltage | Number of operations | Effect of load power factor |
|---|---|---|---|---|
| $MS_A$ | $\dfrac{\bar{U}_S}{R} + \bar{I}_L$ | $\dfrac{1}{2} \cdot (\bar{U}_S + \bar{I}_L \cdot R)$ | N / 4 | maximum duty at p.f. = 1.0 |
| | $\dfrac{\bar{U}_S}{R} - \bar{I}_L$ | $\dfrac{1}{2} \cdot (\bar{U}_S - \bar{I}_L \cdot R)$ | N / 4 | |
| $MS_B$ | $\dfrac{\bar{U}_S}{R} + \bar{I}_L$ | $\dfrac{1}{2} \cdot (\bar{U}_S + \bar{I}_L \cdot R)$ | N / 4 | maximum duty at p.f. = 1.0 |
| | $\dfrac{\bar{U}_S}{R} - \bar{I}_L$ | $\dfrac{1}{2} \cdot (\bar{U}_S - \bar{I}_L \cdot R)$ | N / 4 | |

Table 2.1-12: Transition contact duty of a symmetrical pennant cycle diverter switch operation

| Contact | Transition contact duty | | | |
|---|---|---|---|---|
| | Switched current | recovery voltage | Number of operations | Effect of load power factor |
| $T_A$ | $\dfrac{\bar{U}_S}{R}$ | $\bar{U}_S$ | N / 2 | none |
| $T_B$ | $\dfrac{\bar{U}_S}{R}$ | $\bar{U}_S$ | N / 2 | none |

### 2.1.2.4 ASYMMETRICAL PENNANT CYCLE OPERATION (SELECTOR SWITCH)

Typical of this method used to perform a tap-change operation is that, in one direction of movement of the OLTC, the circulating current starts flowing before the through-current is diverted from the main contacts, while in the other direction of movement the through-current is diverted from the main contacts before the circulating current starts flowing. Tap-changers employing the asymmetrical pennant cycle are normally selector switches and are used with a load current flow in one direction only.

Table 2.1-13 shows the different operating steps of an asymmetrical pennant cycle selector switch operation and the relevant phasor diagrams for both switching directions. The main switching contact has to break the through-current in one switching direction and the circulating current minus the through-current in the other switching direction. The power factor only affects the contact duty of the main switching contact, when the circulating current minus the through-current is being switched. The maximum current to be switched appears when the vectorial sum of these two currents becomes maximal. This is reached when the phase angle between the two currents is 90 degrees, that means at power factor 0. The transition contact has to break the circulating current in one direction and no current in the other one. The circulating current is determined by the relevant step voltage and the transition resistor.
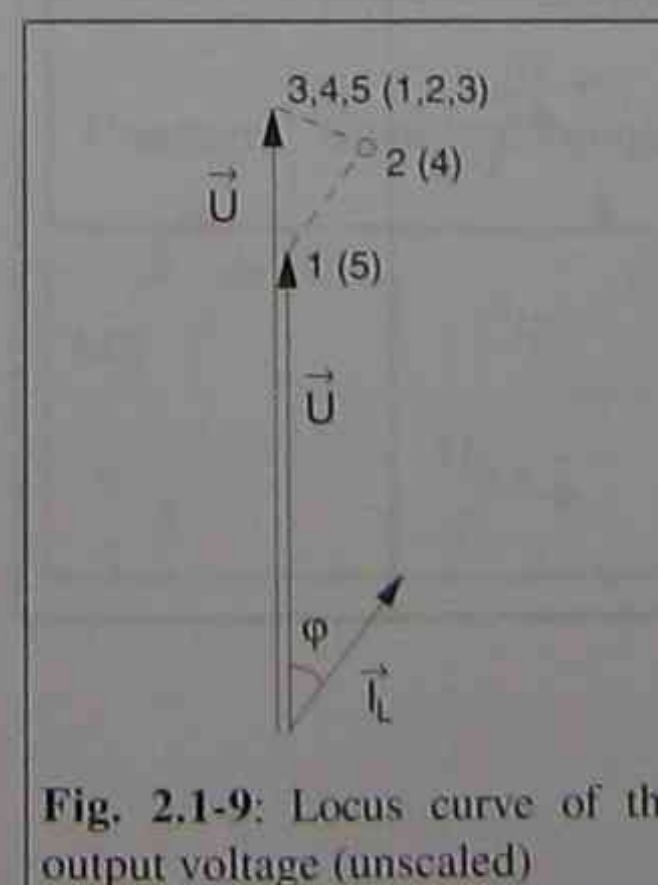
Fig. 2.1-9 shows the locus curve of the output voltage $\bar{U}$ of the transformer when moving from one tapping to the adjacent one, derived from the phasor diagrams listed in Table 2.1-13.



**Fig. 2.1-9**: Locus curve of the output voltage (unscaled)

Table 2.1-13: Connection diagrams, operating order of contacts and phasor diagrams of an asymmetrical pennant cycle selector switch operation

| switching direction with through-current is diverted before circulating current starts to flow | | | | |
|---|---|---|---|---|
| | MS breaks | MS makes | T breaks | T makes |

| switching direction with circulating current starts to flow before through-current is diverted | | | | |
|---|---|---|---|---|
| | T breaks | T makes | MS breaks | MS makes |

Table 2.1-14 shows the operating order of contacts of the selector switch for some consecutive switching operations of the OLTC in both directions (adding and substracting turns).

The duties on the main switching contact and on the transition contact are given in Tables 2.1-15 and 2.1-16. In these tables also the number of operations of every set of contacts is given in relationship to the total number N of operations of the selector switch.

The number of operations of the main switching contact and of the transition contact in the two switching directions can be determined simply as one half of the total number of the operations of the OLTC.

Table 2.1-14: Operating order of contacts of a selector switch for some consecutive switching operations (asymmetrical pennant cycle)

| Switching operation from | Operating order of contacts | | | |
|---|---|---|---|---|
| tap (m) to tap (m+1) | MS breaks | MS makes | T breaks | T makes |
| tap (m+1) to tap (m+2) | MS breaks | MS makes | T breaks | T makes |
| tap (m+2) to tap (m+3) | MS breaks | MS makes | T breaks | T makes |
| ... | and so on | and so on | and so on | and so on |
| tap (n) to tap (n-1) | T breaks | T makes | MS breaks | MS makes |
| tap (n-1) to tap (n-2) | T breaks | T makes | MS breaks | MS makes |
| tap (n-2) to tap (n-3) | T breaks | T makes | MS breaks | MS makes |
| ... | and so on | and so on | and so on | and so on |

Table 2.1-15: Main contact duty of an asymmetrical pennant cycle selector switch operation

| Main contact duty | | | | |
|---|---|---|---|---|
| Contact | Switched current | recovery voltage | Number of operations | Effect of load power factor |
| MS | $\vec{I}_L$ | $\vec{I}_L \cdot R$ | $N/2$ | none |
| | $\dfrac{\vec{U}_S}{R} - \vec{I}_L$ | $\vec{U}_S - \vec{I}_L \cdot R$ | $N/2$ | maximum duty at p.f. = 0 |

Table 2.1-16: Transition contact duty of an asymmetrical pennant cycle selector switch operation

| Contact | Transition contact duty | | | Effect of load power factor |
|---------|------------|-----------|-----------|------|
|         | Switched current | recovery voltage | Number of operations | |
| $T_A$ | $\dfrac{\bar{U}_S}{R}$ | $\bar{U}_S$ | $N/2$ | none |
|         | $0$ | $0$ | $N/2$ | none |

## 2.1.2.5 MULTIPLE RESISTOR CYCLE OPERATION (DIVERTER SWITCH)

This method used to perform a tap-change operation is an extension of either the flag cycle or the pennant cycle. It was shown in the previous paragraphs that the transition resistors determine the recovery voltage at the main switching contacts as well as the circulating current. To increase the allowable step voltage or the breaking capacity of the OLTC this method can be used.

To reduce the recovery voltage and with this the stress on the main switching contacts a small transition resistor is required (comp. eq. 2.1_1). To limit the circulating current with increasing step voltages a larger transition resistor is required (comp. eq. 2.1_2). These requirements cannot be satisfied by only one set of transition resistors. Therefore the multiple resistor diverter switch was designed to fullfill these requirements.

Todays most used multiple resistor cycle diverter switch is introduced here. This diverter switch is equipped with two transition resistors each side which are connected into the circuit one after the other during a diverter switch cycle. The first transition resistor has a small value to reduce the recovery voltage at the main switching contacts and the second one has a high value to limit the circulating current.

Table 2.1-17 shows the different operating steps of a multiple resistor cycle diverter switch operation and the relevant phasor diagrams for "light" and "heavy" switching direction. The definition for the designations "heavy" and "light" was given in paragraph 2.1.2.1. The first and second transition resistors of both sides of the diverter switch are assumed to be equal.

In the starting position of the diverter switch (main contacts are not examined) the main switching contact and the two transition contacts of the opening side (here $MS_A$, $T_{1A}$ and $T_{2A}$) are closed. The main switching contact bypasses the transition contacts and carries the through-current. The main switching contact opens and

breaks the through-current usually in the first current zero after contact separation. After quenching of the arc the through-current $\bar{I}_L$ passes through the parallel connected transition resistors $R_1$ and $R_2$. The recovery voltage at the opening contact MS is

$$\bar{U}_{rMS} = \bar{I}_L \cdot \frac{R_1 \cdot R_2}{R_1 + R_2} \qquad (2.1\_11)$$

In the next position the transition contact $T_2$ of the closing side (here $T_{2B}$) closes. The through-current is shared between the parallel connected transition resistors $R_1$ and $R_2$ of the opening side and the transition resistor $R_2$ of the closing side. In this position a circulating current $\bar{I}_{C1}$ flows. The circulating current is determined by the step voltage and the transition resistor network:

$$\bar{I}_{C1} = \frac{\bar{U}_S}{\dfrac{R_1 \cdot R_2}{R_1 + R_2} + R_2} = \frac{\bar{U}_S \cdot (R_1 + R_2)}{R_2 \cdot (2 \cdot R_1 + R_2)} \qquad (2.1\_12)$$

Now the transition contact $T_1$ of the opening side (here $T_{1A}$) breaks its current which is composed by a portion of the circulating current plus or minus a portion of the through-current and is determined by the current splitting by the transition resistors, in the first current zero after contact separation.

$$\bar{I}_{T1} = \bar{I}_{C1} \cdot \left( \frac{R_2}{R_1 + R_2} \right) \pm \bar{I}_L \cdot \left( \frac{R_2}{R_1 + R_2} \right) \cdot \left\{ \frac{R_2}{\dfrac{R_1 \cdot R_2}{R_1 + R_2} + R_2} \right\} \qquad (2.1\_13a)$$

$(\ )$:  current splitting between the transition resistors $R_1$ and $R_2$ of the opening side

$\{\ \}$:  current splitting between the opening and closing side

With eq. 2.1_12 follows

$$\bar{I}_{T1} = \frac{\bar{U}_S \cdot (R_1 + R_2)}{R_2 \cdot (2 \cdot R_1 + R_2)} \cdot \frac{R_2}{R_1 + R_2} \pm \bar{I}_L \cdot \frac{R_2}{2 \cdot R_1 + R_2} = (\bar{U}_S \pm \bar{I}_L \cdot R_2) \cdot \frac{1}{2 \cdot R_1 + R_2} \qquad (2.1\_13b)$$

The recovery voltage at the opening transition contact $T_1$ (here $T_{1A}$) is determined by the voltage drop at the transition resistor $R_2$ of the closing side caused by the current flowing through the resistor. After quenching of the arc the circulating current becomes

$$\bar{I}_{C2} = \frac{\bar{U}_S}{2 \cdot R_2} \qquad (2.1\_14)$$

The recovery voltage at the opening transition contact $T_1$ (here $T_{1A}$) becomes with eq. 2.1_14

**Table 2.1-17:** Connection diagrams, operating order of contacts and phasor diagrams of a multiple resistor cycle diverter switch operation

**Table 2.1-17 (cont.):** Connection diagrams, operating order of contacts and phasor diagrams of a multiple resistor cycle diverter switch operation

$$\bar{U}_{/T1} = \bar{I}_{C2} \cdot R_2 \pm \bar{I}_L \cdot \frac{R_2}{R_2 + R_2} \cdot R_2 = (\bar{U}_S \pm \bar{I}_L \cdot R_2) \cdot \frac{1}{2}. \qquad (2.1\_15)$$

In the next position the transition contact $T_1$ (here $T_{1B}$) closes. The through-current is shared between the transition resistor $R_2$ of the opening side and the parallel connected transition resistors $R_1$ and $R_2$ of the closing side. In this position the circulating current becomes

$$\bar{I}_{C3} = \frac{\bar{U}_S}{R_2 + \dfrac{R_1 \cdot R_2}{R_1 + R_2}} = \frac{\bar{U}_S \cdot (R_1 + R_2)}{R_2 \cdot (2 \cdot R_1 + R_2)} = \bar{I}_{C1}. \qquad (2.1\_16)$$

Now the transition contact $T_2$ (here $T_{2A}$) opens and breaks its current in the first current zero after contact separation

$$\bar{I}_{T2} = \bar{I}_{C3} \pm \bar{I}_L \cdot \frac{\dfrac{R_1 \cdot R_2}{R_1 + R_2}}{R_2 + \dfrac{R_1 \cdot R_2}{R_1 + R_2}} = \frac{\bar{U}_S \cdot (R_1 + R_2)}{R_2 \cdot (2 \cdot R_1 + R_2)} \pm \bar{I}_L \cdot \frac{R_1 \cdot R_2}{R_1 + R_2} \cdot \frac{(R_1 + R_2)}{R_2 \cdot (2 \cdot R_1 + R_2)}$$

$$\bar{I}_{T2} = \left(\bar{U}_S \pm \bar{I}_L \cdot \frac{R_1 \cdot R_2}{R_1 + R_2}\right) \cdot \frac{R_1 + R_2}{R_2 \cdot (2 \cdot R_1 + R_2)} \qquad (2.1\_17)$$

The recovery voltage at the opening transition contact $T_2$ (here $T_{2A}$) is determined by the step voltage plus or minus the voltage drop at the parallel connected transition resistors $R_1$ and $R_2$ of the closing side caused by the through-current:

$$\bar{U}_{T2} = \bar{U}_S \pm \bar{I}_L \cdot \frac{R_1 \cdot R_2}{R_1 + R_2} \qquad (2.1\_18)$$

By closing the main switching contact MS of the closing side the diverter switch operation is completed (neglecting the operation of the main contacts).

For the next tap-change operation in the same direction the above-mentioned sequence will be repeated, but now the side B of the diverter switch becomes the opening side and side A becomes the closing side (comp. Table 2.1-2). Consequently the two sides of the diverter switch alternate operation during consecutive tap-change operations. The arising stresses on the contacts are the same for both sides of the diverter switch and only differ with the switching direction (adding or subtracting turns).

The switched currents $\bar{I}_{T1}$ and $\bar{I}_{T2}$ given in equations 2.1_13b and 2.1_17 are affected by the power factor as shown in paragraph 2.1.2.1. The currents become a maximum in the "heavy" switching direction at power factor 1.

Fig. 2.1-10 shows the locus curve of the output voltage $\bar{U}$ of the transformer when moving from one tapping to the adjacent one, derived from the phasor diagrams listed in Table 2.1-17. This multiple resistor diverter switch cycle is also known as flag-pennant cycle, derived from the locus curve. From the phasor diagrams we can derive that power factor only affects the duty on the transition contacts.
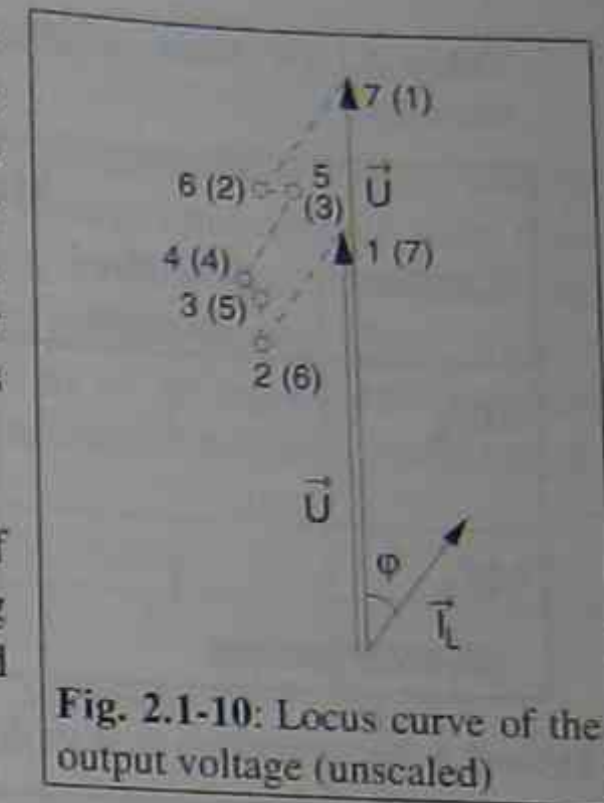


Fig. 2.1-10: Locus curve of the output voltage (unscaled)

Table 2.1-18 shows the operating order of contacts of the diverter switch for some consecutive switching operations of the OLTC in both directions (adding and subtracting turns).

The duties on the main switching contacts and on the transition contacts are given in the Tables 2.1-19 and 2.1-20. In these tables also the number of operations of every set of contacts is given in relationship to the total number N of operations of the diverter switch.

The number of operations of the main switching contacts of the two sides of the diverter switch can be determined simply as one half of the total number of the operations of the OLTC, since the two sides of the diverter switch alternate operation.

In case of the transition contacts the same is valid. In addition it has to be considered that not every operation is a heavy operation. It can be assumed as a mean value that the operations of one side (N/2) are distributed evenly into heavy (N/4) and light (N/4) operations.

Table 2.1-18: Operating order of contacts of a diverter switch for some consecutive switching operations (multiple resistor cycle "flag-pennant cycle")

| Switching operation from | Operating order of contacts (br: breaks, ma: makes) | | | | | |
|---|---|---|---|---|---|---|
| tap (m) to tap (m+1) | $MS_A$ br | $T_{1B}$ ma | $T_{1A}$ br | $T_{2B}$ ma | $T_{2A}$ br | $MS_B$ ma |
| tap (m+1) to tap (m+2) | $MS_B$ br | $T_{1A}$ ma | $T_{1B}$ br | $T_{2A}$ ma | $T_{2B}$ br | $MS_A$ ma |
| tap (m+2) to tap (m+3) | $MS_A$ br | $T_{1B}$ ma | $T_{1A}$ br | $T_{2B}$ ma | $T_{2A}$ br | $MS_B$ ma |
| ... | and s.o. | and s.o. | and s.o. | and s.o. | and s.o. | and s.o. |
| tap (n) to tap (n-1) | $MS_B$ br | $T_{1A}$ ma | $T_{1B}$ br | $T_{2A}$ ma | $T_{2B}$ br | $MS_A$ ma |
| tap (n-1) to tap (n-2) | $MS_A$ br | $T_{1B}$ ma | $T_{1A}$ br | $T_{2B}$ ma | $T_{2A}$ br | $MS_B$ ma |
| tap (n-2) to tap (n-3) | $MS_B$ br | $T_{1A}$ ma | $T_{1B}$ br | $T_{2A}$ ma | $T_{2B}$ br | $MS_A$ ma |
| ... | and s.o. | and s.o. | and s.o. | and s.o. | and s.o. | and s.o. |

Table 2.1-19: Main switching contact duty of a multiple resistor cycle diverter switch operation

| Main switching contact duty | | | | |
|---|---|---|---|---|
| Contact | Switched current | recovery voltage | Number of operations | Effect of load power factor |
| $MS_A$ | $\bar{I}_L$ | $\bar{I}_L \cdot \dfrac{R_1 \cdot R_2}{R_1 + R_2}$ | $N/2$ | none |
| $MS_B$ | $\bar{I}_L$ | $\bar{I}_L \cdot \dfrac{R_1 \cdot R_2}{R_1 + R_2}$ | $N/2$ | none |

Table 2.1-20: Transition contact duty of a multiple resistor cycle diverter switch operation

| Contact | Switched current | recovery voltage | No. of operations | Effect of load power factor |
|---|---|---|---|---|
| $T_{1A}$ | $(\bar{U}_S + \bar{I}_L \cdot R_2) \cdot \dfrac{1}{2 \cdot R_1 + R_2}$ | $\dfrac{1}{2} \cdot (\bar{U}_S + \bar{I}_L \cdot R_2)$ | $N/4$ | maximum duty at p.f. = 1.0 |
| | $(\bar{U}_S - \bar{I}_L \cdot R_2) \cdot \dfrac{1}{2 \cdot R_1 + R_2}$ | $\dfrac{1}{2} \cdot (\bar{U}_S - \bar{I}_L \cdot R_2)$ | $N/4$ | |
| $T_{2A}$ | $\left(\bar{U}_S + \bar{I}_L \dfrac{R_1 \cdot R_2}{R_1 + R_2}\right) \dfrac{R_1 + R_2}{R_2(2R_1 + R_2)}$ | $\bar{U}_S + \bar{I}_L \cdot \dfrac{R_1 \cdot R_2}{R_1 + R_2}$ | $N/4$ | maximum duty at p.f. = 1.0 |
| | $\left(\bar{U}_S - \bar{I}_L \dfrac{R_1 \cdot R_2}{R_1 + R_2}\right) \dfrac{R_1 + R_2}{R_2(2R_1 + R_2)}$ | $\bar{U}_S - \bar{I}_L \cdot \dfrac{R_1 \cdot R_2}{R_1 + R_2}$ | $N/4$ | |
| $T_{1B}$ | $(\bar{U}_S + \bar{I}_L \cdot R_2) \cdot \dfrac{1}{2 \cdot R_1 + R_2}$ | $\dfrac{1}{2} \cdot (\bar{U}_S + \bar{I}_L \cdot R_2)$ | $N/4$ | maximum duty at p.f. = 1.0 |
| | $(\bar{U}_S - \bar{I}_L \cdot R_2) \cdot \dfrac{1}{2 \cdot R_1 + R_2}$ | $\dfrac{1}{2} \cdot (\bar{U}_S - \bar{I}_L \cdot R_2)$ | $N/4$ | |
| $T_{2B}$ | $\left(\bar{U}_S + \bar{I}_L \dfrac{R_1 \cdot R_2}{R_1 + R_2}\right) \dfrac{R_1 + R_2}{R_2(2R_1 + R_2)}$ | $\bar{U}_S + \bar{I}_L \cdot \dfrac{R_1 \cdot R_2}{R_1 + R_2}$ | $N/4$ | maximum duty at p.f. = 1.0 |
| | $\left(\bar{U}_S - \bar{I}_L \dfrac{R_1 \cdot R_2}{R_1 + R_2}\right) \dfrac{R_1 + R_2}{R_2(2R_1 + R_2)}$ | $\bar{U}_S - \bar{I}_L \cdot \dfrac{R_1 \cdot R_2}{R_1 + R_2}$ | $N/4$ | |

## 2.2 REACTOR TYPE OLTC

The reactor type also called reactance type OLTC is manufactured today mainly according to two principles with respect to the arcing switch. One concept uses two arcing switches with the preventive autotransformer, which acts as transition impedance, located at the current terminal as a center-tapped reactor (Fig. 2.2-1). Such an OLTC can be designed as a selector switch or as an arcing switch (transfer switch) plus a tap selector. The transfer switches can be constructed as a usual set of transfer contacts or as vacuum interrupters.

The historical differentiation of the two basic principles (high-speed resistor type and reactor type OLTC) by means of their breaking contact velocity has lost its correctness today. Especially when considering the today mainly used reactor type OLTC with vacuum interrupters, where the breaking contacts are moved with a comparable



Fig. 2.2-1: Principle scheme of a reactance type OLTC with arcing switch and tap selector (non-bridging and bridging position)

speed as in case of the resistor type OLTC. In the beginning the reactor type OLTC was designed for the application at the low voltage side of the transformer. Therefore it is dimensioned to break, make and carry large currents. Today such arrangements are used mainly in Northamerica.
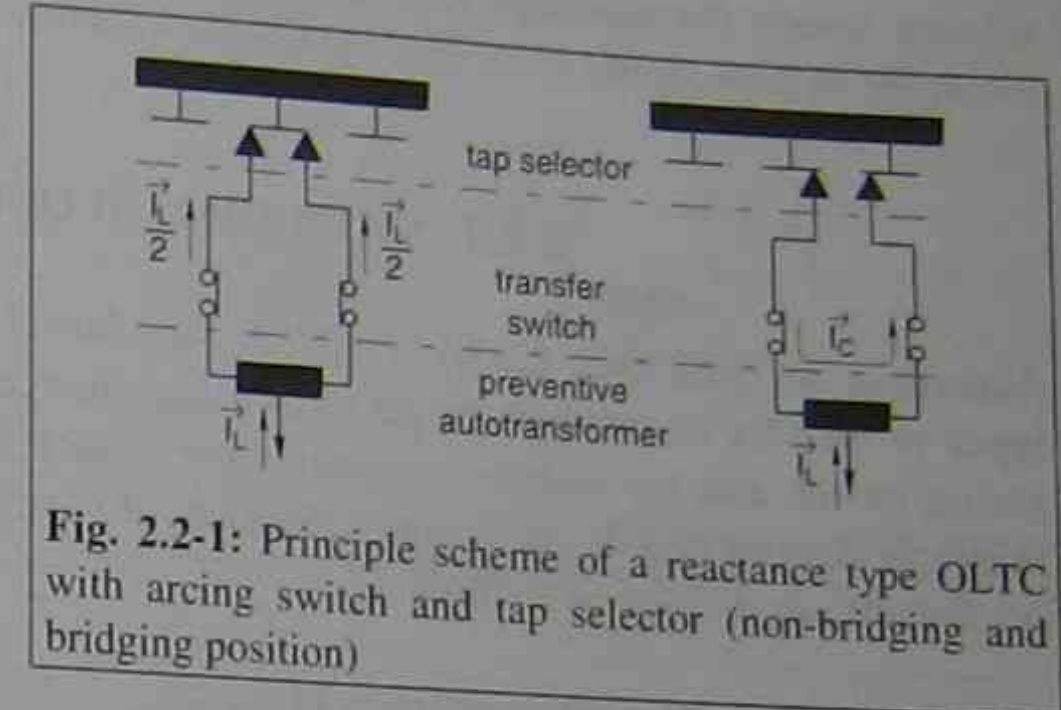
A tap-changing operation acc. to this switching principle is performed in three steps. The tap-changer is operated by a motor drive mechanism, which drives the reduction gears to open and close the transfer switches and the tap selector in proper sequence.

When moving from one position to the next, the transfer switch opens first by a spring-operated mechanism and breaks the current. Then the proper tap selector selects the next position. The transfer switch is then reclosed. In case of the selector switch design (also called arcing tap switch) these three steps are carried out at once. The arcing tap switch combines the basic functions of breaking the current, selecting the next tap and making current.
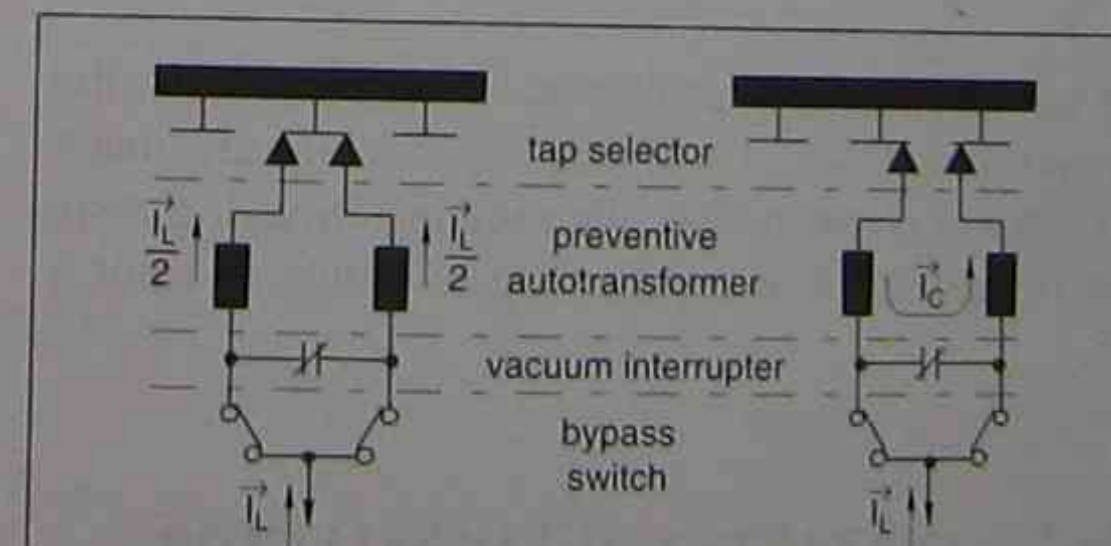
The second principle (Fig. 2.2-2) is uses one vacuum interrupter acting as arcing



Fig. 2.2-2: Principle scheme of a reactance type OLTC with vacuum interrupter, bypass switch and tap selector (non-bridging and bridging position)

switch and two bypass switches. The preventive autotransformer (transition impedance) has to be divided in two halfs and each has to be located between the tap selector and the vacuum interrupter. The tap-changer is also operated by a motor drive mechanism, which drives the reduction gears to open and close the bypass switches, the vacuum interrupter and the tap selector in proper sequence.

When moving from one tap position to the next, one bypass switch opens and commutates the current to the vacuum interrupter path. The second one stays closed. The vacuum interrupter opens by a spring-operated mechanism before the proper tap selector selects the next tap. After reclosing of the vacuum interrupter under spring force, the bypass switch closes and shunts the vacuum interrupter.

## 2.2.1 SWITCHING SEQUENCE

According to IEEE Std. C57.131 *[IEEE Standard C57.131 1995]* there are three types of OLTCs or methods to perform a tap-change operation (arcing tap switch, arcing switch and tap selector, vacuum interrupter). Figure 2.2-3 to 2.2-5 show the principle designs and the switching sequences of these OLTCs. The different switches or contacts are defined as follows:

**arcing switch (transfer switch) (TFS$_{A,B}$):**
A switching device used in conjunction with a tap selector to carry, make and break current in circuits that have already been selected. The contacts of these switches usually are made from a copper-tungsten alloy.

It is also possible to use vacuum interrupters as switching devices.

**arcing tap switch (ATS$_{A,B}$):**
A switching device capable of carrying current and also breaking and making current while selecting a tap position. It, thereby, combines the duties of an arcing switch and a tap selector. The contacts of these switches usually are made from a copper-tungsten alloy.

**bypass contacts (BYC$_{A,B}$):**
A set of through-current carrying contacts that commutates the current to the transfer switch (e.g. vacuum interrupter (VI)). These contacts usually are made from copper. To control the processes of commutation often the last breaking resp. the first making contact section is made from a copper-tungsten alloy to limit a possible contact wear.

## 2.2.1.1 OLTC WITH ARCING CONTACTS AND TAP SELECTOR

The switching sequence for example from one non-bridging position to the next non-bridging position of an OLTC with arcing contacts and tap selector is given in Fig.
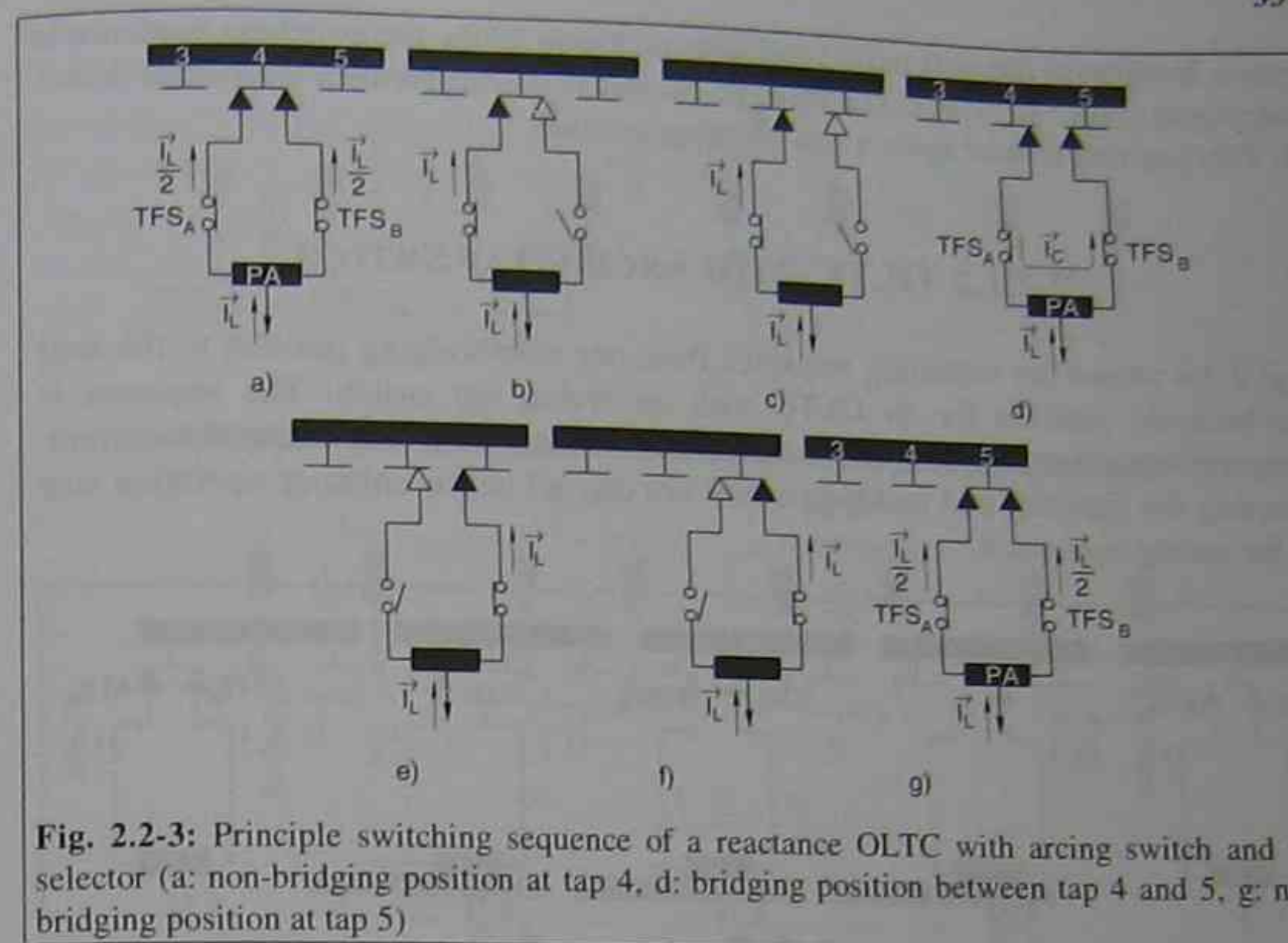
**Fig. 2.2-3:** Principle switching sequence of a reactance OLTC with arcing switch and tap selector (a: non-bridging position at tap 4, d: bridging position between tap 4 and 5, g: non-bridging position at tap 5)

2.2-3. In this example the tap selectors are connected to tap 4 (Fig. 2.2-3a). This is a non-bridging position. The through-current $\bar{I}_L$ is shared between the two pathes A and B, each carrying one half of the current. The switching sequence starts with the opening of the arcing switch TFS$_B$. The current breaks usually in the first current zero after the contact separation (Fig. 2.2-3b). The through-current flows now only through path A.

The tap selector of path B moves loadfree from tap 4 to tap 5 (Fig. 2.2-3c). After completion of the tap selector operation the transfer switch TFS$_B$ recloses (Fig. 2.2-3d). The through-current is shared again between the pathes A and B. In addition a circulating current $\bar{I}_C$ flows because the two tap selectors are connected to different tappings of the winding. The circulating current is determined by the step voltage and the impedance Z of the preventive autotransformer. The magnitude of the circulating current often is given as a percentage of the through-current (pa)

$$\left|\bar{I}_C\right| = \left|\frac{\bar{U}_S}{Z}\right| = \frac{pa}{100\%} \cdot \left|\bar{I}_L\right| \qquad (2.2\_1)$$

The circulating current is 90 degrees lagging to the step voltage. This position is called bridging position and, usually, is used as a service position.

The next switching sequence is started by the opening of the arcing switch TFS$_A$. After breaking the current in the first current zero after contact separation the through-current flows only through path B (Fig. 2.2-3e). The tap selector of path A

moves loadfree to the next tap (5) and after reclosing TFS$_A$ the switching sequence is completed (Figs. 2.2-3f+g). The through-current is shared between the pathes A and B. This position is once again a non-bridging position.

### 2.2.1.2 OLTC WITH ARCING TAP SWITCH

Fig. 2.2-4 shows the switching sequence from one non-bridging position to the next non-bridging position for an OLTC with an arcing tap switch. The sequence is comparable to the previously described, but the three steps, breaking the current, selecting the next tap and making current are carried out in only one operation step by the arcing tap switch.
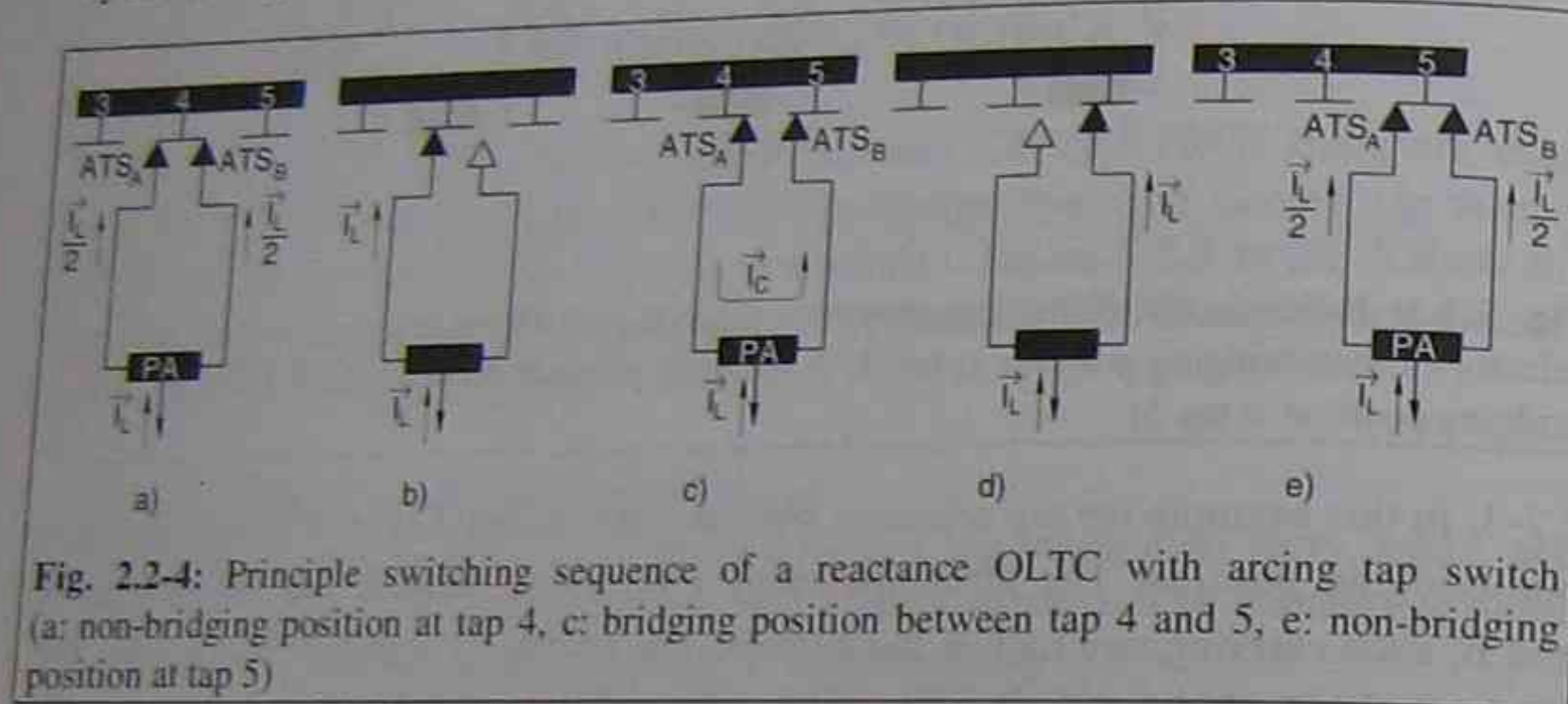


**Fig. 2.2-4:** Principle switching sequence of a reactance OLTC with arcing tap switch (a: non-bridging position at tap 4, c: bridging position between tap 4 and 5, e: non-bridging position at tap 5)

### 2.2.1.3 OLTC WITH VACUUM INTERRUPTER

The introduction of vacuum interrupters into the OLTC technique brings the advantage of a large number of possiblke operations combined with a small contact wear. In addition there is practically no carbonizing of the oil by arcing with this design.

The switching sequence of an OLTC with vacuum interrupter (designation acc. to IEEE Std. C57.131) requires more steps to carry out the tap-changing operation as shown in Fig. 2.2-5. Starting from the non-bridging position at tap 4 (Fig. 2.2-5a), first the bypass contact BYC$_B$ opens. During this operation the relevant part of the through-current is commutated to the vacuum interrupter path (Fig. 2.2-5b). Then the vacuum interrupter VI opens and breaks the current in the first current zero after contact separation. The through-current flows now only in path A (Fig. 2.2-5c). The tap selector moves loadfree to the next tapping and the vacuum interrupter recloses (Figs. 2.2-5d+e). With the reclosing of the vacuum interrupter a circulating current starts to flow. By reclosing the bypass contacts BYC$_B$ the bridging position is reached (Fig. 2.2-5f). Now the circulating current is shared between the vacuum interrupter
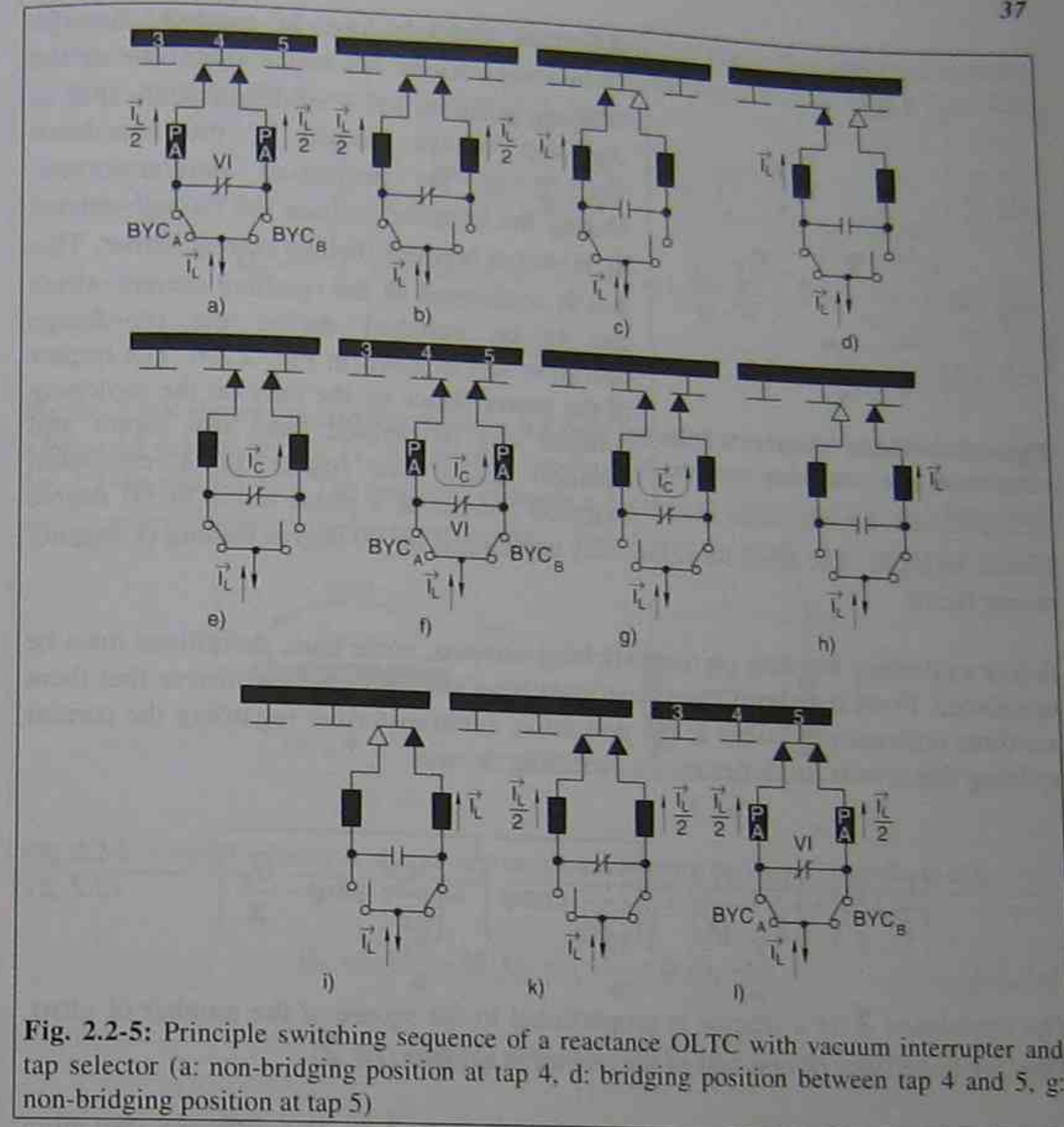
**Fig. 2.2-5:** Principle switching sequence of a reactance OLTC with vacuum interrupter and tap selector (a: non-bridging position at tap 4, d: bridging position between tap 4 and 5, g: non-bridging position at tap 5)

path (approx. 30%) and the bypass contacts (approx. 70%). The distribution depends on the contact resistance relation. Also for this OLTC the bridging position is a service position. The continuation of the switching sequence to the next non-bridging position is carried out in the same manner as described before, but now the path A has to break the current (Fig. 2.2-5g to l).

### 2.2.2 DUTY ON SWITCHING CONTACTS

The duty on the switching contacts of reactance type OLTCs depends on the method used to perform the tap-change operation. As mentioned above different basic methods are used for this purpose [IEEE Std. C57.131 1995].
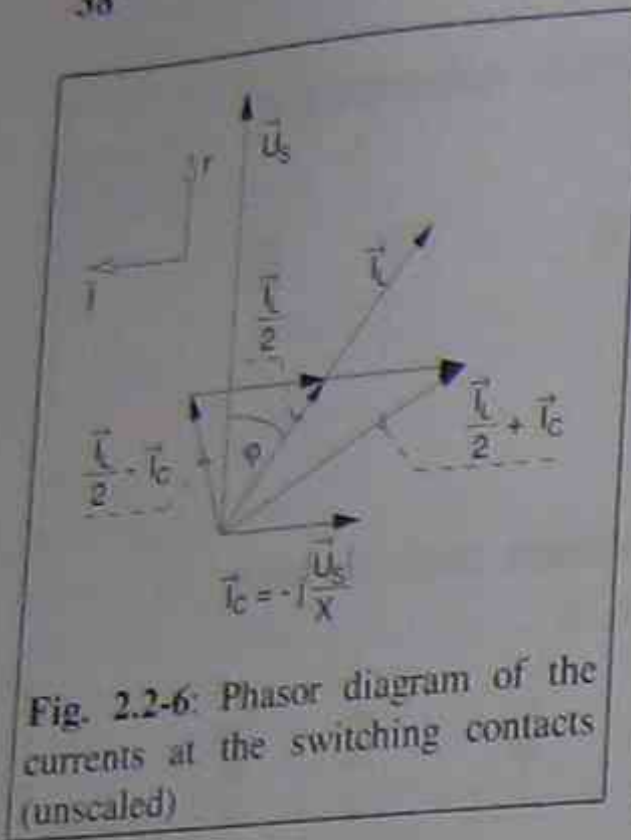
All these methods have in common that the circulating current $\bar{I}_C$, which flows during the bridging position, has a 90 degree phase shift to the step voltage, caused by the impedance $\bar{Z} \cong j \cdot X$ of the preventive autotransformer. During the bridging position the through-current $\bar{I}_L$ is shared between the two current pathes. This fact is considered in the resulting current which has to be switched during the tap-change operation and is given in Fig. 2.2-6. The impact of the power factor on the duty on the switching contacts can be derived from this figure and equation 2.2_2 and results in a maximum switched current at a phase angle of 90 degree (power factor 0). The absolute values stay unchanged for 90 degree leading or lagging power factor.



Fig. 2.2-6: Phasor diagram of the switching contacts currents at the switching contacts (unscaled)

Before evaluating the duty on the switching sequences we can derive that there introduced. From the above mentioned preventive autotransformer regarding the current are three different conditions at the splitting that affects the duties on the switching devices.

$$\left|\frac{\bar{I}_L}{2} + \bar{I}_C\right| = \left|\frac{\bar{I}_L}{2} + \frac{\bar{U}_S}{jX}\right| = \sqrt{\left(\left|\frac{\bar{I}_L}{2}\right| \cdot \cos\varphi\right)^2 + \left(\left|\frac{\bar{I}_L}{2}\right| \cdot \sin\varphi - \frac{\bar{U}_S}{X}\right)^2} \quad (2.2\_2)$$

The impedance $\bar{Z}$ of a reactor is proportional to the square of the number of turns. Thus the impedance of one half of the reactor is a quarter of $\bar{Z}$.

The relations of currents and voltages do not depend on the different switching principles and therefore do not depend on the two designs of preventive autotransformer usually used (center-tapped reactor and reactor with two single windings). The magnetic coupling M is equal to 1.
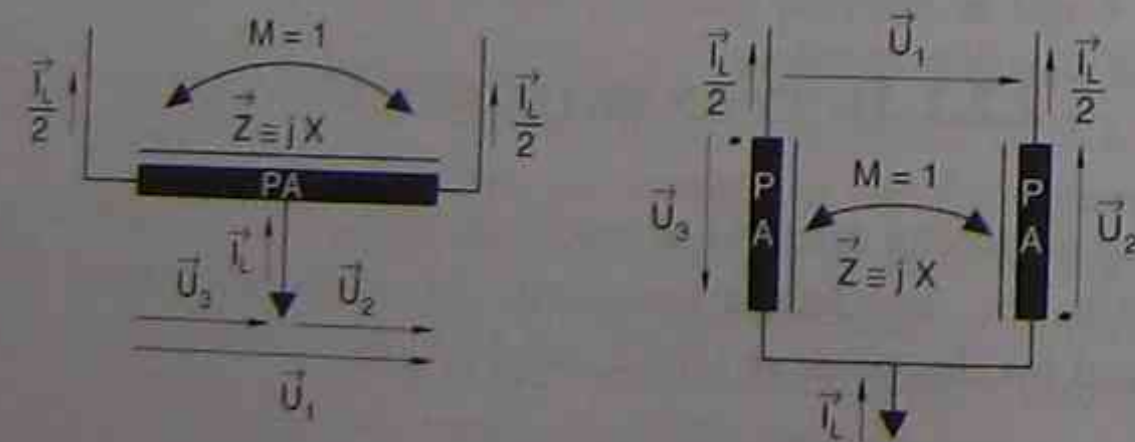


Fig. 2.2-7: Current splitting at the preventive autotransformer during non-bridging position

Figure 2.2-7 shows the current splitting for both types of preventive autotransformers in the non-bridging position of the OLTC (compare Figs. 2.2-3a to 2.2-5a). The resulting voltages are given in equations 2.2_3a to c.

$$\bar{U}_2 = \frac{\bar{I}_L}{2} \cdot \frac{jX}{4} + M \cdot \bar{U}_3 = \frac{\bar{I}_L}{2} \cdot \frac{jX}{4} - 1 \cdot \frac{\bar{I}_L}{2} \cdot \frac{jX}{4} = 0 \quad (2.2\_3a)$$

$$\bar{U}_3 = -\frac{\bar{I}_L}{2} \cdot \frac{jX}{4} + M \cdot \bar{U}_2 = -\frac{\bar{I}_L}{2} \cdot \frac{jX}{4} + 1 \cdot \frac{\bar{I}_L}{2} \cdot \frac{jX}{4} = 0 \quad (2.2\_3b)$$

$$\bar{U}_1 = \bar{U}_2 + \bar{U}_3 = 0 \quad (2.2\_3c)$$

Figure 2.2-8 shows the current splitting for both types of preventive autotransformers when one side of the OLTC is carrying the through-current (compare e.g. Figs. 2.2-3b, 2.2-4b and 2.2-5c). The resulting voltages are given in equations 2.2_4a to c.
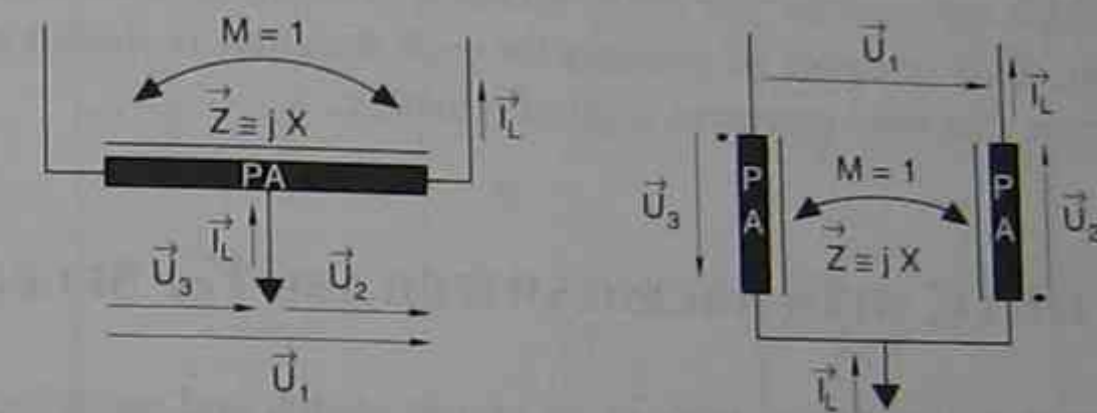


Fig. 2.2-8: Current splitting at the preventive autotransformer during opening of one side

$$\bar{U}_2 = \bar{I}_L \cdot \frac{jX}{4} + M \cdot \bar{U}_3 = \bar{I}_L \cdot \frac{jX}{4} + 0 = \bar{I}_L \cdot \frac{jX}{4} \quad (2.2\_4a)$$

$$\bar{U}_3 = 0 + M \cdot \bar{U}_2 = 0 + 1 \cdot \bar{I}_L \cdot \frac{jX}{4} = \bar{I}_L \cdot \frac{jX}{4} \quad (2.2\_4b)$$

$$\bar{U}_1 = \bar{U}_2 + \bar{U}_3 = 2 \cdot \left(\bar{I}_L \cdot \frac{jX}{4}\right) \quad (2.2\_4c)$$

Figure 2.2-9 shows the current splitting for both types of preventive autotransformers during the bridging position of the OLTC (compare e.g. Figs. 2.2-3d, 2.2-4c and 2.2-5f). The resulting voltages are given in equations 2.2_5a to c.

$$\bar{U}_2 = \left(\frac{\bar{I}_L}{2} + \bar{I}_C\right) \cdot \frac{jX}{4} + M \cdot \bar{U}_3 = \left(\frac{\bar{I}_L}{2} + \bar{I}_C\right) \cdot \frac{jX}{4} - 1 \cdot \left(\frac{\bar{I}_L}{2} - \bar{I}_C\right) \cdot \frac{jX}{4} = \bar{I}_C \cdot \frac{jX}{2} \quad (2.2\_5a)$$
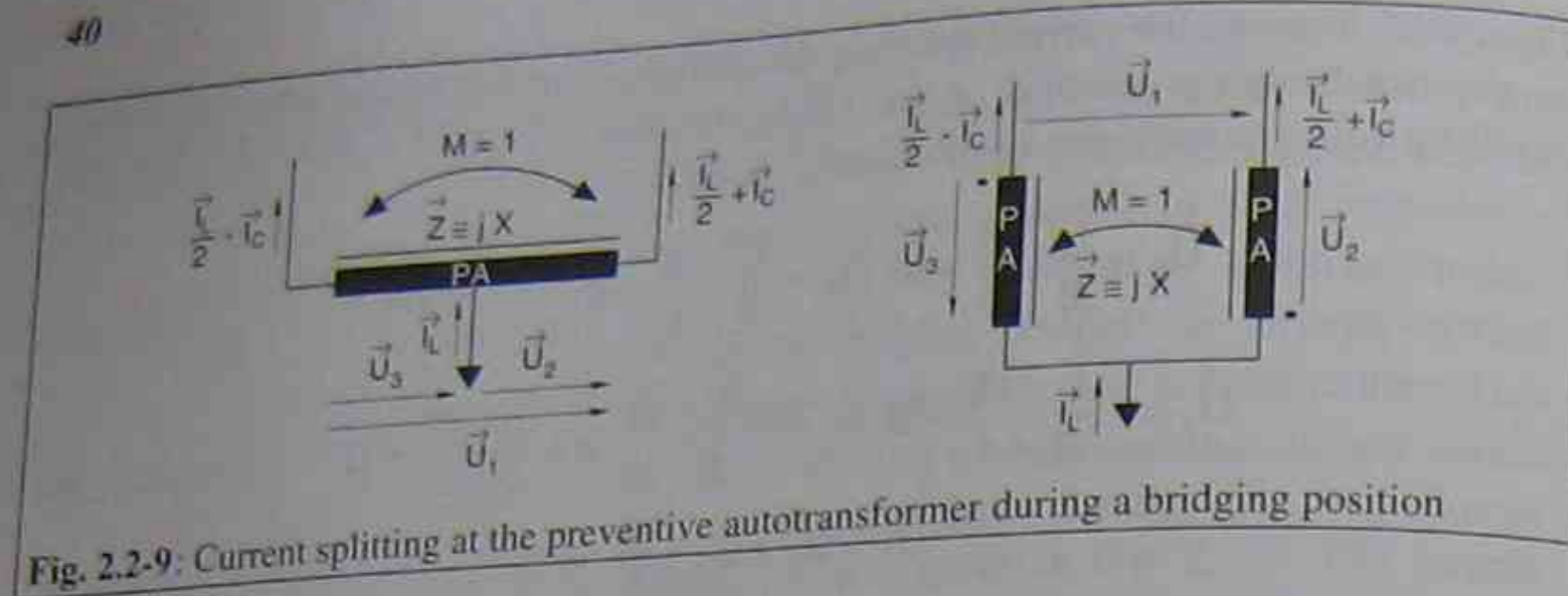
$$\bar{U}_3 = -\left(\frac{\bar{I}_L}{2} - \bar{I}_C\right) \cdot \frac{jX}{4} + M \cdot \bar{U}_2 = -\left(\frac{\bar{I}_L}{2} - \bar{I}_C\right) \cdot \frac{jX}{4} + 1 \cdot \left(\frac{\bar{I}_L}{2} + \bar{I}_C\right) \cdot \frac{jX}{4} = \bar{I}_C \cdot \frac{jX}{2} \quad (2.2\_5b)$$

**Fig. 2.2-9**: Current splitting at the preventive autotransformer during a bridging position

$$\vec{U}_1 = \vec{U}_2 + \vec{U}_3 = 2 \cdot \left( \vec{I}_C \cdot \frac{jX}{2} \right) = \vec{I}_C \cdot jX \qquad (2.2\_5c)$$

The tables in the following paragraphs show typical contact or switching device arrangements which are used for the above mentioned methods used to perform a tap-change operation. Only one pair of contacts for each function is shown in the figures, although in practice this may represent a set of contacts.

## 2.2.2.1 OLTC with Arcing switch and Tap Selector

Table 2.2-1 shows those operating steps of an arcing switch and tap selector reactance type OLTC which are relevant to the switching duty or to the output voltage of the transformer. The whole switching sequence is shown in Fig. 2.2-3. The example shows a tap-changing operation from the non-bridging position at tap 4 to the non-bridging position at tap 5 and vice versa.

For the non-bridging position the current splitting and the voltages are given in Fig. 2.2-7 and equations 2.2_3a to c.

During the tap-change from the non-bridging position at tap 4 to the bridging position at taps 4-5, first the transfer switch TFS$_B$ must break its current:

$$\vec{I}_{TFSB} = \frac{1}{2} \cdot \vec{I}_L \qquad (2.2\_6)$$

The recovery voltage at the opening contacts after arc quenching is determined by the voltage drop at the reactor (compare Fig. 2.2-8 and eq. 2.2_4a-c):

$$\vec{U}_{rTFSB} = 2 \cdot \left( \vec{I}_L \cdot \frac{jX}{4} \right) \qquad (2.2\_7)$$

After the tap selector operation from tap 4 to tap 5 and reclosing of the transfer switch the bridging position is reached. For the bridging position the current splitting and the voltages are given in Fig. 2.2-9 and equations 2.2_5a to c.

**Table 2.2-1**: Connection diagrams, operating order of contacts and phasor diagrams of an arcing switch and tap selector operation

The change of taps from this position to the next non-bridging position starts with the opening of the transfer switch TFS$_A$. This transfer switch must break the through-current and the circulating current:

$$\bar{I}_{TFSA} = \frac{1}{2} \cdot \bar{I}_L - \bar{I}_C \qquad (2.2\_8)$$

The recovery voltage at the opening contacts becomes:

$$\bar{U}_{rTFSA} = \bar{U}_S - 2 \cdot \left( \bar{I}_L \cdot \frac{jX}{4} \right) \qquad (2.2\_9)$$

This operation is called a "light" operation (minus signs in equations 2.2_8 and 2.2_9). The opposite operation from the non-bridging position at tap 5 to tap 4 is a "heavy" operation (plus signs in equations 2.2_12 and 2.2_13). The distribution of light and heavy operations to the transfer switches or to the switching direction depends on the signs of the through-current and the step voltage.

The following equations are valid for the operation from the non-bridging position at tap 5 to 4:

$$\bar{I}_{TFSA} = \frac{1}{2} \cdot \bar{I}_L \qquad (2.2\_10)$$

$$\bar{U}_{rTFSA} = 2 \cdot \left( \bar{I}_L \cdot \frac{jX}{4} \right) \qquad (2.2\_11)$$

$$\bar{I}_{TFSB} = \frac{1}{2} \cdot \bar{I}_L + \bar{I}_C \qquad (2.2\_12)$$

$$\bar{U}_{rTFSB} = \bar{U}_S + 2 \cdot \left( \bar{I}_L \cdot \frac{jX}{4} \right) \qquad (2.2\_13)$$

Fig. 2.2-10 shows the locus curve of the output voltage $\bar{U}$ of the transformer when moving from a non-bridging position to the next non-bridging position. This figure is derived from the phasor diagrams listed in Table 2.2-1. The shape of the curve (compare designations of the high-speed resistor type OLTC) looks like a pennant (non-bridging to bridging position or vice versa) or a double pennant (non-bridging to non-bridging position).
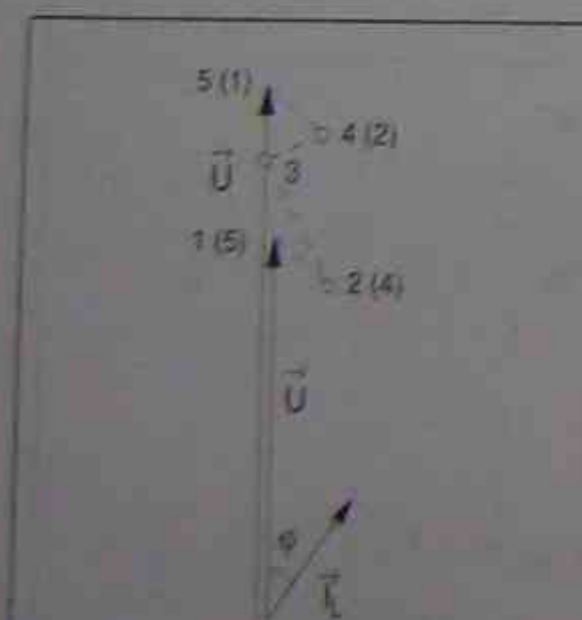
Table 2.2-2 shows the operating order of the switching contacts for some consecutive switching operations of the OLTC in both directions (adding and subtracting turns). The duties on the switching contacts (transfer switches) are given in Table 2.2-3. In there, also the number of operations of every set of



Fig. 2.2-10: Locus curve of the output voltage (unscaled)

**Table 2.2-2**: Operating order of contacts for some consecutive switching operations of an arcing switch and tap selector type OLTC (transfer switches)

| Switching operation from | Operating order of contacts | |
|---|---|---|
| non-bridging to bridging (raise) | TFS$_B$ breaks | TFS$_B$ makes |
| bridging to non-bridging (raise) | TFS$_A$ breaks | TFS$_A$ makes |
| non-bridging to bridging (raise) | TFS$_B$ breaks | TFS$_B$ makes |
| bridging to non-bridging (raise) | TFS$_A$ breaks | TFS$_A$ makes |
| ... | and so on | and so on |
| non-bridging to bridging (lower) | TFS$_A$ breaks | TFS$_A$ makes |
| bridging to non-bridging (lower) | TFS$_B$ breaks | TFS$_B$ makes |
| non-bridging to bridging (lower) | TFS$_A$ breaks | TFS$_A$ makes |
| bridging to non-bridging (lower) | TFS$_B$ breaks | TFS$_B$ makes |
| ... | and so on | and so on |

**Table 2.2-3**: Transfer switch duty of an arcing switch and tap selector type OLTC operation

| Contact | Switched current | recovery voltage | Number of operations | Effect of load power factor |
|---|---|---|---|---|
| TFS$_A$ | $\frac{1}{2} \cdot \bar{I}_L$ | $\frac{1}{2} \cdot \bar{I}_L \cdot jX$ | N / 4 | none |
| | $\frac{1}{2} \cdot \bar{I}_L - \frac{\bar{U}_S}{jX}$ | $\bar{U}_S - \frac{1}{2} \cdot \bar{I}_L \cdot jX$ | N / 4 | |
| TFS$_B$ | $\frac{1}{2} \cdot \bar{I}_L$ | $\frac{1}{2} \cdot \bar{I}_L \cdot jX$ | N / 4 | none |
| | $\frac{1}{2} \cdot \bar{I}_L + \frac{\bar{U}_S}{jX}$ | $\bar{U}_S + \frac{1}{2} \cdot \bar{I}_L \cdot jX$ | N / 4 | maximum duty at p.f. = 0 |

contacts, in relationship to the total number N of operations of the OLTC, and the effect of the power factor on the switching duties are given.

With the definition that one switching operation of the OLTC is the transition from a non-bridging to a bridging position (or vice versa) the number of operations of the transfer switches can be derived from the switching sequence (Fig. 2.2-3) and results to N/2 each. The duty on the contacts for half of these operations (N/4) is according

to equations 2.2_6 and 2.2_7 resp. 2.2_10 and 2.2_11. The other half (N/4) is for one transfer switch light operations and for the second transfer switch heavy operations. The question which of the both transfer switches must handle the heavy or the light operation depends on the signs of through-current and step voltage, as mentioned before. Fig. 2.2-6 explains the effect of the power factor on the duty on the switching contacts. The maximum current is reached at power factor 0.

### 2.2.2.2 OLTC with Arcing Tap Switch

The switching principle in regards to the switching duties of these OLTCs is the same as that of OLTCs with arcing switch and tap selector. However, the switching device is in this case the arcing tap selector, which must break the current and select the tapping. The resulting duties on the arcing tap switches, the number of operations, heavy and light operations and the effect of the power factor on the switched currents are the same as mentioned in the previous paragraph 2.2.2.1 for the transfer switches of the arcing switch and tap selector type OLTC. For this reason a description can be left out at this point.

### 2.2.2.3 OLTC with Vacuum Interrupter

Table 2.2-4 shows those operating steps of a vacuum interrupter reactance type OLTC which are relevant to the switching duty or to the output voltage of the transformer. The whole switching sequence is shown in Fig. 2.2-5. The example shows a tap-changing operation from the non-bridging position 4 to non-bridging position 5 and vice versa.

For the non-bridging position the current splitting and the voltages are given in Fig. 2.2-7 and equations 2.2_3a to c. During the tap-change from the non-bridging position at tap 4 to the bridging position at taps 4-5, first the bypass contacts $BYC_B$ must commutate its current to the vacuum interrupter (VI) path. Then the vacuum interrupter opens and breaks its current:

$$\vec{I}_{VI} = \frac{1}{2} \cdot \vec{I}_L \qquad (2.2\_14)$$

The recovery voltage at the opening contacts after arc quenching is determined by the voltage drop at the reactor (compare Fig. 2.2-8 and eq. 2.2_4a-c):

$$\vec{U}_{VI} = 2 \cdot \left( \vec{I}_L \cdot \frac{jX}{4} \right) \qquad (2.2\_15)$$

After the tap selector operation from tap 4 to tap 5 and reclosing of the vacuum interrupter the bridging position is reached. For the non-bridging position the current splitting and the voltages are given in Fig. 2.2-9 and equations 2.2_5a to c.

**Table 2.2-4:** Connection diagrams, operating order of contacts and phasor diagrams for an operation of an OLTC with vacuum interrupter

The tap-change from this position to the next non-bridging position starts with the opening of the bypass contacts $BYC_A$ and commutation of its current to the vacuum interrupter path. Now the vacuum interrupter opens and breaks the through-current plus the circulating current:

$$\bar{I}_{VI} = \frac{1}{2} \cdot \bar{I}_L - \bar{I}_C \qquad (2.2\_16)$$

and the recovery voltage at the opening contacts becomes:

$$\bar{U}_{rVI} = \bar{U}_S - 2 \cdot \left( \bar{I}_L \cdot \frac{jX}{4} \right) \qquad (2.2\_17)$$

This operation is called a "light" operation (minus signs in equations 2.2_16 and 2.2_17). The opposite operation from the non-bridging position at tap 5 to tap 4 is a "heavy" operation (plus signs in equations 2.2_20 and 2.2_21). These relations can change related to the vacuum interrupter when the through-current or the step voltage are in an opposite direction.

The following equations are valid for the opposite operation from the non-bridging position at tap 5 to tap 4:

$$\bar{I}_{VI} = \frac{1}{2} \cdot \bar{I}_L \qquad (2.2\_18)$$

$$\bar{U}_{rVI} = 2 \cdot \left( \bar{I}_L \cdot \frac{jX}{4} \right) \qquad (2.2\_19)$$

$$\bar{I}_{VI} = \frac{1}{2} \cdot \bar{I}_L + \bar{I}_C \qquad (2.2\_20)$$

$$\bar{U}_{rVI} = \bar{U}_S + 2 \cdot \left( \bar{I}_L \cdot \frac{jX}{4} \right) \qquad (2.2\_21)$$

A comparison of the equations 2.2_6 to 2.2_13 with equations 2.2_14 to 2.2_21 shows that the currents switched and recovery voltages for the transfer switches are identical with those of the vacuum interrupter.

The locus curve of the output voltage $\bar{U}$ of the transformer when moving from one non-bridging position to the next non-bridging position is the same as for the arcing switch and tap selector type OLTC as shown in Fig. 2.2-10.

Table 2.2-5 shows the operating order of switching contacts for some consecutive switching operations of the OLTC in both directions (adding and subtracting turns). The duties on the switching contacts (vacuum interrupter) are given in Table 2.2-6. In there, also the number of operations of every set of contacts, in relationship to the total number N of operations of the OLTC, and the effect of the power factor on the switching duties are given.

The vacuum interrupter is involved in every switching operation of the OLTC. If the transition from a non-bridging to a bridging position (or vice versa) is defined as one switching operation, the number of operations of the vacuum interrupter can be defined as N. Further, it has to be considered that every operation is neither a heavy nor a light operation. It can be assumed as a mean value that the operations of the vacuum interrupter are distributed evenly into heavy (N/2) and light (N/2) operations.

Fig. 2.2-6 explains the effect of the power factor on the duty on the switching contacts. The maximum current will be reached at power factor 0.

Table 2.2-5: Operating order of contacts for some consecutive switching operations of a vacuum interrupter type OLTC

| Switching operation from | Operating order of contacts | |
|---|---|---|
| non-bridging to bridging (raise) | VI breaks | VI makes |
| bridging to non-bridging (raise) | VI breaks | VI makes |
| non-bridging to bridging (raise) | VI breaks | VI makes |
| bridging to non-bridging (raise) | VI breaks | VI makes |
| ... | and so on | and so on |
| non-bridging to bridging (lower) | VI breaks | VI makes |
| bridging to non-bridging (lower) | VI breaks | VI makes |
| non-bridging to bridging (lower) | VI breaks | VI makes |
| bridging to non-bridging (lower) | VI breaks | VI makes |
| ... | and so on | and so on |

Table 2.2-6: Contact duty of a vacuum interrupter type OLTC operation

| | Transition contact duty | | | |
|---|---|---|---|---|
| Contact | Switched current | recovery voltage | Number of operations | Effect of load power factor |
| VI | $\frac{1}{2} \cdot \bar{I}_L$ | $\frac{1}{2} \cdot \bar{I}_L \cdot jX$ | N/2 | none |
| | $\frac{1}{2} \cdot \bar{I}_L - \frac{\bar{U}_S}{jX}$ | $\bar{U}_S - \frac{1}{2} \cdot \bar{I}_L \cdot jX$ | N/4 | |
| | $\frac{1}{2} \cdot \bar{I}_L + \frac{\bar{U}_S}{jX}$ | $\bar{U}_S + \frac{1}{2} \cdot \bar{I}_L \cdot jX$ | N/4 | maximum duty at p.f. = 0 |

## 2.3 TAP SELECTOR

The purpose of a tap selector is to transfer connection from a common terminal to a multiplicity of leads connected to the transformer tapped winding. The simplest type of tap selector therfore takes the form of a rotary or linear multiway indexing switch. When using the rotary form, the tap-selector terminals are arranged in a circular manner or on the arc of a circle. Whichever design is choosen, one method of driving such a device is by Geneva wheels and driving cam (Geneva crank). This method provides the single- or double-selector motion, but also locks the moving contacts firmly on position between operations. Other systems include elliptical drive gears or normal and partial toothed gear-reduction methods [Webb 1979].

Theoretically, the number of positions for a tap selector with contact terminals arranged in a circular manner can be increased until the distance between the adjacent contact terminals reaches the minimum that can be tolerated in regards to the withstand voltage between two taps. If a symmetrical contact pitch is choosen, the maximum voltage stress appears at those two adjacent contact terminals which are connected to the beginning and end of the tap winding. The voltage between two taps being insignificant compared with the voltage across the whole tap winding.

In practice, the number of positions is mainly in the range of 17 to 35 positions. In some special cases (industrial transformers) OLTCs with up to 107 operating positions have been realized. It needs to be considered that the number of tapping sections of the transformer winding is determined by the transformer design and is limited by the impulse level that appears across the tap winding. To increase the number of operating positions but not the electrical length of the tap winding, the tap selector can be equipped with a change-over selector (reversing or coarse) which approximately allows to double the tapping range and with it the number of operating positions (see paragraph 3).

When using a tap selector with change-over selector, a fully circular tap selector is mandatory to allow the tap selector to move through a second revolution.

On the basis of different OLTC designs (in-tank or compartment type) and different switching principles (resistor or reactor type) different tap selector designs are necessary and have been introduced. The single-multiway selector design is only possible when using a resistor type selector switch, whereas the tap selectors of all other OLTC designs (resistor and reactor type) must be taken as double-multiway selectors.

### 2.3.1 TAP SELECTORS OF IN-TANK TYPE OLTCs

OLTCs designed according to the selector switch principle consist basically of an oil compartment and a tap-changer insert (Fig. 2.3-1). The oil compartment is a cylinder, nowadays made from glassfibre reinforced epoxy resin (FRP), and is gas and
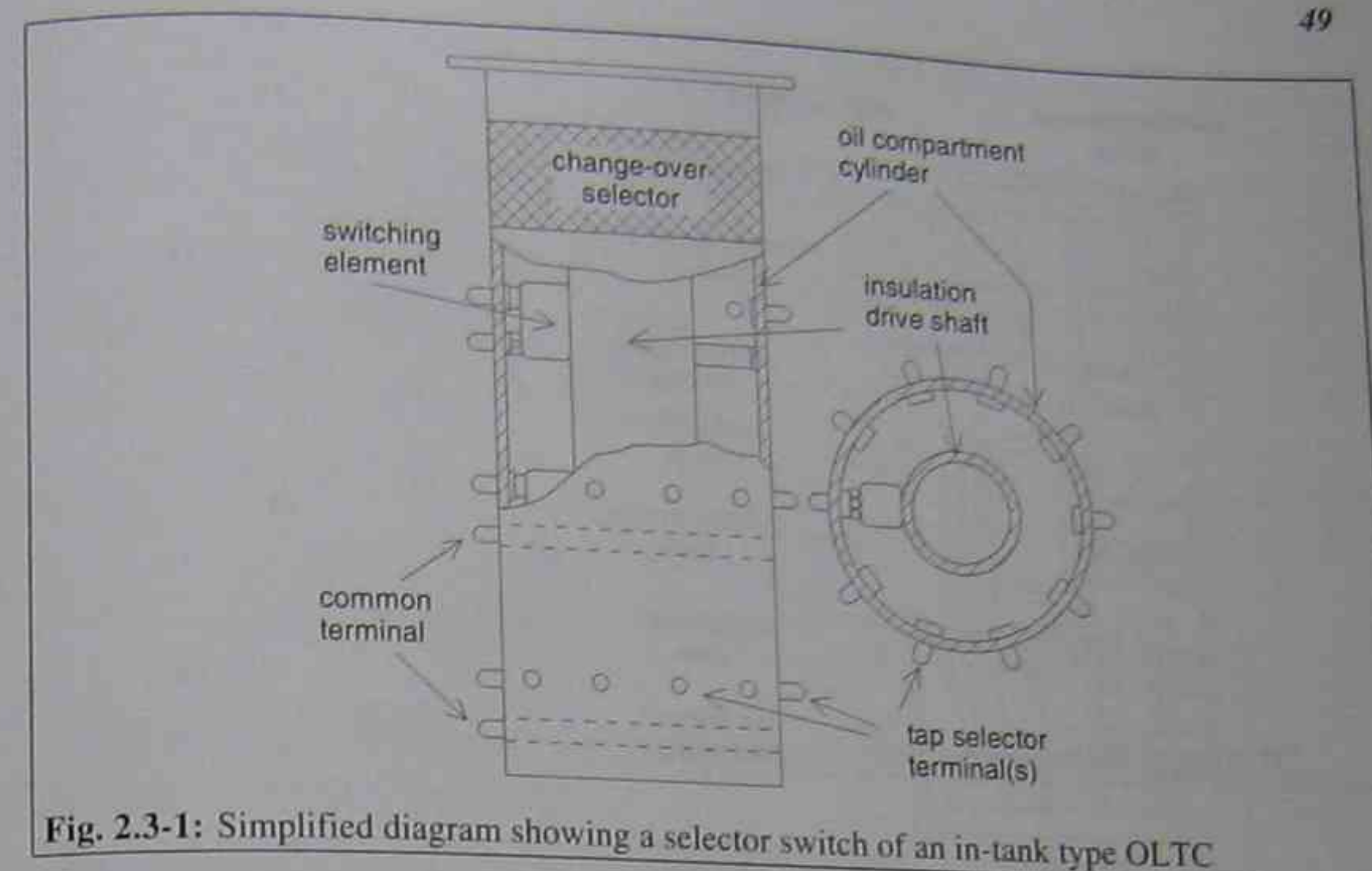
**Fig. 2.3-1:** Simplified diagram showing a selector switch of an in-tank type OLTC

oil tight to the surrounding transformer main tank. The fixed contacts of the selector switch and, if present, of the change-over selector, are arranged on seperate contact levels, mounted on the internal side of the oil compartment cylinder and connected to the outside terminals. According to the switching principle of the selector switch (compare paragraph 2.1.1) only one contact circle (one level) is needed (single-multiway indexing switch) per phase.

The tap-changer insert comprises the entire movable contact system of the selector switch. It consists of the selector switch insulating drive shaft, nowadays also made from FRP, the switching elements and, if required, the change-over selector contact carrier. The selector switch insulating drive shaft is connected at the top to the Geneva gearing mechanism.

The tap selector of resistor type OLTCs consisting of a diverter switch and a tap selector is located in the transformer main tank without a separate compartment. The tap selector is usually located below the diverter switch oil compartment. The insulating drive shafts of the tap selector are coupled through a Geneva gearing mechanisms to the motor drive through an additional drive shaft, which may be located at the center or outside of the diverter switch oil compartment.

The fixed contacts of the tap selector are arranged in a circular manner and mounted on bars made from laminated paper or FRP, or on shells made from FRP (Fig. 2.3-2). The tap selector may also include a change-over selector. Each phase consists of two levels of contacts (even and odd contact numbers) which connect through the movable contact assembly (called contact bridge) to take-off rings. The take-off rings of the two levels of every phase are connected through leads to the corresponding side of the diverter switch of every phase.
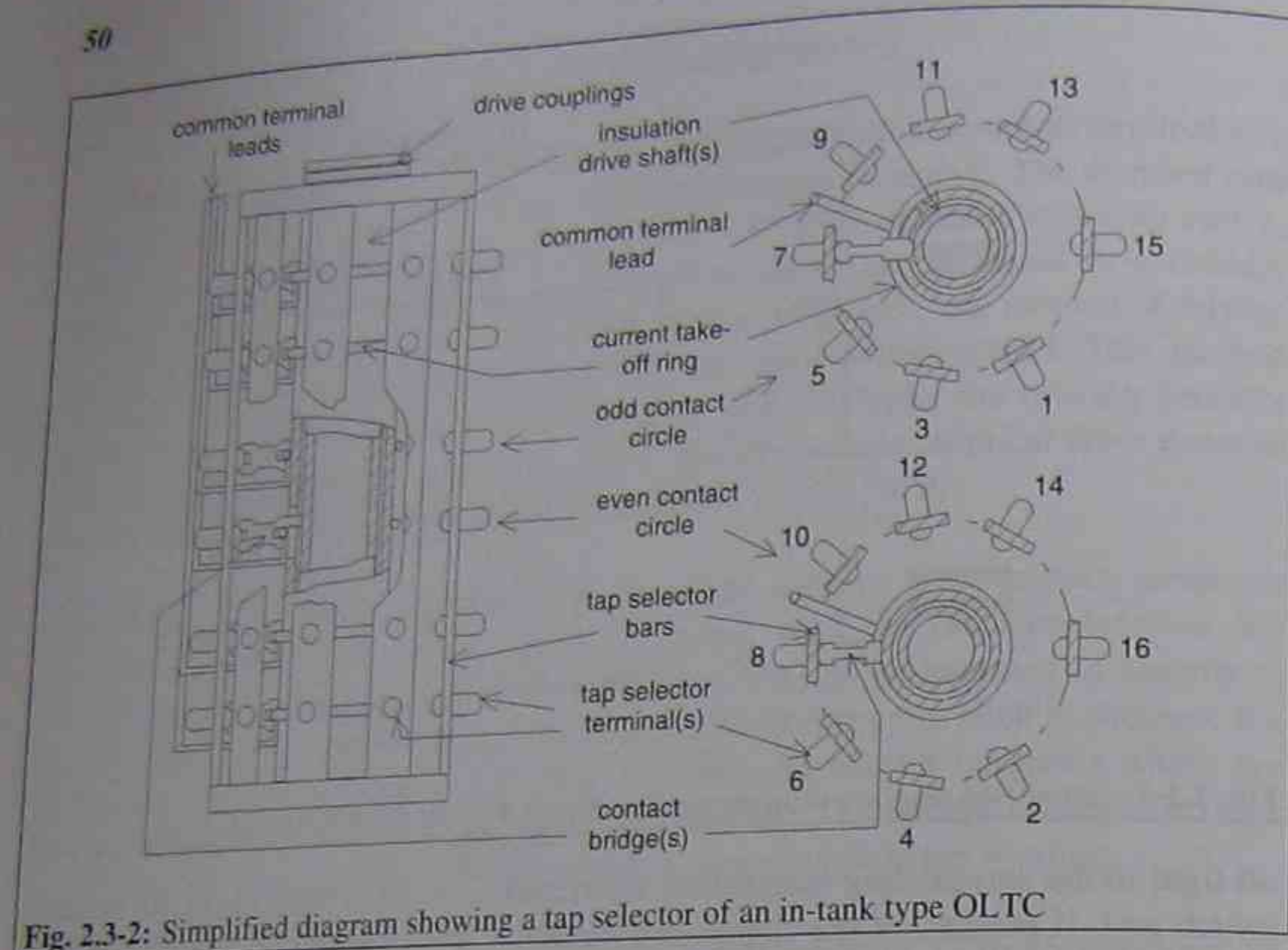
**Fig. 2.3-2:** Simplified diagram showing a tap selector of an in-tank type OLTC

As described in paragraph 2.1.1 the contact bridges of the even and odd contact circles alternate operation during consecutive tap-change operations. For this purpose the gearing may be a step by step gear operated by two Geneva wheels and a Geneva crank with two driving cams. With the tap selector design shown in Fig. 2.3-2 the two concentric insulation drive shafts are coupled with one Geneva wheel each. Such a design requires that the leads, which connect the diverter switch with the tap selector take-off ring, must be located outside the tap selector cage.

The coupling is designed in such a way that in the event of a reversal of the tap-change direction the motor drive action does not move the movable tap selector contact bridge but only the diverter switch.

The insulating distance between the first and last fixed contact of the tap selector (this means the beginning and the end of the tap winding) often is enlarged due to the impulse level, which appears across the tap winding.

## 2.3.2 TAP SELECTORS OF COMPARTMENT TYPE OLTCs

Physically, there are two basic configurations possible for the compartment type OLTC with a circular tap selector:

The tap selector in line with the barrier board (Fig. 2.3-3)
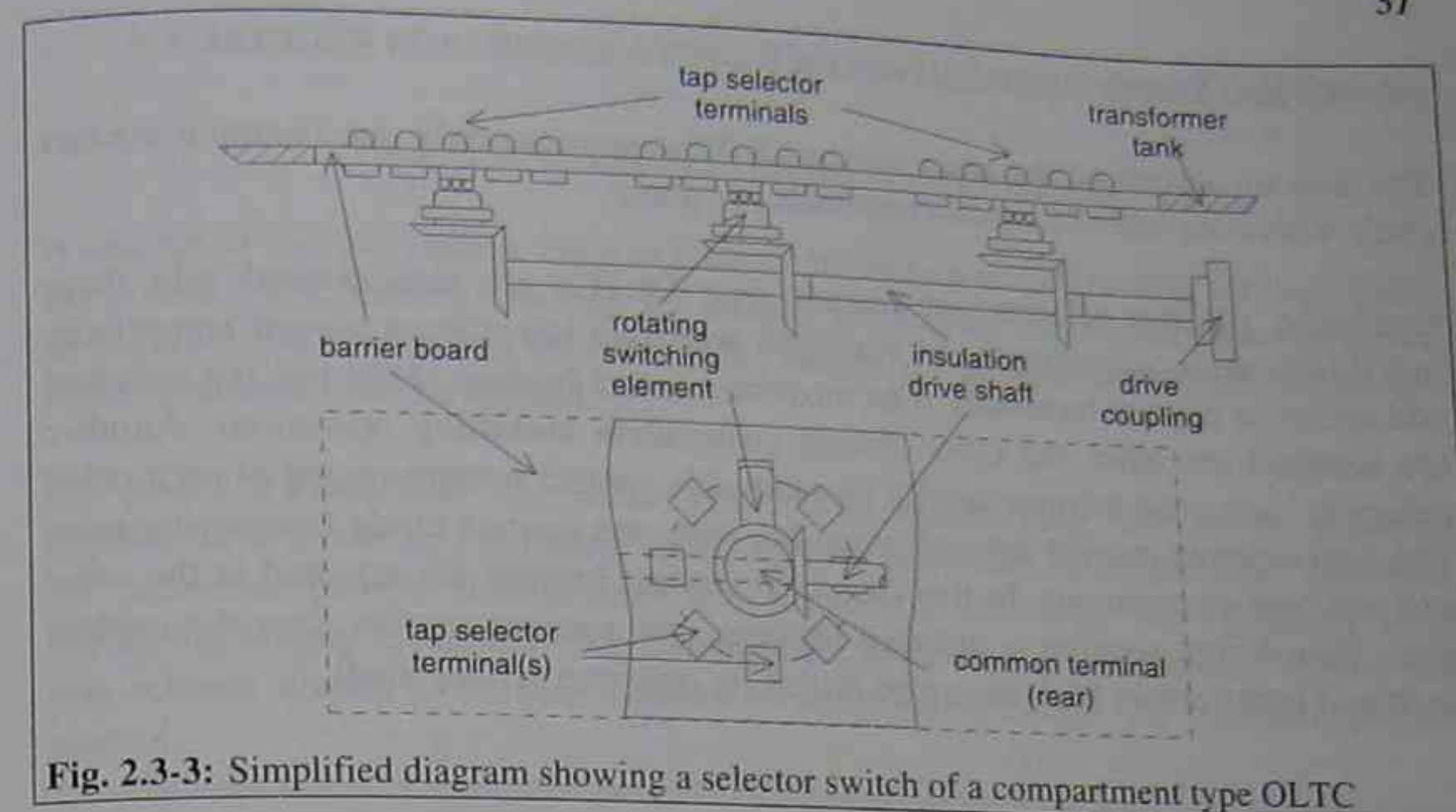The tap selector perpendicular to the barrier board (Fig. 2.3-4)

**Fig. 2.3-3:** Simplified diagram showing a selector switch of a compartment type OLTC

The first option makes for the simplest electrical path while the other allows the use of a single drive shaft, although connecting leads to the terminals mounted on the barrier board are needed.

The tap selectors themselves are divided into three individual phase assemblies. In case of the resistor type OLTC with diverter switch plus tap selector each phase assembly comprises two tap selectors, one for the odd numbered and the other for the even numbered tappings. The two contact circles can be located on the top of each
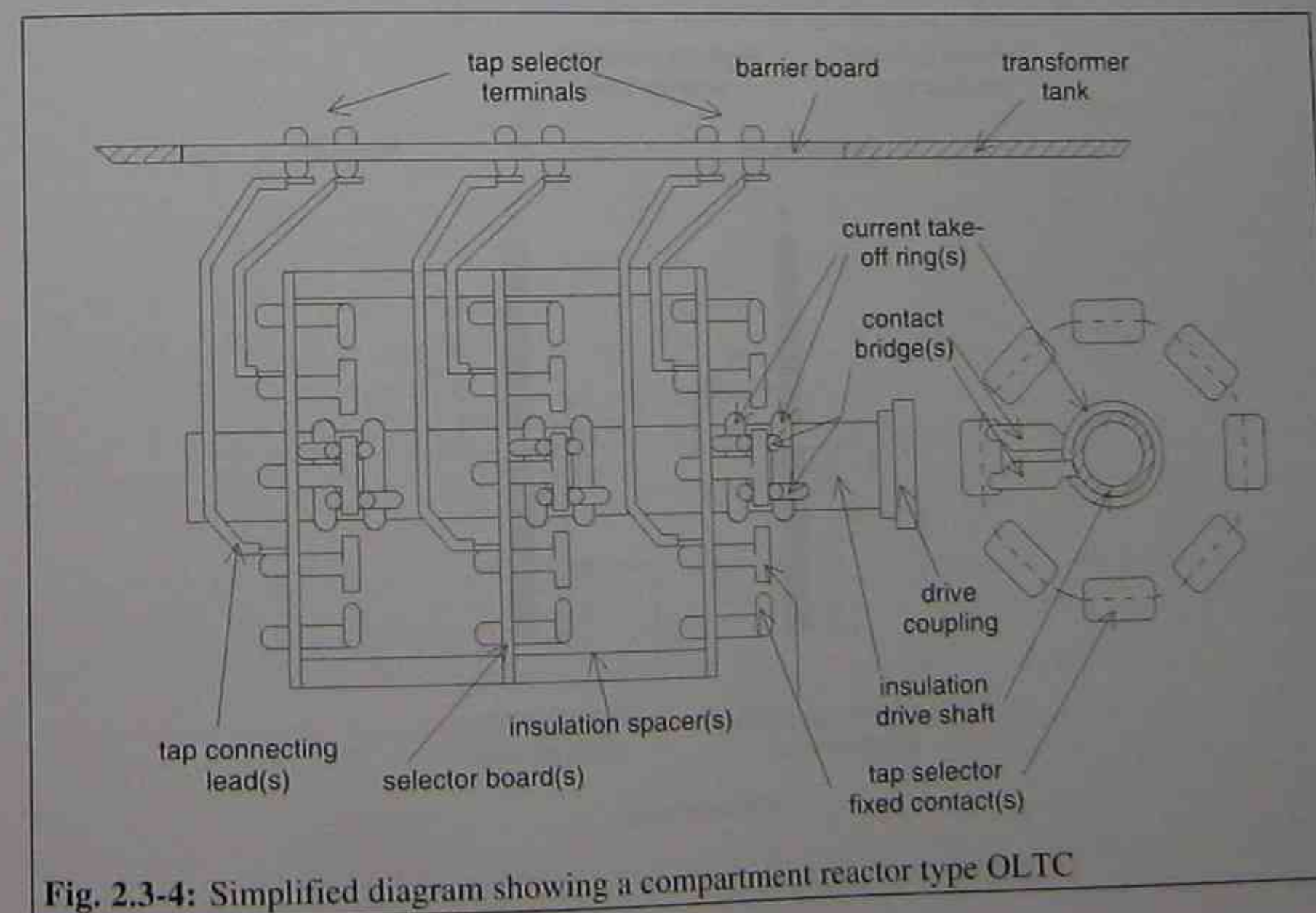
**Fig. 2.3-4:** Simplified diagram showing a compartment reactor type OLTC

other or next to each other.

The selector switch of the resistor type OLTC comprises only one common contact circle with even and odd contact terminals per phase.

Generally, the tap selectors of reactor type OLTCs are also divided into three individual phase assemblies and equipped with two tap selectors, each comprising odd and even contact terminals. The movable contact bridges of the two tap selectors are actuated one after the other during consecutive switching operations. Another design of such a tap selector is with two movable contact bridges on top of each other with two seperate current take-off rings but only one contact circle comprising even and odd contact terminals. In this case both contact bridges are actuated at the same time. This design requires a distance between two contacts smaller than the contact itself and both contact bridges can be driven by only one driving shaft.

# 3 CIRCUITS FOR REGULATING TRANSFORMERS WITH OLTCs

## 3.1 FUNDAMENTALS OF REGULATION

A change of the transformer ratio is effected by adding or subtracting turns to either the primary or secondary winding. Three basic connecting schemes are used as shown in Figure 3.1-1. Depending on system and design parameters of the transformer any of these schemes can be applied.

On power transformers the linear connecting scheme (Fig. 3.1-1a) is generally applied for a moderate regulating range up to a maximum of 20 per cent. However, for industrial process transformers this scheme is also used for extremely large regulating ranges. Generally such transformers work with a variable flux density and this scheme allows a variable number of turns between taps for optimum process control.
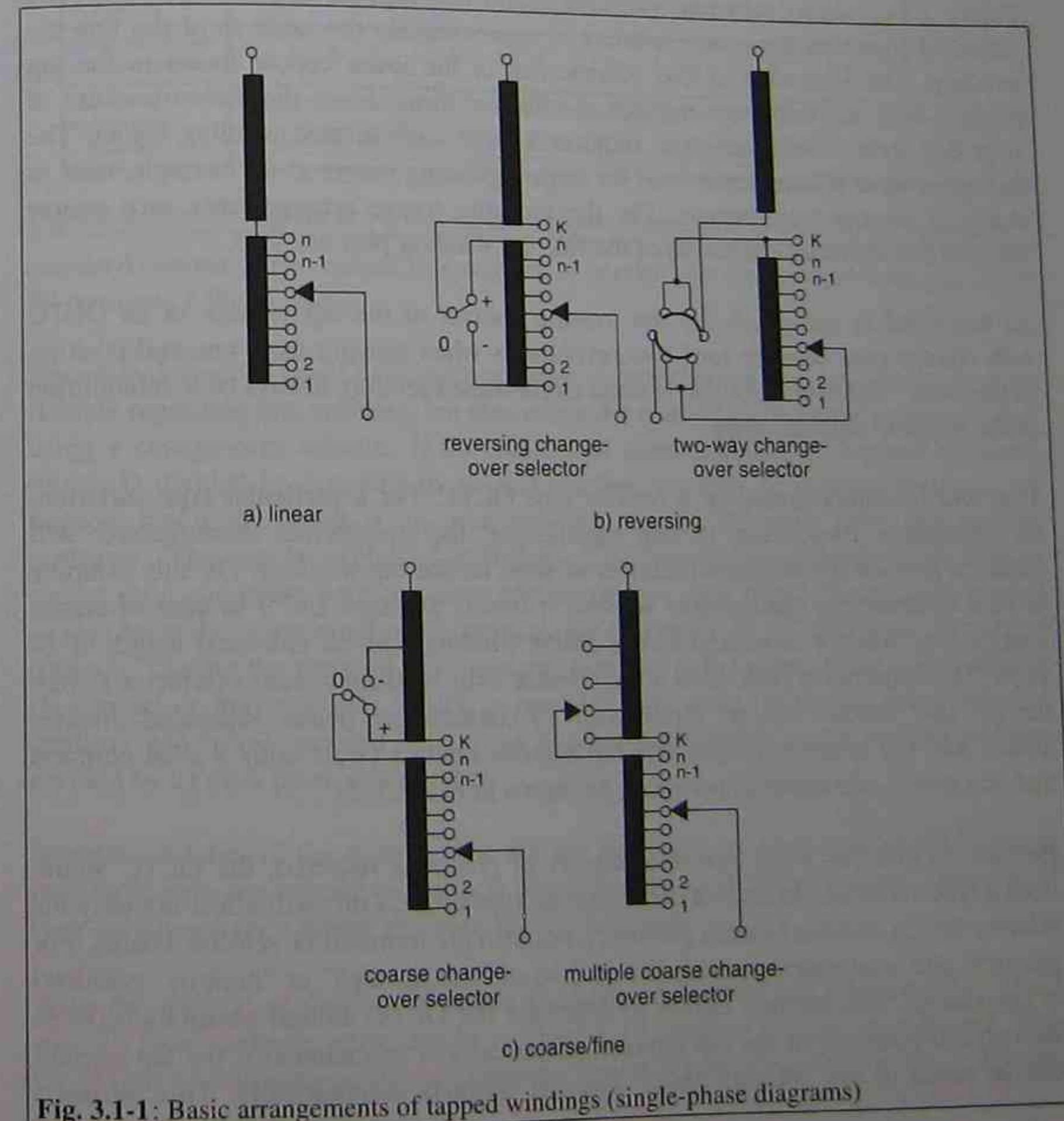


Fig. 3.1-1: Basic arrangements of tapped windings (single-phase diagrams)

As shown in Figs. 3.1-1b and 3.1-1c, the tapping range can be approximately doubled by using a change-over selector. A reversing change-over selector (Fig. 3.1-1b) allows the tapped winding to be connected in vectorial addition (boost) or substraction (buck) to the main winding. This enables to enlarge the regulating range or to reduce the number of taps of the tapped winding. However, in the circuit causing maximum number of effective turns the entire tap winding is in the circuit causing maximum copper losses in the transformer. Usually the design with a single pole reversing change-over selector is applied. For large single-phase tansformers using line-end tap-changers also a two-way change-over selector can be applied. This design has the advantage that during the reversing switch operation the tapped winding remains connected to the main winding. When using a two-way change-over selector a special gear for the tap selector is necessary. The sequences of events of a single pole reversing change-over selector and of the two-way change-over selector are compared in detail in paragraph 4.3.3.1.

Figure 3.1-1c shows schemes with coarse and fine tap winding arrangements. The electrical length of the coarse winding is approximately the same as of the fine tap winding. The advantage of this scheme lies in the lower copper losses in the tap position with the minimum number of effective turns. From the dielectric point of view this arrangement, however, requires a more sophisticated winding layout. The multiple coarse scheme lends itself for large regulating ranges as for example, used in chemical process transformers. For the multiple coarse arrangements each coarse winding has the electrical length of the fine tap winding plus one step.

As described in paragraph 2.3 the moving contact of the tap selector of an OLTC with change-over selector runs two revolutions when moving from one end-position to the other. Unfortunately, the contact circle must therefore always be a submultiple of the required tapping range.

This will be demonstrated on a resistor type OLTC. For a particular type variation, for example a 19-position 18-step transformer, the transformer manufacturer will prefer to provide the minimum number of steps on the tap winding. For this example in case of reversing change-over selector it means 10 steps and 9 in case of coarse change-over selector combined with a coarse winding with an electrical length of 10 steps. This requires in both cases a tap selector with 10 fixed contacts (selector switch design: one selector contact circle with 10 contacts per phase; separated diverter switch and tap selector design: one tap selector contact circle with 5 even contacts and one with 5 odd contacts per phase as shown in Fig. 3.1-2).

Because of this, for every possible number of positions required, the OLTC would need a type variation. In case of compartment type OLTCs this will affect not only the selector design and the Geneva geometry, but also the terminal or selector boards. For practical and economical reasons the method of "run through" or "dummy" positions is introduced. This method allows to distribute the OLTC unused positions between the two end-positions of the tap selector. Electrically or mechanically, the tap selector can be made to run through these common contacts automatically. This allows a
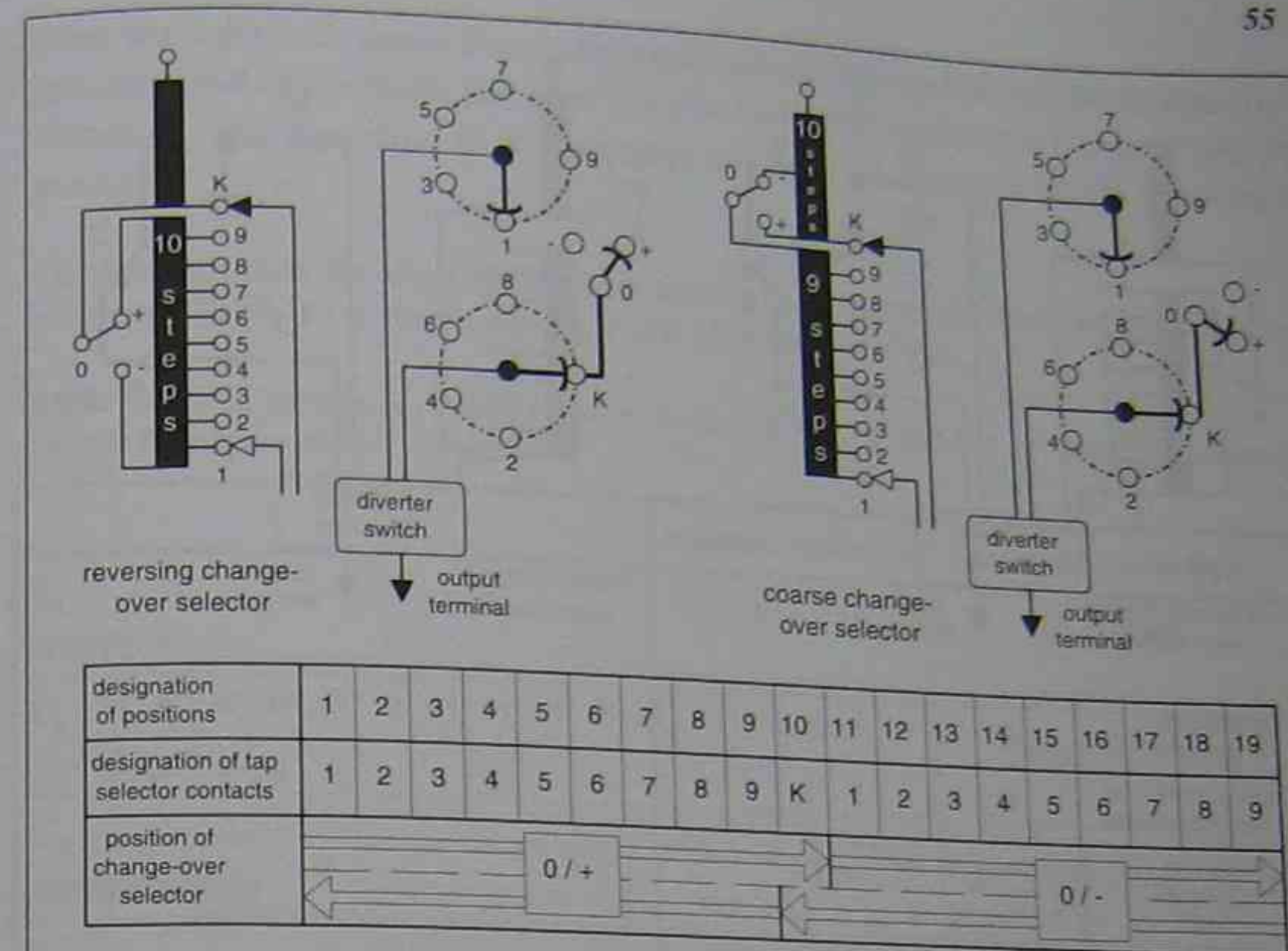
**Fig. 3.1-2**: Circuit diagram of a reversing and a coarse change-over selector with 19 positions

standard contact circle molded in a selector or barrier board to be used from e.g. 33 to 39 positions [ Webb 1979].

The in-tank resistor type OLTC with seperate diverter switch and tap selector is more flexible regarding this problem, but also needs the method of "dummy" contacts when using a change-over selector. If the number of steps (number of required positions minus 1) divided by 2 results in an odd number, usually, no dummy positions are needed, but if the result is an even number, the OLTC must have two dummy positions . This can be explained as follows. The tap selector consists of two contact circles (odd and even) with the same contact pitches each phase. Hence both contact circles have the same number of contacts, which results in an even total number of contacts. During the running from one end-position to the other, there is one contact (K-contact or mid-position), which is operated only once. With this the number of contacts which are operated twice (this number corresponds to the number of steps divided by 2) must be an odd number.

Selector switches of the in-tank type are not subjected to these restrictions, because they have only one contact circle each phase, but for economical reasons (decrease of type variations) they follow the same circuit diagrams.

With the method of dummy positions the above described tap selector (Fig. 3.1-2) with 10 fixed contacts must also be used for a 17-position 16-step transformer. This OLTC has two dummy positions (positions 9a and 9c) as shown in Fig. 3.1-3. The tap
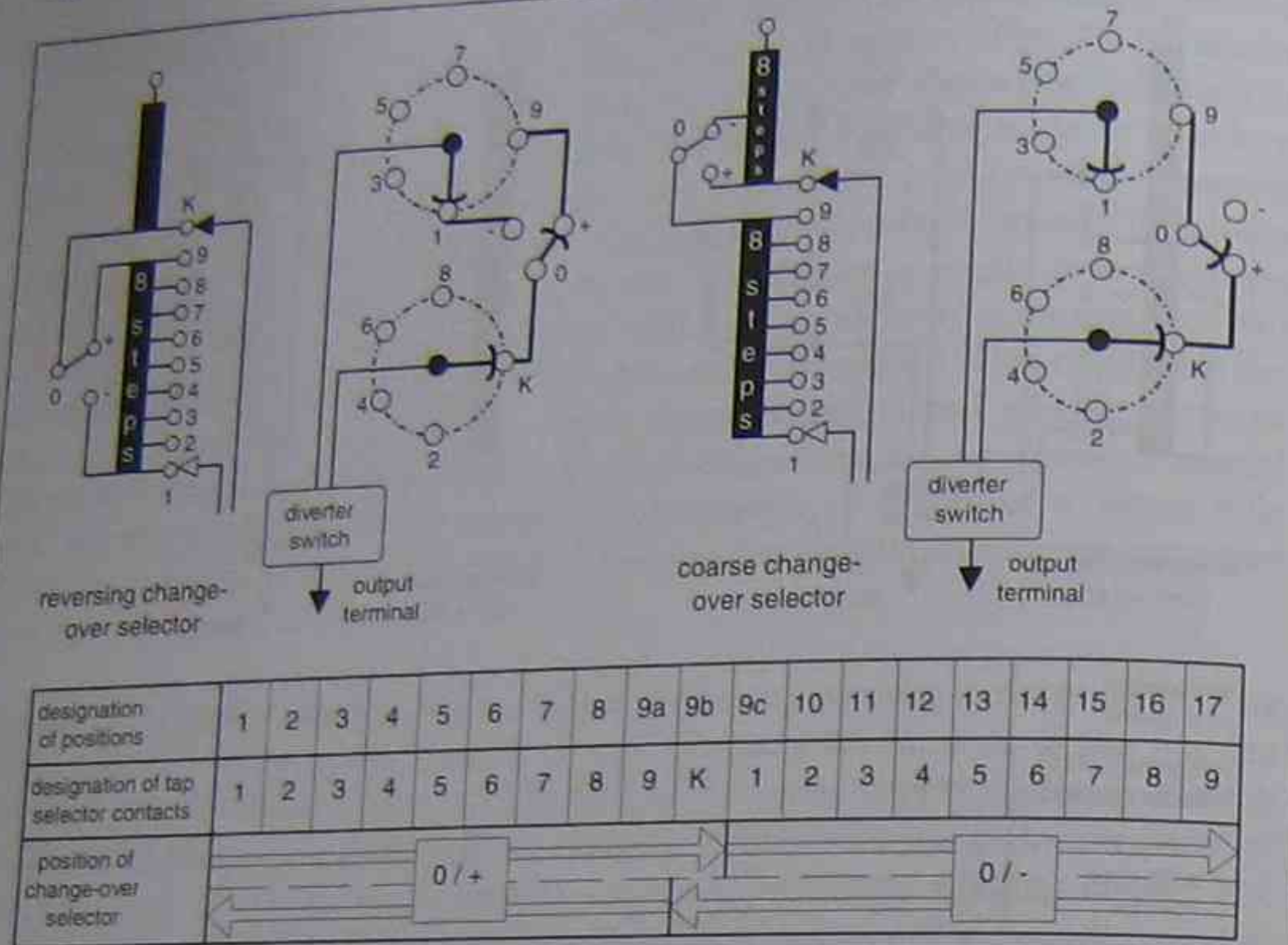
**Fig. 3.1-3**: Circuit diagram of a reversing and a coarse change-over selector with 17 positions

| designation of positions | 1 | 2 | 3 | 4 | 5 | 6 | 7 | 8 | 9a | 9b | 9c | 10 | 11 | 12 | 13 | 14 | 15 | 16 | 17 |
|---|---|---|---|---|---|---|---|---|---|---|---|---|---|---|---|---|---|---|---|
| designation of tap selector contacts | 1 | 2 | 3 | 4 | 5 | 6 | 7 | 8 | 9 | K | | 1 | 2 | 3 | 4 | 5 | 6 | 7 | 8 | 9 |
| position of change-over selector | | | | | 0 / + | | | | | | | | | 0 / − | | | | | |

winding must have 8 steps, independently of the type of change-over selector used. If a coarse winding is used, it also has the electrical length of 8 steps.

In the following an arrangement according to Fig. 3.1-2 will be called OLTC with "one mid-position" and according to Fig. 3.1-3 OLTC with "three mid-positions".

Physically, every regulation can be carried out with constant induction or with variable induction. Fig. 3.1-4 shows one phase of a two-winding, three-phase power transformer with tap winding and linear regulation. If the winding that includes the tap winding (in Fig. 3.1-4 the primary winding 1U1-1U2) is fed with a constant input voltage $\bar{U}_1$, the induction is variable. The number of turns ($w_{HV} + w_{TV}$) that see the constant input voltage varies and leads to a variable voltage per turn. This affects the secondary winding 2U1-2U2 and the result is a variable output voltage $\bar{U}_2$ corresponding to the constant number of turns $w_{LV}$ of the secondary winding. Also the step voltage at the tap winding varies with the number of active turns and reaches its maximum in the OLTC position with the minimum number of turns (maximum voltage per turn). This has to be considered when selecting the OLTC.
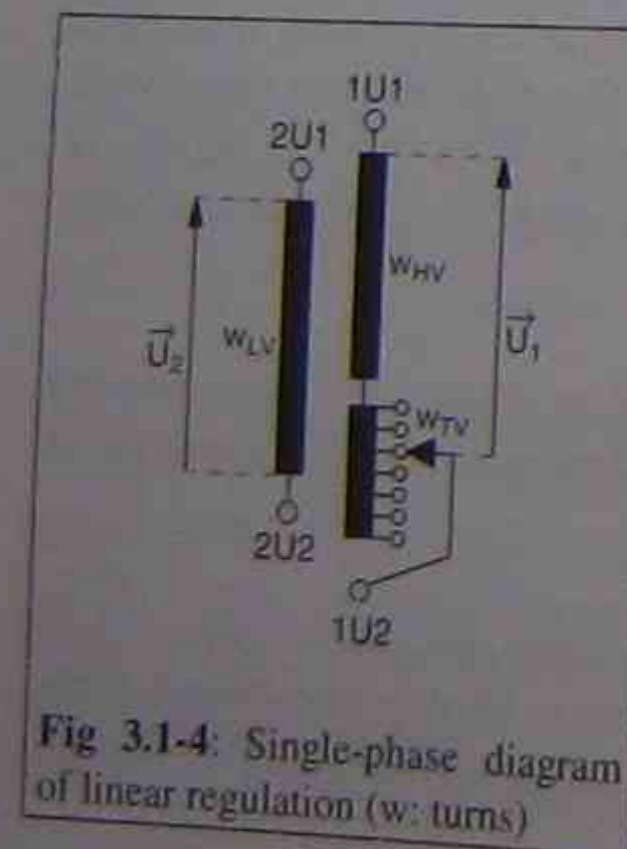


**Fig 3.1-4**: Single-phase diagram of linear regulation (w: turns)

When the voltage $\bar{U}_1$ across the winding that includes the tap winding is variable, the induction and the voltage per turn are constant. The result is a constant output voltage $\bar{U}_2$ corresponding to the constant number of turns $w_{LV}$ of the secondary winding.

The relevant data for the OLTC dimensioning is different for constant or variable induction. Table 3.1-1 shows a comparison of the relevant data.

**Table 3.1-1**: Comparison of data relevant to the OLTC for variable or constant induction (circuit diagram as shown in Fig. 3.1-4)

| | | constant induction | variable induction |
|---|---|---|---|
| $U_1$ primary voltage | | $U_{1min} \leq U_1 \leq U_{1max}$ | $U_1 = \text{const.}$ |
| $U_2$ secondary voltage | | $U_2 = \text{const.}$ | $U_{2min} \leq U_2 \leq U_{2max}$ |
| $U_R$ regulating range | | $U_R = U_{1max} - U_{1min}$ | $U_{Rmax} = U_1 \cdot \dfrac{U_{2max} - U_{2min}}{U_{2min}}$ |
| $I_{max}$ max. through-current (OLTC) | | $I_{max} = \dfrac{S_N}{3 \cdot U_{1min}}$ | $I_{max} = \dfrac{S_N}{3 \cdot U_1} = \text{const.}$ |
| $U_S$ step voltage | | $U_S = \dfrac{U_{TV}}{m}$ | $U_{Smax} = \dfrac{U_{TVmax}}{m}$ |
| *linear regulation* | | | |
| $U_{TV}$ voltage across tap winding | | $U_{TV} = U_R$ | $U_{TVmax} = U_{Rmax}$ |
| *regulation with reversing change-over selector* | | | |
| $U_{TV}$ voltage across tap winding | 1 mid-pos. | $U_{TV} = \dfrac{U_R}{2} \cdot \dfrac{m}{m-1}$ | $U_{TVmax} = \dfrac{U_{Rmax}}{2} \cdot \dfrac{m}{m-1}$ |
| | 3 mid-pos. | $U_{TV} = \dfrac{U_R}{2}$ | $U_{TVmax} = \dfrac{U_{Rmax}}{2}$ |
| *regulation with coarse change-over selector* | | | |
| $U_{TV}$ voltage across tap winding | | $U_{TV} = \dfrac{U_R}{2}$ | $U_{TVmax} = \dfrac{U_{Rmax}}{2}$ |
| $U_{CV}$ voltage across coarse winding | 1 mid-pos. | $U_{CV} = U_{TV} + U_S$ | $U_{CVmax} = U_{TVmax} + U_{Smax}$ |
| | 3 mid-pos. | $U_{CV} = U_{TV}$ | $U_{CVmax} = U_{TVmax}$ |

(with: $S_N$: 3 phase power of the transformer
and m: number of steps of the tap winding)

Depending on the system and operating requirements the described basic connection schemes are applied to two-winding transformers, autotransformers, phase shifting transformers as well as booster circuits.

The symbols used in the following paragraphs are listed below:

$S_N$:    3 phase power of the transformer
$U_1$:    primary voltage (phase to phase)
$U_R$:    regulating range (phase to phase)
$I_{max}$:    max. through current of OLTC
$U_S$:    step voltage
$U_{TV}$:    voltage across tap winding
$U_{CV}$:    voltage across coarse winding
$m$:    number of steps of the tap winding

## 3.2 CIRCUITS FOR REGULATION AT THE NEUTRAL END

On two-winding power transformers the most popular arrangement is the regulation at the neutral end of the Y-connected windings as shown in Fig. 3.2-1. This solution provides a most economical tap winding arrangement and generally graded insulation combined with a compact three-phase star point OLTC.

The following data is important with respect to the dimensioning of the OLTC (regulation as shown in Fig. 3.2-1, symbols see end of paragraph 3.1):

$$U_{1min} \leq U_1 \leq U_{1max} \; ; \; S_N = \text{const.} \; ; \; \text{induction} = \text{const.}$$

$$U_R = U_{1max} - U_{1min} \quad \text{and} \quad I_{max} = \frac{S_N}{\sqrt{3} \cdot U_{1min}} \quad \text{and} \quad U_S = \frac{U_{TV}}{m} \qquad (3.2\_1, 3.2\_2, 3.2\_3)$$

for linear regulation (constant turns per step):

$$U_{TV} = \frac{U_R}{\sqrt{3}} \qquad (3.2\_4)$$

for regulation with reversing change-over selector:

1 mid-position:
$$U_{TV} = \frac{U_R}{2 \cdot \sqrt{3}} \cdot \frac{m}{m-1} \qquad (3.2\_5)$$

3 mid-positions:
$$U_{TV} = \frac{U_R}{2 \cdot \sqrt{3}} \qquad (3.2\_6)$$

$\vec{U}_{HV}$ : voltage at the main winding     $\vec{U}_{TV}$ : voltage at the tap winding
$\vec{U}_{CV}$ : voltage at the coarse winding     $\vec{U}_{S}$ : voltage at the transformer terminals
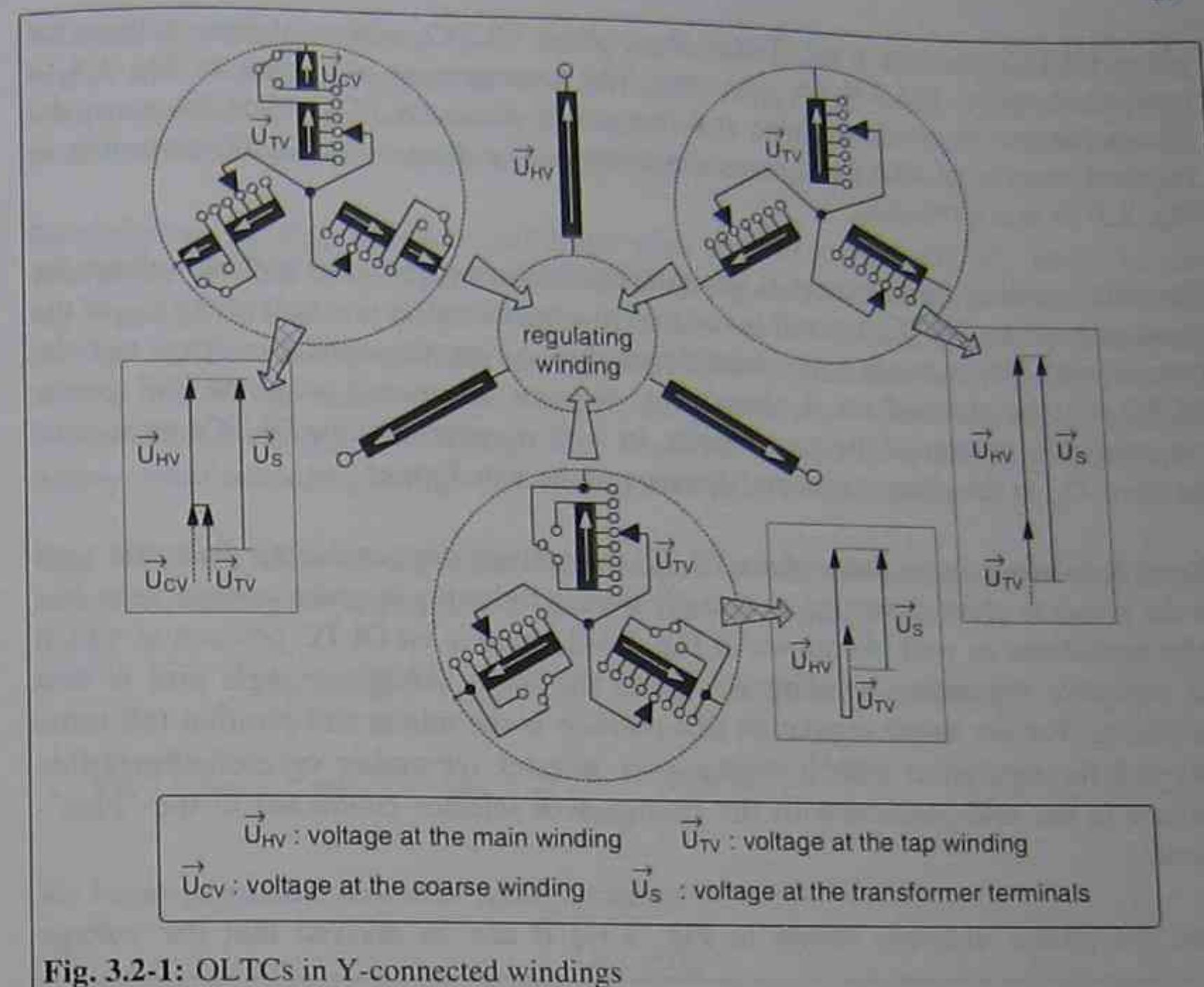
**Fig. 3.2-1:** OLTCs in Y-connected windings

for regulation with coarse change-over selector:

$$U_{TV} = \frac{U_R}{2 \cdot \sqrt{3}} \qquad (3.2\_7)$$

1 mid-position:
$$U_{CV} = U_{TV} + U_S \qquad (3.2\_8)$$

3 mid-positions:
$$U_{CV} = U_{TV} \qquad (3.2\_9)$$

## 3.3 CIRCUITS FOR REGULATION IN DELTA CONNECTED WINDINGS

For the voltage regulation in delta connected windings the arrangements shown in Fig. 3.3-1 can be applied. This figure only shows winding arrangements with reversing change-over selector. For the other regulation principles (coarse/fine or linear regulation) the tap winding arrangements have to be replaced by the corresponding ones (compare Fig. 3.2-1).

The choice of the winding arrangement (3-pole line end, 2-pole + 1-pole line end or 3-pole mid-winding) depends on the highest voltage for equipment $U_m$ and parameters such as transformer impedance, BIL level and the OLTC design itself. In case of the 3-pole line-end arrangement either a three-phase OLTC or three single-

phase OLTCs must be used. Today three-phase OLTCs with a highest voltage for equipment up to 145 kV are available. The arrangement according to Fig 3.3-1c allows the use of one two-phase and one single-phase OLTC, which decreases the required number of OLTCs if an arrangement with a three-phase OLTC according to Fig. 3.3-1a is not feasable.

The mid-winding arrangement is advantegous with respect to the highest voltage for equipment of the OLTC, since it is reduced to approximately one half of the $U_m$ of the transformer. But it needs to be considered that during the applied voltage test the OLTC will be stressed on its insulating distance to ground with the full power frequency test voltage of the transformer. In such transformers the OLTCs must have the same $U_m$ at the phase to ground distance as the transformer.

However, when using a three-phase OLTC the voltage stresses during dielectric tests, especially during lightning impulse voltage tests, has on the phase to phase distances to be considered as well. As shown in Fig. 3.3-2, there is an OLTC position at which the complete regulating winding is outside the main voltage triangle and is free oscillating. For the linear regulation this position is the minus end-position (all turns out) and for regulation with a change-over selector (reversing or coarse/fine) this position is the mid-position with the change-over selector connected to the "plus"-contact.

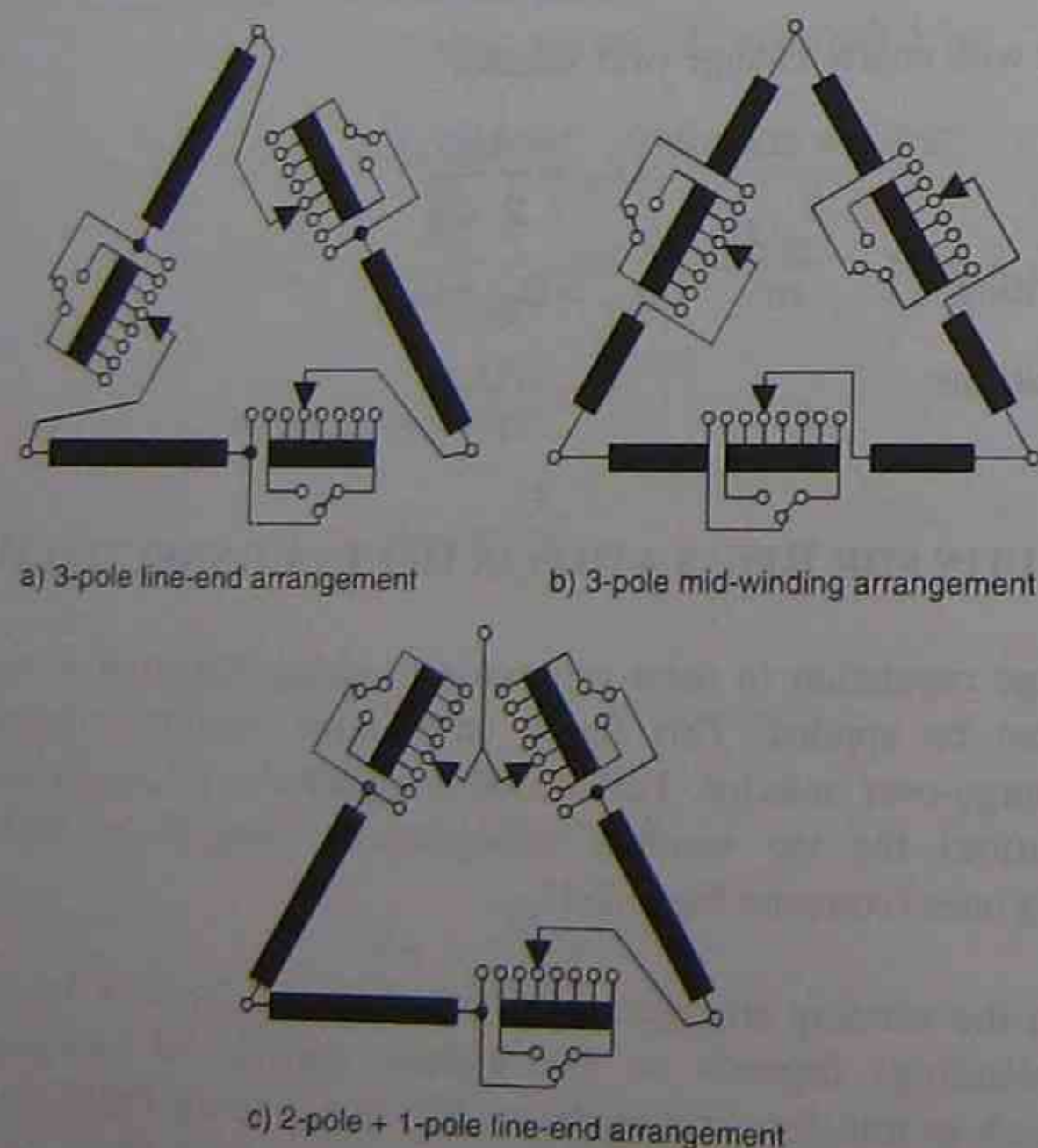From the phasor diagram shown in Fig. 3.3-2 it can be derived that the voltage



a) 3-pole line-end arrangement        b) 3-pole mid-winding arrangement

c) 2-pole + 1-pole line-end arrangement

**Fig. 3.3-1**: OLTCs in delta connected windings

between two free oscillating ends of the tap windings of different phases ($U_{res}$) is higher than the test voltage at the input terminals ($U_{test}$). The value of the voltage $U_{res}$ which arises during impuls testing depends on the transformer design. This fact has to be considered during transformer design and selection of the OLTC.

Nevertheless, if $U_{res}$ becomes too high with respect to the OLTC, there is the possibility, in case of a coarse/fine winding arrangement, to connect electrically the tap winding between the main winding and the coarse winding (shown alternatively in Fig. 3.3-2). Such a winding arrangement ensures that the tap winding remains always within the main voltage triangle. In case of the other connection schemes (linear and reversing) the voltage $U_{res}$ must be limited or a winding and OLTC arrangement according to Figs. 3.3-1b or 3.3-1c must be chosen.

The following data is important with respect to the dimensioning of the OLTC (regulation as shown in Fig. 3.3-1, symbols see end of paragraph 3.1):

$$U_{1min} \leq U_1 \leq U_{1max} \; ; \; S_N = const. \; ; \; induction = const.$$

$$U_R = U_{1max} - U_{1min} \text{ and } I_{max} = \frac{S_N}{3 \cdot U_{1min}} \text{ and } U_S = \frac{U_{TV}}{m} \quad (3.3\_1, 3.3\_2, 3.3\_3)$$

for linear regulation (constant turns per step):

$$U_{TV} = U_R \quad (3.3\_4)$$

for regulation with reversing change-over selector:

1 mid-position:
$$U_{TV} = \frac{U_R}{2} \cdot \frac{m}{m-1} \quad (3.3\_5)$$



linear

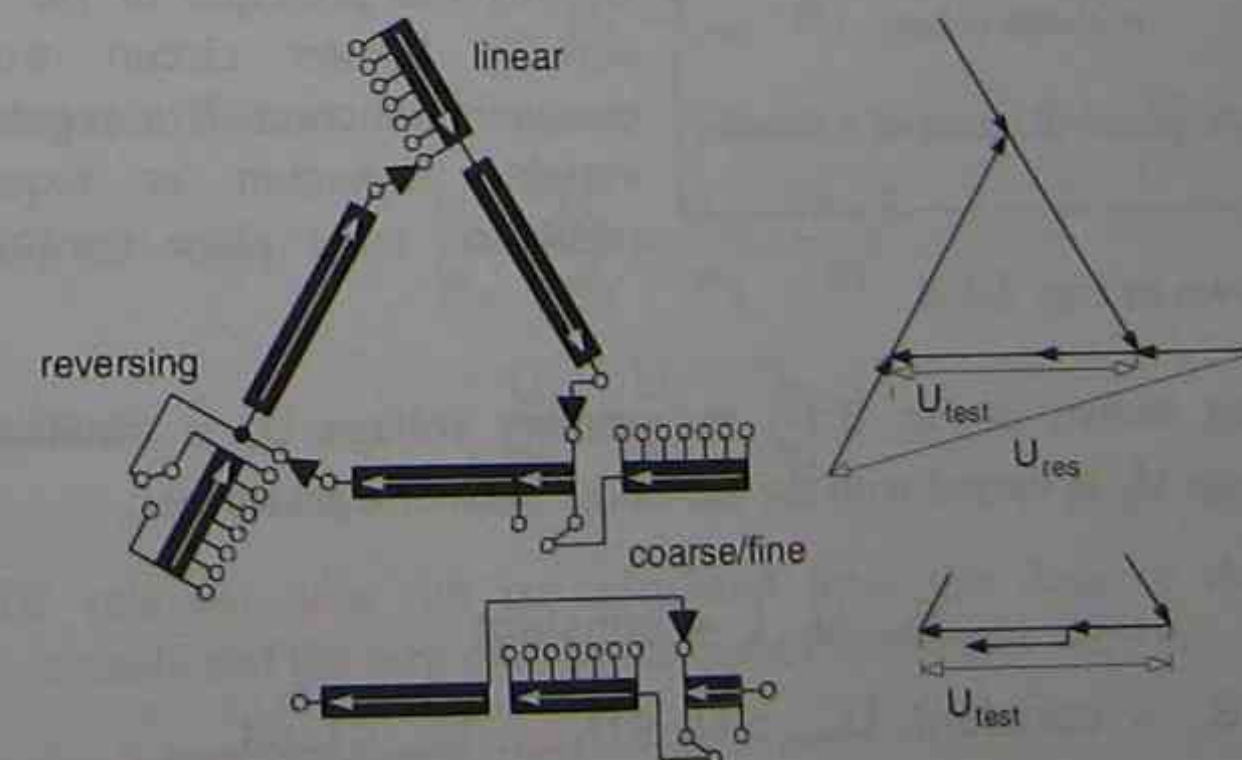reversing

$U_{test}$

$U_{res}$

coarse/fine

$U_{test}$

**Fig. 3.3-2:** Free oscillating tap windings in delta connected winding arrangements during dielectric tests   (the figure shows all three connection schemes in the delta connected windings)

$$U_{TV} = \frac{U_R}{2} \qquad (3.3\_6)$$

3 mid-positions:

for regulation with coarse change-over selector:

$$U_{TV} = \frac{U_R}{2} \qquad (3.3\_7)$$

$$U_{CV} = U_{TV} + U_S \qquad (3.3\_8)$$

1 mid-position:

$$U_{CV} = U_{TV} \qquad (3.3\_9)$$

3 mid-positions:

## 3.4 CIRCUITS FOR REGULATION IN BOOSTER TRANSFORMERS

Circuits with booster transformers are often used for industrial process transformers (through-currents of some kiloamps) adjusting the data of the intermediate circuit to accommodate OLTCs. Fig. 3.4-1 shows the principle mode of operation. Booster circuits can be applied to two winding transformers as well as to autotransformers.
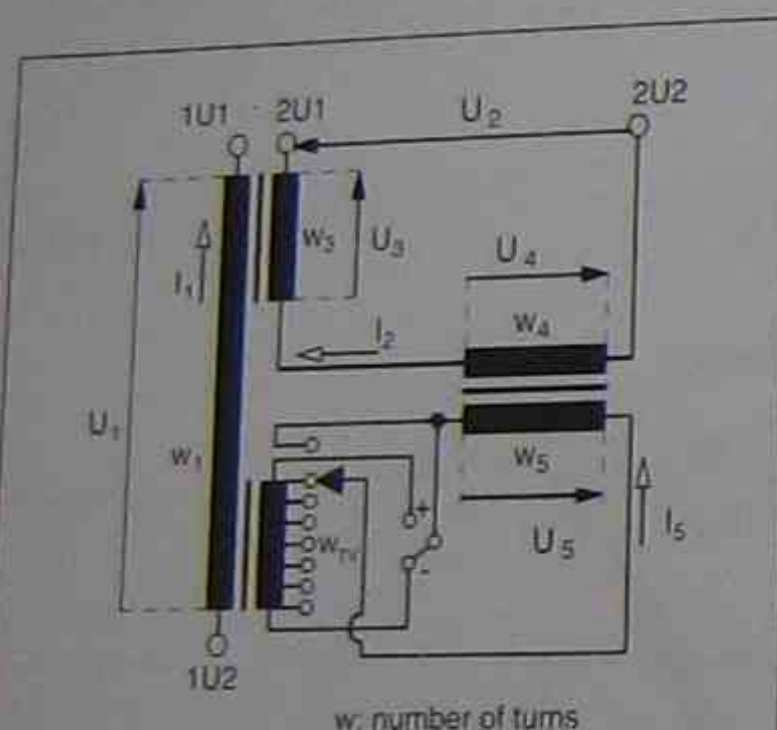


Fig. 3.4-1: Single-phase diagram of a booster circuit

w: number of turns

For the calculation of the data relevant for the OLTC (voltage across the tap winding $U_{TV}$, step voltage $U_S$ and max. through-current $I_{max}$) details of the primary and secondary circuits only are not sufficient. Also the details of the intermediate or booster circuit are needed (minimum data: the turn ratio of one booster of the circuit).

Usually the principle of the regulation with a booster circuit works with constant induction. If a regulation with variable induction is required, the regulation takes place on the primary winding as shown in Fig. 3.1-4.

With the circuit shown in Fig. 3.4-1 the primary voltage $U_1$ is constant and the secondary voltage $U_2$ is varied with the aid of the booster transformer:

primary: $\qquad S_N, U_1, I_1 = $ constant

secondary: $\qquad S_N = $ constant, $U_{2min} \leq U_2 \leq U_{2max}$, $I_{2min} \leq I_2 \leq I_{2max}$

With the definitions chosen in Fig. 3.4-1 follows:

$$U_{2min} = U_3 - U_4 \text{ and } U_{2max} = U_3 + U_4 \qquad (3.4\_1a, 3.4\_1b)$$

$$I_{2min} = \frac{S_N}{3 \cdot U_{2max}} \text{ and } I_{2max} = \frac{S_N}{3 \cdot U_{2min}} \qquad (3.4\_2a, 3.4\_2b)$$

In case of constant induction the voltage across the tap winding is independent of the position of the OLTC.

The current $I_5$ represents the through-current of the OLTC. $I_5$ reaches its maximum, when $I_2$ reaches its maximum (equilibrium of ampere-turns). The maximum of $I_2$ correlates (eq. 3.4_2b) with $U_{2min}$. This corresponds to the minus end-position of the OLTC as shown in Fig. 3.4-1.

The following basic equations are valid for the OLTC in the minus end-position.

**main transformer**

from the equilibrium of the ampere-turns follows:

1 mid-position: $\qquad I_1 \cdot w_1 = I_{max} \cdot w_{TV} \cdot \dfrac{m-1}{m} + I_{2max} \cdot w_3 \qquad (3.4\_3a)$

3 mid-positions: $\qquad I_1 \cdot w_1 = I_{max} \cdot w_{TV} + I_{2max} \cdot w_3 \qquad (3.4\_3b)$

from the turn ratio follows:

$$\frac{U_1}{w_1} = \frac{U_{TV}}{w_{TV}} = \frac{U_3}{w_3} \qquad (3.4\_4)$$

**booster transformer**

from the equilibrium of the ampere-turns follows:

$$I_{max} \cdot w_5 = I_{2max} \cdot w_4 \qquad (3.4\_5)$$

from the turn ratio follows:

1 mid-position: $\qquad \dfrac{U_4}{w_4} = \dfrac{U_5}{w_5} = \dfrac{U_{TV}}{w_5} \cdot \dfrac{m-1}{m} \qquad (3.4\_6a)$

3 mid-positions: $\qquad \dfrac{U_4}{w_4} = \dfrac{U_5}{w_5} = \dfrac{U_{TV}}{w_5} \qquad (3.4\_6b)$

The OLTC relevant data can be calculated from the data of the primary and secondary circuits and the turn ratio of the main transformer $w_1 / w_{TV}$.

With equation 3.4_4 follows:

$$U_{TV} = U_1 \cdot \frac{w_{TV}}{w_1} \qquad (3.4\_7)$$

and the step voltage can be calculated to:

$$U_S = \frac{U_{TV}}{m} \qquad (3.4\_8)$$

The maximum through-current can be determined with equations 3.4_3a resp. 3.4_3b using 3.4_4, 3.4_1a and 3.4_1b to:

1 mid-position:
$$I_{max} = \left(I_1 - I_{2max} \cdot \frac{U_{2max} + U_{2min}}{2 \cdot U_1}\right) \cdot \frac{w_1}{w_{TV}} \cdot \frac{m}{m-1} \qquad (3.4\_9a)$$

3 mid-positions:
$$I_{max} = \left(I_1 - I_{2max} \cdot \frac{U_{2max} + U_{2min}}{2 \cdot U_1}\right) \cdot \frac{w_1}{w_{TV}} \qquad (3.4\_9b)$$

The calculation of the OLTC relevant data is also possible with the data of the primary and secondary circuits and the turn ratio of the booster transformer $w_4 / w_5$.

From equation 3.4_6a resp. 6b follows using 3.4_1a and 3.4_1b:

1 mid-position:
$$U_{TV} = \frac{U_{2max} - U_{2min}}{2} \cdot \frac{w_5}{w_4} \cdot \frac{m}{m-1} \qquad (3.4\_10a)$$

3 mid-positions:
$$U_{TV} = \frac{U_{2max} - U_{2min}}{2} \cdot \frac{w_5}{w_4} \qquad (3.4\_10b)$$

and the step voltage can be calculated with eq. 3.4_8 as $U_S = \dfrac{U_{TV}}{m}$

The maximum through-current becomes with eq. 3.4_5:

$$I_{max} = I_{2max} \cdot \frac{w_4}{w_5} \qquad (3.4\_11)$$

A typical application for industrial or process transformers is the regulation of the secondary voltage to keep the secondary current constant (furnace transformers). The above equations are also valid in this case, but with $S_N$ = variable and $I_{2max} = I_2 = $ cons tan t.

## 3.5 CIRCUITS FOR REGULATION IN AUTOTRANSFORMERS

Single autotransformers (one three-phase unit or three single-phase units) working as interconnection transformers between two high voltage networks must be solidly grounded. If more autotransformers are connected in parallel to the high voltage system (e.g. connented to one busbar) and feeding seperate mean voltage (autopoint) systems, it may be advantageous not to ground solidly all starpoints of the
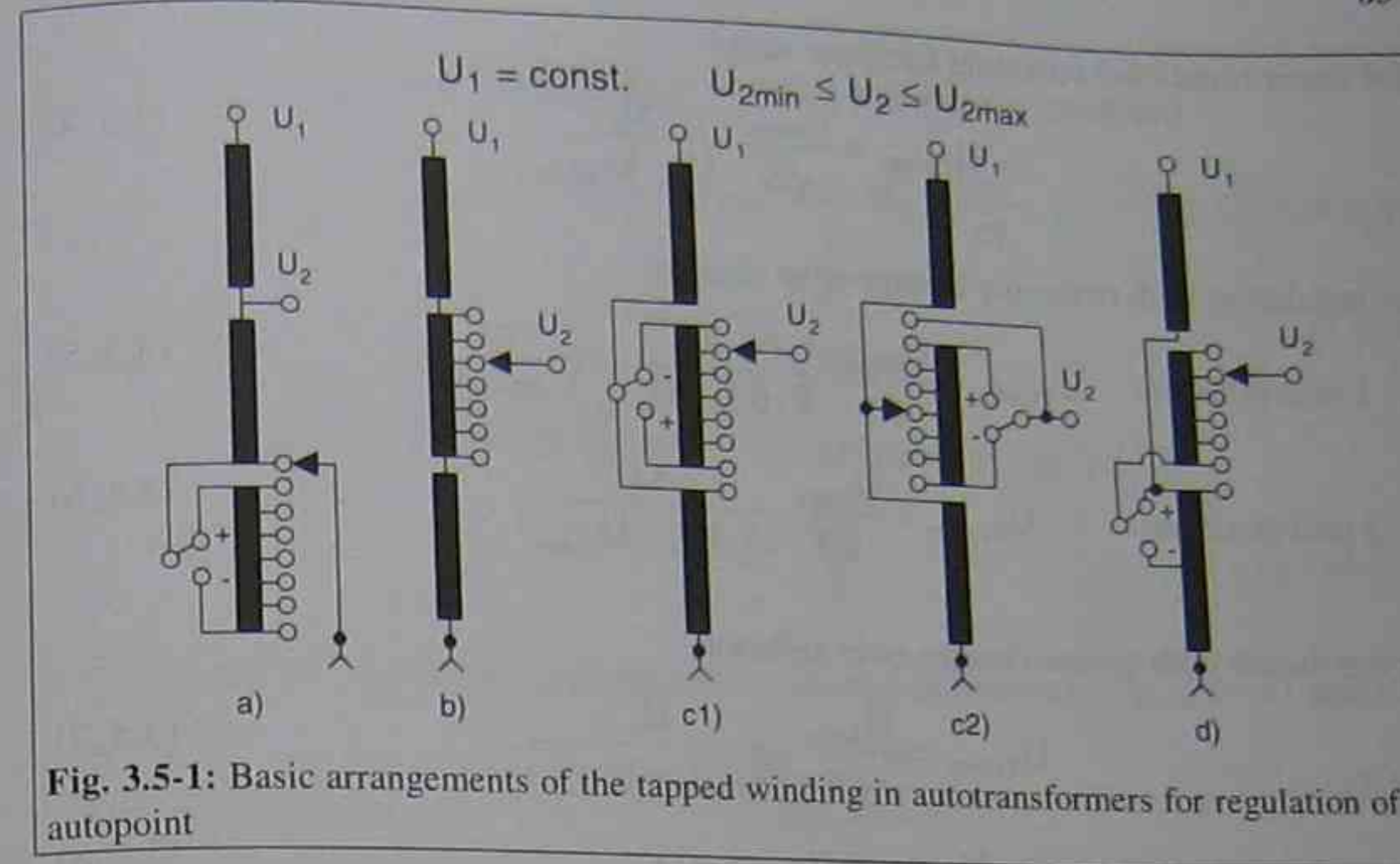
Fig. 3.5-1: Basic arrangements of the tapped winding in autotransformers for regulation of the autopoint

autotransformers with regard to limitation of the ground-fault current [Schlosser 1961, Schlosser 1965].

Regulating autotransformers can principally be classified into units with direct regulation using a regulating winding on the autotransformer and units with indirect regulation using a series regulating transformer. Different possibilities for the direct regulation are given in Figs. 3.5-1 and 3.5-2 and for the indirect regulation in Fig. 3.5-3. Principally, for the evaluation of the OLTC and the type of regulation, it is necessary to consider if the high voltage is constant and the mean voltage (autopoint) subjected to variations or vice versa [Heller 1973].

The winding arrangements according to Figs. 3.5-1 a to d serve for regulation of the autopoint. The high voltage stays constant. The advantage of the direct regulation in the neutral point of the autotransformer (Fig. 3.5-1a) is that an OLTC with a lower highest voltage for equipment $U_m$ can be applied, irrespectively of the rated voltage of the high and mean voltage windings. Nevertheless, considerable variations of the magnetic induction and tertiary voltage are associated with this method of regulation.

The following data is important with respect to the dimensioning of the OLTC (regulation as shown in Fig. 3.5-1a, symbols see end of paragraph 3.1):

$$U_{2min} \le U_2 \le U_{2max} \; ; \; S_N = \text{const.} \; ; \; \text{induction} = \text{variable}$$

$$U_{Rmax} = U_{2max} - U_{2min} \text{ and } U_{Smax} = \frac{U_{TVmax}}{m} \qquad (3.5\_1, \, 3.5\_2)$$

$$I_{max} = \frac{S_N}{\sqrt{3}} \cdot \left(\frac{1}{U_{2min}} - \frac{1}{U_1}\right) \qquad (3.5\_3)$$

for linear regulation (constant turns per step):

$$U_{TVmax} = \frac{U_{Rmax}}{\sqrt{3}} \cdot \frac{U_1}{U_1 - U_{2max}} \qquad (3.5\_4)$$

for regulation with reversing change-over selector:

1 mid-position:
$$U_{TVmax} = \frac{U_{Rmax}}{\sqrt{3}} \cdot \frac{U_1}{2 \cdot (U_1 - U_{2max})} \cdot \frac{m}{m-1} \qquad (3.5\_5)$$

3 mid-positions:
$$U_{TVmax} = \frac{U_{Rmax}}{\sqrt{3}} \cdot \frac{U_1}{2 \cdot (U_1 - U_{2max})} \qquad (3.5\_6)$$

for regulation with coarse change-over selector:

$$U_{TVmax} = \frac{U_{Rmax}}{\sqrt{3}} \cdot \frac{U_1}{2 \cdot (U_1 - U_{2max})} \qquad (3.5\_7)$$

1 mid-position:
$$U_{CVmax} = U_{TVmax} + U_{Smax} \qquad (3.5\_8)$$

3 mid-positions:
$$U_{CVmax} = U_{TVmax} \qquad (3.5\_9)$$

The other variations of the autopoint regulation operate with constant induction. Fig. 3.5-1b shows a linear regulation and Fig. 3.5-1d a regulation with coarse and fine tap winding. The arrangements in Figs. 3.5-1c1 and c2 are equivalent with respect to the transformer design and the regulating range. In arrangement c2 the common terminal (take-off terminal) of the tap selector, which is directly connected to the diverter switch, has a fixed potential during operation, whereas the potential of the common terminal in arrangement c1 is variable. The highest potential of the diverter switch determines the insulation to ground of the OLTC. However, the insulation to ground is dimensioned with respect to the rated withstand voltages determined by the international standards *[IEC Publ. 60214 1989]* and corresponds to the highest voltage for equipment $U_m$.

The advantage of arrangement c2 shall be demonstrated with an example. For an autotransformer e.g. 700 MVA, 400 kV / 240 kV ± 10 · 1.5 %, the maximum voltage at the diverter switch becomes 240 kV + 15 % = 276 kV when using an arrangement acc. to c1. This requires an OLTC with $U_m$ = 300 kV, because the next lower $U_m$ = 245 kV is not sufficient. When using an arrangement acc. to c2 the maximum voltage at the diverter switch becomes 240 kV = constant. In this case an OLTC with $U_m$ = 245 kV can be chosen.

The withstand voltages of the tap selector (internal insulation) are the same in both arrangements and do not depend on $U_m$.

The calculation of the through-current and the step voltage can be accomplished with the equations listed below:

$$U_{2min} \leq U_2 \leq U_{2max} \; ; \; S_N = const. \; ; \; induction = constant$$

$$U_R = U_{2max} - U_{2min} \quad and \quad U_S = \frac{U_{TV}}{m} \qquad (3.5\_10, \; 3.5\_11)$$

$$I_{max} = \frac{S_N}{\sqrt{3} \cdot U_{2min}} \qquad (3.5\_12)$$

for linear regulation (constant turns per step) as shown in Fig. 3.5-1b:

$$U_{TV} = \frac{U_R}{\sqrt{3}} \qquad (3.5\_13)$$

for regulation with reversing change-over selector as shown in Fig. 3.5-1c1 and c2:

1 mid-position:
$$U_{TV} = \frac{U_R}{2 \cdot \sqrt{3}} \cdot \frac{m}{m-1} \qquad (3.5\_14)$$

3 mid-positions:
$$U_{TV} = \frac{U_R}{2 \cdot \sqrt{3}} \qquad (3.5\_15)$$

for regulation with coarse change-over selector as shown in Fig. 3.5-1d:

$$U_{TV} = \frac{U_R}{2 \cdot \sqrt{3}} \qquad (3.5\_16)$$

1 mid-position:
$$U_{CV} = U_{TV} + U_S \qquad (3.5\_17)$$

3 mid-positions:
$$U_{CV} = U_{TV} \qquad (3.5\_18)$$

The winding arrangements shown in Figs. 3.5-2a to d serve for regulation of the HV line end of the autotransformer while the autopoint is kept at a constant voltage level. The difference between c1 and c2 is the same as mentioned before for c1 and c2. In this case the arrangement acc. to c1 is advantegeous with respect to $U_m$. For an autotransformer e.g. 700 MVA, 400 kV ± 10 · 1.5 % / 240 kV, the maximum voltage at the high voltage terminals is 460 kV. When using the arrangement c2 the maximum voltage at the diverter switch is 460 kV - (400 kV - 240 kV) = 300 kV, maximum voltage at the diverter switch is 460 kV - (400 kV - 240 kV) = 300 kV, whereas with arrangement c1 the voltage at the diverter switch is constant 240 kV. Alternatively, the tap winding can be located at the line end of the HV side, but then the OLTC must be designed according to the insulation level of the HV. For this reason this method is rarely being used.

For the regulation with variable induction in the starpoint as shown in Fig. 3.5-2a, the relevant data for the OLTCs can be calculated with the following equations:
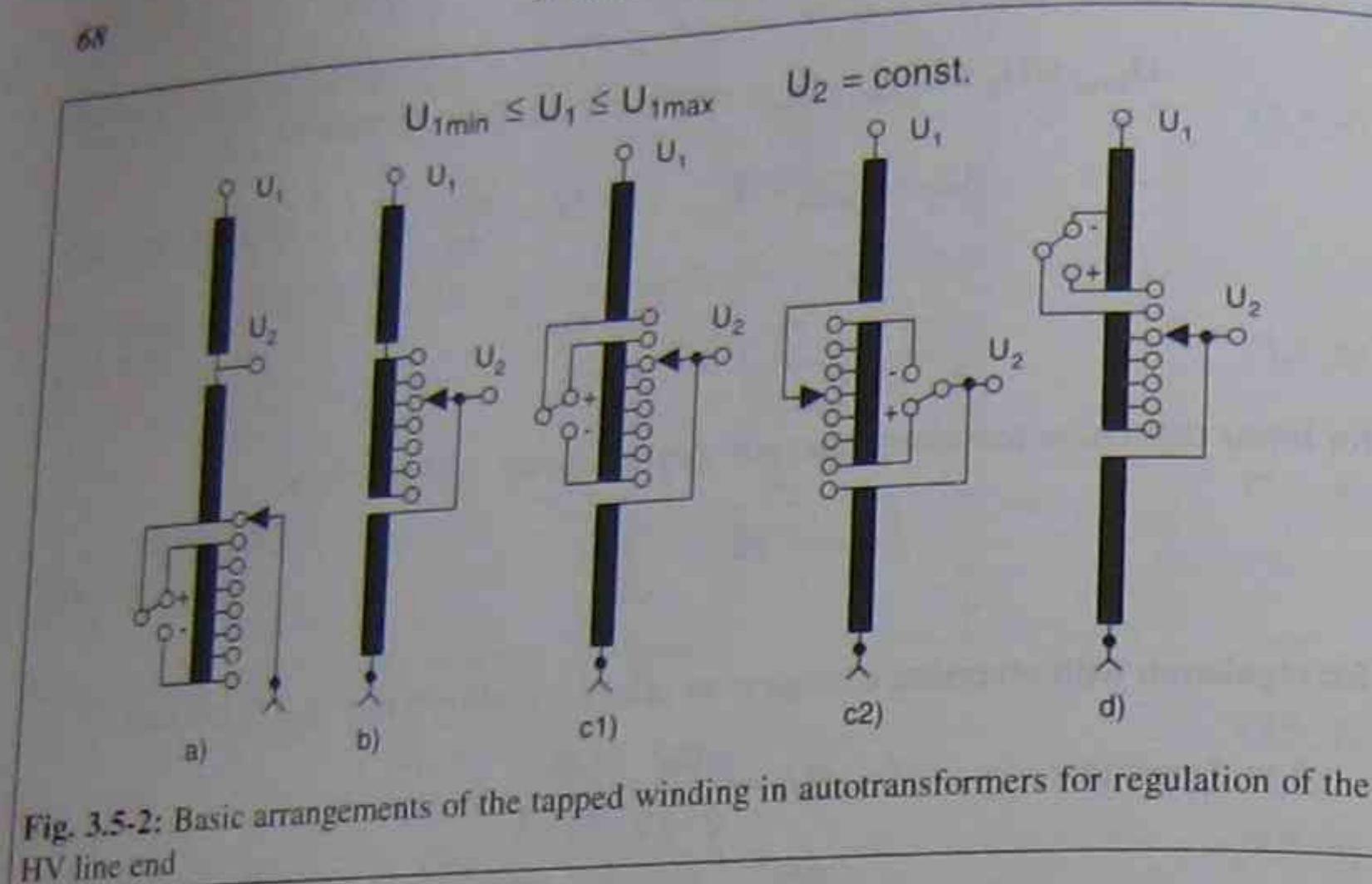
$$U_{1min} \leq U_1 \leq U_{1max} \qquad U_2 = const.$$

**Fig. 3.5-2:** Basic arrangements of the tapped winding in autotransformers for regulation of the HV line end

$$U_{1min} \leq U_1 \leq U_{1max} \; ; \; S_N = const. \; ; \; induction = variable$$

$$U_{Rmax} = U_{1max} - U_{1min} \quad and \quad U_{Smax} = \frac{U_{TVmax}}{m} \qquad (3.5\_19, \; 3.5\_20)$$

$$I_{max} = \frac{S_N}{\sqrt{3}} \cdot \left( \frac{1}{U_2} - \frac{1}{U_{1max}} \right) \qquad (3.5\_21)$$

for linear regulation (constant turns per step):

$$U_{TVmax} = \frac{U_{Rmax}}{\sqrt{3}} \cdot \frac{U_2}{U_{1min} - U_2} \qquad (3.5\_22)$$

for regulation with reversing change-over selector:

1 mid-position:
$$U_{TVmax} = \frac{U_{Rmax}}{\sqrt{3}} \cdot \frac{U_2}{2 \cdot (U_{1min} - U_2)} \cdot \frac{m}{m-1} \qquad (3.5\_23)$$

3 mid-positions:
$$U_{TVmax} = \frac{U_{Rmax}}{\sqrt{3}} \cdot \frac{U_2}{2 \cdot (U_{1min} - U_2)} \qquad (3.5\_24)$$

for regulation with coarse change-over selector:

$$U_{TVmax} = \frac{U_{Rmax}}{\sqrt{3}} \cdot \frac{U_2}{2 \cdot (U_{1min} - U_2)} \qquad (3.5\_25)$$

1 mid-position:
$$U_{CVmax} = U_{TVmax} + U_{Smax} \qquad (3.5\_26)$$

3 mid-positions:
$$U_{CVmax} = U_{TVmax} \qquad (3.5\_27)$$

For the regulation shown in Figs. 3.5-2b to d the relevant OLTC data can be calculated as follows:

$$U_{1min} \leq U_1 \leq U_{1max} \; ; \; S_N = const. \; ; \; induction = constant$$

$$U_R = U_{1max} - U_{1min} \quad and \quad U_S = \frac{U_{TV}}{m} \qquad (3.5\_28, \; 3.5\_29)$$

$$I_{max} = \frac{S_N}{\sqrt{3} \cdot U_{1min}} \qquad (3.5\_30)$$

The following equations are identical as for the regulation of the autopoint. However, to facilitate the calculation they are listed here again:

for linear regulation (constant turns per step) as shown in Fig. 3.5-2b:

as 3.5_13
$$U_{TV} = \frac{U_R}{\sqrt{3}}$$

for regulation with reversing change-over selector as shown in Fig. 3.5-2c1 and c2:

1 mid-position: as 3.5_14
$$U_{TV} = \frac{U_R}{2 \cdot \sqrt{3}} \cdot \frac{m}{m-1}$$

3 mid-positions: as 3.5_15
$$U_{TV} = \frac{U_R}{2 \cdot \sqrt{3}}$$

for regulation with coarse change-over selector as shown in Fig. 3.5-2d:

as 3.5_16
$$U_{TV} = \frac{U_R}{2 \cdot \sqrt{3}}$$

1 mid-position: as 3.5_17
$$U_{CV} = U_{TV} + U_S$$

3 mid-positions: as 3.5_18
$$U_{CV} = U_{TV}$$

Figs. 3.5-3 show two typical arrangements for the indirect regulation of an autotransformer. The mode of operation is described in paragraph 3.4. Both arrangements can be applied in cases where transport limitations restrict the incorporation of the OLTC in the main autotransformer. Additionally, these arrangements have the advantage of providing the possibility to carry out a phase shift if the primary of the booster transformer is connected to one of the other two phases of the autotransformer. The arrangement shown in Fig. 3.5-3b can be used on autotransformers where the mean voltage (autopoint) is higher than the highest $U_m$ available for OLTCs.

With the above mentioned features autotransformers with booster circuits are also built for regulation of the high voltage $U_1$.
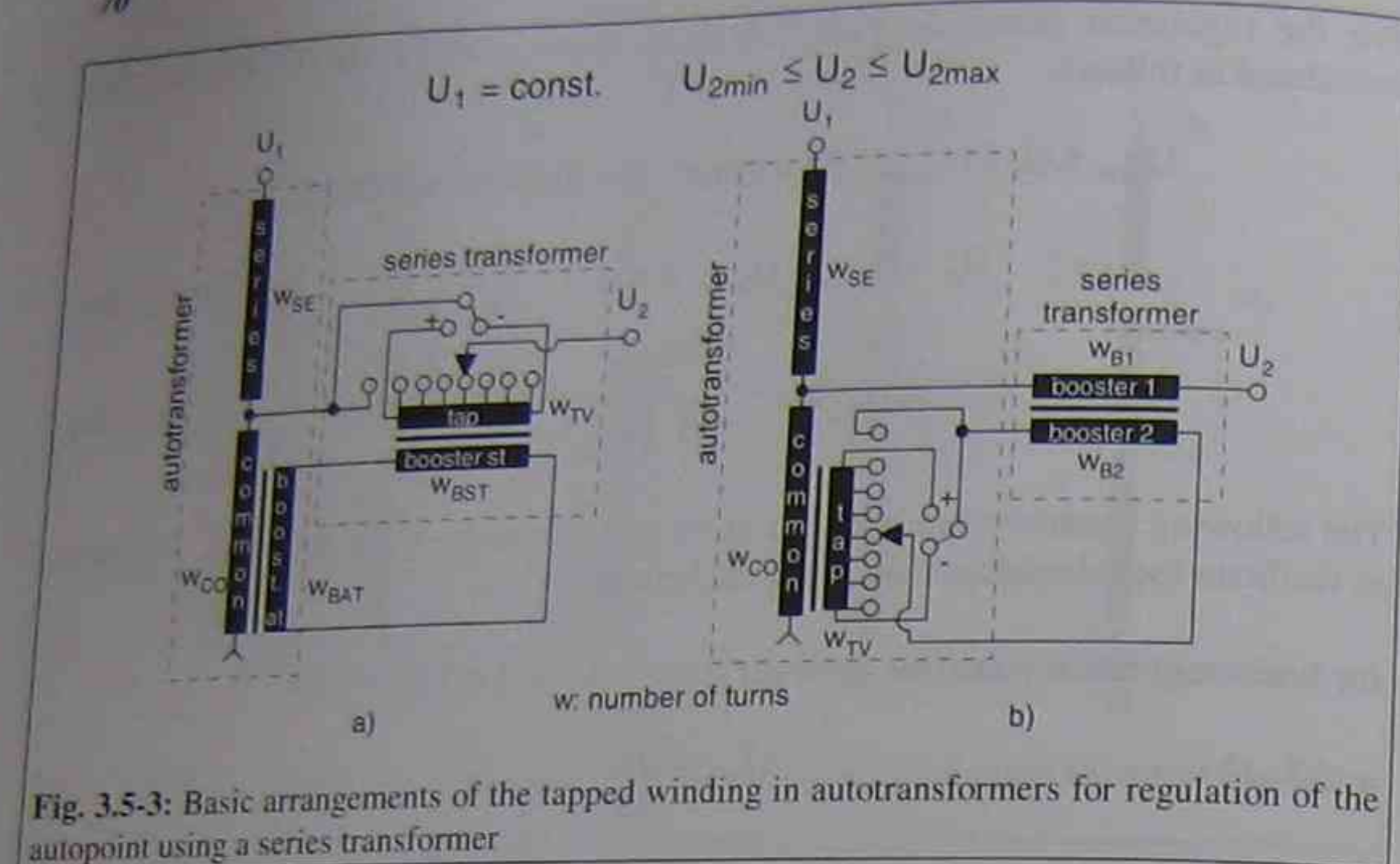
**Fig. 3.5-3:** Basic arrangements of the tapped winding in autotransformers for regulation of the autopoint using a series transformer

It is impossible to decide universaly which of the above mentioned regulation methods is more advantageous or to define limits for both. Each of them offers a row of advantages. The direct regulation is more economical, the indirect regulation is able to carry out also a longitudinal and transversal regulation (phase shifting) and is more suitable for transportation when the regulating transformer is located in a seperate unit.

# 4 SELECTION OF OLTCS

The selection of the adequate OLTC for a certain application or transformer must be made very carefully, although the OLTC represents only a small part of the total cost of the equipment in which it is used. However, the experience of the passed 70 years shows that the OLTC is an important factor with respect to the reliability of the entire equipment. Consequently, account should be taken of the available standard types of OLTCs which should be chosen preferentially.

IEC Publication 60542 *[IEC Publ. 60542 1976]* gives a guideline for the OLTC selection and points out most of the features to be considered during the specification of the OLTC. Additionally, the publication 60542 gives a list of all the information required which should be provided by the transformer manufacturer together with the inquiry or order, to enable the correct OLTC selection. However, in case of special applications such as phase shifting transformers or HVDC rectifier transformers this information is not sufficient (see chapter 5).

The following items, that need to be considered during the OLTC selection, are taken from the IEC Publication 60542 and some additional comments are added:

**Insulation level**

All voltages occuring on all tapping positions of the transformer must be verified against the permissible voltage stresses guaranteed by the OLTC manufacturer. In accordance with IEC Publication 60214 these voltages are:

1. Normal power-frequency operating voltages appearing on the OLTC in service.
2. Power-frequency voltages appearing on the OLTC during transformer tests.
3. Impulse voltages appearing on the OLTC during transformer tests or in service.

Additionally, it must be considered that with some winding arrangements (e.g. neutral-end regulation in autotransformers, line-end regulation in delta connected windings, regulation with booster circuits) abnormal high voltages can appear. These voltages can be affected considerably by the choice of the type of regulation (linear, coarse/fine or reversing tapping arrangements). Variable induction (variable magnetic flux) in the transformer core can also influence the voltages appearing on the OLTC.

Very fast transient overvoltages (VFTO) arise in networks during faults and switching operations. Sources of such VFTOs are high voltage air blast or $SF_6$-breakers with reignition rates below 10 kHz, medium voltage vacuum breakers with reignition rates up to 500 kHz and gas insulated substations (GIS). The most important factors that originate oscillatory waves are the switching of reactor-

loaded transformers, the interruption of inrush currents, close distance faults (2 and 3 phase) and the energizing of transformer terminated lines.

The characteristics of VFTOs originated in GIS are different from those originated in conventioanl substations. Collapse times of 5 to 10 ns are usual in case of conductor-earth breakdowns or disconnector reignitions. The frequencies of the waves lie in the MHz-range due to the short dimensions and the small damping in GIS.

These overvoltages stress the transformer as well as the OLTC. Therefore, the user of the transformer should know the problems in the system and state the requirements clearly in case of critical network conditions [e.g. Müller 1993, Preininger 1993, Cornick et al. 1992, Müller 1992, Stein 1985, WG 12.07 1984, Pretorius, Goosen 1984, D'Heure, Even 1984, Müller, Stein 1983].

Usually when networks or systems are equipped with surge arrester, they are installed phase to ground. When using three-phase OLTCs in line-end applications the voltage appearing at the phase to phase distance of the OLTC may have twice the magnitude of the residual voltage of the surge arrester. This occurs in case of three-phase switching overvoltages when they are in phase opposition

A detailed examination of the insulation distances at the OLTC is given in paragraph 4.1.

### Rated through-current

The maximum rated through-current of the OLTC ($I_{um}$) should not be less than the highest possible current which flows through the tap winding of the transformer and the OLTC (rated through-current $I_{max}$ or $I_u$). Examples for the calculation of the rated through-current depending on the regulation circuit are given in chapter 3.

In paragraph 4.2 remarks are given in regards to the rated through-current and the power factor.

### Overload current

In transformers and OLTCs subjected to overload conditions in accordance with IEC Publication 60354 [IEC Publ. 60354 1991], the OLTC requirements in accordance with IEC Publication 60542 are met , when the maximum rated through-current of the OLTC is at least 1.2 times the rated through-current or when the OLTC does not exceed the temperature rise limits given in IEC Publication 60214 when the contacts carry 1.2 times the maximum rated through-current. The temperature rise of the contacts above the surrounding medium may

not exceed 20 K in the steady state for oil environment (35 to 65 K in air environment dependent on the contact material).

The transition resistors meet the overload requirements if the temperature rise above the surrounding medium does not exceed 350 K for oil environment (400 K for air environment) when carrying 1.5 times the maximum rated through-current. The number of tap-changes for each occasional overload period should be limited to the number of operations required to move from one end of the tapping range to the other. This corresponds to the testing conditions for the transition resistors given in IEC Publication 60214. For further details see paragraph 4.2.

### Short-circuit current

The capability of the OLTC to withstand a certain short-circuit current as specified in IEC Publication 60214 should be not less than the short-circuit current resulting from the overcurrent of the associated transformer as given in IEC Publication 60076-5 [IEC Publ. 60076-5 1976].

Particular care should be taken in case of low-impedance and booster transformers. In some instances, the short-circuit current magnitude can dictate the OLTC selection.

In general the OLTC is only able to carry the short-circuit current but cannot complete a tap-change operation under short-circuit conditions. According to IEC Publication 60214 the r.m.s value of the short-circuit current (2 seconds) which can be applied to the OLTC is 10 to 20 times the maximum rated through-current depending on the value of the maximum rated through-current. The initial peak value of the short-circuit current is 2.5 times the r.m.s. value.

### Breaking capacity

The rated through-current (highest tapping current) and the highest voltage per step of the transformer should be within the values of the maximum rated through-current and the relevant step voltage of the OLTC. In many cases the maximum rated through-current can only be applied with a step voltage (relevant step voltage) smaller than the maximum step voltage.

In general the transition impedance is adjusted to the relevant through-current and the relevant step voltage of the transformer so that the switched currents and recovery voltages in the OLTC do not exceed those covered by the type test. For the determination of the transition impedance, the contact wear and the temperature rise of the transition resistors are also considered.

In certain applications, such as furnace transformers, the OLTC may need to be operated during periods of momentary overloads of two to three times the

transformer maximum continous rating. The OLTC must be chosen with respect to these requirements.

In case of transformers with regulation through the variation of the magnetic induction, it has to be considered that this will affect the step voltage, and consequently the breaking capacity (examples for calculation of the maximum step voltage in case of variable induction are given in chapter 3).

The consequences of adjusted transition impedances with respect to the ratings of the OLTC will be shown in paragraph 4.2.

**Number of tapping positions**

The selection of the service tapping positions should prefarably be made within the range standardized by the OLTC manufacturers (compare paragraph 3.1).

With increasing tapping ranges the voltage stresses at the tap winding during testing or service conditions may increase also. Especially in case of furnace or rectifier transformers feeding electrolytic plants, wide tapping ranges are often necessary. When the OLTC is in the winding with constant voltage, the voltage stress occuring at the tap winding when operating or testing at the minimum winding positions has to be considered as well and precautions have to be taken.

**Discharge problems with change-over selectors**

The operation of the change-over selector takes place in the mid-position of the OLTC. During its operation, the load current does not flow through the tap winding. Therefore the tap winding is temporarily disconnected from the main winding and the potential of the winding floats. In such cases, discharges between the opening and closing contacts occur during the operation of the change-over selector. In order to avoid difficulties regarding the dielectric stress and the possible formation of gases, special precautions may be necessary.

A detailed describtion of this phenomenon, the calculation of the stresses and the countermeasures are given in paragraph 4.3.

**Mechanical life**

The mechanical duty may need consideration if the expected number of operations per year exceeds 50,000. For example, this can occur in transformers for use in rolling mills, electrolytic plants or furnace applications. The mechanical life time of modern OLTCs usually is in the range of 1 to 1.5 million operations or even higher.

**Motor-drive mechanism**

If the motor-drive mechanism is purchased from a manufacturer other than the OLTC manufacturer, then it is the purchaser's responsibility to ensure that the motor-drive mechanism is suitable for all the necessary duties.

**Pressure and vacuum tests**

Modern OLTCs are able to withstand the vacuum procedures during the usual drying process of the transformer (vacuum and vapour phase). Pressure tests are also carried out at the OLTC. If special vacuum or pressure tests should be performed on the OLTC and the associated transformer, all the relevant information should be provided to the OLTC manufacturer.

**Low-temperature conditions**

Should the OLTCs be operated with an oil temperature below -25°C, the OLTC manufacturer needs to be consulted and the quality of the transformer oil needs to be taken into consideration. Important factors are the kinematic viscosity, the pour point and the arc extinguishing capability of the oil at the lowest temperature required *[IEC Publ. 60296 1982]*.

**Continous operation**

If the OLTC is required to make several operations after another, the temperature conditions may need to be verified.

## 4.1 INSULATION LEVEL

### 4.1.1 INTERNAL AND EXTERNAL INSULATION

The voltage stress on the insulation distances respevtively materials of the OLTC is determined by the transformer data such as nominal system voltage, regulating range, regulating mode (linear, coarse/fine, reversing), type of winding (e.g. disk winding, cylindrical winding, coil winding, layer winding) and the winding arrangement.

The insulation of an OLTC is divided into internal and external tap-changer insulation. The withstand voltages of the external insulation are standardized by national and international standards and correspond to the highest voltage for equipment $U_m$. In case of single-pole or three-phase star point OLTCs the external insulation represents the insulation to ground. When three-phase OLTCs are used in delta connected windings, the external insulation represents the insulation to ground and between phases, both determined by $U_m$.
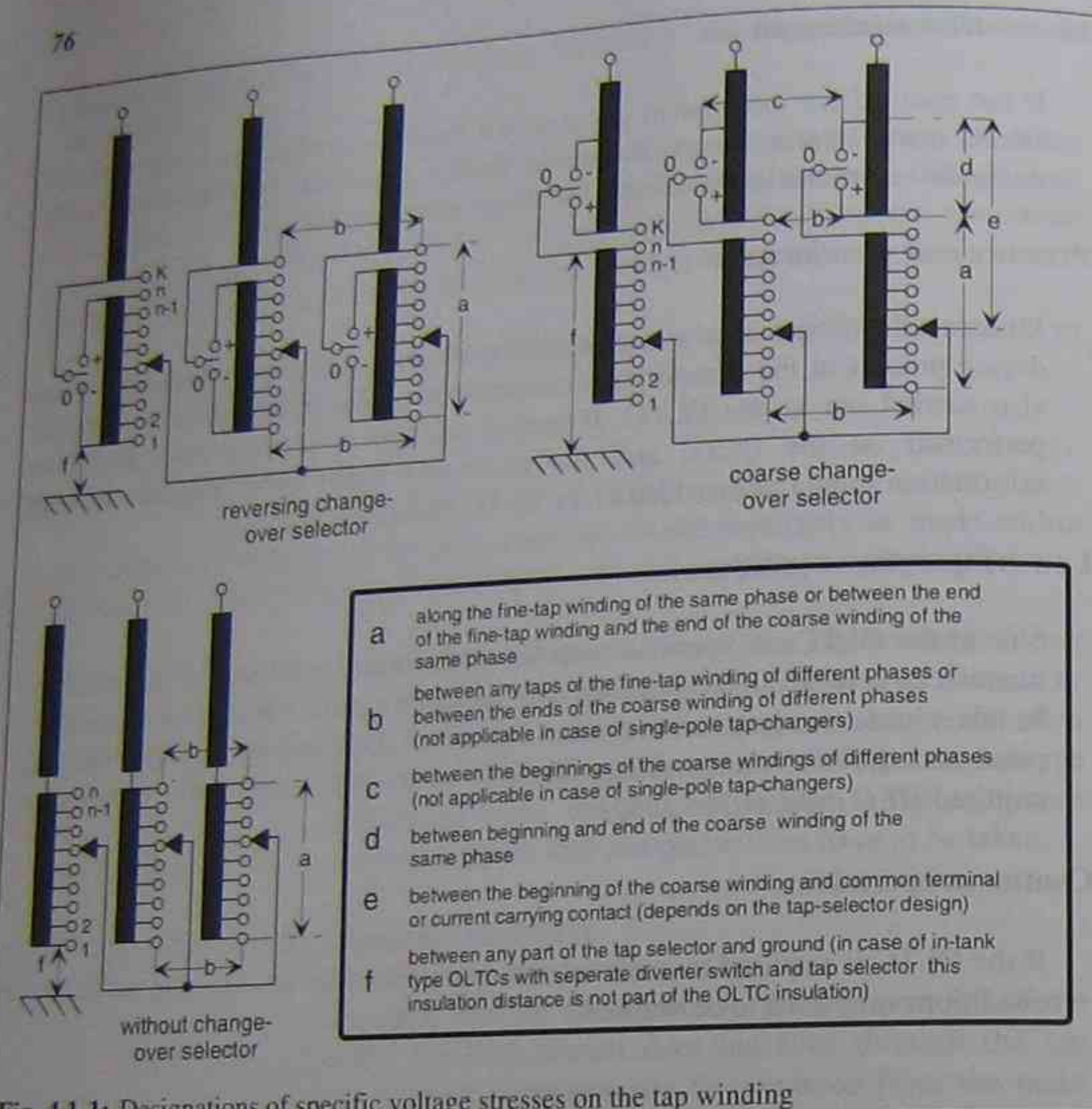
Along/legend box inside figure:

a — along the fine-tap winding of the same phase or between the end of the fine-tap winding and the end of the coarse winding of the same phase

b — between any taps of the fine-tap winding of different phases or between the ends of the coarse winding of different phases (not applicable in case of single-pole tap-changers)

c — between the beginnings of the coarse windings of different phases (not applicable in case of single-pole tap-changers)

d — between beginning and end of the coarse winding of the same phase

e — between the beginning of the coarse winding and common terminal or current carrying contact (depends on the tap-selector design)

f — between any part of the tap selector and ground (in case of in-tank type OLTCs with seperate diverter switch and tap selector this insulation distance is not part of the OLTC insulation)

reversing change-over selector

coarse change-over selector

without change-over selector

**Fig. 4.1-1:** Designations of specific voltage stresses on the tap winding

With respect to the internal tap-changer insulation, a standardization does not exist. However, it is determined by rated withstand voltages that are based on the experiences of the stresses appearing during transformer testing and corresponds to the grading required in practice. The voltage stresses which occur on a three-phase regulating winding can be described by 6 values. Since the OLTC manufacturers use different designations for these values characterizing the tap-selector, the designations shall be defined here as shown in Figure 4.1-1.

These values are often called "insulation distances". This however is misleading since these values do not represent physical distances but the withstand voltage of the relevant part or the internal OLTC insulation, which is stressed by the difference in potential caused by the tap winding. These difference in potential of the tap winding occurs at several insulation distances at the OLTC through the connection leads between tap winding and OLTC. Every "insulation distance" consists of several physical insulation distances which are connected in parallel at the OLTC. With this the withstand voltages defined by the OLTC manufacturers represent the withstand voltage of the relevant poorest distance.

The stress on the internal insulation depends on the OLTC operating position during the transformer testing, and on the transformer design, especially in case of the impulse test. Due to the multitude of transformer designs a classification cannot be made between impulse level of the transformer and the required withstand voltages of the tap selector. The OLTC manufacturers have designed different tap selector sizes which correspond to certain withstand voltages within one phase or between the phases.

In case of in-tank type OLTCs with seperate diverter switch and tap selector, the internal and external OLTC insulation levels can be chosen independently from each other according to the requirements.

The stresses have to be distinguished between stresses occuring during service operation and stresses occuring during transformer testing. Usually, the stresses occuring during service operation should be covered by the standards valid for the equipment. But the tests and the procedure of testing transformers are under discussion worldwide and different users prefer different testing methods.

To meet these different demands, the IEC Publication 60076-3 *[IEC Publ. 60076-3 1980]* offers different combinations of the following tests depending on, e.g., the system voltage and the procedure of testing (method 1 and 2):

- applied power frequency voltage test
- induced power frequency overvoltage test (short duration)
- induced power frequency overvoltage test with partial discharge measurement
- full-wave lightning impulse voltage withstand test for line terminals
- chopped-wave lightning impulse voltage withstand test for line terminals
- full-wave lightning impulse voltage withstand test for the neutral terminal
- switching impulse voltage withstand test for line terminals.

These tests cause different voltage stresses on the insulation of the transformer and the OLTC. Under the lightning impulse test the dielectric stresses are distributed differently depending on the OLTC position and the general design of the transformer. Therefore, if the position of the OLTC during transformer impulse testing is not specified by the customer, usually the two extreme tappings and the principal tapping should be used (minus and plus end-position, mid-position), i.e. the impulse test should be carried out in one position at a time for each of the three individual phases of a three-phase transformer or in one position at a time for each of the three single-phase transformers designed to form a three-phase bank.

In case of the induced power frequency overvoltage test it has to be taken into account that the voltage per turns varies depending on the OLTC position. Therefore the position to be tested has to be specified by the customer.

**Fig. 4.1-2:** Voltage stresses occuring along the transformer windings during testing with different voltages (transformer data: 400 MVA, 400 kV ± 16 % / 120 kV / 30 kV, coarse/fine winding arrangement, regulation at the neutral point) *[Breuer 1984]*
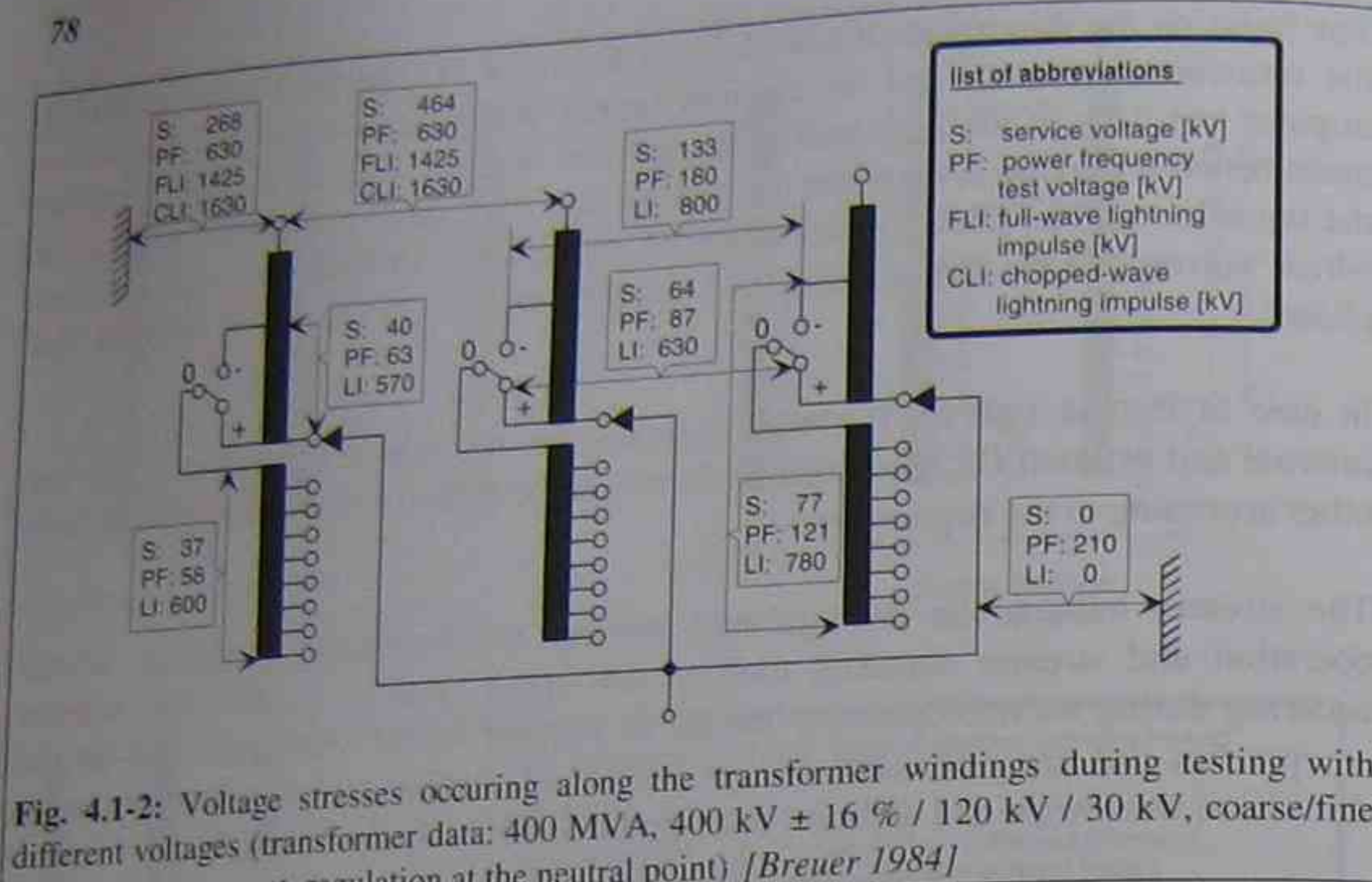
Fig. 4.1-2 gives a basic idea of the stresses of the tapping winding and the OLTC for a power transformer with regulation at the neutral point using a coarse/fine winding arrangement. The listed values of the lightning impulse voltages are maximum values, which do not occur each in the indicated OLTC position.

The highest stresses at the internal insulation of the OLTC occur during full- or chopped-wave lightning impulse withstand tests due to the non-linear voltage distribution along the windings. Hence, these stresses determine the necessary insulation distances. Stresses due to switching impulse tests (voltage distribution along the transformer windings is almost linear) or induced power frequency overvoltage tests (voltage distribution along the winding is linear) are comparatively low and are controled adequately by insulation distances dimensioned for lightning impulse stresses. During testing with applied power frequency voltage the internal insulation of the OLTC will not be stressed.

For the correct selection of the internal OLTC insulation it has to be taken into account that the withstand voltage of an insulation distance is determined not only by the peak value of the stressing voltage but also by the voltage-time area of the occuring voltage wave. From a high number of oscillograms of impulse voltage distribution measurements with transformers of different power ratings and voltage ranges, one can derive that the insulation distances relevant for the internal OLTC insulation will be stressed by unsymmetrical oscillating and damped voltage waves. The frequency of such waves lies in the range of 20 to 50 kHz.

Usually, the lightning impulse withstand voltages of the OLTC are determined using full-wave lightning impulses (1.2/50 µs). As the standard impulse voltage has a

higher stress time compared with the wave appearing in the transformer, one can assume that the OLTC, when tested within the transformer, will withstand a higher level than that one given by a test performed on the seperate OLTC using a 1.2/50 µs wave form. One can assume a gain of voltage withstand capability of 5 to 10 per cent *[Bleibtreu, Widmann 1976, Breuer 1984]*.

Today the tap windings and, if applied, the coarse windings of transformers are increasingly equipped with ZnO-varistors to limit the impulse stresses along the windings. With this measure smaller tap selector sizes can be used, but it has to be considered that the relation of impulse to power frequency voltage stresses decreases. Following this the importance of the power frequency voltage stresses increase and may lead to the conclusion that the power frequency voltage withstand capability limits the tap selector size.

The external insulation is decisively determined by the applied power frequency voltage test. Impulse tests (lightning and switching) play a minor role with respect to the dimensioning of the OLTC.

The above mentioned effect of the individual test voltages to the internal and external insulation becomes clear when comparing the pairs of values of lightning impulse and power frequency voltage stresses. In case of the internal insulation the ratio of lightning impulse to power frequency voltage stress lies between 4.5 and 20 (compare Fig. 4.1-2). The voltage stress on the external insulation, however, is defined by the values of lightning impulse and power frequency voltage levels given in the national and international standards. Depending on the highest voltage for equipment $U_m$ the above ratios lie between 2.5 ($U_m$ = 72.5 kV) and 2.26 ($U_m$ = 420 kV). The comparison of the internal and external test voltage ratios shows clearly the increasing importance of the power frequency voltage stress in case of the external insulation. This becomes also true for the internal insulation of OLTCs of transformers with windings equipped with ZnO-varistors, because the test voltage ratio also decreases.
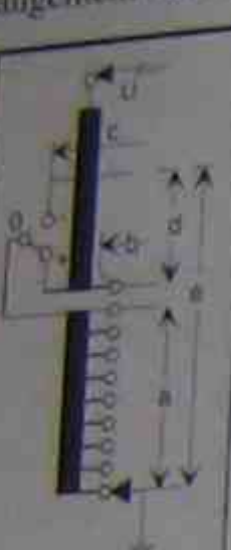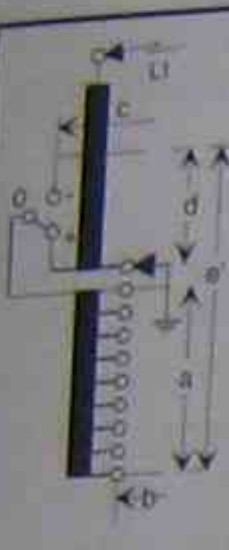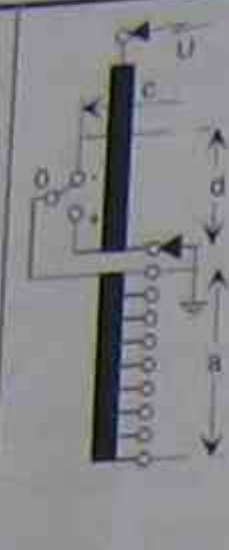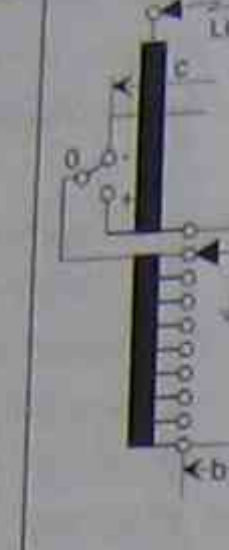
## 4.1.2 VOLTAGE STRESSES ON THE INTERNAL OLTC INSULATION DURING TRANSFORMER IMPULSE TESTING

In the following example the stress levels of the internal insulation of an OLTC will be described when testing the transformer with lightning impulse voltages. As a standard for comparison of the stresses on different insulation distances of the tap selector the stress-ratio will be introduced:

$$ stress-ratio = \frac{stress\ as\ percentage\ of\ the\ input\ impulse}{regulating\ range\ as\ percentage\ of\ the\ nominal\ voltage} $$

This allows to compare transformers of different designs and ratings.

**Table 4.1-1:** Stress-ratios during impulse testing of a transformer with coarse/fine winding arrangement and regulation at the neutral end [Breuer 1984]



| | max. number of turns | mid-position (+) | mid-position (-) | min. number of turns | max. stress | x [1] |
|---|---|---|---|---|---|---|
| a | 1.2 - 2.6 | 1.6 - 3.5 | 1.0 - 3.3 | 1.7 - 3.5 | 3.5 | 2.63 |
| b | 1.2 - 2.6 | 1.6 - 3.5 | - [2] | 2.0 - 3.5 | 3.5 | 2.67 |
| c | 2.2 - 4.0 | 1.7 - 2.7 | 1.7 - 3.1 | - | 4.0 | 3.29 |
| d | 1.4 - 2.4 | 1.8 - 2.4 | 1.8 - 2.4 | 2.0 - 3.4 | 3.5 | 2.55 |
| e | 2.2 - 4.2 | - | - | - | 4.2 | 3.22 |
| e' | - | 3.0 - 5.0 | - | - | 5.0 | - |

**Remarks:**
1) mean value of maximum stresses of all evaluated transformers
2) not evaluated because stresses in mid-position "+" (coarse and fine tap winding connected in series) are greater than in mid-position "-" (coarse and fine tap winding are connected in parallel)
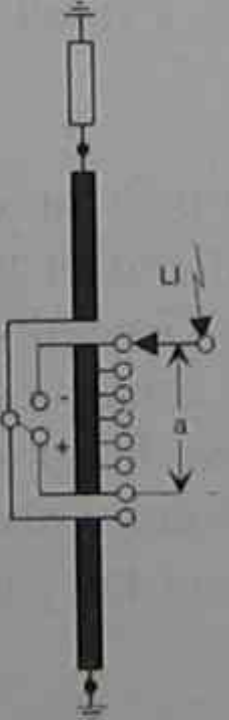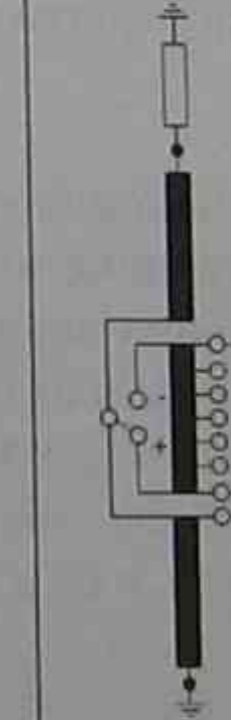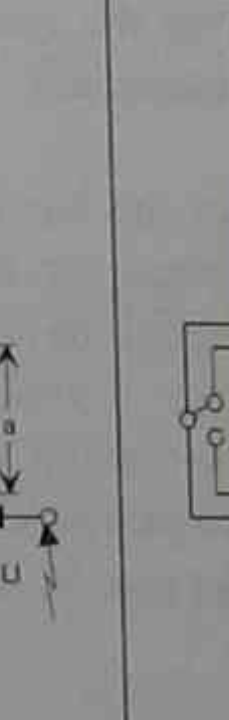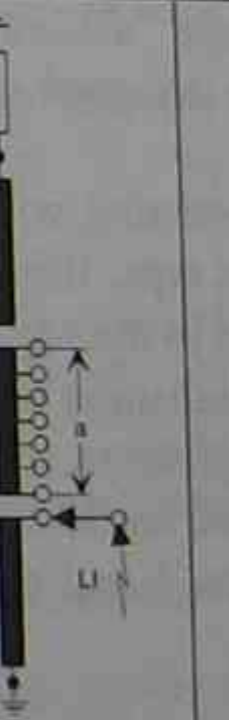e') same insulation distance as "e" but with freely oscillating fine tap winding

Table 4.1-1 shows the stress-ratios for the insulation distances dependent on the OLTC position in case of transformers with coarse/fine winding arrangements and regulation at the neutral end. The values of the stress as percentage of the input impulse are based on voltage distribution measurements or calculations carried out on a multitude of transformers of different manufacturers with power ratings between 15 MVA and 850 MVA and nominal voltages between 110 kV and 525 kV.

The stress-ratios determined for the different insulation distances vary in wide limits. The pairs of values given in Table 4.1-1 represent the minimum and maximum values. The dispersion of the values is caused by the variety of type and arrangement of windings. A direct correlation between the stress-ratios and the rated power or the nominal voltage of the transformers cannot be found. Generally, it can be stated that with increasing ratings of the transformer the stress-ratios will decrease, as in case of bigger units more efforts are undertaken to optimize the voltage distribution along the windings.

The stress-ratios for the insulation distances "a" and "b", shown in Table 4.1-1, are also valid for linear and reversing regulating modes. In the column mid-position (-) there is no value given for the stress on insulation distance "b" and in the circuit diagram the insulation distance "b" is not indicated, because in this position the insulation distance "b" is not maximally stressed. The maximum stress on this insulation distance with the OLTC in mid-position occurs in the mid-position (+), because the coarse and fine tap winding are connected in series, whereas in the mid-position (-) they are connected in parallel.

Table 4.1-2 shows the stress ratios for an autotransformer with regulation of the autopoint with a reversing change-over selector. For the stress-ratio the same definition is valid as given above. In this application only the insulation distance "a" is valid when using single pole OLTCs. Also these stress-ratios are based on voltage distribution measurements or calculations carried out on a multitude of transformers of different manufacturers with power ratings from 140 MVA to 1500 MVA and nominal voltages between 345 kV / 140 kV and 765 kV / 340 kV. Most of the stress-ratios are in the same order as in case of a coarse/fine regulation at the neutral end as shown in Table 4.1-1.

**Table 4.1-2:** Stress-ratios during impulse testing of an autotransformer with regulation with a reversing change-over selector at the autopoint [Breuer 1984]



| | max. number of turns | mid-position (+) | mid-position (-) | min. number of turns | max. stress |
|---|---|---|---|---|---|
| a | 1.7 - 2.5 | 2.2 - 3.1 | 2.3 - 3.7 | 1.7 - 3.2 | 3.7 - 5 [1] |

**Remarks:**
1) in singular cases the stress-ratio can reach this value

## 4.1.3 INTERNAL INSULATION DISTANCES AT TAP SELECTORS OF DIFFERENT DESIGNS

Within the insulation system of the transformer the OLTC represents a device to be switched or operated mechanically under service conditions. Therefore, the same insulation systems cannot be used as in case of the transformer insulation. The insulation distances of the OLTC consist in almost every case in the parallel connection of the following three insulation mediums:

- pure oil or fluid insulation distance
- insulation distance along a boundary fluid-solid insulator
- pure solid insulation distance

The values of the lightning impulse stresses occuring typically at the internal OLTC insulation and their relation to each other determine the insulation coordination within the tap selector and the change-over selector. Not only the design and dimensioning of the particular insulation distances but also the geometric combination of tap selector and change-over selector are committed by the insulation coordination together with aspects of the technology of the mechanism design.

The inner reference diameter of the tap selector is determined by the necessary insulation distances, which are dimensioned according to the voltage stresses between any contacts (insulation distance "a"), and by the space required as a result of the pitch. Usually, all terminals are designed as electrodes.

Naturally, the differences in potential within the tap winding have their maximum between the electrical extreme taps, this means the beginning and end of the tap winding. These taps correspond to the tap selector terminals 1 and n. Generally, with respect to the OLTC only the withstand voltage of these terminals or contacts will be considered and is called voltage stress across the tap winding. When designing the tap selector or selector switch one has to taken into account that this voltage stress not only occurs between the contacts 1 and n but also between 1 or n and the common contact.

In case of tap selectors with reversing change-over selector the maximum in-phase difference in potential caused by the voltage stress across the tap winding occurs between contacts K and n, when the change-over selector is in the minus position, and between K and 1, when the change-over selector is in the plus position. Figure 4.1-3 shows a single-multiway resistor type selector switch (in-tank) and Figure 4.1-4 shows a reactor type OLTC with vacuum interrupter (compartment type), both equipped with reversing change-over selector. In case of single-multiway OLTCs this determines the horizontal contact distance in the contact circle. However, in case of the double-multiway resistor type OLTC not only the contact distance between these two contacts but also the distance between the two contact circles have to be dimensioned for this voltage stress. Although the vertical distance is only necessary at the contact distance K and n (compare Fig. 4.1-3), for physical and geometrical reasons this distance appears at all contacts of the same phase lying above each other.
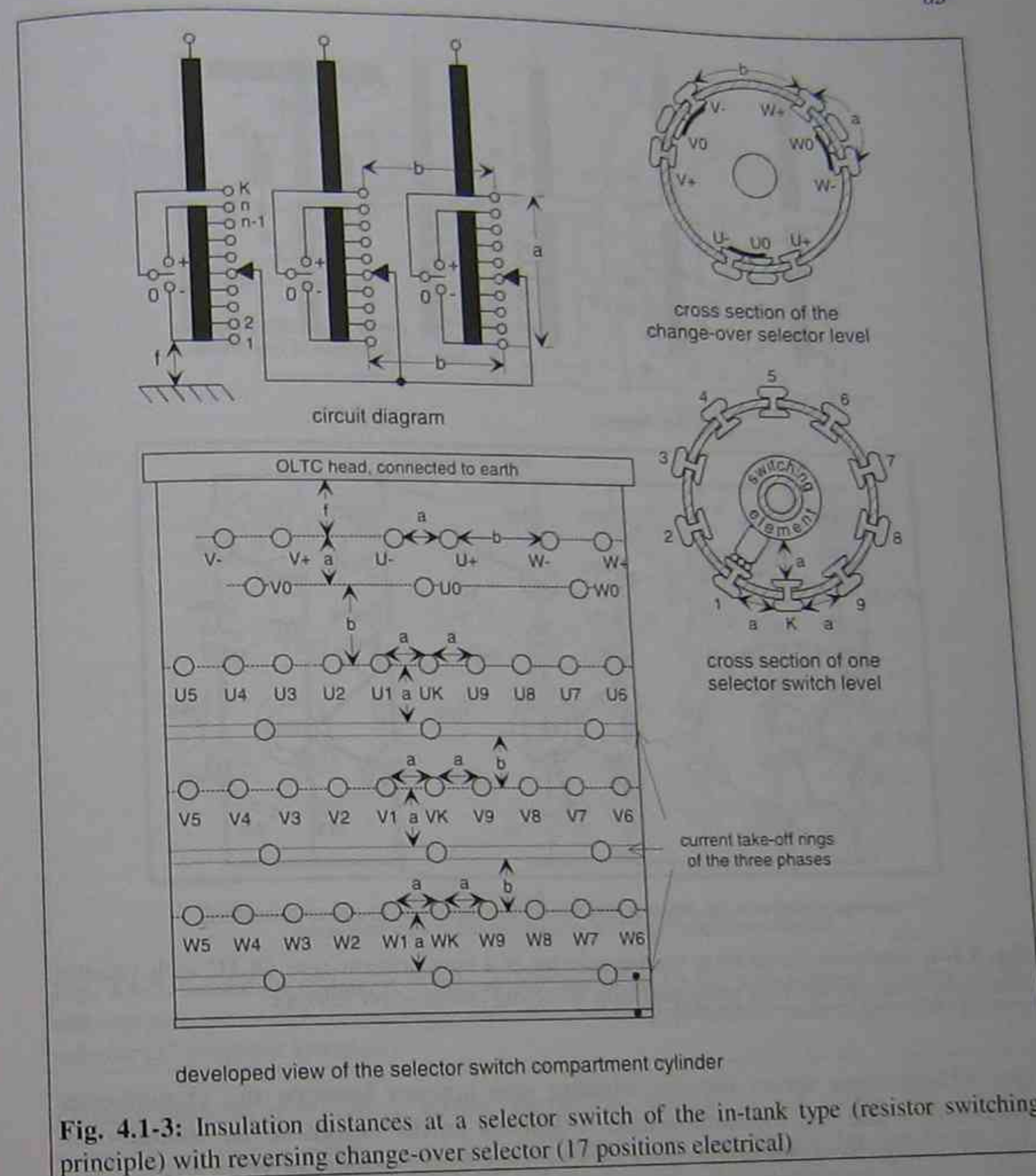
cross section of the change-over selector level

circuit diagram

OLTC head, connected to earth

cross section of one selector switch level

current take-off rings of the three phases

developed view of the selector switch compartment cylinder

**Fig. 4.1-3:** Insulation distances at a selector switch of the in-tank type (resistor switching principle) with reversing change-over selector (17 positions electrical)

A method to decrease this distance is to turn the even or odd contact circle by 180 degrees. With this measure the K-contact lies above the contact which is connected to the middle of the tap winding. The stress on this distance can be assumed to be roughly 80% of the stress across the tap winding, caused by the non-linear voltage distribution. In case of resistor type OLTCs of the compartment type the even and odd contact circles are often arranged on the terminal board side by side. With this design the even and odd contact circles can be turned by 180 degrees to each other to reach closer dimensions (the distance between contacts K and n respectively K and 1 becomes then two times the contact circle diameter).
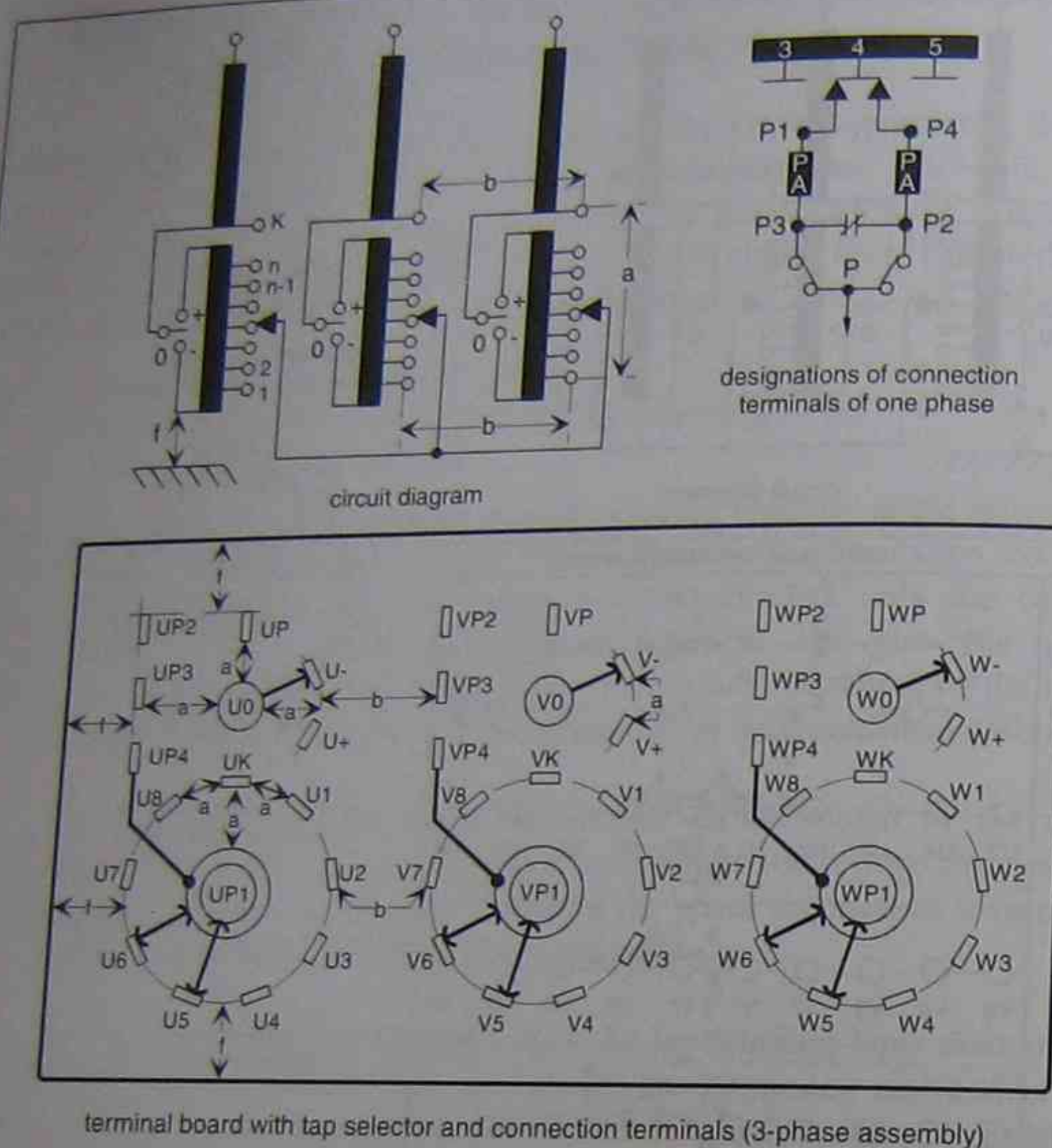
circuit diagram

designations of connection terminals of one phase

terminal board with tap selector and connection terminals (3-phase assembly)

**Fig. 4.1-4:** Insulation distances at the tap selector of a compartment type OLTC with vacuum interrupter (reactor switching principle) with reversing change-over selector



circuit diagram

cross section of the tap selector

common terminal

common terminal

developed view of the tap selector and the change-over selector

**Fig. 4.1-5:** Insulation distances at the tap selector of an OLTC with seperate diverter switch and tap selector of the in-tank type (resistor switching principle) with coarse change-over selector (17 positions electrical)

The voltage stress across the tap winding also appears between the change-over contacts 0, + and - of the same phase. It depends on the design of the change-over selector, if this stress determines the contact distance horizontally or vertically.

Usually, the impulse withstand voltages of the inter-phase insulation distances "b" of a three-phase OLTC for application at the neutral end have the same order as those of the in-phase insulation distances "a". This can be explained as follows. During impulse testing of one phase of a three-phase transformer, the adjacent phases are grounded directly or through low-ohmic resistors. For OLTCs connected to the neutral end one can assume that all tap selector contacts of the grounded phases have ground potential or a potential which is very close to ground. Therefore, all potential differences which occur in-phase between any contact and the common terminal (ground) must occur in the same order between any contact of the tested phase and the contacts of the grounded phases.
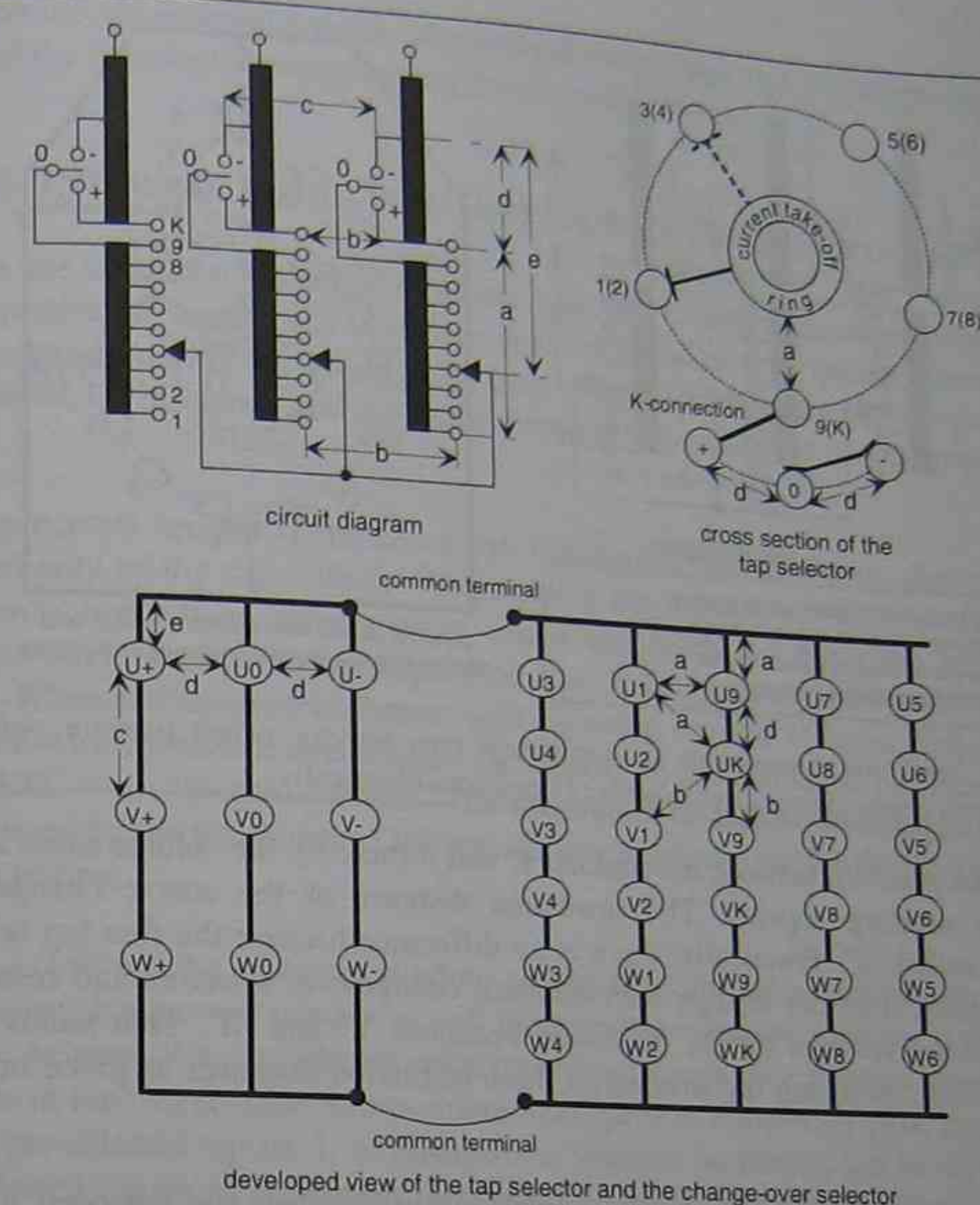
During induced overvoltage testing the above relation is not valid. The stresses occuring on the inter-phase insulation distances "b" are greater by the factor $\sqrt{3}$ compared to the in-phase insulation distances "a". As mentioned before, when selecting an OLTC this fact has to be considered, because the inter-phase voltage stress at the insulation distance "b" can become the determining factor with respect to the tap selector size, especially when using ZnO-varistors to limit the impulse stresses. Usually, the power frequency withstand voltages of the tap selector insulation distances are two times the maximum permissible service voltage.

When considering tap selectors with coarse change-over selector, in principle, the above mentioned is also valid, but the designations differ. Figure 4.1-5 shows a double-multiway resistor type OLTC with seperate diverter switch and tap selector (in-tank) and Figure 4.1-6 shows a resistor type selector switch (compartment type), both equipped with coarse change-over selector. With the coarse change-over selector

circuit diagram

All insulation distances (b and c)
between phases are not shown here.
They are located between the
seperate selector boards

selector board with selector switch and
coarse change-over selector of one phase

**Fig. 4.1-6:** Insulation distances in a compartment type selector switch (resistor switching principle) with coarse change-over selector (17 positions electrical)

in the minus position, between the contacts K and n (here 9), the voltage stress across the coarse winding appears. The insulation distance at the coarse change-over selector is called "d". Practically, there is no difference because the fine tap selector design, usually, does not change with different change-over selectors and results in equal withstand voltages for the insulation distances "a" and "d". That seems to be tolerable when comparing the stresses on these insulation distances as given in table 4.1-1.

However, the voltage stresses on the insulation distances between the open minus-contact of the coarse change-over selector and the current take-off terminal (common terminal, insulation distance "e") and between the open minus-contacts of different phases (insulation distance "c") reach higher values compared to the stresses on the insulation distances "a", "b" and "d", which are all in the same order. This is caused by the fact that in this change-over selector position the fine tap winding and the coarse winding are connected in series.

An additional specific characteristic of the tap selector with coarse change-over selector is the OLTC position, where the coarse change-over selector is connected to the plus-contact and the tap selector is connected to the K-contact. In this position the tap selector contact that is not carrying a current is connected to last contact of the fine tap winding (here 9). The lower end of the fine tap winding, which is linked to contact 1, is therefore able to oscilate freely. Thus the contact 1 can reach a very high difference in potential to the open minus-conatct of the change-over selector. In table 4.1-1 the relevant insulation distance in this OLTC position is indicated with "e' ". The importance of this insulation distance depends on the OLTC design. In case of OLTCs with geometrical seperated tap selector and change-over selector, usually, this distance is insignificant.

The specific characteristics during the induced overvoltage test are comparable with those of the tap selector with reversing change-over selector.

### 4.1.4 INTERNAL INSULATION DISTANCE AT THE DIVERTER SWITCH

Within the insulation system of a resistor type OLTC with seperate diverter switch and tap selector, there is one insulation distance at the diverter switch which is highly stressed during the testing of the transformer. This distance ($a_0$) is a part of the internal OLTC insulation and is found between the tap in service and the pre-selected tap.

During normal service operation of the transformer the insulation distance $a_0$ is stressed only by the step voltage. When testing the transformer with induced power frequency, overvoltage stresses occur which can reach 2.5 times the service step voltage. These stresses do not depend on the OLTC position and can be controled easily. When testing the transformer with lightning impulse voltages (full-wave and chopped-wave) transient overvoltages can appear on the insulation distance $a_0$ when the OLTC is in the mid-position. The magnitude of these overvoltages is mainly determined by the oscillation of the transformer windings and by the OLTC position during testing.

Fig. 4.1-7 shows the principle winding arrangement for tap selectors with reversing and coarse change-over selector as well as the voltage stresses occuring at the diverter switch. In case of a tap selector with reversing change-over selector the maximum stresses in the two possible mid-positions (change-over selector on plus, tap in service on K, pre-selected tap on 1, or change-over selector on minus, tap in service on K, pre-selected tap on n) are almost identical. In both positions the oscillating potential of the tap winding occurs at the $a_0$-distance. When using a tap selector with coarse change-over selector the two mid-positions (change-over selector on minus, tap in service on K, pre-selected tap on 1, or change-over selector on minus, tap in service on 1, pre-selected tap on K) can lead to different stresses at the $a_0$-distance, but usually in the same order. The stress on the $a_0$-distance of the first mentioned critical mid-position is characterized by the potential of the oscillating fine tap winding, whereas in the second mentioned critical mid-position it is characterized by the potential of the oscillating coarse winding.

The voltage stresses measured on several transformers of different designs demonstrate clearly that especially in coarse/fine winding arrangements very high impulse stresses must be expected between the two diverter switch sides. This impulse stresses must be expected between the two diverter switch sides. This although the stress caused by power frequency voltages is only one step in case of tap selectors with one mid-position and no step in case of tap selectors with three mid-positions (compare 3.1).
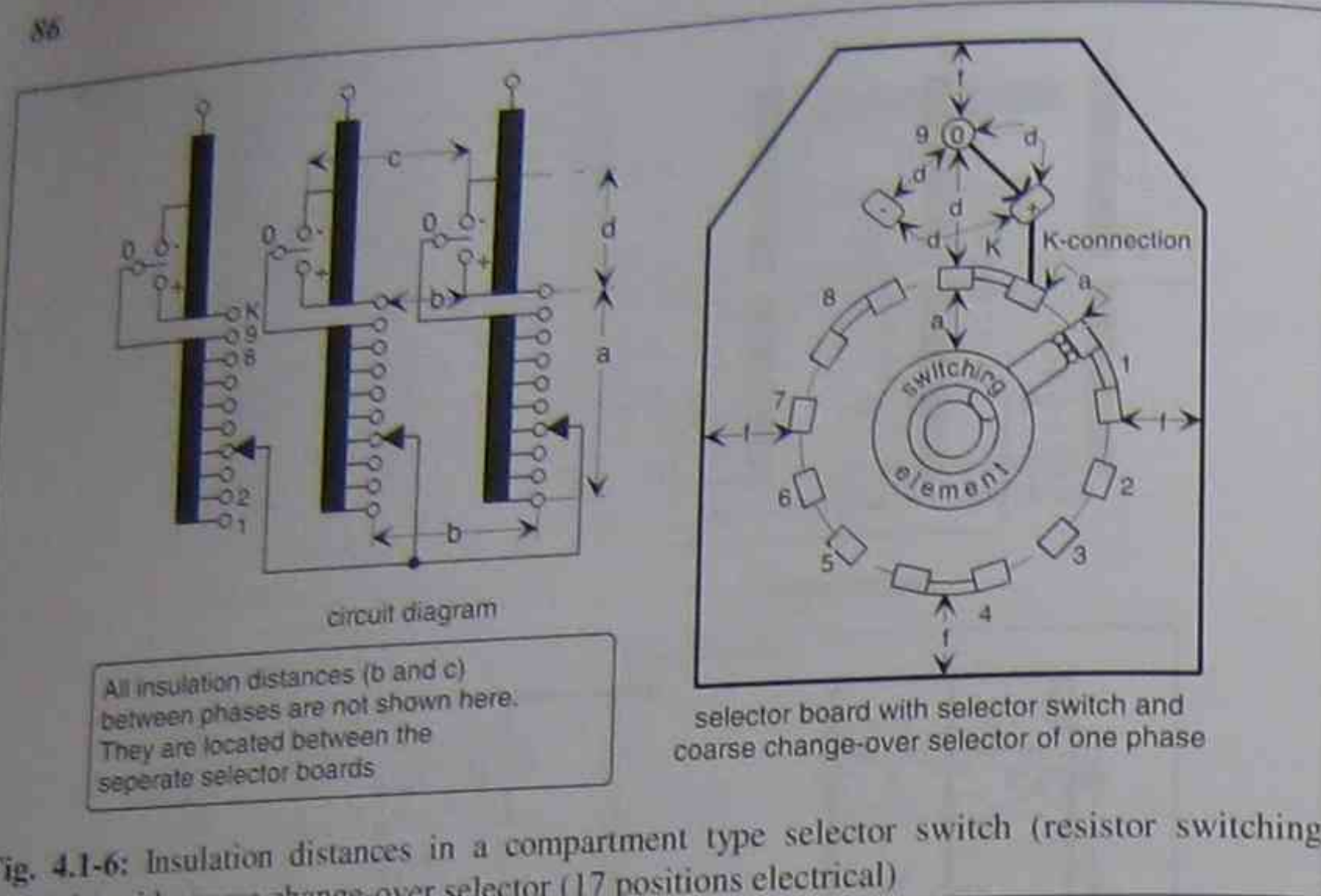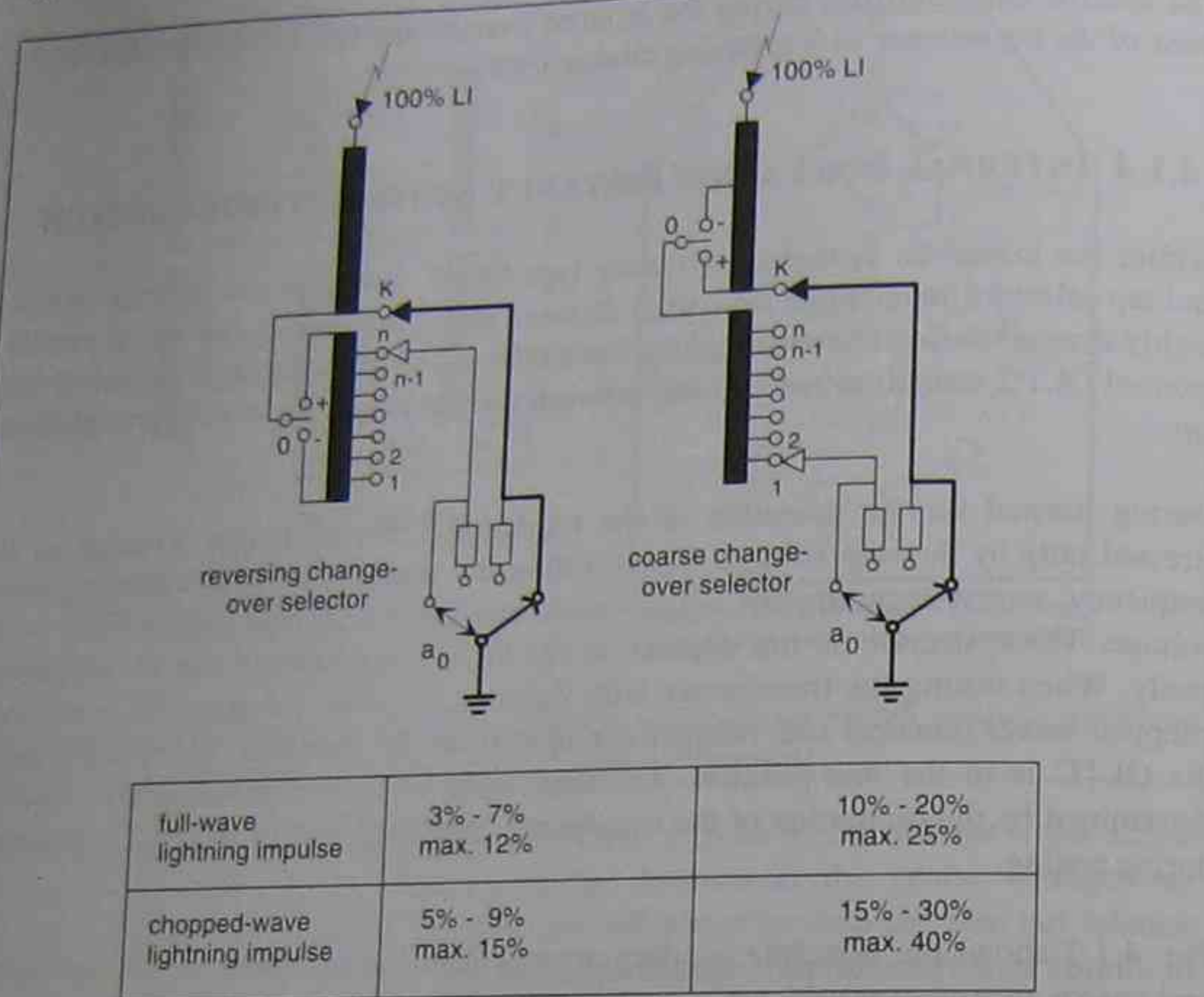
| full-wave lightning impulse | 3% - 7% max. 12% | 10% - 20% max. 25% |
|---|---|---|
| chopped-wave lightning impulse | 5% - 9% max. 15% | 15% - 30% max. 40% |

**Fig. 4.1-7:** Voltage stresses on the $a_0$-distance with reversing and coarse change-over selector

The measurements (Fig. 4.1-7) show that in case of tap selector with coarse change-over selectors upto 25% of the input impulse level appears at the $a_0$-distance when testing with full-wave lightning impulses and upto 40% when testing with chopped-wave lightning impulses respectively. When considering a transformer with $U_m = 245$ kV and a BIL of 950 kV, the stresses on the $a_0$-distance can reach values of 238 kV and 380 kV respectively. For economic reasons the insulation distance $a_0$ within the diverter switch cannot be designed for stresses in this order. Usually, lightning impulse withstand voltages in the range of 120 kV to 160 kV can be accomplished.
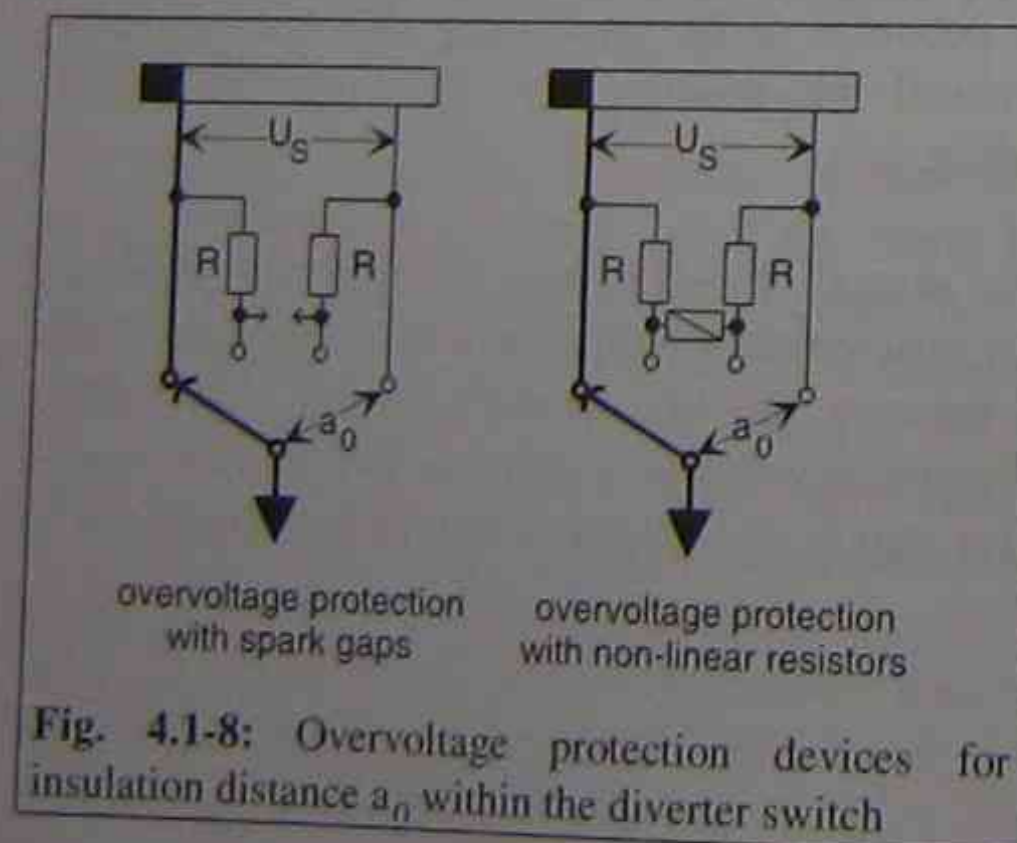
To guarantee a safe and proper operation of the OLTC countermeasures have to be taken. Fig. 4.1-8 shows two possible principles of overvoltage protection of the $a_0$-distance within the diverter switch. The voltages that stress the insulation can be limited by using spark gaps



**Fig. 4.1-8:** Overvoltage protection devices for insulation distance $a_0$ within the diverter switch

as well as non-linear resistors. They are installed into the diverter switch and connected in series with the transition resistors. Both methods are applied today successfully.

The response level of spark gaps, usually, is chosen in the range between 90 kV (0%) and 130 kV (100%). When the spark gap fires a follow current flows caused by the step voltage and limited by the transition resistors. This current breaks at the first current zero and is normally in the range of 100 A to 300 A. The firing of the spark gap leads to wear of the arcing horns. Therefore Spark gaps should be used in applications where an occasional or rare firing of the overvoltage protection system is to be expected. During impulse testing of the transformer it has to be considered that a firing of the spark gap in the critical mid-position is possible when the occuring impulse stress exceeds the response level.

Non-linear resistors should be used as overvoltage protection of the diverter switch in applications where frequent stresses caused by overvoltages have to be expected. Due to the connection of the non-linear resistors in series with the transition resistors, they are continuously exposed to the step voltage. The electrical losses caused by the step voltage can be neglected however, since the non-linear resistors are designed for a protection level of 15 times to 20 times the service power frequency stress caused by the step voltage.

Non-linear resistors limit the overvoltage without delayed and with continuous action, and prevent an overshooting of the voltage above the protection level set by their characteristics. This overshooting of the voltage cannot be avoided when using spark gaps because of their response delay time.

In the early stages 25 years ago, silicon carbide elements (SiC) were used as non-linear resistors. After introduction of high power zinc oxide varistors (ZnO) 20 years ago, today mainly these elements are used. In Fig. 4.1-9 the current/voltage
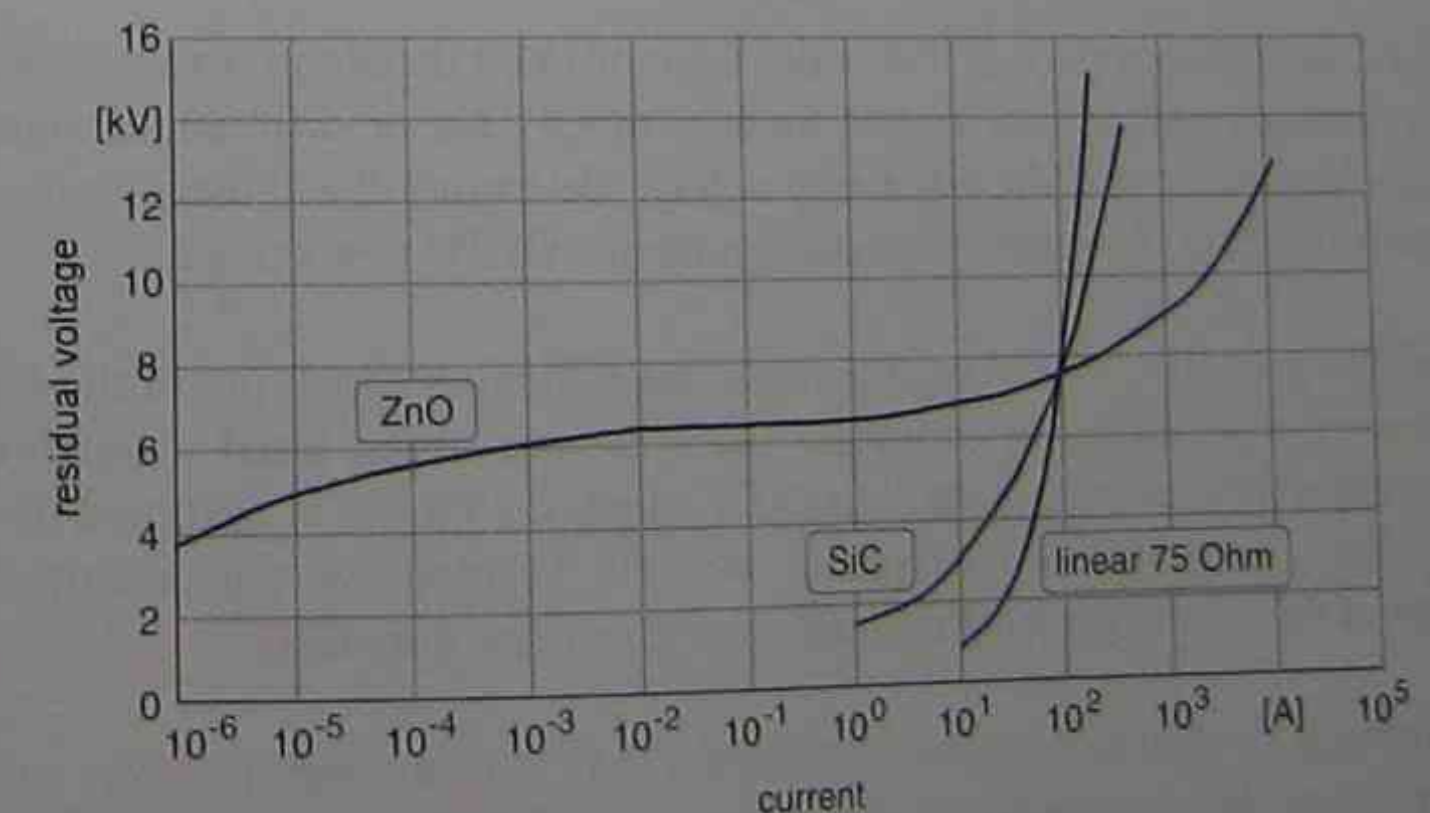


**Fig. 4.1-9:** Voltage/current characteristics of linear and non-linear resistors

characteristics of zinc oxide varistors, silicon carbide elements and those of linear resistors are shown. To allow a better comparison all plots of the resistor elements are dimensioned for the working point 7,500 V/100 A (75 $\Omega$) so that all three curves meet this point. Fig. 4.1-9 demonstrates the advantage of ZnO resulting from its extreme non-linearity.

The dimensioning of the non-linear resistors is performed individually by the OLTC manufacturer according to the stresses of the OLTC application (step voltage, full-wave and chopped-wave). OLTCs have been lightning impulse levels for equipped successfully with non-linear resistors for more than 20 years. But still these have to be checked during routine inspections of the diverter switch.

## 4.2 SWITCHING CAPABILITY

According to IEC 60214 [IEC Publ. 60214 1989] the following definitions apply:

**rated through-current ($I_u$ or $I_{max}$)**
The current flowing through the OLTC towards the external circuit, which the apparatus is capable of transferring from one tapping to the other at the relevant step voltage and which can be carried continuously while meeting the technical data of the OLTC manufacturer.

**maximum rated through-current ($I_{um}$)**
The rated through-current for which both the temperature rise of the contacts and the service duty test apply.

Within the maximum rated through-current of the OLTC there may be different assigned combinations of values of rated through-current and corresponding rated step voltage. When a value of rated step voltage is referred to a specific value of rated through-current, it is called relevant rated step voltage.

The OLTC manufacturers cover the wide range of rated through-currents needed for different transformers with a limited number of OLTCs of different designs. The rated through-current and the rated step voltage determine the dimensioning of the transition resistors of the resistor switching principle OLTC (see 4.2.3).

When fulfilling the IEC 60214 requirements, the switching capability of the OLTC is also tested (40 operations) by switching twice the maximum rated through-current $I_{um}$ at the relevant maximum step voltage for which the OLTC is designed (breaking capacity test). In addition the contact wear is verified by performing 50,000 operations at the maximum rated through-current (service duty test).

The switching or breaking capacity test of OLTCs using the resistor switching principle has to be performed at the maximum rated through-current and power factor 1 (IEC Publ. 60214).
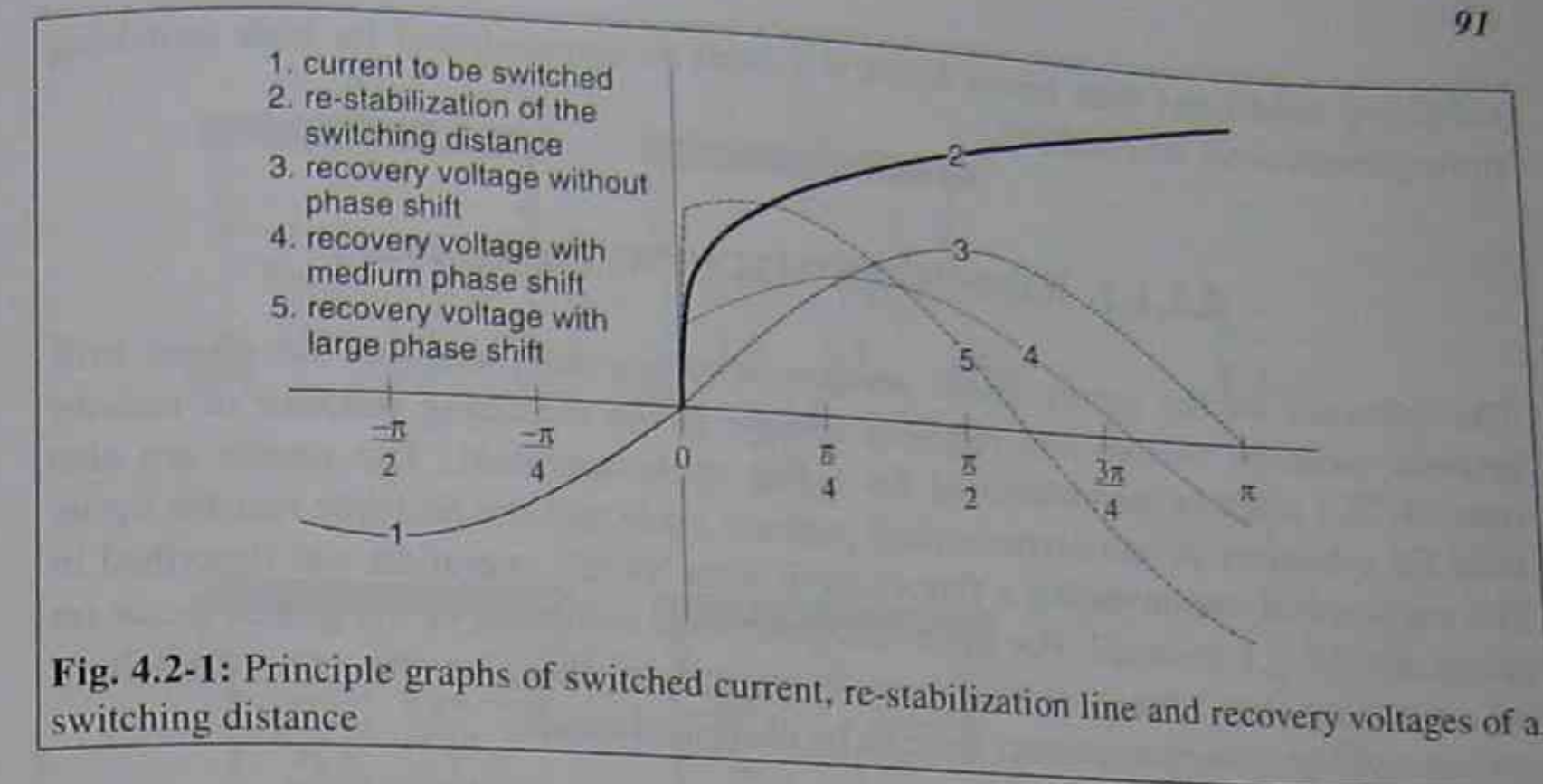
**Fig. 4.2-1:** Principle graphs of switched current, re-stabilization line and recovery voltages of a switching distance

In case of OLTCs using the reactor switching principle the service duty test has to be performed at the maximum rated-through-current, a circulating current of 50% (generated by the preventive autotransformer) and a power factor of 0.8 (IEEE Standard C57.131), and the breaking capacity test at twice the maximum rated through-current and power factor 0 respectively.

## 4.2.1 POWER FACTOR

Although material characteristics, geometry and velocity of the opening contacts influence, the arc quenching capability of a switching distance, it is mainly determined by the shape and magnitude of the current to be switched and the recovery voltage. Fig. 4.2-1 shows as an example the graphs for the switched current, the re-stabilization of the switching distance and the recovery voltages for different phase shifts.

The recovery voltage without phase shift (curve 3) corresponds to the breaking of an ohmic load. It can be recognized that the re-stabilization line (curve 2) is transgressed only if the peak of the recovery voltage (sine curve which starts at current zero) is too high. In such cases only the r.m.s. value of the recovery voltage has to be considered.

But things look different when a phase shift arises due to an inductive or capacitive characteristic of the recovery voltage. In such cases it is important how large the phase shift becomes (compare curves 4 and 5). A transgression of the re-stabilization line may result in a re-ignition of the switching distance and may lead to a short circuit of a portion of the tap winding.

OLTC users often have questions regarding the influence of the power factor on the switching capability and on the above mentioned phase shift. In the following the

switching conditions with power factor $\neq 1$ shall be demonstrated for both switching principles (resistor and reactor).

### 4.2.1.1 RESISTOR SWITCHING PRINCIPLE

The influence of the power factor on the switching duty and on the phase shift between switched current and recovery voltage at the switching distance of resistor type OLTCs shall be demonstrated for a flag cycle operation. The results are also valid for symmetrical and asymmetrical pennant cycle and the multiple resistor cycle. The sequence of events during a flag cycle diverter switch operation was described in paragraph 2.1.2.1 in detail. For the evaluation of the influence of the power factor on the switching duty, the two moments of current breaking at the main switching contact and the transition contact have to be examined closer.

Figures 4.2-2a through d show the circuit diagrams of these two moments (just before and after current zero) for a heavy switching operation. For the further evaluation it shall be agreed that the phasors of the transformer voltage $\bar{U}$ and the step voltage $\bar{U}_S$ are on the real coordinate axis. The through-current $\bar{I}_L$ shall have a phase angle $\varphi$ to the voltage as shown in the phasor diagram in Figure 4.2-2e. With this the through-current can be expressed as:

$$\bar{I}_L = \left| \bar{I}_L \right| \cdot (\cos\varphi - j\sin\varphi) \qquad (4.2\_1)$$

During the switching sequence, first the main switching contact $MS_A$ opens. Until the first current zero after contact separation, an arc short-circuits the opening contacts (Fig. 4.2-2a) and the through-current still flows through this path. At the current zero the main switching contact has to break the through-current

$$\bar{I}_{MSA} = \left| \bar{I}_L \right| \cdot (\cos\varphi - j\sin\varphi) \qquad (4.2\_2)$$

After quenching of the arc a recovery voltage $\bar{U}_{rMSA}$ arises at the open contacts (Fig. 4.2-2b). The recovery voltage can be determined as the voltage drop at the transition resistor $R_A$ caused by the through-current $\bar{I}_L$:

$$\bar{U}_{rMSA} = \left| \bar{I}_L \right| \cdot R_A \cdot (\cos\varphi - j\sin\varphi) \qquad (4.2\_3)$$

Comparing equations 4.2_2 and 4.2_3, it can be stated that the switched current $\bar{I}_{MSA}$ and the recovery voltage $\bar{U}_{rMSA}$ are always in phase (at leading as well as lagging power factors):

$$\varphi_{IMSA} = \operatorname{arctg}\frac{\operatorname{Im}(\bar{I}_{MSA})}{\operatorname{Re}(\bar{I}_{MSA})} = \operatorname{arctg}\frac{-\sin\varphi}{\cos\varphi} = \operatorname{arctg}\frac{\operatorname{Im}(\bar{U}_{rMSA})}{\operatorname{Re}(\bar{U}_{rMSA})} = \varphi_{UMSA} \qquad (4.2\_4)$$
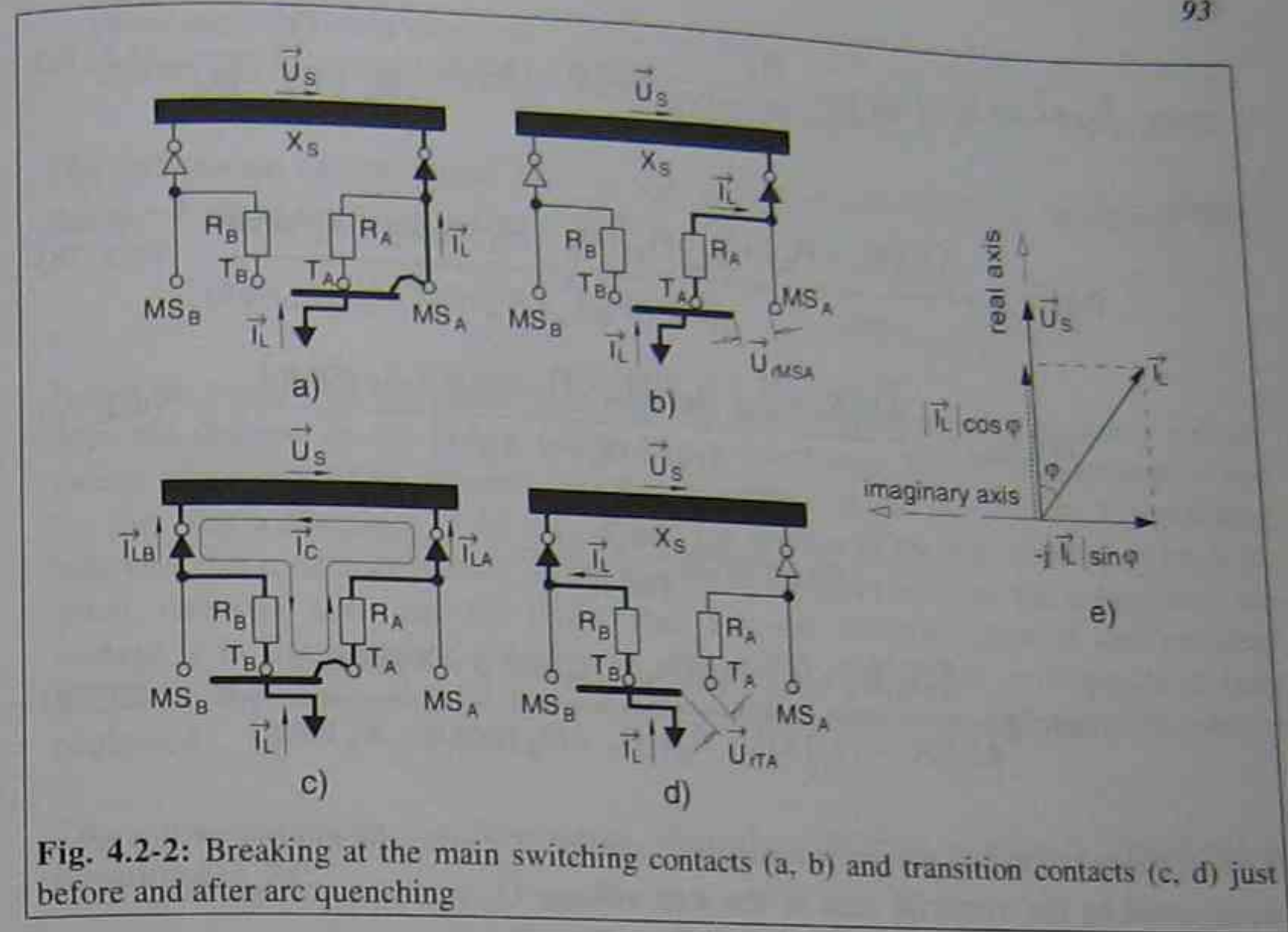
Fig. 4.2-2: Breaking at the main switching contacts (a, b) and transition contacts (c, d) just before and after arc quenching

Following the further switching sequence the next event is the current breaking at the transition contact. As long as the arc has not extinguished the through-current $\bar{I}_L$ is shared between the two transition resistor pathes A and B (Fig. 4.2-2c). The share ratio is determined by the impedances of the two paths. For the calculation of the phase shift one tap section of the tap winding is represented by its equivalent voltage source $\bar{U}_S$ and its reactance $X_S$.

The portion of the through-current which flows through the path A can be determined to:

$$\bar{I}_{LA} = \bar{I}_L \cdot \frac{R_B}{R_B + R_A + jX_S} = \left| \bar{I}_L \right| \cdot \frac{R_B}{R_B + R_A + jX_S}(\cos\varphi - j\sin\varphi) \qquad (4.2\_5)$$

In addition to the through-current, the step voltage $\bar{U}_S$ generates a circulating current $\bar{I}_C$ that flows through the transition resistors and the impedance of the tap section:

$$\bar{I}_C = \frac{\bar{U}_S}{R_A + R_B + jX_S} \qquad (4.2\_6)$$

With equations 4.2_5 and 4.2_6 the switched current at the transition contact $T_A$ is calculated to:

$$\bar{I}_{TA} = \bar{I}_{LA} + \bar{I}_C = |\bar{I}_L| \cdot \frac{R_B}{R_A + R_B + jX_S} (\cos\varphi - j\sin\varphi) + \frac{\bar{U}_S}{R_A + R_B + jX_S} \qquad (4.2\_7a)$$

with:

$$Re(\bar{I}_{TA}) = \frac{|\bar{U}_S|(R_A + R_B) + |\bar{I}_L| \cdot R_B((R_A + R_B)\cos\varphi - X_S\sin\varphi)}{(R_A + R_B)^2 + X_S^2} \qquad (4.2\_7b)$$

$$Im(\bar{I}_{TA}) = -\frac{|\bar{U}_S|X_S + |\bar{I}_L| \cdot R_B((R_A + R_B)\sin\varphi + X_S\cos\varphi)}{(R_A + R_B)^2 + X_S^2} \qquad (4.2\_7c)$$

$$\varphi_{ITA} = \text{arctg}\frac{Im(\bar{I}_{TA})}{Re(\bar{I}_{TA})} =$$

$$= \text{arctg}\frac{-(|\bar{U}_S|X_S + |\bar{I}_L| \cdot R_B((R_A + R_B)\sin\varphi + X_S\cos\varphi))}{|\bar{U}_S|(R_A + R_B) + |\bar{I}_L| \cdot R_B((R_A + R_B)\cos\varphi - X_S\sin\varphi)} \qquad (4.2\_7d)$$

The recovery voltage at the open transition contacts $T_A$ after quenching of the arc is determined by the vectorial sum of the step voltage $\bar{U}_S$ and the voltage drop at the transition resistor $R_B$ caused by the through-current $\bar{I}_L$ (Fig. 4.2-2d):

$$\bar{U}_{rTA} = \bar{U}_S + \bar{I}_L \cdot R_B = |\bar{U}_S| + |\bar{I}_L| \cdot R_B \cdot (\cos\varphi - j\sin\varphi) \qquad (4.2\_8a)$$

$$\varphi_{UTA} = \text{arctg}\frac{Im(\bar{U}_{rTA})}{Re(\bar{U}_{rTA})} = \frac{-|\bar{I}_L| \cdot R_B\sin\varphi}{|\bar{U}_S| + |\bar{I}_L| \cdot R_B\cos\varphi} \qquad (4.2\_8b)$$

Now the phase shift between the switched current $\bar{I}_{TA}$ and the recovery voltage $\bar{U}_{rTA}$ at the transition contact can be calculated to:

$$|\Delta\varphi_{TA}| = |\varphi_{UTA} - \varphi_{ITA}| \qquad (4.2\_9)$$

In the following a calculation of the phase shift $\varphi_{UTA}$ is performed with exemplary values to get an idea of the order of the phase shift:

step voltage: $\quad \bar{U}_S = 2,000\,V \quad$ transition resistors: $\quad R_A = R_B = 1.5\Omega$

rated through-current: $\bar{I}_L = 1,300\,A \quad$ power factor: $\quad \cos\varphi = 0.8$

reactance of one tap: $X_S = 50m\Omega$

phase angle of the switched current: $\quad \varphi_{ITA} = \text{arctg}\dfrac{-3,688\,V\Omega^2}{10,621.50\,V\Omega^2} = -19.15°$

phase angle of the recovery voltage: $\quad \varphi_{UTA} = \text{arctg}\dfrac{-1,170\,V}{3,560\,V} = -18.19°$

phase angle between switched current and recovery voltage: $\quad |\Delta\varphi_{TA\cos\varphi=0.8}| = |(-18.19°) - (-19.15°)| = 0.96°$

The calculation of the phase shift at the transition contact for a $\cos\varphi = 0$ and $\cos\varphi = 1$ shows the same result:

$$|\Delta\varphi_{TA\cos\varphi=0}| = 0.96° \qquad \text{and} \qquad |\Delta\varphi_{TA\cos\varphi=1}| = 0.96°$$

It can be stated that the phase shift between switched current and recovery voltage does not depend on the power factor, but is determined by the relationship of the values of the transition resistors and the impedance of one tap section. Considering the fact that a reactance of 50 mΩ of one tap section of the tap winding is on high side and the resistance values of the transition resistors used in the calculation are usual, one can state that the phase shift between switched current and recovery voltage is in the range of 1 degree. A phase shift of 1 degree corresponds to only 1.75% of the peak value of the recovery voltage sine wave and therefore can be neglected.

The same conclusion can be reached when the following relation is considered in equation 4.2_7d:

$$R_A = R_B = R \gg X_S \cong 0 \qquad (4.2\_10)$$

Using this relation the phase angle of the switched current at the transition contact can be simplified to:

$$\varphi_{ITA} = \text{arctg}\frac{-(0 + |\bar{I}_L| \cdot R \cdot [(2R)\sin\varphi + 0])}{|\bar{U}_S| \cdot (2R) + |\bar{I}_L| \cdot R \cdot [(2R)\cos\varphi - 0]} \qquad (4.2\_11a)$$

and becomes equal to the phase angle of the recovery voltage at the transition contact:

$$\varphi_{ITA} = \text{arctg}\frac{-|\bar{I}_L| \cdot R\sin\varphi}{|\bar{U}_S| + |\bar{I}_L| \cdot R\cos\varphi} = \varphi_{UTA} \qquad (4.2\_11b)$$

As shown above, the phase shift generated by the power factor does not increase the switching duty. However, the power factor does affect the absolute values of recovery voltage and switched current. With equation 4.2_7a follows that the switched current $\bar{I}_{TA}$ reaches its maximum when $\bar{I}_{LA}$ and $\bar{I}_C$ are in phase. This occurs at power factor 1. The recovery voltage $\bar{U}_{rTA}$ (eq. 4.2_8a) reaches its maximum at power factor 1 as well ($\bar{U}_S$ and $\bar{I}_L \cdot R_B$ are in phase). With this the maximum duty on the transition contact occurs at power factor 1. This fact is considered in the standards which require to carry out the service duty test and the breaking capacity test at power factor 1.

The last mentioned conclusions are only valid if equation 4.2_10 is true. This is normally met with almost all tap operations within the fine tap winding. In case of resistor type OLTCs with coarse change-over selector when operating from the end of the fine tap winding to the end of the coarse winding, or vice versa, it can happen that the equation 4.2_10 is not fullfilled and large phase shifts can occur (for further information see paragraph 4.5).

## 4.2.1.2 REACTOR SWITCHING PRINCIPLE

It was demonstrated in the foregoing chapter that a leading or lagging power factor only affects the absolute value of the switching duty, but does not produce a phase shift between switched current and recovery voltage. This maximum value occurs at power factor 1.

These relations may change in case of reactor type OLTCs. The switching sequence of the different types of reactor type OLTCs were given in section 2.2. From Tables 2.2-3 and 2.2-6, where the duties of the switching contacts are summarized for different reactor type OLTCs, it can be determined that there are two values of switching duties which must be controlled.

For the evaluation of the influence of the power factor on the switching duty, the two current breaking moments at the breaking contacts have to be examined closer. Figure 4.2-3 shows as an example the circuit diagrams, just before and after current zero, of these two moments for a reactor type OLTC with arcing switch.

For our purposes, the through-current is expressed in the same manner as given in equation 4.2_1. With this the equations 2.2_10 to 2.2_13 and 2.2_18 to 2.2_21 reach the following forms.

**Tap-changing operation from a non-bridging to a bridging position**
**(Fig. 4.2-3 a and b)**

Switched current at the breaking contact (TFS$_A$) (compare eq. 2.2_10 and 2.2_18):

$$\overline{I}_{TFSA} = \frac{1}{2} \cdot \overline{I}_L = \frac{1}{2} \cdot \left| \overline{I}_L \right| \cdot (\cos\varphi - j\sin\varphi) \qquad (4.2\_12)$$

Recovery voltage at the open contact distance (compare eq. 2.2_11 and 2.2_19):

$$\overline{U}_{ITFSA} = 2\left( \overline{I}_L \cdot \frac{jX}{4} \right) = \left| \overline{I}_L \right| \cdot \frac{X}{2}(\sin\varphi + j\cos\varphi) \qquad (4.2\_13)$$
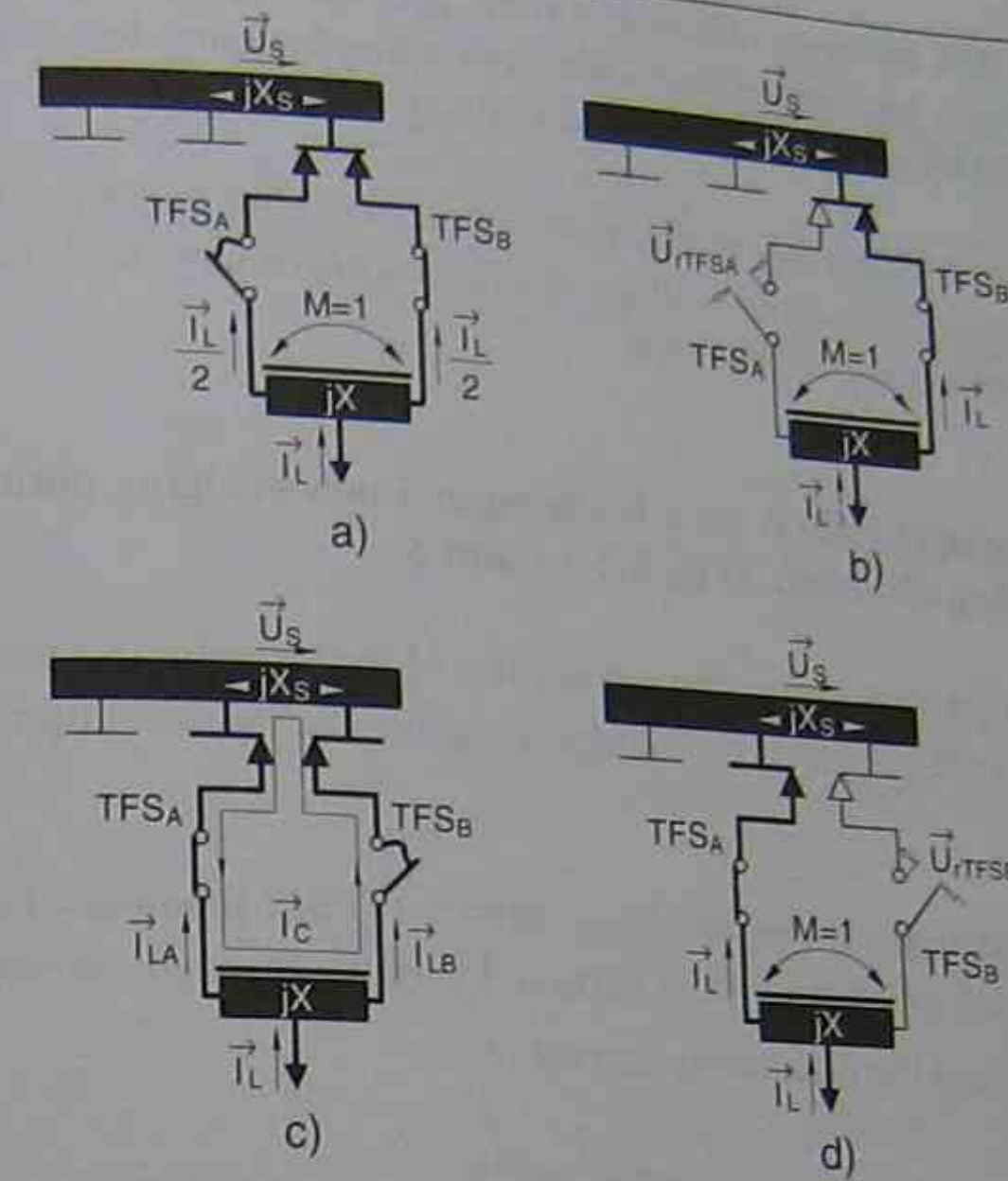
**Fig. 4.2-3:** Breaking at the transfer switches during operation from a non-bridging to bridging position (a, b) and from a bridging to a non-bridging position (c, d) just before and after arc quenching

With

$$\varphi_{ITFSA} = \text{arctg}\frac{\text{Im}\left(\overline{I}_{TFSA}\right)}{\text{Re}\left(\overline{I}_{TFSA}\right)} = \text{arctg}\frac{-\sin\varphi}{\cos\varphi} \qquad (4.2\_14a)$$

and

$$\varphi_{UTFSA} = \text{arctg}\frac{\text{Im}\left(\overline{U}_{TFSA}\right)}{\text{Re}\left(\overline{U}_{TFSA}\right)} = \text{arctg}\frac{\cos\varphi}{\sin\varphi} \qquad (4.2\_14b)$$

the phase shift between switched current and recovery voltage is calculated to:

$$\left|\Delta\varphi_{TFSA}\right| = \left|\varphi_{UTFSA} - \varphi_{ITFSA}\right| = \left|\text{arctg}\frac{\cos\varphi}{\sin\varphi} - \text{arctg}\frac{-\sin\varphi}{\cos\varphi}\right| \qquad (4.2\_14c)$$

With the relation $\text{arctg}(X) - \text{arctg}(Y) = \text{arctg}\frac{X-Y}{1+X\cdot Y}$ follows:

$$\left|\Delta\varphi_{TFSA}\right| = \left|\text{arctg}\frac{\dfrac{\sin\varphi}{\cos\varphi} - \dfrac{\cos\varphi}{\sin\varphi}}{1 + \dfrac{\sin\varphi}{\cos\varphi}\cdot\dfrac{\cos\varphi}{-\sin\varphi}}\right| = \left|\text{arctg}\frac{\dfrac{\sin\varphi}{\cos\varphi} - \dfrac{\cos\varphi}{\sin\varphi}}{1-1}\right| = 90° \quad (4.2\_14d)$$

The phase shift between switched current and recovery voltage at the breaking contact during a tap-change operation from a non-bridging to a bridging position is not affected by the power factor and is always 90 degrees.

A phase shift of 90 degrees is the most severe switching condition for an opening contact, because the recovery voltage reaches its maximum (peak value) when the arc extinguishes in the current zero.

**Tap-changing operation from a bridging to a non-bridging position in case of heavy switching direction (Fig. 4.2-3 c and d)**

For the following evaluation one tap section of the tap winding is represented by its equivalent voltage source $\bar{U}_S$ and its reactance $X_S$, the winding resistance shall be neglected.

The switched current at the breaking contact (TFS$_B$) (compare eq. 2.2_12 and 2.2_20) is the vectorial sum of the portion $\bar{I}_{LB}$ of the through-current which flows through path B and the circulating current $\bar{I}_C$:

$$\bar{I}_{TFSB} = \bar{I}_{LB} + \bar{I}_C \qquad (4.2\_15)$$

$\bar{I}_{LB}$ can be derived from:

$$j\bar{I}_{LB}\cdot\frac{X}{4} + jM\bar{I}_{LB}\cdot\frac{X}{4} + j\bar{I}_{LB}\cdot X_S = j\bar{I}_{LA}\cdot\frac{X}{4} + jM\bar{I}_{LA}\cdot\frac{X}{4} \qquad (4.2\_16a)$$

and

$$\bar{I}_{LB} + \bar{I}_{LA} = \bar{I}_L \qquad (4.2\_16b)$$

to

$$\bar{I}_{LB} = \bar{I}_L\cdot\frac{\dfrac{X}{2}}{X+X_S} \qquad (4.2\_16c)$$

The circulating current $\bar{I}_C$ is determined by:

$$\bar{I}_C = -j\frac{\bar{U}_S}{X+X_S} \qquad (4.2\_17)$$

For the switched current at the breaking contacts (TFS$_B$) follows with 4.2_16c and 4.2_17:

$$\bar{I}_{TFSB} = |\bar{I}_L|\frac{\dfrac{X}{2}}{X+X_S}\cos\varphi - j\left(|\bar{I}_L|\frac{\dfrac{X}{2}}{X+X_S}\sin\varphi + \frac{\bar{U}_S}{X+X_S}\right) \qquad (4.2\_18a)$$

with: $\varphi_{ITFSB} = \text{arctg}\dfrac{\text{Im}(\bar{I}_{TFSB})}{\text{Re}(\bar{I}_{TFSB})} = \text{arctg}\dfrac{-\left(|\bar{I}_L|\dfrac{\dfrac{X}{2}}{X+X_S}\sin\varphi + \dfrac{|\bar{U}_S|}{X+X_S}\right)}{|\bar{I}_L|\dfrac{\dfrac{X}{2}}{X+X_S}\cos\varphi}$ (4.2_18b)

$$\varphi_{ITFSB} = \text{arctg}\dfrac{-\left(|\bar{I}_L|\dfrac{X}{2}\sin\varphi + |\bar{U}_S|\right)}{|\bar{I}_L|\dfrac{X}{2}\cos\varphi} \qquad (4.2\_18c)$$

The recovery voltage at the open contact distance of TFS$_B$ is the verctorial sum of the voltage drop at the preventive autotransformer caused by the through-current and the step voltage (compare eq. 2.2_13 and 2.2_21):

$$\bar{U}_{rTFSB} = \bar{U}_S + j\bar{I}_L\cdot\frac{X}{4} + j\bar{I}_L M\cdot\frac{X}{4} = \bar{U}_S + j\bar{I}_L\cdot\frac{X}{2} \qquad (4.2\_19a)$$

$$\bar{U}_{rTFSB} = \bar{U}_S + j\bar{I}_L\cdot\frac{X}{2} = |\bar{U}_S| + |\bar{I}_L|\frac{X}{2}\sin\varphi + j|\bar{I}_L|\frac{X}{2}\cos\varphi \qquad (4.2\_19b)$$

with: $\varphi_{UTFSB} = \text{arctg}\dfrac{\text{Im}(\bar{U}_{rTFSB})}{\text{Re}(\bar{U}_{rTFSB})} = \text{arctg}\dfrac{|\bar{I}_L|\dfrac{X}{2}\cos\varphi}{|\bar{U}_S| + |\bar{I}_L|\dfrac{X}{2}\sin\varphi}$ (4.2_19c)

The equations 4.2_18c and 4.2_19c show that the phase angles of the switched current and the recovery voltage do not depend on the reactance $X_S$ of the tap section. With this the phase shift can be expressed as:

$$|\Delta\varphi_{TFSB}| = |\varphi_{UTFSB} - \varphi_{ITFSB}| \qquad (4.2\_20a)$$

$$|\Delta\varphi_{TFSB}| = \left|\text{arctg}\dfrac{|\bar{I}_L|\dfrac{X}{2}\cos\varphi}{|\bar{U}_S| + |\bar{I}_L|\dfrac{X}{2}\sin\varphi} - \text{arctg}\dfrac{-\left(|\bar{U}_S| + |\bar{I}_L|\dfrac{X}{2}\sin\varphi\right)}{|\bar{I}_L|\dfrac{X}{2}\cos\varphi}\right| \qquad (4.2\_20b)$$

$$|\Delta\varphi_{TFSB}| = \left|\text{arctg}\dfrac{\dfrac{|\bar{I}_L|\dfrac{X}{2}\cos\varphi}{|\bar{U}_S| + |\bar{I}_L|\dfrac{X}{2}\sin\varphi} + \dfrac{|\bar{U}_S| + |\bar{I}_L|\dfrac{X}{2}\sin\varphi}{|\bar{I}_L|\dfrac{X}{2}\cos\varphi}}{1 + \dfrac{|\bar{I}_L|\dfrac{X}{2}\cos\varphi}{|\bar{U}_S| + |\bar{I}_L|\dfrac{X}{2}\sin\varphi}\cdot\dfrac{-\left(|\bar{U}_S| + |\bar{I}_L|\dfrac{X}{2}\sin\varphi\right)}{|\bar{I}_L|\dfrac{X}{2}\cos\varphi}}\right| \qquad (4.2\_20c)$$

$$|\Delta\varphi_{TFSB}| = \left| \mathrm{arctg} \frac{\frac{|\bar{I}_L| \frac{X}{2} \cos\varphi}{|\bar{U}_S| + |\bar{I}_L| \frac{X}{2} \sin\varphi} + \frac{|\bar{U}_S| + |\bar{I}_L| \frac{X}{2} \sin\varphi}{|\bar{I}_L| \frac{X}{2} \cos\varphi}}{1-1} \right| = 90° \quad (4.2\_20d)$$

The phase shift between switched current and recovery voltage at the breaking contact during a tap-change operation from a bridging to a non-bridging position is not affected by the power factor and is always 90 degrees. Things look different when considering in addition to the reactance of the tap section also its resistance. The resulting phase shift must be smaller than 90 degrees and that means that the switching duty is less severe.

It was shown above that the phase angle between switched current and recovery voltage for operations from a non-bridging to a bridging position and vice versa is always 90 degrees and is not affected by the power factor. Only the phase angles of these two values relative to the step voltage are affected by the power factor.

One can conclude that the maximum switching duty occurs when the vectorial sums of the switched current on one hand and of the recovery voltage on the other hand reach their maximum. This occurs at power factor 0 ($\bar{I}_{LB}$ and $\bar{I}_C$ are in phase). This fact is considered in the standards which require to carry out the breaking capacity test at power factor 0, which represents the testing of the switching capacity of the OLTC.

### 4.2.2 PERMISSIBLE OVERLOAD OF OLTCs IN OIL-IMMERSED POWER TRANSFORMERS

The basic demands for overload of power transformers are given in IEC Publication 60076-1, Power Transformers - General, [IEC Publ. 60076-1 1993]. If specified, the transformer may be assigned, in addition to its rated power for continous loading, a temporary load cycle which it shall be capable of performing under conditions specified in IEC Publication 60076-2, Power Transformers - Temperature Rise, [IEC Publ. 60076-2 1993]. This option is to be used in particular to give a basis for design and guarantees concerning temporary emergency loading of large power transformers.

In the absence of such specification, guidance on loading of transformers may be found in IEC Publication 60354, Loading Guide for Oil-immersed Power Transformers, [IEC Publ. 60354 1991].

When OLTCs are used in transformers which are subjected to overload conditions, their selection should be such that they do not restrict the loading capability of the transformer. Same is valid for bushings or other auxiliary equipment.

All OLTC contacts and current paths which carry current continously must be dimensioned for all current stresses that occur on the transformer under rated load and permissible overload. If the overload conditions are in accordance with the IEC Publication 60354, the requirements with respect to the OLTC are met, in accordance with IEC Publication 60542 Application Guide for On-Load Tap-Changers, when the maximum rated through-current of the OLTC is at least 1.2 times the rated through-current or when the OLTC does not exceed the temperature rise limits given in IEC Publication 60214 On-Load Tap-Changers, when the contacts carry 1.2 times the maximum rated through-current. In addition, the transition resistors meet the overload conditions if the temperature rise above the surrounding medium does not exceed the temperature rise limits given in IEC Publication 60214 when carrying 1.5 times the maximum rated through-current. The number of tap-changes for each occasional overload period should be limited to the number of operations corresponding to one half of a complete operating cycle (number of operations as is required to move from one end of the tapping range to the other).

Also according to IEEE Standard C57.131 Requirements for Load Tap Changers [IEEE Standard C57.131 1995] the OLTC is suitable for the overload conditions specified in IEEE Standard C57.91 Guide for Loading Mineral-Oil-Immersed Transformers [IEEE Standard C57.91 1995] when the above mentioned requirements are fullfilled.

For particular applications, when OLTCs are subject to overload conditions that are not in accordance with the limitations stated in IEC Publication 60076-1 with regard to IEC Publication 60354, the OLTC manufacturer should be consulted for the correct OLTC selection based on the current magnitude and overload duration.

The Loading Guide for Oil-immersed Power Transformers (IEC Publication 60354) or other national standards indicate the values by which the transformers may be loaded above the rated conditions. The limits of loading are determined from the electrical, thermal and mechanical characteristics of the transformer insulation (usually: oil-paper) taking into consideration the loss of normal life expectancy of the transformer. These life expectancy considerations are not applicable to OLTCs, but overload factors and loading periods are important for OLTCs.

Between the national and the international standards there are deviations regarding the permissible overload. Therefore in the following only IEC requirements are considered. The loading periods are defined in IEC Publication 60354, paragraph 1.3.4 and 1.3.5:

### 1.3.4 Cyclic loading

*Loading with cyclic variations (the duration of the cycle usually being one day) which is regarded in terms of the average amount of ageing that occurs during the cycle. The cyclic loading may either be a normal loading, or a long-time emergency loading.*

#### a) Normal cyclic loading

*A higher ambient temperature or a higher than rated load current is applied during part of the cycle, but, from the point of view of thermal ageing (according to the mathematical model), this loading is equivalent to the rated load at normal ambient temperature. This is achieved by taking advantage of low ambient temperatures or low-load currents during the rest of the load cycle. For planning purposes, this principle can be extended to provide for long periods of time whereby cycles with ageing rates greater than unity are compensated for by cycles with ageing rate less than unity.*

#### b) Long-time emergency cyclic loading

*Loading resulting from the prolonged outage of same system elements that will not be reconnected before a steady state temperature rise is reached in the transformer. This is not a normal operating condition and its occurrence is expected to be rare, but it may persist for weeks or even months and can lead to considerable ageing. However, it should not be the cause of breakdown due to thermal destruction or reduction of dielectric strength.*

### 1.3.5 Short-time emergency loading

*Unusually heavy loading due to the occurrence of one or more unlikely events which seriously disturb normal system loading, causing the conductor hot spots to reach dangerous levels and, possibly, a temporary reduction in the dielectric strength. However, acceptance of this condition for a short time may be preferable to other alternatives. This type of loading is expected to occur rarely and it must be rapidly reduced or the transformer disconnected within a short time in order to avoid its failure. The permissible duration of this load is shorter than the thermal time constant of the transformer and depends on the operating temperature before the increase in the loading; typically, it would be less than half an hour.*

Furthermore, in accordance with IEC Publication 60354 power transformers can be divided into three classes with respect to their rated capacity. For these three classes different current and temperature limits are valid. With respect to the overload considerations of OLTCs Table 4.2-1 shows only the current limits. The indicated overload factors are covered by the type tests performed on OLTCs according to IEC Publication 60214.

**Table 4.2-1:** Current limitations applicable to loading beyond nameplate rating (excerpt from Table 1 in IEC 60354)

| Type of loading<br><br>Transformer class | Normal cyclic loading<br><br>current (p.u.) | Long-time emergency loading<br>current (p.u.) | Short-time emergency loading<br>current (p.u.) |
|---|---|---|---|
| **Distribution transformers**<br><br>(acc. to IEC 60354, paragraph 1.3.1: three-phase ≤ 2,500 kVA single-phase ≤ 833 kVA) | 1.5 | 1.8 | 2.0 |
| **Medium power transformers**<br><br>(acc. to IEC 60354, paragraph 1.3.2: three-phase ≤ 100 MVA single-phase ≤ 33.3 MVA) | 1.5 | 1.5 | 1.8 |
| **Large power transformers**<br><br>(acc. to IEC 60354, paragraph 1.3.3: three-phase > 100 MVA) | 1.3 | 1.3 | 1.5 |

### 4.2.2.1 NORMAL CONTINUOUS LOADING

In case of continuous loading the difference between transformer and OLTC must be considered. The acceptable load factors for transformers are defined in IEC Publication 60354. If the load current over a certain period of time shows no pronounced variation, a constant equivalent load current may be used. Table 4.2-2, taken from IEC Publication 60354, gives acceptable load factors for transformers $K = K_{24}$ ($K_{24}$: load factor for 24 hours per day) for continuous duty for different ambient temperatures.

**Table 4.2-2:** Acceptable load factor for continuous duty $K_{24}$ at different ambient temperatures (ONAN, ON, OF and OD cooling) [IEC Publ. 60354 1991]

| Ambient temperature °C | | | -25 | -20 | -10 | 0 | 10 | 20 | 30 | 40 |
|---|---|---|---|---|---|---|---|---|---|---|
| Hot-spot-temperature rise K | | | 123 | 118 | 108 | 98 | 88 | 78 | 68 | 58 |
| $K_{24}$ | Distribution Transformers | ONAN | 1.37 | 1.33 | 1.25 | 1.17 | 1.09 | 1.00 | 0.91 | 0.81 |
| | Power Transformers | ON | 1.33 | 1.30 | 1.22 | 1.15 | 1.08 | 1.00 | 0.92 | 0.82 |
| | | OF | 1.31 | 1.28 | 1.21 | 1.14 | 1.08 | 1.00 | 0.92 | 0.83 |
| | | OD | 1.24 | 1.22 | 1.17 | 1.11 | 1.06 | 1.00 | 0.94 | 0.87 |

These load factors consider the fact that, in case of transformers, different ambient temperatures or different methods of cooling lead to different oil temperatures within the transformer at constant load current, or vice versa, that a constant (or maximum) oil temperature within the transformer can be reached with different load currents under the above mentioned circumstances.

Taking for example a power transformer with forced oil cooling, the load factors of 1.31 at -25°C and of 0.92 at 30°C can be derived from Table 4.2-2. Both loadings lead to the same oil temperature within the transformer. Therefore, an OLTC which is installed in the transformer tank (in-tank type) is surrounded by transformer oil that shows a constant temperature. Consequently the OLTC conditions do not change in regards to the ambient temperature at different loadings. Things look different if the OLTC is mounted in its own oil compartment (compartment type). It can be stated that the load factors given in Table 4.2-2 for continuous loading are not generally valid for OLTCs. This fact must be taken into account when selecting an OLTC and it is considered in the standards.

In IEC Publication 60076-1, sub-clause 4.1, it is stated that the rated power of a transformer, which shall be marked on the rating plate, must refer to the continuous loading. If different values of apparent power are assigned under different circumstances (for example with different methods of cooling) the highest of these values is the rated power. This sentence is also applicable to different ambient temperatures.

Furthermore, according to IEC Publication 60542 the OLTC must be selected for the highest magnitude of the tapping current which results from the rated power, and must be capable of carrying and breaking occasional overload currents.

From these statements two conclusions can be made:

- The normal continuous loading is not an overload condition with respect to the OLTC, but a normal service condition.

- The OLTC must be selected in such a way that the rated through-current of the OLTC is not less than the highest tapping current with normal continuous loading under different circumstances.

## 4.2.2.2 CYCLIC LOADING

The following three examples show the permissible cyclic loading according to IEC Publication 60354 for normal, long- and short-time emergency cyclic loading with respect to the transformer and the OLTC. The ambient temperature, the initial load (load factor and duration) and the peak load (load factor and duration) are kept constant for all three examples. Other examples at different ambient temperatures or

The values given in the following tables have been determined with the diagrams and tables of IEC Publication 60354.

| Example A |
|---|
| Three-phase medium power transformer 16 MVA, 66 (1 ± 10 · 1.0%) kV |

Regulation: neutral end          Type of cooling: ON (natural cooling)

max. tapping current:     156A          step voltage:     $\dfrac{660V}{\sqrt{3}} = 381V$

selected OLTC:          three-phase OLTC for neutral end application
max. rated through-current:     200A
max. rated step voltage:     1,400V
rated switching capacity:     280kVA

Table 4.2-3: Permissible load factors for a medium power transformer according to example A

| Type of loading | Normal cyclic loading | Long-time emergency cyclic loading | Short-time emergency cyclic loading |
|---|---|---|---|
| Ambient temperature $\theta_A$ | 10°C | | |
| **Initial load** | | | |
| Duration | 22 hours | | |
| Factor $K_1$ | 0.8 | | |
| Capacity | 12.8 MVA | | |
| max. tapping current | 125 A | | |
| **Peak Load** | | | |
| Duration | 2 hours | | |
| Factor $K_2$ | 1.47 (Figure 10)[1] | 1.5 (Tables 1 and 15)[1] | 1.7 (Tables 1 and 15)[1] |
| Capacity | 23,5 MVA | 24.0 MVA | 27.2 MVA |
| max. tapping current | 229 A | 233 A | 264 A |
| Loss of life (Table 15)[1] | normal | 1.32 · normal | 15.6 · normal |
| Hot-spot temperature (Table 15)[1] | - | 132°C | 156°C |

**Remarks:**
1) Designations of tables and figures refer to IEC Publication 60354

**Example B**

Three-phase medium power transformer 63 MVA, 110 (1 ± 13 · 1.69%) kV

Regulation: neutral end          Type of cooling: OF (forced cooling)

max. tapping current:     424A          step voltage:     $\dfrac{1{,}859V}{\sqrt{3}} = 1{,}074V$

selected OLTC:     three-phase OLTC for neutral end application
                           max. rated through-current:     500A
                           max. rated step voltage:          3,300V
                           rated switching capacity:        1,400kVA

Table 4.2-4: Permissible load factors for a medium power transformer according to example B

| Type of loading | Normal cyclic loading | Long-time emergency cyclic loading | Short-time emergency cyclic loading |
|---|---|---|---|
| Ambient temperature $\theta_A$ | 10°C | | |
| **Initial load** | | | |
| Duration | 22 hours | | |
| Factor $K_1$ | 0.8 | | |
| Capacity | 50.4 MVA | | |
| max. tapping current | 339 A | | |
| **Peak Load** | | | |
| Duration | 2 hours | | |
| Factor $K_2$ | 1.33 (Figure 11)[1] | 1.4 (Tables 1 and 21)[1] | 1.5 (Tables 1 and 21)[1] |
| Capacity | 83.8 MVA | 88.2 MVA | 94.5 MVA |
| max. tapping current | 564 A | 593 A | 636 A |
| Loss of life (Table 21)[1] | normal | 2.9 · normal | 14.2 · normal |
| Hot-spot temperature (Table 21)[1] | - | 137°C | 152°C |

**Remarks:**
1) Designations of tables and figures refer to IEC Publication 60354

**Example C**

Three-phase large power transformer 1000 MVA, 420 (1 ± 9 · 1.25%) kV

Regulation: neutral end          Type of cooling: OD (forced and directional cooling)

max. tapping current:     1,549A          step voltage:     $\dfrac{5{,}250V}{\sqrt{3}} = 3{,}031V$

selected OLTC:     three-phase OLTC for neutral end application
                           max. rated through-current:     1,600A
                           max. rated step voltage:          5,000V
                           rated switching capacity:        5,000kVA

Table 4.2-5: Permissible load factors for a large power transformer according to example C

| Type of loading | Normal cyclic loading | Long-time emergency cyclic loading | Short-time emergency cyclic loading |
|---|---|---|---|
| Ambient temperature $\theta_A$ | 10°C | | |
| **Initial load** | | | |
| Duration | 22 hours | | |
| Factor $K_1$ | 0.8 | | |
| Capacity | 800 MVA | | |
| max. tapping current | 1239 A | | |
| **Peak Load** | | | |
| Duration | 2 hours | | |
| Factor $K_2$ | 1.28 (Figure 21)[1] | 1.3[2] (Tables 1 and 27)[1] | 1.4 (Tables 1 and 27)[1] |
| Capacity | 1,280 MVA | 1,300 MVA | 1,400 MVA |
| max. tapping current | 1,983 A | 2,014 A | 2.168 A |
| Loss of life (Table 27)[1] | normal | 1.81 · normal | 14.2 · normal |
| Hot-spot temperature (Table 27)[1] | - | 133°C | 153°C |

**Remarks:**
1) Designations of tables and figures refer to IEC Publication 60354
2) When using the Tables 1 and 27 of IEC Publication 60354 the peak loading for 2 hours during long-time emrgency cyclic loading reaches a value of 1.2 (limitation: permissible hot-spot temperature of 130°C). Since it does not make sense that the peak loading of the normal cyclic loading is larger than the long-time emergency cyclic loading, a load factor $K_2$ of 1.3 has been chosen. This although the hot-spot temperature limitation is exceeded by 3°C.

initial loads do not provide any new facts regarding the OLTC and therefore have not been included.

Independent on the thermal based load factors resulting from IEC Publication 60354, OLTCs can be operated at up to twice the maximum tapping current of the transformer if the selection of the OLTC is done according to the IEC Publications 60076-1, 60542 and 60214 (maximum tapping current is smaller than the maximum rated through-current). However, for safety reasons it is recommended to include a protective device in the motor drive to prevent operation of the motor drive or to interrupt the tap-change in operation when the transformer load exceeds 1.5 times the maximum tapping current (compare IEC Publication 60542, sub-clause 4.1).

The OLTCs used in the examples can withstand the overloading given in Tables 4.2-3 to 4.2-5 as long as they fullfill the IEC Publication 60214 requirements. The figures of loss of life do not relate to the OLTC life time, they relate to the transformer insulation only.

### 4.2.3 TRANSITION RESISTOR LAYOUT

The reliability of the load-transfer system of the OLTC is largely determined by the ability of the diverter switch contact system to quench the through-current within the predetermined switching sequence. This ability depends on design parameters as contact speed, contact stroke, contact material and the design of the arcing area as well as the transition resistor layout (ohmic value and thermal capacity).

The most important condition which has to be fullfilled during a diverter switch operation is that the arc at the main switching contact of the opening side (connected to the tap in service) is quenched before the main switching contact of the closing side (connected to the pre-selected tap) has been closed. This has to be considered when judging the switching capability or the safety of operation of a diverter switch. Arc quenching at the transition contacts is of secondary importance even if such arcs are prolonged until the main switching contact of the closing side has been closed.

The breaking capacity of the OLTC is defined as the product of the relevant rated step voltage and the rated through-current. However, the switching duty of main and transition contacts within the OLTC not only depends on the above mentioned pair of values but also on the method of performing the tap-change operation and the ohmic value of the transition resistor (compare chapter 2).

Usually the transition resistors are to be adjusted to the rated through-current and the relevant rated step voltage of the transformer so that the switched currents and recovery voltages at the several contacts do not exceed those covered by the type test. In general, the through-current of the OLTC may vary along the regulating range. The rated through-current is the highest possible current which can flow through the tap winding of the transformer.

The adjustment of the transition resistors covers aspects like temperature rise of the transition resistors, contact wear (contact life) of the several contacts, differences in contact wear between the main switching and the transition contacts and compliance with the limits of switched currents and recovery voltages. However, the number of different transition resistor values should be limited for economic reasons.

Besides all material and design aspects, the contact wear of breaking contacts is determined by the arc-drop voltage, the switched current and the arcing time. It can be assumed for a given design that the arc-drop voltage does not depend on the switched current. However, the arcing time does depend on the switched current and the recovery voltage. On condition that the current breaks in the first current zero after contact separation (arc quenching within one halfwave of the sinusoidal current), the contact wear of the main switching and transition contacts can be assumed to be a function only of the switched current. The condition of arc quenching within one halfwave usually is fullfilled if the arising recovery voltage is equal or below value confirmed in the type tests.

In the following it will be shown how the transition resistor influences the switched current and recovery voltage. For this purpose a flag cycle operating diverter switch has been chosen (refer to paragraph 2.1.2.1).

The following equations for the main switching contact duty and the transition contact duty are taken from Tables 2.1-3 and 2.1-4:

**main switching contact**

switched current: $\bar{I}_{MS} = \bar{I}_L$          recovery voltage: $\bar{U}_{rMS} = \bar{I}_L \cdot R$

**transition contact (heavy switching direction)**

switched current: $\bar{I}_{Th} = \left(\bar{U}_S + \bar{I}_L \cdot R\right) \cdot \dfrac{1}{2 \cdot R}$     recovery voltage: $\bar{U}_{rTh} = \bar{U}_S + \bar{I}_L \cdot R$

**transition contact (light switching direction)**

switched current: $\bar{I}_{Tl} = \left(\bar{U}_S - \bar{I}_L \cdot R\right) \cdot \dfrac{1}{2 \cdot R}$     recovery voltage: $\bar{U}_{rTl} = \bar{U}_S - \bar{I}_L \cdot R$

The equations above show that the contact wear at the main switching contact only depends on the through-current resp. the load current.

For the estimation of the contact wear of the transition contact it has to be considered that not every operation is a heavy operation. It can be assumed as a mean value that the operations are distributed evenly into heavy and light operations. Following this the switched current at the transition contact $\bar{I}_T$ can be expressed as a mean value of the heavy $\bar{I}_{Th}$ and light $\bar{I}_{Tl}$ switching operations.
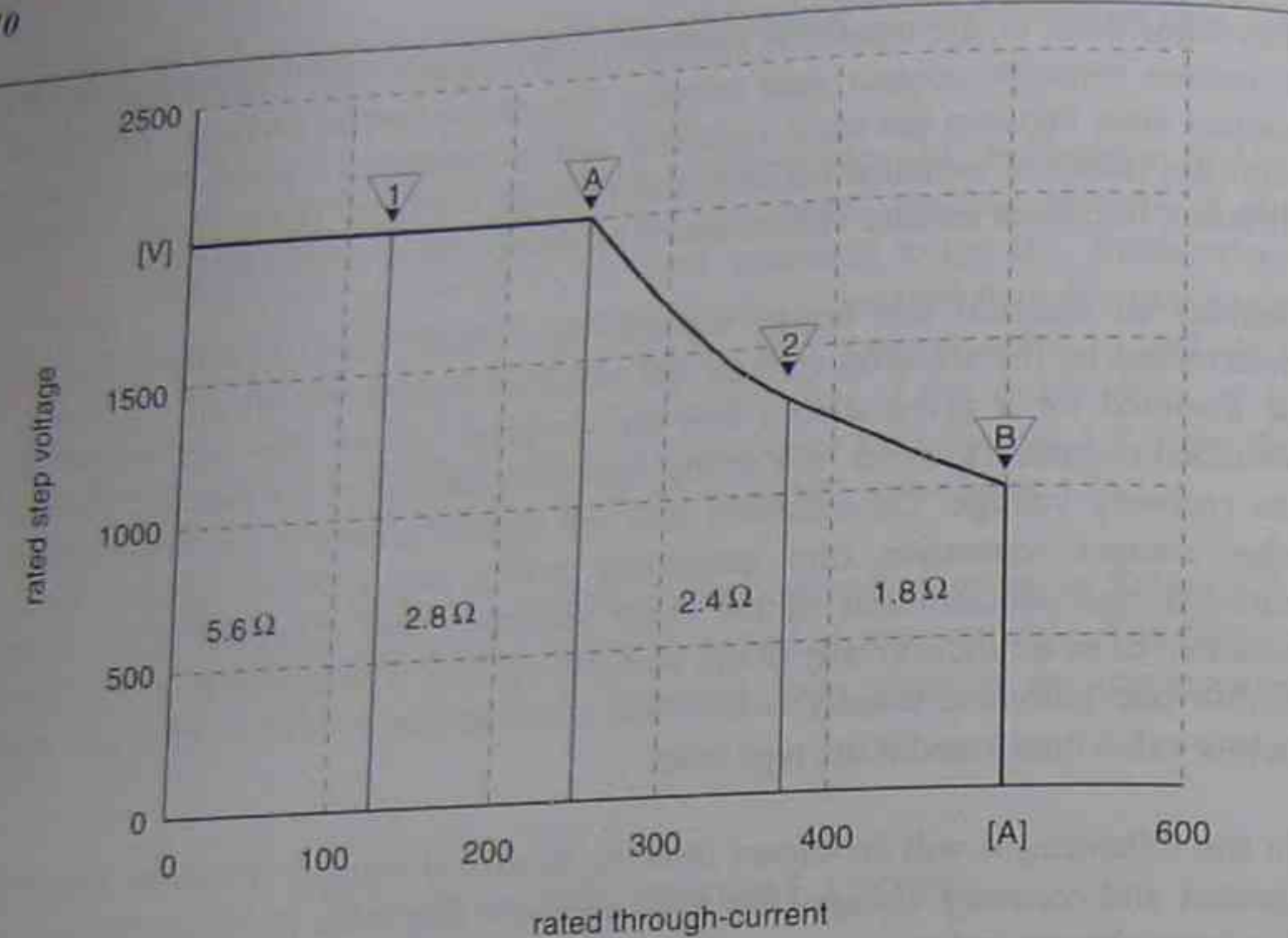
**Fig. 4.2-4:** Rated breaking capacities and transition resistor matrix of a 500 A, 500 kVA OLTC (simplified example)

**transition contact (mean value of light and heavy switching direction)**

$$\text{switched current:} \quad \overline{I}_T = \frac{\overline{I}_{Th} + \overline{I}_{Tl}}{2} = \frac{\overline{U}_S}{2 \cdot R}$$

It can be seen that the mean value of the switched current at the transition contact only depends on the step voltage and the transition resistor. This current value is equal to the circulating current $\overline{I}_c$ (compare equation 2.1_4). The design of the OLTC and the loading of the transformer (network transformer, generator transformer, industrial process transformer) determine the preferred relation between the switched currents at the transition and main switching contacts. Of course, in addition the maximum permissible recovery voltages have to be taken into account when designing the transition resistor.

Figure 4.2-4 shows a simplified example of the rated breaking capacities (relevant rated step voltages vs. rated through-currents) of an OLTC using the flag cycle operation with a maximum rated through-current of 500 A and a maximum step voltage of 2.000 V. The rated switching capacity is 500 kVA.

Within the rated breaking capacity curve there are application areas with different transition resistor values. The maximum switching stresses occur at the upper edges of the application areas (in Fig. 4.2-4 indicated with numbered triangles). For these load points the switching stresses on the main switching and transition contacts were

calculated at twice the rated through-current and are shown in Table 4.2-6. The calculation was performed at twice the rated through-current, because the breaking capacity of a diverter switch is tested during the type test. This breaking capacity test (40 operations) must be carried out at twice the maximum rated through-current and the relevant rated step voltage (load point B). If necessary, a second breaking capacity test (40 operations) must be carried out at the maximum rated step voltage and twice the relevant rated through-current (load point A).

In Table 4.2-6 it can be seen also that for the chosen transition resistor selection matrix all switched currents and recovery voltages at the main switching and transition contacts do not exceed those covered by the type test (load points A and B).

The adjustment of the transition resistors to the maximum load current and the relevant step voltage of the transformer is done once the ratings have been defined by the customer. This adjustment limits the current for the OLTC application. Herewith the rated load current of the OLTC is determined by the selected transition resistors and, usually, this load current is less than the maximum rated through-current for which the OLTC was designed. Significant changes of the rated through-current and/or the relevant rated step voltage lateron in service have to be checked by the OLTC manufacturer with respect to the transition resistor selection. This shall be demonstrated with an example.

**Table 4.2-6:** Switching stresses at twice the through-current on the main switching and transition contacts of a diverter switch according to the breaking capacities and transition resistor selection matrix of Fig. 4.2-4

| load point | through-current [A] | step voltage [V] | transition resistor [Ω] | main switching contatcts | | | transition contacts | | |
|---|---|---|---|---|---|---|---|---|---|
| | | | | switched current [A] | recovery voltage [V] | switching duty [kVA] | switched current [A] | recovery voltage [V] | switching duty [kVA] |
| A | 250 | 2000 | 2.80 | 500.00 | 1400.00 | 700.00 | 607.14 | 3400.00 | 2064.29 |
| B | 500 | 1000 | 1.80 | 1000.00 | 1800.00 | 1800.00 | 777.78 | 2800.00 | 2177.78 |
| 1 | 125 | 2000 | 5.60 | 250.00 | 1400.00 | 350.00 | 303.57 | 3400.00 | 1032.14 |
| | | | 2.80 | 250.00 | 700.00 | 175.00 | 482.14 | 2700.00 | 1301.79 |
| A | 250 | 2000 | 2.80 | 500.00 | 1400.00 | 700.00 | 607.14 | 3400.00 | 2064.29 |
| | | | 2.40 | 500.00 | 1200.00 | 600.00 | 666.67 | 3200.00 | 2133.33 |
| 2 | 375 | 1333 | 2.40 | 750.00 | 1800.00 | 1350.00 | 652.78 | 3133.33 | 2045.37 |
| | | | 1.80 | 750.00 | 1350.00 | 1012.50 | 745.37 | 2683.33 | 2000.07 |

OLTC according to Fig. 4.2-4:

max. rated through-current:     500 A
rated load point 1:             500 A / 1,000 V
rated load point 2:             250 A / 2,000 V

The transition resistors are selected for:

step voltage:                           1,675 V
rated through-current (max. value):     230 A

This pair of values leads to a transition resistor of $2.8\Omega$ (according to Fig. 4.2-4).

The values for the breaking capacity, recovery voltage and switched current at the main switching and transition contacts at rated through-current and twice rated through-current are given in Table 4.2-7. In addition, this table shows the values confirmed during the type tests (load points A and B at twice the rated through-current). All occuring stresses including twice the rated through-current during overload are covered by the type test.

Now the the same OLTC with transition resistors of $2.8\Omega$ shall be used with a different rating:

step voltage:                           1,250 V
rated through-current (max. value):     450 A

The new rating is within the rated breaking capacities for which the OLTC was designed, but the selected transition resistors are not adjusted. The occuring stresses are also given in Table 4.2-7.

**Table 4.2-7:** Switching stresses at rated through-current and at twice rated through-current at different load points (the transition resistors are adjusted to only one of these load points)

| | rated through-current I [A] | rated step voltage [V] | selected transi-tion resistor [Ω] | main switching contatcts | | | transition contacts (heavy dir.) | | |
|---|---|---|---|---|---|---|---|---|---|
| | | | | switched current [A] | recovery voltage [V] | switching duty [kVA] | switched current [A] | recovery voltage [V] | switching duty [kVA] |
| A | 250 | 2000 | 2.80 | 500.00 | 1400.00 | 700.00 | 607.14 | 3400.00 | 2064.29 |
| B | 500 | 1000 | 1.80 | 1000.00 | 1800.00 | 1800.00 | 777.78 | 2800.00 | 2177.78 |
| $1 \cdot I_u$ | 230 | 1675 | 2.80 | 230.00 | 644.00 | 148.12 | 379.61 | 2319.00 | 880.31 |
| $2 \cdot I_u$ | | | | 460.00 | 1288.00 | 592.48 | 529.11 | 2963.00 | 1567.74 |
| $1 \cdot I_u$ | 450 | 1250 | 2.80 | 450.00 | 1260.00 | 567.00 | 380.71 | 2510.00 | 955.59 |
| $2 \cdot I_u$ | | | | 900.00 | 2520.00 | 2268.00 | 673.21 | 3770.00 | 2538.02 |
| $2 \cdot I_u$ | 320 | 1250 | 2.80 | 640.00 | 1792.00 | 1146.88 | 543.21 | 3042.00 | 1652.46 |

Table 4.2-7 shows that the occuring stresses at the main switching and transition contacts also at twice the rated through-current are covered by the type tested values in case of a rated through-current and rated step voltage for which the transition resistors were selected (230 A \ 1,675 V). The use of the same transition resistors for the second pair of values of rated through-current and rated step voltage (450 A \ 1,250V) leads to stresses at twice the rated through-current which are not covered by the type test.

To prevent exceeding the type tested limits at twice the rated through-current with the given step voltage of 1,250 V and the selected transition resistor of $2.8\Omega$, the maximum load current should not exceed 320 A. The occuring stresses at the breaking contacts are given in the last line of Table 4.2-7. The most limiting factor in this case is the recovery voltage at the main switching contact. This is the application limit for the selected transition resistor at the given step voltage when fullfilling the overload requirements of the IEC standards.

For this OLTC with the selected transition resistor ($2.8\Omega$) the change from the original rating (230 A \ 1,675 V) to the new rating (450 A \ 1,250V) is equivalent to a continous overload of 41% (450 A / 320 A).

### 4.2.4 IMPROVEMENT OF THE THROUGH-CURRENT BY PARALLEL CONNECTION

Generally it is possible to increase the rated through-current when connecting diverter switches or OLTCs in parallel. However, there are some specific consideration that have to be taken into account and which result in some restrictions.

A direct connection of two or more diverter switches to one tap winding is only permitted if the diverters are driven by one common energy accumulator. If, for example, two diverter switches are driven by separate energy accumulators, it cannot be prevented that the diverters operate one after the other (the operation of the first diverter is completed before the operation of the second has started). In this case a short-circuit of one tap section of the tap winding will occur, because two different taps will be in service at the same time without limiting impedances. Therefore, the connection of two or more separate OLTCs to one tap winding is not permitted.

However, the principle of diverter switches connected in parallel and driven by one energy accumulator is used by OLTC manufacturers to increase the bandwith of their products and is available for most designs of resistor switching type OLTCs. However, it needs to be considered that the use, for example, of three diverter switches connected in parallel does not result in three times the switching capability of a single unit. The possible increase depends on the design.

## 4.2.4.1 DIVERTER SWITCHES CONNECTED IN PARALLEL WITH ENFORCED CURRENT SPLITTING

When using transformer winding designs with two or more parallel winding branches, it is possible to reach an enforced current splitting. If the parallel current pathes have the same impedance a symmetrical current splitting occurs and n diverter switches connected in parallel can be loaded with n-times the rated through-current of one of the diverter switches.

The impedance of one current path consists of the impedance of the winding and the impedance of the OLTC. Requirements on the value of the winding impedance cannot be deduced from the OLTC when the diverter switch is in the neutral position, because the impedance of the current pathes of the diverter switches and tap selectors being connected in parallel do not differ considerably. This may change when considering the different steps during the diverter switch operation, where the current splitting must also be symmetrical. This demand on the current splitting must be fulfilled across the entire regulating range, also in that position where the fine tap winding is not effective (linear and coarse/fine regulation: position of minimum winding number of turns; boost and buck regulation: K-position). The symmetrical splitting cannot be achieved only by dividing the fine tap winding in parallel branches. On the contrary, the entire transformer winding has to be divided in parallel branches.

To get an idea of the necessary impedance between the windings the following assumptions are made. The diverter switches connected in parallel are driven by one energy accumulator and are of the same design with an identical transition resistor layout. Further, it is assumed that the mechanical opening and closing moments of the breaking contacts of the different diverters are within ± 1.5 ms. Consequently, the operation of the parallel diverter switches can be judged as being simultaneous and the different operating steps of the diverters can be evaluated separately (see 2.1.1).

**First operating step (breaking of the main switching contact)**

There are different chronological orders of arc quenching possible at the switching contacts that are connected in parallel. These will be shown for two typical applications:

Case 1:   Parallel connection of three diverter switches

Case 1.1: The current breaks at the three main switching contacts in the same current zero after contact separation.
Case 1.2: The current breaks at one main switching contact in the first current zero, whereas the other two main switching contacts break current in the second current zero after contact separation.

Case 1.3: The current breaks at two main switching contacts in the first current zero, whereas the last main switching contact breaks current in the second current zero after contact separation.

Case 2:   Parallel connection of two diverter switches

Case 2.1: The current breaks at the two main switching contacts in the same current zero after contact separation.
Case 2.2: The current breaks at one main switching contact in the first current zero and at the other main switching contact in the second current zero after contact separation.

In cases 1.1 and 2.1 the symmetrical current splitting is ensured and the switched current at every main switching contact $\bar{I}_{MSx}$ is one third and one half respectively of the through-current $\bar{I}_L$:

Case 1.1:
$$\bar{I}_{MS-C11} = \frac{\bar{I}_L}{3} \qquad (4.2\_21a)$$

Case 2.1:
$$\bar{I}_{MS-C21} = \frac{\bar{I}_L}{2} \qquad (4.2\_21b)$$

These relations may change for the other cases, because the transition resistor becomes effective after arc quenching and results in a current displacement, i.e. the switched current of the residual contacts increases. The magnitude of the current displacement is a function of the relation of the impedances of the winding and the transition resistors. As an example case 1.2 will be calculated in detail on the following. Figure 4.2-5 shows the circuit diagram of an OLTC with multiple resistor cycle mode of operation valid for the calculation of the switching conditions of case 1.2.

Further, the following simplification is considered:

$$Z_1 = Z_2 = Z_3 = jX \qquad (4.2\_22a)$$

$$\bar{I}_2 = \bar{I}_3 \quad resp. \quad \bar{I}_{MS2} = \bar{I}_{MS3} = \bar{I}_{MS-C12} \qquad (4.2\_22b)$$

It can be assumed that both transition contacts of the opening side are closed when the second arc quenching attempt at the residual main switching contacts ($MS_2$ and $MS_3$) takes place. Therefore, the two transition contacts are connected in parallel and can be expressed with their equivalent resistor

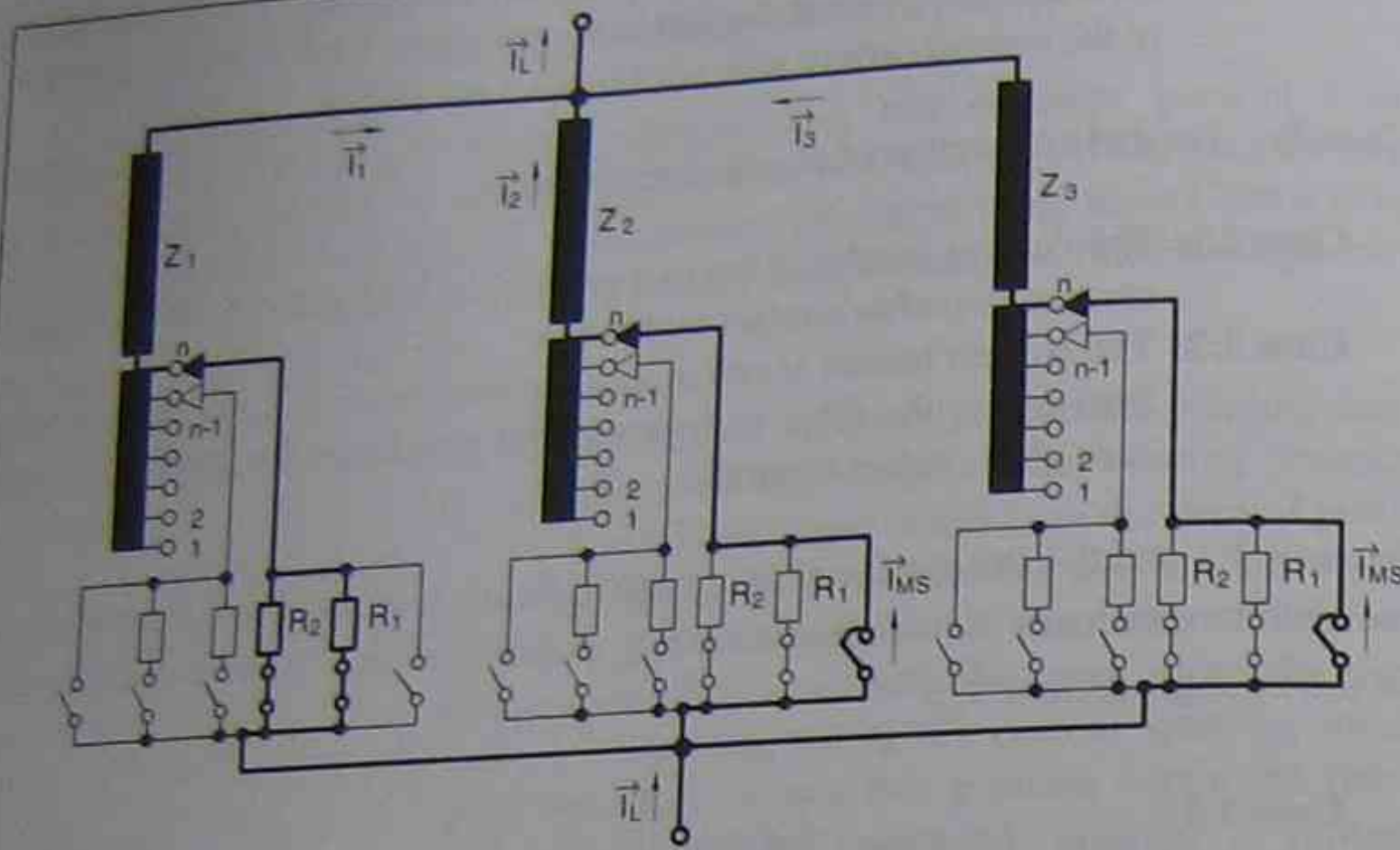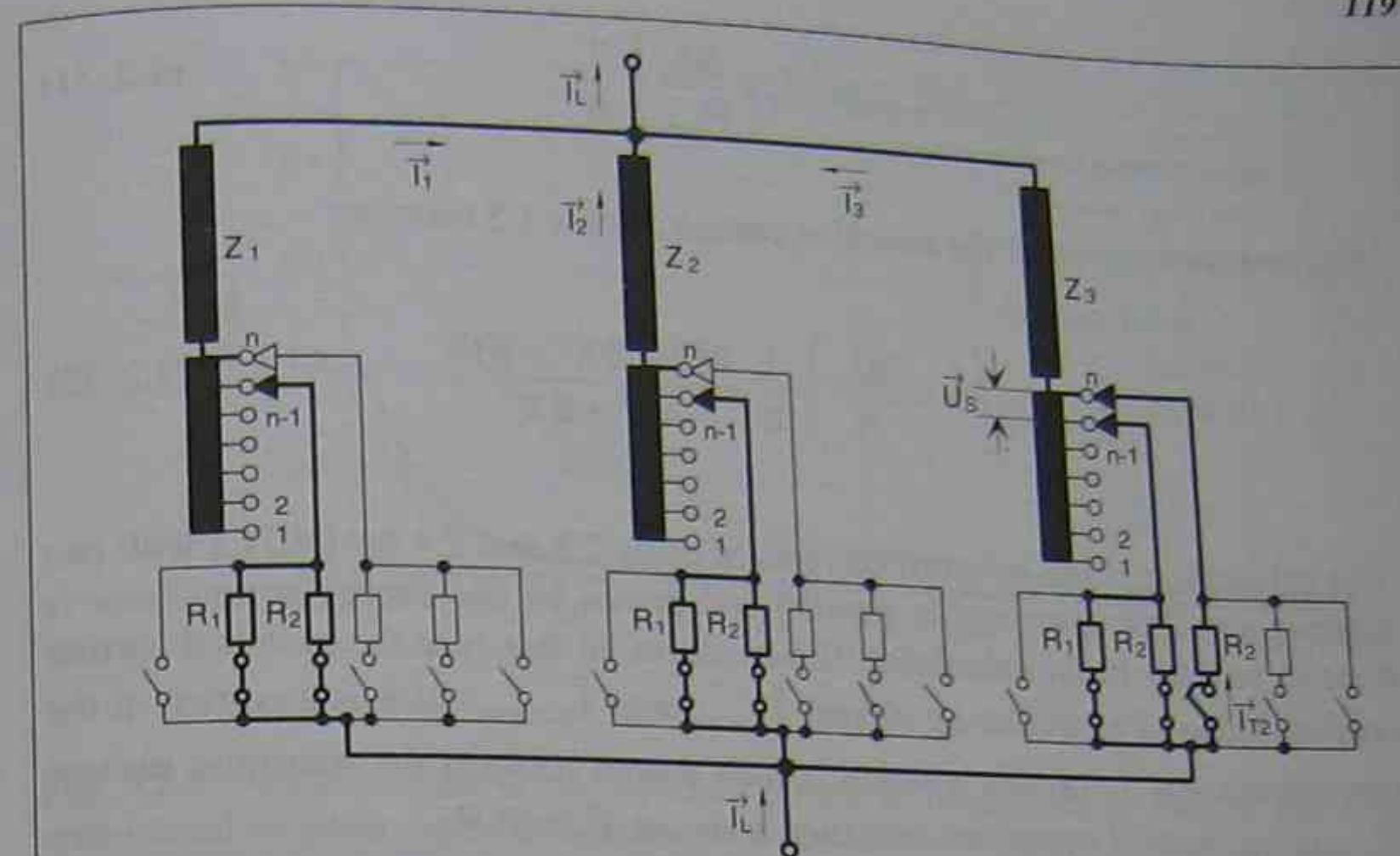$$R_{par} = \frac{R_1 \cdot R_2}{R_1 + R_2} \qquad (4.2\_23)$$

**Fig. 4.2-5:** Circuit diagram valid for case 1.2 of current splitting for three diverter switches connected in parallel

The calculation of the switched current $\overline{I}_{MS-C12}$ at the main switching contacts, that have not yet interrupted the current, is as follows

$$\overline{I}_L = \overline{I}_1 + \overline{I}_2 + \overline{I}_3 = \overline{I}_1 + \overline{I}_{MS2} + \overline{I}_{MS3} = \overline{I}_1 + 2 \cdot \overline{I}_{MS-C12} \quad (4.2\_24a)$$

$$\overline{I}_1 \cdot (R_{par} + jX) = \overline{I}_{MS-C12} \cdot jX \quad (4.2\_24b)$$

and results to

$$\overline{I}_{MS-C12} = \overline{I}_L \cdot \frac{2R_{par}^2 + 3X^2 - jXR_{par}}{4R_{par}^2 + 9X^2}. \quad (4.2\_25)$$

The same calculation for the case 1.3 leads to the switched current $\overline{I}_{MS-C13}$

$$\overline{I}_{MS-C13} = \overline{I}_L \cdot \frac{R_{par}^2 + 3X^2 - j2XR_{par}}{R_{par}^2 + 9X^2} \quad (4.2\_26)$$

and for case 2.2 to the switched current $\overline{I}_{MS-C22}$

$$\overline{I}_{MS-C22} = \overline{I}_L \cdot \frac{R_{par}^2 + 2X^2 - jXR_{par}}{R_{par}^2 + 4X^2}. \quad (4.2\_27)$$
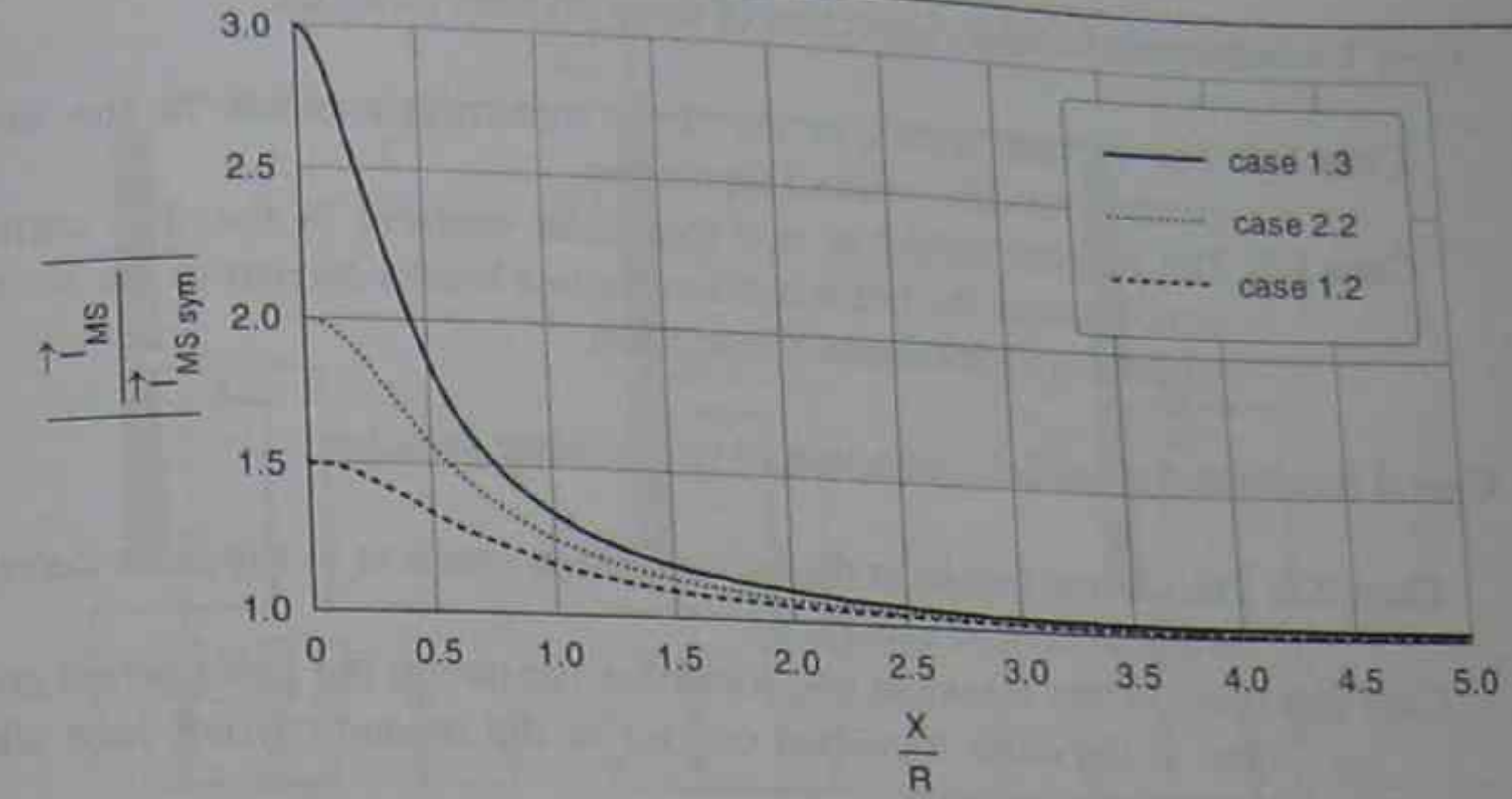


**Fig. 4.2-6:** Absolute value of the switched current in relationship to that of the relevant symmetrical switched current as function of the X/R-ratio.

The equations 4.2_25 to 4.2_27 can also be used for OLTCs with flag cycle mode of operation (compare 2.1.2.1) when taking the resistor $R_{par}$ as the effective transition resistor $R$ of one diverter.

Figure 4.2-6 shows the absolute value of the switched current at the main switching contacts in relationship to that of the ideal switched current (symmetrical current splitting) for the different cases. For small X/R-ratios the current displacement reaches values up to three times the symmetrical current. The magnitude of the admissible displacement depends on the design. Regarding the rated through-current and the switching capability of the single diverter switches, X/R-ratios of 2 to 3 and higher seem to be acceptable. This results in an unsymmetry of 5 to 10%, i.e. the switched current may vary between 90% and 110% of the symmetrical current.

**Second and third operating step (breaking of the (last) transition contact)**

The aforementioned shows that the maximum current displacements occur in case 1.3, when connecting three diverters in parallel, or in case 2.2, when connecting two diverters in parallel. Therefore, in the following only these two chronological orders of arc quenching will be investigated for the second operating step. In case of an OLTC with multiple resistor cycle mode of operation the more severe condition is the arc quenching at the second transition contact (third operating step).

**Case 1 (continued):Parallel connection of three diverter switches**

**Case 1.4:** The current breaks at the three transition contacts in the same current zero after contact separation.

**Case 1.5:** The current breaks at two transition contacts in the first current zero, whereas the last transition contact breaks current in the second current zero after contact separation.

**Case 2 (continued):Parallel connection of two diverter switches**

**Case 2.3:** The current breaks at the two transition contacts in the same current zero after contact separation.

**Case 2.4:** The current breaks at one transition contact in the first current zero and at the other transition contact in the second current zero after contact separation.

**OLTC with multiple resistor cycle mode of operation**

In case 1.4 the symmetrical current splitting is ensured and the switched current at every main switching contact $\bar{I}_{T2x}$ can be determined with the help of the equations given in Table 2.1-20. Using these equations the mentioned through-current $\bar{I}_L$ has to be divided by three. This leads to:

$$\bar{I}_{T2-C14} = \left( \bar{I}_L + \frac{3\bar{U}_S}{R_{par}} \right) \cdot \frac{R_{par}}{3} \cdot \frac{R_2^2}{R_2^3 + R_2^2 R_{par}} \qquad (4.2\_28)$$

Figure 4.2-7 shows the circuit diagram valid for the calculation of the switching conditions of case 1.5. For simplification reasons equation 4.2_22a describing the transformer impedances should still be valid. In addition the equivalent resistor $R_{par}$ of the transition resistors $R_1$ and $R_2$ connected in parallel as defined in equation 4.2_23 shall be used. It has to be considered that the switched current $\bar{I}_{T2-C15}$ at the second transition contact consists of two portions as shown in Figure 4.2-7. The circulating current $\bar{I}_{C-C15}$, which is driven by the step voltage $\bar{U}_S$ and limited by the resistor and impedance network, and $\bar{I}_{3-C15}$, which is a portion of the through-current $\bar{I}_3$ of this winding branch shared between the transition resistor $R_2$ and the parallel connected transition resistors $R_1$ and $R_2$.

In this diverter switch position the circulating current is determined by a parallel connection of the winding branches 1 and 2 with the resistor $R_{par}$ of the third branch and, in addition, the resistor at the breaking transition contact $R_2$ connected in series.

**Fig. 4.2-7:** Circuit diagram valid for case 1.4 of current splitting of three diverter switches connected in parallel

With
$$\bar{I}_L = \bar{I}_1 + \bar{I}_2 + \bar{I}_3 = 2 \cdot \bar{I}_1 + \bar{I}_3 \qquad (4.2\_29a)$$

$$\bar{I}_1 \cdot (R_{par} + jX) = \bar{I}_3 \cdot \left( \frac{R_2 \cdot R_{par}}{R_2 + R_{par}} + jX \right) \qquad (4.2\_29b)$$

and
$$\bar{I}_{3-C15} = \bar{I}_3 \cdot \frac{R_{par}}{R_2 + R_{par}} \qquad (4.2\_29c)$$

$$\bar{I}_{C-C15} = \frac{\bar{U}_S}{R_2 + \dfrac{R_{par} \cdot (R_{par} + j3X)}{3R_{par} + j3X}} \qquad (4.2\_29d)$$

the switched current at the transition contact in case 1.5 becomes

$$\bar{I}_{T2-C15} = \left( \bar{I}_L + \frac{3\bar{U}_S}{R_{par}} \right) \cdot \frac{R_{par}^3 (R_{par} + 3R_2) + 3X^2 R_{par}(R_{par} + R_2) - j2XR_{par}^3}{\left[ R_{par}(R_{par} + 3R_2) \right]^2 + \left[ 3X(R_{par} + R_2) \right]^2} \qquad (4.2\_30)$$

**OLTC with flag cycle mode of operation**

In case 1.4 the symmetrical current splitting is ensured and the switched current at every main switching contact $\bar{I}_{Tx}$ can be determined with the help of the equations given in Table 2.1-4. Using these equations the mentioned through-current $\bar{I}_L$ has to be divided by three. With $R_2 = R_{par} = R$ this leads to:

$$\bar{I}_{T-C14} = \left( \bar{I}_L + \frac{3\bar{U}_S}{R_{par}} \right) \cdot \frac{1}{6} \tag{4.2_31}$$

The switched current at the transition contact in case 1.5 becomes

$$\bar{I}_{T-C15} = \left( \bar{I}_L + \frac{3\bar{U}_S}{R} \right) \cdot \frac{1}{2} \cdot \frac{2R^2 + 3X^2 - jRX}{4R^2 + 9X^2} \tag{4.2_32}$$

The calculation of the switched currents of cases 2.3 and 2.4 for OLTCs with two diverter switches connected in parallel and driven by one energy accumulator is done in analogy to the calculation shown above. In this case the switched current consists again of a circulating current $\bar{I}_{C-C23}$ and $\bar{I}_{2-C23}$, which is a portion of the through-current $\bar{I}_2$ of this winding branch shared between the transition resistor $R_2$ and the parallel connected transition resistors $R_1$ and $R_2$.

**OLTC with multiple resistor cycle mode of operation**

The current switched during symmetrical current splitting and simultaneous arc quenching according to case 2.3 is

$$\bar{I}_{T2-C23} = \left( \bar{I}_L + \frac{2\bar{U}_S}{R_{par}} \right) \cdot \frac{R_{par}}{2} \cdot \frac{R_2^2}{R_2^3 + R_2^2 R_{par}} \tag{4.2_33}$$

and according to case 2.4 with arc quenching in different current zeros

$$\bar{I}_{T2-C24} = \left( \bar{I}_L + \frac{2\bar{U}_S}{R_{par}} \right) \cdot \frac{R_{par}^3(R_{par} + 2R_2) + 2X^2 R_{par}(R_{par} + R_2) - jXR_{par}^3}{\left[ R_{par}(R_{par} + 2R_2) \right]^2 + \left[ 2X(R_{par} + R_2) \right]^2} \tag{4.2_34}$$

**OLTC with flag cycle mode of operation**

$$\bar{I}_{T-C23} = \left( \bar{I}_L + \frac{2\bar{U}_S}{R_{par}} \right) \cdot \frac{1}{4} \tag{4.2_35}$$

$$\bar{I}_{T-C24} = \left( \bar{I}_L + \frac{2\bar{U}_S}{R} \right) \cdot \frac{3R^2 + 4X^2 - jRX}{9R^2 + 16X^2} \tag{4.2_36}$$

Figure 4.2-8 shows the absolute value of the switched current at the transition contacts in relationship to that of the ideal switched current (symmetrical current splitting) for the different cases. For small X/R-ratios the current displacement reaches values up to 1.5 times the symmetrical current. The magnitude of the
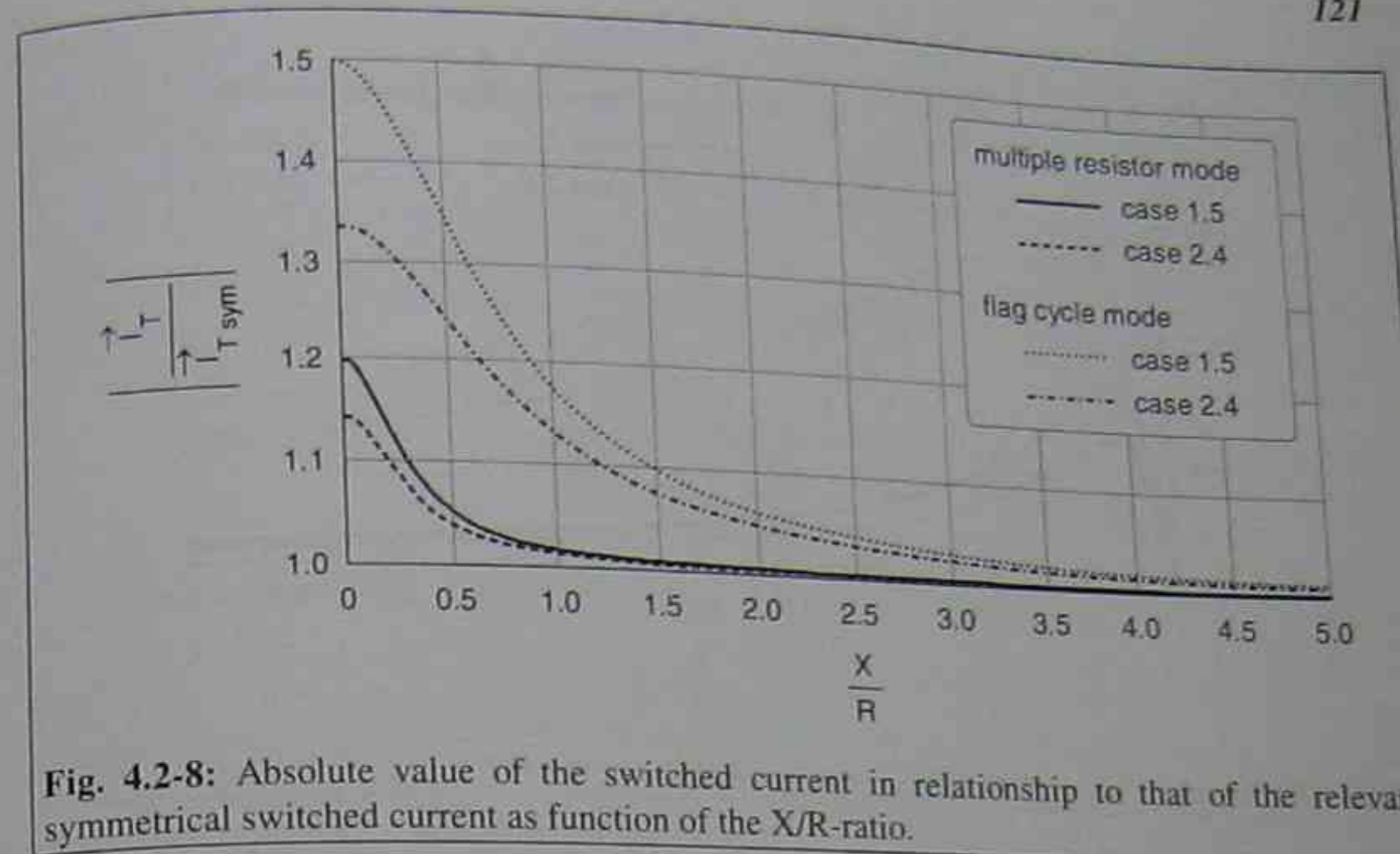
**Fig. 4.2-8:** Absolute value of the switched current in relationship to that of the relevant symmetrical switched current as function of the X/R-ratio.

admissible displacement depends on the OLTC design. A X/R-ratio of 2 to 3, which seemed to be acceptable at the main switching contact, can also be accepted here and results in an unsymmetry of up to 7%.

In addition to the above mentioned it has to be considered when judging the switching stresses at the transition contacts in cases 1.5 and 2.4, that a phase shift between the switched current and the recovery voltage occurs. This phase shift is caused by the circulating current which flows through the impedances X of the parallel winding branches. As shown in paragraph 4.2.1 during normal switching operations only the reactance of one tap section is effective and the resulting phase shift can be neglected.

The recovery voltages can be calculated using the equations given in Tables 2.1-4 and 2.1-20. As shown in paragraph 4.2.1.1 the resulting phase shift between the switched current and the recovery voltage in such cases does not depend on the power factor. Therefore, the introduction of the power factor is not necessary at this point. Following this the phase angle of the recovery voltages becomes 0 degree in relationship to the step voltage. Therefore, the phase shift can be calculated directly with equation 4.2_37 as the phase angle of the switched currents.

$$\varphi_{IUT} = \arctan \frac{\text{imaginary component of the switched current}}{\text{real component of the switched current}} \tag{4.2_37}$$

Figure 4.2.9 shows the occuring phase shift depending on the X/R-ratio. The resistor R in here represents the transition resistor R in case of an OLTC with flag cycle mode of operation and $R_2$ in case of an OLTC with multiple resistor cycle mode of operation respectively. Applying the same limits for X/R as given before,
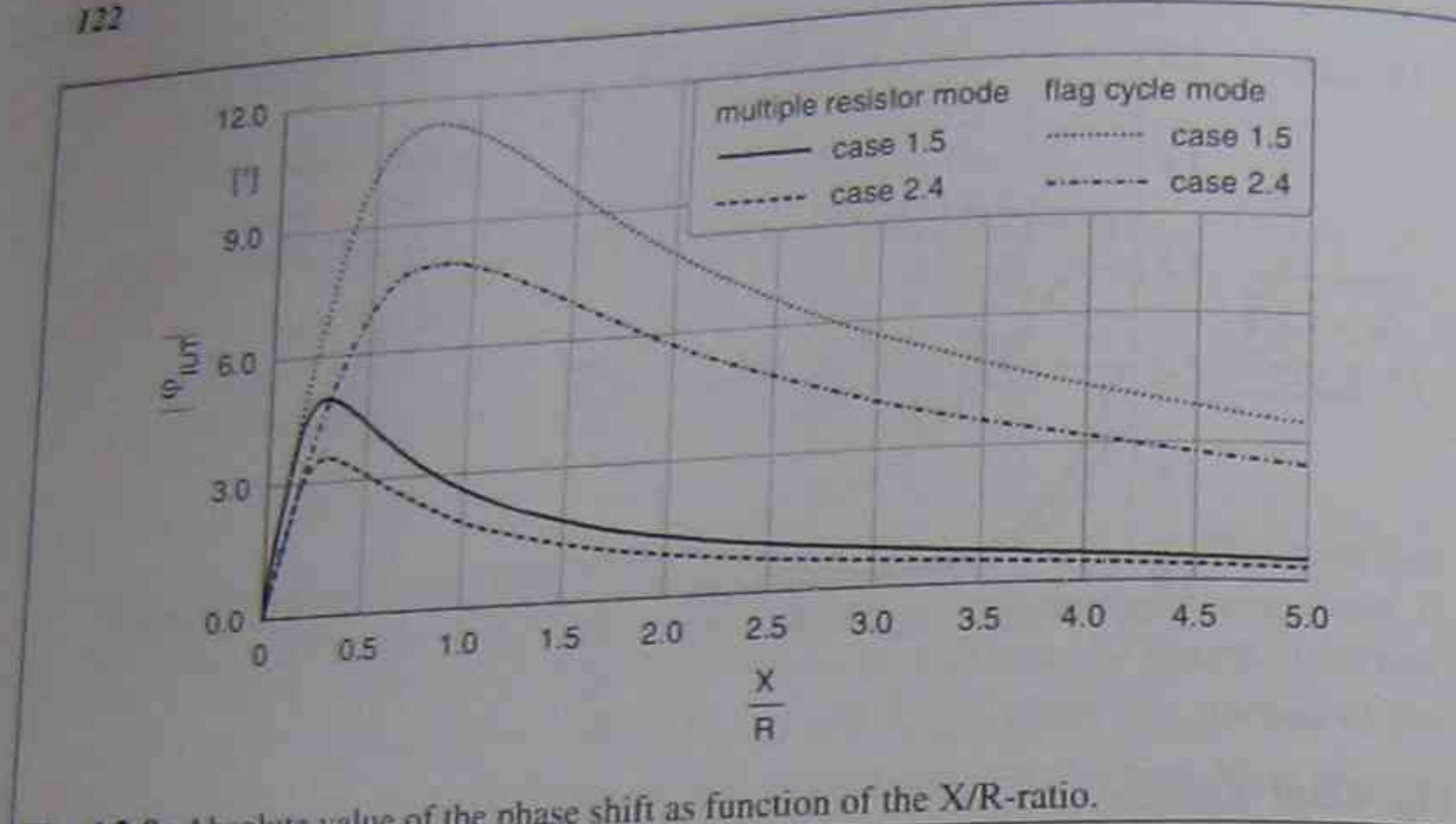
Fig. 4.2-9: Absolute value of the phase shift as function of the X/R-ratio.

phase shifts of up to 8 degree may occur at the transition contact of three parallel connected diverter switches with the flag cycle mode of operation.

When using OLTCs in applications as described in this paragraph, the compliance with the admissible limits needs to be checked by the OLTC manufacturer.

### 4.2.4.2 SEPARATE OLTCS CONNECTED IN PARALLEL

As previously described, the method of parallel connection of different diverter switches driven by one common energy accumulator is used by the OLTC manufacturers to increase the rated through-current and the switching capacity of an OLTC. The method of paralleling separate OLTCs is sometimes used by transformer makers in cases where the switching capacity of one OLTC is not sufficient. As mentioned before, this solution is only permitted if the entire transformer winding is splitted into parallel winding branches. But still, when using such a method certain limitations apply which have to be fulfilled by the transformer design.

It needs to be considered that two separate OLTCs connected in parallel will not operate simultaneously, even if they are driven by one common motor drive mechanism. Minimum time differences of 300 ms can be reached when the driving shaft arrangement is adjusted to an optimum. During this time period the two OLTCs are connected to different taps of the tap winding and a circulating current flows driven by the step voltage and only limited by the winding impedances. The limitation of such arrangements is defined by the admissible magnitude of the circulating current, which depends on the OLTC design. A value of 5 to 10% of the relevant through-current of a single OLTC seems to be acceptable and leads to switching stresses which are comparable to that of parallel connected diverter switches as shown in 4.2.4.1. In case of two OLTCs connected in parallel this results

in a value of 2.5 to 5% of the total current of the transformer. Generally, the OLTC manufacturer should check the stresses and must define the admissible limits for such applications.

The electrical situation of parallel connected OLTCs with splitted winding branches is comparable to that of parallel connected transformers (refer to sub-clause 5.5).

## 4.3 POTENTIAL CONNECTION OF THE TAP WINDING

### 4.3.1 INTRODUCTION

The operation of the change-over selector takes place in the mid-position of the OLTC, i.e. when the tap selectors are in position "K" (see Fig. 4.3-1). During this operation, the load current does not flow through the tap winding. Therefore the tap winding is temporarily disconnected from the main winding and the potential of the winding floats. The floating potential of the tap winding is determined by the voltages of the adjacent windings as well as by the coupling capacities to these windings and to the grounded parts. The floating potential usually is different from the potential of the tap winding when it is connected to the main winding.
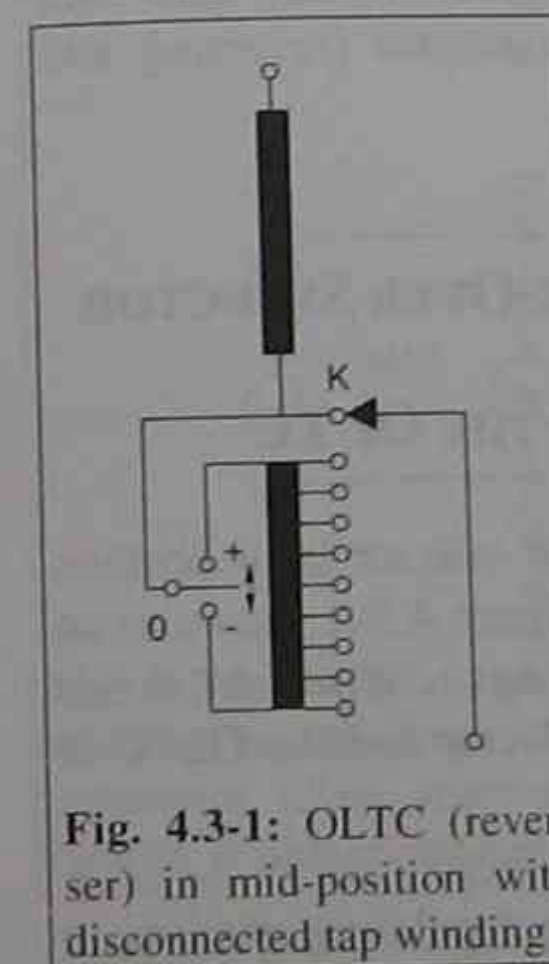


Fig. 4.3-1: OLTC (reverser) in mid-position with disconnected tap winding

In such cases, discharges between the opening and closing contacts occur during the operation of the change-over selector. In order to avoid difficulties in regards to the dielectric stress and the formation of gases which could arise, special precautions are necessary. The stresses on an opening contact are determined by the current flowing before the contacts open and the voltage (here called recovery voltage) which arises when the arc or the discharge extinguishes.

If the values reach the admissible limits, there are many different methods to overcome this problem. Some examples are the use of two-way change-over selectors (double reverser), control resistors (tie-in resistor) or capacitive control between the adjacent potentials and the tap winding.

The permissible stresses are determined by the discharge occuring during the change-over selector operation. The discharge time is mainly dependent on the magnitude of the recovery voltage. The magnitude of the switched capacitive current, in comparison, is of smaller importance. The admissible discharge time limit is in the range of half of the switching time of the change-over selector (time between electrical opening and closing).

The values of admissible recovery voltages and switched currents differ with the design of the change-over selector. For every application the stresses on the change-over selector contacts needs to be calculated to avoid a possible short-circuit of the tap winding or the formation of a great volume of gases.

Discharges in the admissible limits produce a certain volume of gases in the range of a few millilitres per operation. The amount depends on the switched current and the arcing time, and is neligible compared with the gases which are produced in the transformer by aging of the insulating oil and the paper. The main composites of the gases are hydrogen ($H_2$: 70% - 75%), acetylen ($C_2H_2$: 5% - 15%), nitrogen ($N_2$: 5% - 10%), oxygen ($O_2$: 2% -5%) and methane ($CH_4$: 2% - 4%). The common international failure codes characterize this gas composition as a partial discharge.

### 4.3.2 CALCULATION OF RECOVERY VOLTAGE AND SWITCHED CURRENT

The stresses which occur during the change-over selector operation at the change-over selector contacts have to be calculated for the correct dimensioning of the OLTC. The principle of calculation will be demonstrated in detail using typical examples for different locations of the tap winding (neutral-end and delta connection, auto- and phase-shifting transformer) and for different regulation principles (reversing and coarse change-over selector).

#### 4.3.2.1 REGULATION WITH REVERSING CHANGE-OVER SELECTOR

##### 4.3.2.1.1 NEUTRAL-END CONNECTION OF THE OLTC

Before the change-over selector operation takes place the tap selector is in position "K" and the change-over selector is in position "+" or "-". Figure 4.3-2 shows as an example a typical windings arrangement and the windings connection for a regulation at the neutral-end with a reversing change-over selector and the OLTC in the mid-position.

The load current of the transformer does not flow through the regulating winding in this position. When the change-over selector is still closed a current flows through the change-over selector contacts "+" or "-" and the winding capacitances $C_1$ and $C_2$. The source for this capacitive current $I_{S+}$ or $I_{S-}$ is the voltage $U_{HV}$ and $U_{TV}$. The current $I_{S+}$ or $I_{S-}$ has to be switched off during the change-over selector operation. The recovery voltage $U_{r+}$ or $U_{r-}$ is defined as the difference in potential between the change-over selector contacts "+" or "-" and the contact "0" when the contacts are open. In case of the reversing change-over selector the potentials of the "+"- and "-"- contacts which are connected to the tap winding float. Whereas the potential of the common change-over selector contact "0" is fixed by the connection to the main
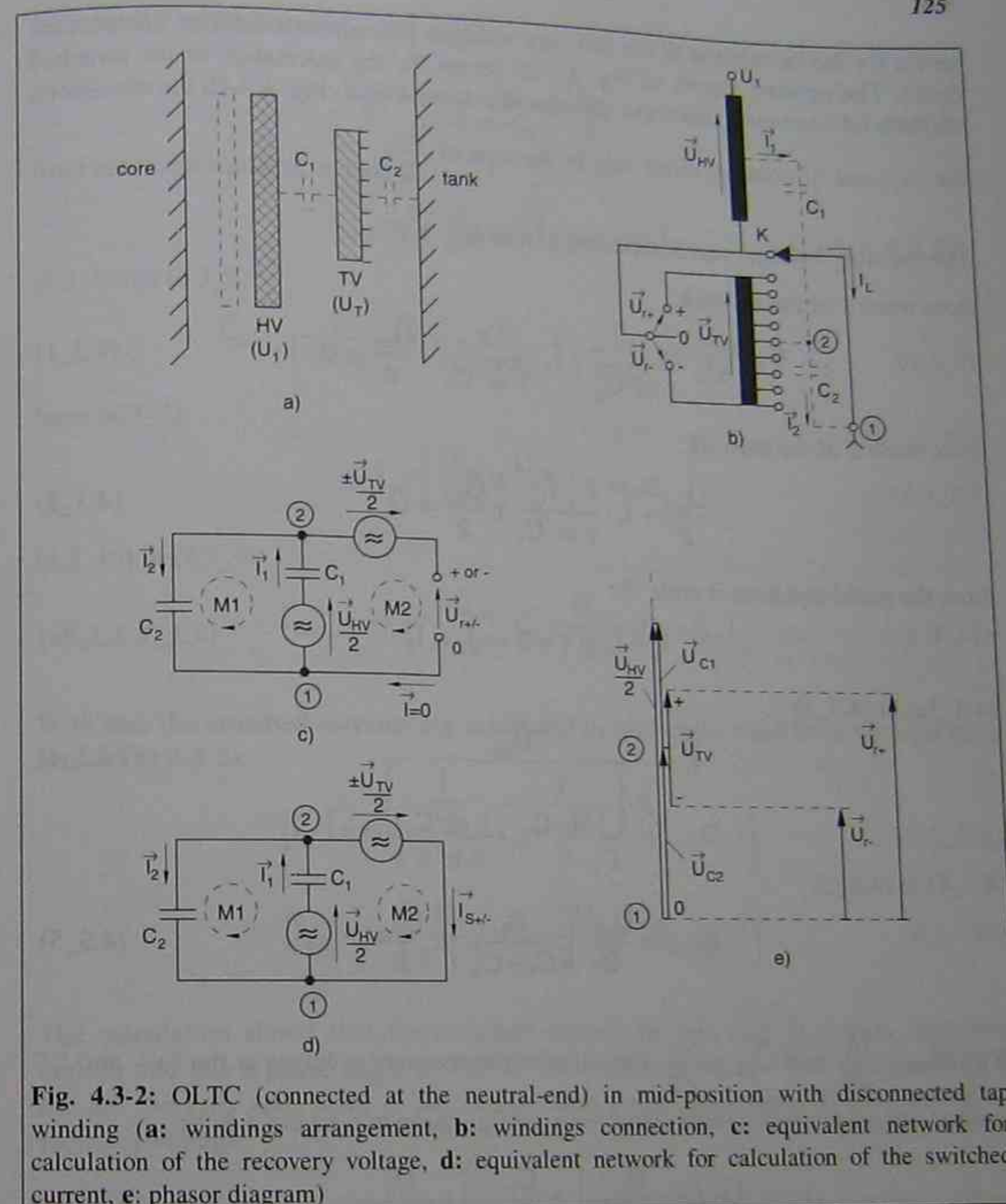
Fig. 4.3-2: OLTC (connected at the neutral-end) in mid-position with disconnected tap winding (a: windings arrangement, b: windings connection, c: equivalent network for calculation of the recovery voltage, d: equivalent network for calculation of the switched current, e: phasor diagram)

winding. In case of a coarse change-over selector floating and fixed potentials are different. This will be explained lateron.

The winding capacities and the capacities to ground are represented in Fig. 4.3-2b as lumped capacitors connected to the middle of the windings and fed by one half of the voltages $\vec{U}_{HV}$ and $\vec{U}_{TV}$. This simplification is used in the equivalent electrical networks (4.3-2c and d). The voltages $\frac{\vec{U}_{HV}}{2}$ and $\frac{\vec{U}_{TV}}{2}$ are represented by the equivalent voltage sources. The equivalent electrical network shown in Fig. 4.3-2c

serves for the calculation of the recovery voltages (change-over selector contacts are open). The network shown in Fig. 4.3-2d serves for the calculation of the switched currents (change-over selector is still closed). According to Fig. 4.3-2b the stresses on the "+"- and "-" contacts differ only by the sign of $\dfrac{\bar{U}_{TV}}{2}$.

The recovery voltages can be calculated from Fig. 4.3-2c:

from mesh 1 of the network:

$$-\bar{I}_2 \cdot \frac{1}{j \cdot \omega \cdot C_2} - \bar{I}_1 \cdot \frac{1}{j \cdot \omega \cdot C_1} - \frac{\bar{U}_{HV}}{2} = 0 \qquad (4.3\_1)$$

from mesh 2 of the network:

$$\frac{\bar{U}_{HV}}{2} + \bar{I}_1 \cdot \frac{1}{j \cdot \omega \cdot C_1} \pm \frac{\bar{U}_{TV}}{2} = \bar{U}_{r+/-} \qquad (4.3\_2)$$

from the nodal equation at node ①:

$$\bar{I}_1 - \bar{I}_2 = \bar{I} = 0 \Rightarrow \bar{I}_1 = \bar{I}_2 \qquad (4.3\_3, 4.3\_3a)$$

(4.3_3a) in (4.3_1)

$$\bar{I}_1 = \frac{-\bar{U}_{HV}}{2 \cdot \left( \dfrac{1}{j \cdot \omega \cdot C_1} + \dfrac{1}{j \cdot \omega \cdot C_2} \right)} \qquad (4.3\_4)$$

(4.3_4) in (4.3_2)

$$\bar{U}_{r+/-} = \frac{\bar{U}_{HV}}{2} \cdot \left( \frac{C_1}{C_1 + C_2} \right) \pm \frac{\bar{U}_{TV}}{2} \qquad (4.3\_5)$$

With $\bar{U}_{HV} = \dfrac{U_1}{\sqrt{3}}$ and $\bar{U}_{TV} = \dfrac{U_T}{\sqrt{3}}$ the value of the recovery voltages at the "+"- and "-" contacts are calculated to (only valid for a configuration acc. to Fig 4.3-2):

$$\left| \bar{U}_{r+} \right| = \frac{U_1}{2 \cdot \sqrt{3}} \cdot \left( \frac{C_1}{C_1 + C_2} \right) + \frac{U_T}{2 \cdot \sqrt{3}} \qquad (4.3\_5a)$$

$$\left| \bar{U}_{r-} \right| = \frac{U_1}{2 \cdot \sqrt{3}} \cdot \left( \frac{C_1}{C_1 + C_2} \right) - \frac{U_T}{2 \cdot \sqrt{3}} \qquad (4.3\_5b)$$

The switched currents can be calculated from Fig. 4.3-2d:

from mesh 1 of the network:

$$-\bar{I}_2 \cdot \frac{1}{j \cdot \omega \cdot C_2} - \bar{I}_1 \cdot \frac{1}{j \cdot \omega \cdot C_1} - \frac{\bar{U}_{HV}}{2} = 0 \qquad (4.3\_6)$$

from mesh 2 of the network:

$$\frac{\bar{U}_{HV}}{2} + \bar{I}_1 \cdot \frac{1}{j \cdot \omega \cdot C_1} \pm \frac{\bar{U}_{TV}}{2} = 0 \qquad (4.3\_7)$$

from the nodal equation at node ①:

$$\bar{I}_{S+/-} = \bar{I}_1 - \bar{I}_2 \Rightarrow -\bar{I}_2 = \bar{I}_{S+/-} - \bar{I}_1 \qquad (4.3\_8, 4.3\_8a)$$

(4.3_8a) in (4.3_6)

$$\bar{I}_{S+/-} \cdot \frac{1}{j \cdot \omega \cdot C_2} - \bar{I}_1 \cdot \left( \frac{1}{j \cdot \omega \cdot C_1} + \frac{1}{j \cdot \omega \cdot C_2} \right) - \frac{\bar{U}_{HV}}{2} = 0 \qquad (4.3\_9)$$

from (4.3_7)

$$-\bar{I}_1 = \left( \frac{\bar{U}_{HV}}{2} \pm \frac{\bar{U}_{TV}}{2} \right) \cdot j \cdot \omega \cdot C_1 \qquad (4.3\_10)$$

(4.3_10) in (4.3_9)

$$\bar{I}_{S+/-} = -j \cdot \omega \cdot \left( \frac{\bar{U}_{HV}}{2} \cdot C_1 \pm \frac{\bar{U}_{TV}}{2} \cdot (C_1 + C_2) \right) \qquad (4.3\_11)$$

With this the switched currents are calculated to (also only valid for a configuration acc. to Fig 4.3-2):

$$\left| \bar{I}_{S+} \right| = \omega \cdot \left( \frac{U_1}{2 \cdot \sqrt{3}} \cdot C_1 + \frac{U_T}{2 \cdot \sqrt{3}} \cdot (C_1 + C_2) \right) \qquad (4.3\_11a)$$

$$\left| \bar{I}_{S-} \right| = \omega \cdot \left( \frac{U_1}{2 \cdot \sqrt{3}} \cdot C_1 - \frac{U_T}{2 \cdot \sqrt{3}} \cdot (C_1 + C_2) \right) \qquad (4.3\_11b)$$

The calculation shows that the switched current in this case is a pure capacitive current and has a phase angle of -90° to the recovery voltage. The extinguishing of the arc can only take place at the current zero point, this means at the peak of the recovery voltage.

In some cases - as a quicker solution - it is easier to calculate the recovery voltage with the aid of the phasor diagram shown in Fig. 4.3-2e. The capacitors $C_1$ and $C_2$ represent a capacitive divider fed by $\dfrac{\bar{U}_{HV}}{2}$. With this the voltages $U_{C1}$ and $U_{C2}$ can be expressed as follows:

$$\bar{U}_{C1} = \frac{\bar{U}_{HV}}{2} \cdot \left( \frac{C_2}{C_1 + C_2} \right) \qquad (4.3\_12)$$

$$\bar{U}_{C2} = \frac{\bar{U}_{HV}}{2} \cdot \left( \frac{C_1}{C_1 + C_2} \right) \qquad (4.3\_13)$$

Fig. 4.3-2b shows that the "0" contact of the reverser is directly connected to the neutral-end. The "+" contact is located at the tip of the $U_{TV}$-phasor and the "-" contact at the bottom. With this the recovery voltages $U_{r+}$ and $U_{r-}$ are defined and shown as dotted lines in the phasor diagram (Fig. 4.3-2e). The calculation of the recovery voltages is now very simple (going from "0" to "+" or "-").

$$\bar{U}_{r+} = \bar{U}_{C2} + \frac{\bar{U}_{TV}}{2} = \frac{\bar{U}_{HV}}{2} \cdot \left(\frac{C_1}{C_1 + C_2}\right) + \frac{\bar{U}_{TV}}{2}$$

$$\bar{U}_{r-} = \bar{U}_{C2} - \frac{\bar{U}_{TV}}{2} = \frac{\bar{U}_{HV}}{2} \cdot \left(\frac{C_1}{C_1 + C_2}\right) - \frac{\bar{U}_{TV}}{2}$$

The result is the same as found with 4.3_5.

*Example:*
(windings arrangement and nomenclature acc. to Fig. 4.3-2)

*Transformer data:*
*325 MVA, 240 kV (1±10 1,25%)/31,5 kV, 50 Hz, regulation at the neutral-end*

HV: $U_1 = 240 \, kV$
TV: $U_T = U_1 \cdot 0.125 = 30.0 \, kV$

capacity to the adjacent winding: $C_1 = 1950 \, pF$
capacity to grounded parts: $C_2 = 450 \, pF$

$$\left|\bar{U}_{r+}\right| = \frac{240 kV}{2 \cdot \sqrt{3}} \left(\frac{1950 pF}{1950 pF + 450 pF}\right) + \frac{30 kV}{2 \cdot \sqrt{3}} = 64.95 \, kV$$

$$\left|\bar{U}_{r-}\right| = \frac{240 kV}{2 \cdot \sqrt{3}} \cdot \left(\frac{1950 pF}{1950 pF + 450 pF}\right) - \frac{30 kV}{2 \cdot \sqrt{3}} = 47.63 \, kV$$

$$\left|\bar{I}_{s+}\right| = 2\pi \cdot 50 \frac{1}{s} \cdot \left(\frac{240 kV}{2 \cdot \sqrt{3}} 1950 pF + \frac{30 kV}{2 \cdot \sqrt{3}} (1950 pF + 450 pF)\right) = 48.97 \, mA$$

$$\left|\bar{I}_{s-}\right| = 2\pi \cdot 50 \frac{1}{s} \cdot \left(\frac{240 kV}{2 \cdot \sqrt{3}} 1950 pF - \frac{30 kV}{2 \cdot \sqrt{3}} (1950 pF + 450 pF)\right) = 35.91 \, mA$$

### 4.3.2.1.2 DELTA CONNECTION OF THE OLTC

In the following examples the calculation of the recovery voltages and the switched currents is performed on an application with the OLTC located at the end of a delta winding. Figs. 4.3-3 shows an example for the calculation with the same windings arrangement as used in 4.3.2.1.1.
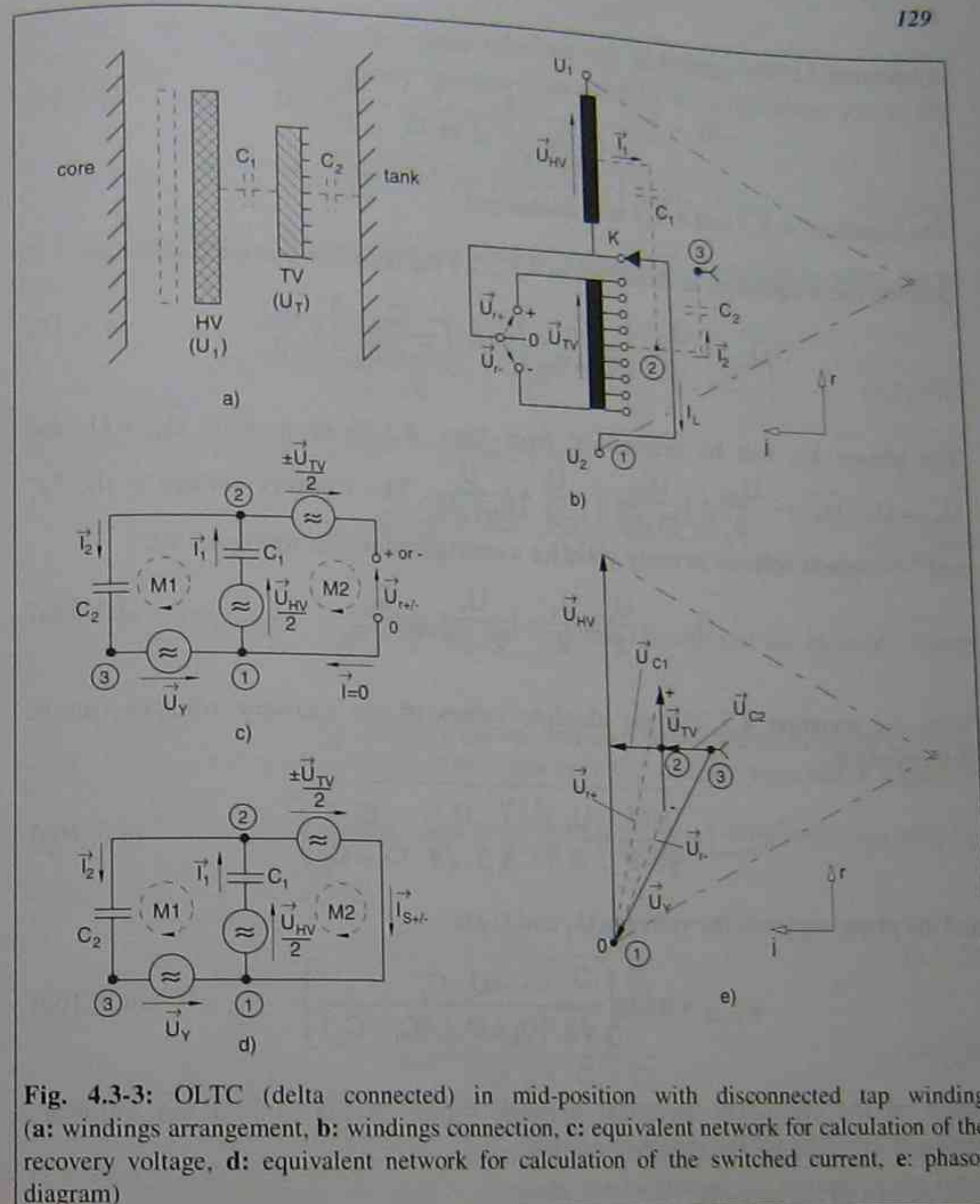
**Fig. 4.3-3:** OLTC (delta connected) in mid-position with disconnected tap winding (**a:** windings arrangement, **b:** windings connection, **c:** equivalent network for calculation of the recovery voltage, **d:** equivalent network for calculation of the switched current, **e:** phasor diagram)

The equivalent electrical networks shown in Figs. 4.3-3c and d are very similar to the networks shown in Figs. 4.3-2c and d. The only difference is an additional equivalent voltage source $U_Y$ between nodes ① and ③. This additional voltage source represents the voltage difference between the grounded middle of the voltage triangle, where the capacitor $C_2$ is connected, and the common contact "0" of the change-over selector (comp. 4.3.2.1.1: in case of a regulation at the neutral-end this voltage is zero).

The calculation of the recovery voltages is performed in the same way as described under 4.3.2.1.1:

from mesh 1 of the network:

$$-\bar{U}_Y - \bar{I}_2 \cdot \frac{1}{j \cdot \omega \cdot C_2} - \bar{I}_1 \cdot \frac{1}{j \cdot \omega \cdot C_1} - \frac{\bar{U}_{HV}}{2} = 0 \qquad (4.3\_14)$$

The equations 4.3_2 and 4.3_3 stay unchanged.

Solving these equations as described in 4.3.2.1.1 the recovery voltage follows as:

$$\bar{U}_{r+/-} = \frac{\bar{U}_{HV}}{2} \cdot \left( \frac{C_1}{C_1 + C_2} \right) - \bar{U}_Y \cdot \left( \frac{C_2}{C_1 + C_2} \right) \pm \frac{\bar{U}_{TV}}{2} \qquad (4.3\_15)$$

The phasor $\bar{U}_Y$ can be determined from Figs. 4.3-3b or e, with $\bar{U}_{HV} = U_1$ and $\bar{U}_{TV} = U_T$: $\bar{U}_Y = -\frac{U_{HV}}{2} + j \frac{U_{HV}}{2 \cdot \sqrt{3}} = -\frac{U_1}{2} + j \frac{U_1}{2 \cdot \sqrt{3}}$. The recovery voltage at the "+" and "-" contacts follows as (only valid for a configuration acc. to Fig 4.3-3):

$$\bar{U}_{r+/-} = \frac{U_1}{2} \pm \frac{U_T}{2} - j \frac{U_1}{2 \cdot \sqrt{3}} \cdot \frac{C_2}{C_1 + C_2} \qquad (4.3\_15a)$$

With the equation 4.3_15a the absolute values of the recovery voltages can be determined to:

$$|U_{r+/-}| = \sqrt{ \left( \frac{U_1}{2} \pm \frac{U_T}{2} \right)^2 + \left( \frac{U_1}{2 \cdot \sqrt{3}} \cdot \frac{C_2}{C_1 + C_2} \right)^2 } \qquad (4.3\_16a)$$

and the phase angles to the voltages $U_1$ and $U_T$ to:

$$\varphi_{+/-Ur} = \arctan\left( \frac{-U_1 \cdot C_2}{\sqrt{3} \cdot (U_1 \pm U_T) \cdot (C_1 + C_2)} \right) \qquad (4.3\_16b)$$

Based on the equivalent electrical network shown in Fig. 4.3-3d the following equations are valid for the switched current:

from mesh 1 of the network:

$$-\bar{U}_Y - \bar{I}_2 \cdot \frac{1}{j \cdot \omega \cdot C_2} - \bar{I}_1 \cdot \frac{1}{j \cdot \omega \cdot C_1} - \frac{\bar{U}_{HV}}{2} = 0 \qquad (4.3\_17)$$

The equations 4.3_7 and 4.3_8 stay unchanged.

With these equations the switched currents can be determined to:

$$\bar{I}_{S+/-} = -j \cdot \omega \cdot \left( \frac{\bar{U}_{HV}}{2} \cdot C_1 \pm \frac{\bar{U}_{TV}}{2} (C_1 + C_2) - \bar{U}_Y \cdot C_2 \right) \qquad (4.3\_18)$$

For the switched currents, the same relations for $\bar{U}_Y$, $\bar{U}_{HV}$ and $\bar{U}_{TV}$ apply as mentioned before for the recovery voltages (only valid for a configuration acc. to Fig 4.3-3):

$$\bar{I}_{S+/-} = -\frac{U_1}{2 \cdot \sqrt{3}} \cdot \omega \cdot C_2 - j \cdot \left( \frac{U_1 \pm U_T}{2} \right) \cdot \omega \cdot (C_1 + C_2) \qquad (4.3\_18a)$$

With the equations 4.3_18a and b the absolute values of the switched currents can be determined:

$$|I_{S+/-}| = \omega \cdot \sqrt{ \left( \frac{U_1}{2 \cdot \sqrt{3}} \cdot C_2 \right)^2 + \left( \left( \frac{U_1 \pm U_T}{2} \right) \cdot (C_1 + C_2) \right)^2 } \qquad (4.3\_19a)$$

The phase angles to the voltages $U_H$ and $U_T$ are:

$$\varphi_{+/-Is} = \arctan\left( \frac{\sqrt{3} \cdot (U_1 \pm U_T) \cdot (C_1 + C_2)}{U_1 \cdot C_2} \right) \qquad (4.3\_19b)$$

The differential phase angle between the switched current and the recovery voltage becomes -90°.

As shown in 4.3.2.1.1 the recovery voltage can also be calculated easily by using the phasor diagram in Fig. 4.3-3e. The capacitors $C_1$ and $C_2$ represent a capacitive divider fed by the voltage $\bar{U}_{C1} + \bar{U}_{C2} = \frac{\bar{U}_{HV}}{2 \cdot \sqrt{3}} = j \cdot \frac{U_{HV}}{2 \cdot \sqrt{3}}$. The voltages $U_{C1}$ and $U_{C2}$ can be expressed as follows:

$$\bar{U}_{C1} = j \cdot \frac{U_{HV}}{2 \cdot \sqrt{3}} \cdot \frac{C_2}{C_1 + C_2} \qquad (4.3\_20)$$

$$\bar{U}_{C2} = j \cdot \frac{U_{HV}}{2 \cdot \sqrt{3}} \cdot \frac{C_1}{C_1 + C_2} \qquad (4.3\_21)$$

With the knowledge that the "0" contact of the reverser is connected to the bottom of the $U_{HV}$-phasor and the "+" and "-" contacts are located at the tip and at the bottom of the $U_{TV}$-phasor respectively the recovery voltages are defined (see the dotted lines in Fig. 4.3-3e). Going from "0" to "+" or "-" the recovery voltages are found as:

$$\bar{U}_{r+} = \frac{\bar{U}_{HV}}{2} - \bar{U}_{C1} + \frac{\bar{U}_{TV}}{2} = \frac{U_{HV}}{2} + \frac{U_{TV}}{2} - j \cdot \frac{U_{HV}}{2 \cdot \sqrt{3}} \cdot \left( \frac{C_2}{C_1 + C_2} \right)$$

$$\bar{U}_{r-} = \frac{\bar{U}_{HV}}{2} - \bar{U}_{C1} - \frac{\bar{U}_{TV}}{2} = \frac{U_{HV}}{2} - \frac{U_{TV}}{2} - j \cdot \frac{U_{HV}}{2 \cdot \sqrt{3}} \cdot \left( \frac{C_2}{C_1 + C_2} \right)$$

The equation 4.3_15a can be reached by inserting the values of $\bar{U}_{HV} = U_1$ and $\bar{U}_{TV} = U_T$.

$$\bar{U}_{rec} = \frac{U_1}{2} \pm \frac{U_T}{2} - j \frac{U_1}{2 \cdot \sqrt{3}} \left( \frac{C_2}{C_1 + C_2} \right)$$

**Example:**
(windings arrangement and nomenclature acc. to Fig. 4.3-3)

**Transformer data:**
13 MVA, 132 kV (1±8) 1.25% √24 kV, 50 Hz, regulation at line end

HV:    $U_1 = 132$ kV
TV:    $U_T = U_1 \cdot 0.1 = 13.2$ kV

capacity to the adjacent winding:    $C_1 = 1810$ pF
capacity to grounded parts:    $C_2 = 950$ pF

$$|\bar{U}_{r+}| = \sqrt{\left(\frac{132kV}{2} + \frac{13.2kV}{2}\right)^2 + \left(\frac{132kV}{2 \cdot \sqrt{3}} \cdot \frac{950\,pF}{1810\,pF + 950\,pF}\right)^2} = 73.78\,kV$$

$$|\bar{U}_{r-}| = \sqrt{\left(\frac{132kV}{2} - \frac{13.2kV}{2}\right)^2 + \left(\frac{132kV}{2 \cdot \sqrt{3}} \cdot \frac{950\,pF}{1810\,pF + 950\,pF}\right)^2} = 60.83\,kV$$

$$|\bar{I}_{s+}| = \sqrt{\left(\frac{132kV}{2 \cdot \sqrt{3}} \cdot 2\pi \cdot 50 \frac{1}{s} \cdot 950\,pF\right)^2 + \left(\frac{145.2kV}{2} \cdot 2\pi \cdot 50 \frac{1}{s} \cdot 2760\,pF\right)^2} = 63.97\,mA$$

$$|\bar{I}_{s-}| = \sqrt{\left(\frac{132kV}{2 \cdot \sqrt{3}} \cdot 2\pi \cdot 50 \frac{1}{s} \cdot 950\,pF\right)^2 + \left(\frac{118.8kV}{2} \cdot 2\pi \cdot 50 \frac{1}{s} \cdot 2760\,pF\right)^2} = 52.75\,mA$$

### 4.3.2.1.3 OLTCs IN AUTOTRANSFORMERS

Besides the two above mentioned applications of an OLTC, autotransformers with voltage regulation are very often used. Also for this kind of application an example of a calculation of the recovery voltages and the switched currents is provided.

For the example an autotransformer with regulation of the low voltage is selected. The OLTC is located between the common and the series winding at the low-voltage line-end. Fig. 4.3-4a shows a typical windings arrangement of such an application. The corresponding windings connection are given in Fig. 4.3-4b. As in the previous examples these configurations are represented by the equivalent electrical networks to allow the calculation of the recovery voltages (Fig. 4.3-4c) and the switched currents (Fig. 4.3-4d).
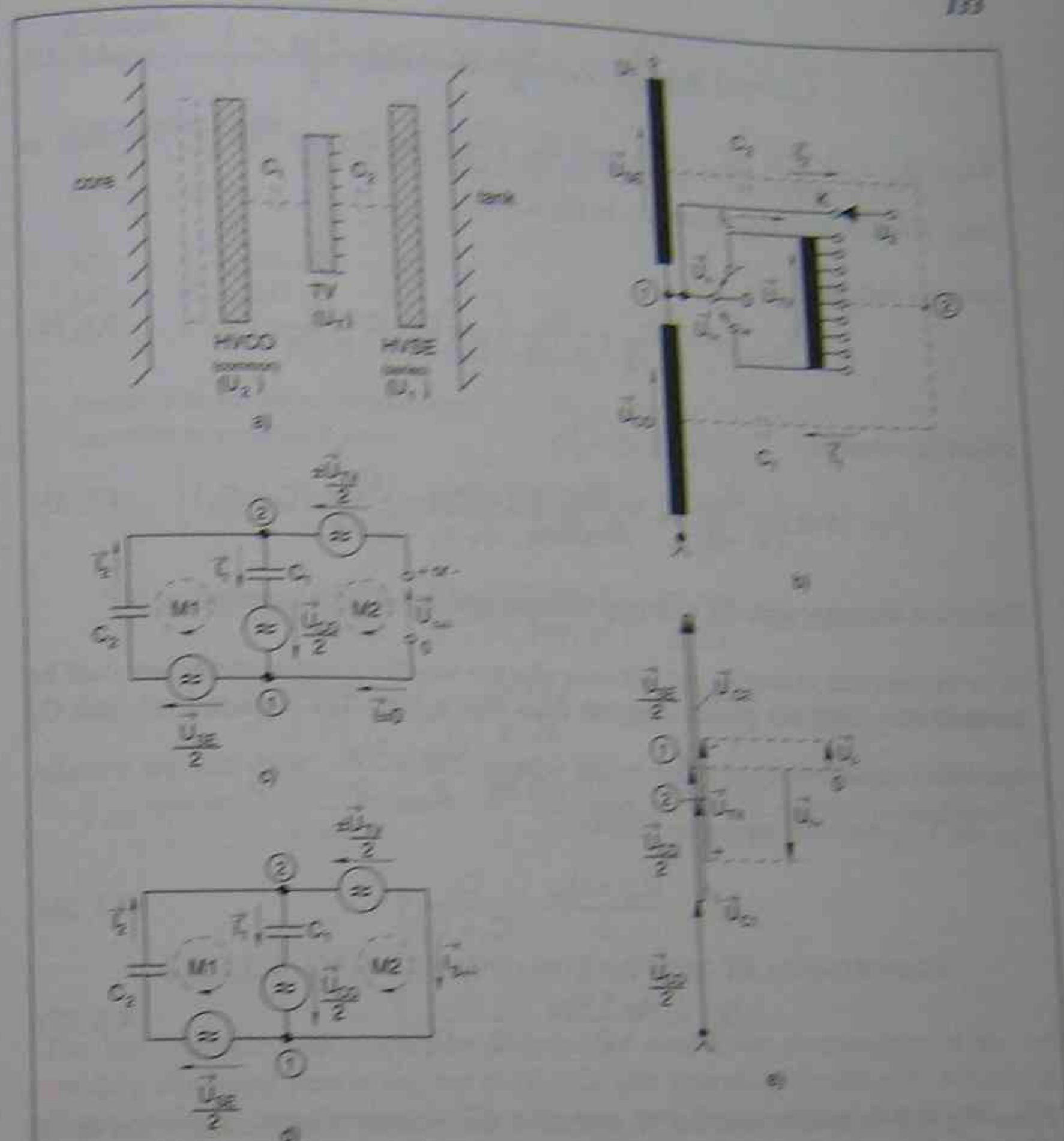
Fig. 4.3-4: OLTC (autotransformer) in mid-position with disconnected tap winding (a: windings arrangement, b: windings connection, c: equivalent network for calculation of the recovery voltage, d: equivalent network for calculation of the switched current, e: phasor diagram)

The calculation of the recovery voltages can be performed acc. to Fig. 4.3-4c with comparable basic formulations as demonstrated in 4.3.2.1.1 and 4.3.2.1.2. With the same mathematical operations the recovery voltages can be determined to:

$$\bar{U}_{rec} = -\frac{\bar{U}_{CO}}{2} \cdot \left(\frac{C_1}{C_1 + C_2}\right) + \frac{\bar{U}_{SE}}{2} \cdot \left(\frac{C_2}{C_1 + C_2}\right) \pm \frac{\bar{U}_{TV}}{2} \quad (4.3\_22)$$

and for the switched currents follows:

$$\bar{I}_{s+/-} = -j \cdot \omega \cdot \left( \frac{\bar{U}_{SE}}{2} \cdot C_2 \mp \frac{\bar{U}_{TV}}{2} \cdot (C_1 + C_2) - \frac{\bar{U}_{CO}}{2} \cdot C_1 \right) \qquad (4.3\_23)$$

With $\bar{U}_{SE} = \dfrac{U_1 - U_2}{\sqrt{3}}$, $\bar{U}_{CO} = \dfrac{U_2}{\sqrt{3}}$ and $\bar{U}_{TV} = \dfrac{U_T}{\sqrt{3}}$ the stresses can be expressed as

(only valid for a configuration acc. to Fig 4.3-4):

recovery voltages:

$$\left| \bar{U}_{r+/-} \right| = -\frac{U_2}{2 \cdot \sqrt{3}} + \frac{U_1}{2 \cdot \sqrt{3}} \cdot \left( \frac{C_2}{C_1 + C_2} \right) \mp \frac{U_T}{2 \cdot \sqrt{3}} \qquad (4.3\_24)$$

switched currents:

$$\left| \bar{I}_{s+/-} \right| = \omega \cdot \left( \frac{U_1}{2 \cdot \sqrt{3}} \cdot C_2 \mp \frac{U_T}{2 \cdot \sqrt{3}} \cdot (C_1 + C_2) - \frac{U_2}{2 \cdot \sqrt{3}} \cdot (C_1 + C_2) \right) \qquad (4.3\_25)$$

The phase angle between the recovery voltages and the switched currents is -90°.

As in the previous examples, for this case also the way for a rapid calculation shall be demonstrated using the phasor diagram from Fig. 4.3-4e. The capacitors $C_1$ and $C_2$ represent a capacitive divider fed by the voltage $\dfrac{\bar{U}_{CO}}{2} + \dfrac{\bar{U}_{SE}}{2}$. With this the voltages $U_{C1}$ and $U_{C2}$ can be expressed as follows:

$$\bar{U}_{C1} = \frac{\bar{U}_{SE} + \bar{U}_{CO}}{2} \cdot \left( \frac{C_2}{C_1 + C_2} \right) \qquad (4.3\_26)$$

$$\bar{U}_{C2} = \frac{\bar{U}_{SE} + \bar{U}_{CO}}{2} \cdot \left( \frac{C_1}{C_1 + C_2} \right) \qquad (4.3\_27)$$

From Fig. 4.3-4b follows that the "0" contact of the reverser is connected to the tip of the $U_{CO}$-phasor and to the bottom of the $U_{SE}$-phasor. The "+" contact of the reverser is located at the bottom of the $U_{TV}$-phasor and the "-" contact at the tip. With this the recovery voltages $U_{r+}$ and $U_{r-}$ are defined. They are shown as dotted lines in the phasor diagram (Fig. 4.3-4e). Going from "0" to "+" or "-" the recovery voltages can be expressed as:

$$\bar{U}_{r+} = \frac{\bar{U}_{SE}}{2} - \bar{U}_{C2} - \frac{\bar{U}_{TV}}{2} = \frac{U_{SE}}{2} - \frac{U_{SE} + U_{CO}}{2} \cdot \left( \frac{C_1}{C_1 + C_2} \right) - \frac{U_{TV}}{2}$$

$$\bar{U}_{r-} = \frac{\bar{U}_{SE}}{2} - \bar{U}_{C2} - \frac{\bar{U}_{TV}}{2} = \frac{U_{SE}}{2} - \frac{U_{SE} + U_{CO}}{2} \cdot \left( \frac{C_1}{C_1 + C_2} \right) + \frac{U_{TV}}{2}$$

With a small conversion of these equations it is easily seen that these equations are equivalent to the equation 4.3_22.

*Example:*
*(windings arrangement and nomenclature acc. to Fig. 4.3-4)*

**Transformer data:**
*3 · 167 MVA, 550 kV/245 kV (1±10·1,2%)/30 kV, 50 Hz, regulation at the low-voltage line end*

HV:  $U_1 = 550\ kV$
LV:  $U_2 = 245\ kV$
TV:  $U_T = U_2 \cdot 0.12 = 29.4\ kV$

capacity to the adjacent winding:  $C_1 = 1750\ pF$
capacity to grounded parts:  $C_2 = 2150\ pF$

$$\left| \bar{U}_{r+} \right| = -\frac{245\,kV}{2 \cdot \sqrt{3}} + \frac{550\,kV}{2 \cdot \sqrt{3}} \left( \frac{2150\,pF}{3900\,pF} \right) - \frac{29.4\,kV}{2 \cdot \sqrt{3}} = 8.32\,kV$$

$$\left| \bar{U}_{r-} \right| = -\frac{245\,kV}{2 \cdot \sqrt{3}} + \frac{550\,kV}{2 \cdot \sqrt{3}} \left( \frac{2150\,pF}{3900\,pF} \right) + \frac{29.4\,kV}{2 \cdot \sqrt{3}} = 25.29\,kV$$

$$\left| \bar{I}_{s+} \right| = 2\pi \cdot 50 \frac{1}{s} \left( \frac{550\,kV}{2 \cdot \sqrt{3}} 2150\,pF - \frac{29.4\,kV}{2 \cdot \sqrt{3}} 3900\,pF - \frac{245\,kV}{2 \cdot \sqrt{3}} 3900\,pF \right) = 10.19\,mA$$

$$\left| \bar{I}_{s-} \right| = 2\pi \cdot 50 \frac{1}{s} \left( \frac{550\,kV}{2 \cdot \sqrt{3}} 2150\,pF + \frac{29.4\,kV}{2 \cdot \sqrt{3}} 3900\,pF - \frac{245\,kV}{2 \cdot \sqrt{3}} 3900\,pF \right) = 30.99\,mA$$

### 4.3.2.1.4 OLTCs IN PHASE-SHIFTING TRANSFORMERS

The last example with respect to the potential connection phenomenon of the tap winding discussed here is the use of OLTCs with reversing change-over selector in Phase-Shifting Transformers (PST) with one core design (direct regulation). The occuring recovery voltages and switched currents are often very high. Therefore the calculation of these values is very important and can have a deep influence on the design of the transformer.

The generation of the phase angle is achieved by adding a cross voltage to the voltages of the source- and load-side. This can be realized in a three-phase system by ntroducing a tap winding in one phase and adding it to another phase. A typical windings arrangement and the appropriate windings connection are shown in Figs. 4.3-5a and b.

The basic formulations for the equivalent network shown in Fig. 4.3-6a and prepared in the same way as shown in the previous paragraphs leads to:
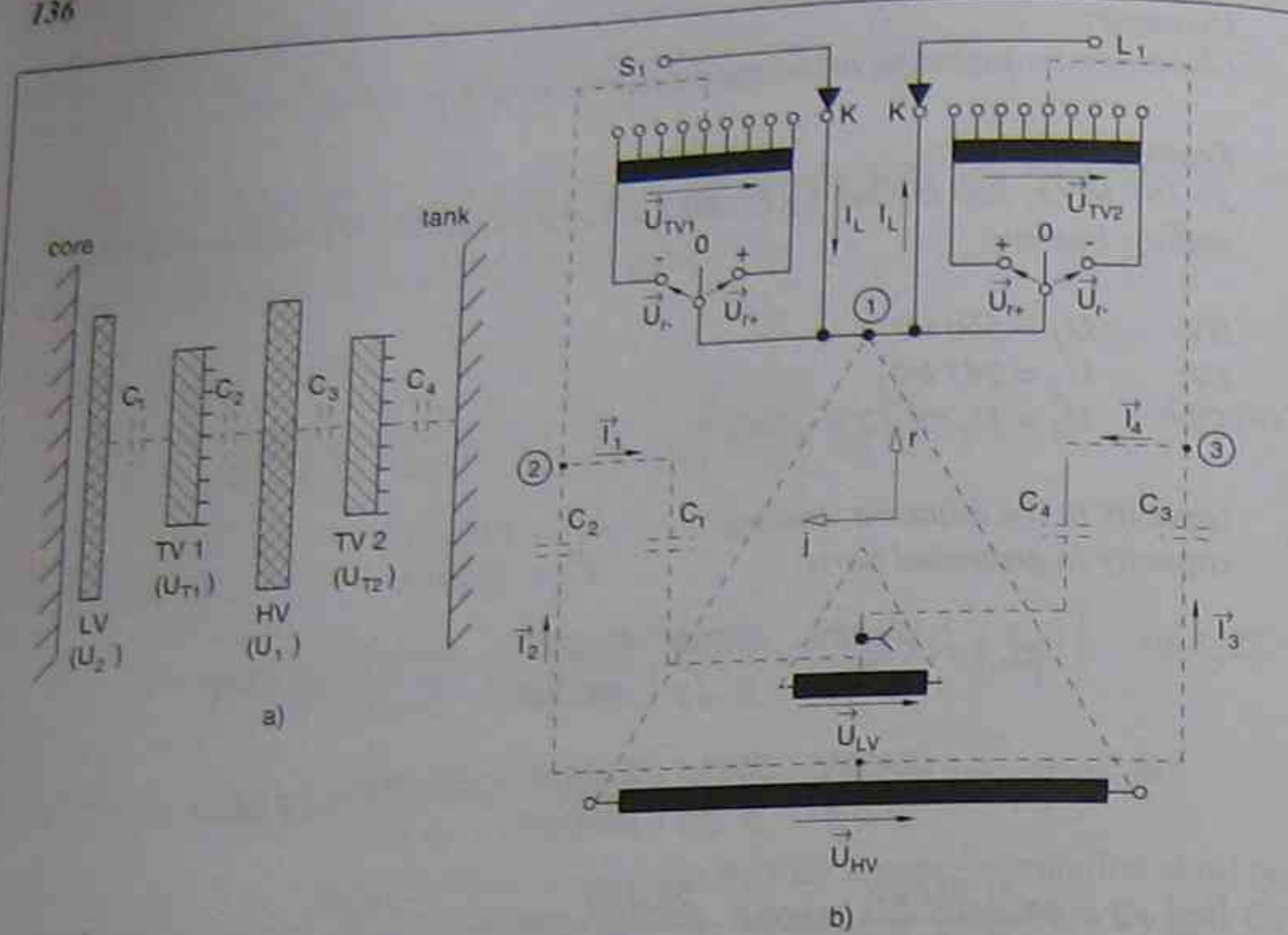
**Fig. 4.3-5:** OLTC (phase-shifting transformer) in mid-position with disconnected tap winding (**a:** windings arrangement, **b:** windings connection)

$$\bar{U}_{r+/-} = \bar{U}_Y \cdot \left( \frac{C_1}{C_1 + C_2} \right) + \bar{U}_Z \cdot \left( \frac{C_2}{C_1 + C_2} \right) \pm \frac{\bar{U}_{TV1}}{2} \qquad (4.3\_28)$$

and for the equivalent electrical network in Fig. 4.3_6b $I_S$ follows to:

$$\bar{I}_{S+/-} = -\bar{U}_Y \cdot j \cdot \omega \cdot C_1 - \bar{U}_Z \cdot j \cdot \omega \cdot C_2 \mp \frac{\bar{U}_{TV1}}{2} \cdot j \cdot \omega \cdot (C_1 + C_2) \qquad (4.3\_29)$$

From the phasor diagram (Fig. 4.3-6c) the voltages $\bar{U}_Y$, $\bar{U}_Z$ and $\bar{U}_{TV1}$ can be determined to:

$$\bar{U}_Y = -\frac{U_1}{\sqrt{3}} - \frac{U_2}{2 \cdot \sqrt{3}} \quad , \quad \bar{U}_Z = -\frac{3 \cdot U_1}{2 \cdot \sqrt{3}} \quad , \quad \bar{U}_{TV1} = j \cdot U_{T1}$$

Applying these relations to equation 4.3_28 the recovery voltages follow as (only valid for a configuration acc. to Fig. 4.3-5):

$$\bar{U}_{r+/-} = -\frac{U_1}{\sqrt{3}} \cdot \left( \frac{2 \cdot C_1 + 3 \cdot C_2}{2 \cdot (C_1 + C_2)} \right) - \frac{U_2}{2 \cdot \sqrt{3}} \cdot \left( \frac{C_1}{C_1 + C_2} \right) \pm j \cdot \frac{U_{T1}}{2} \qquad (4.3\_30)$$
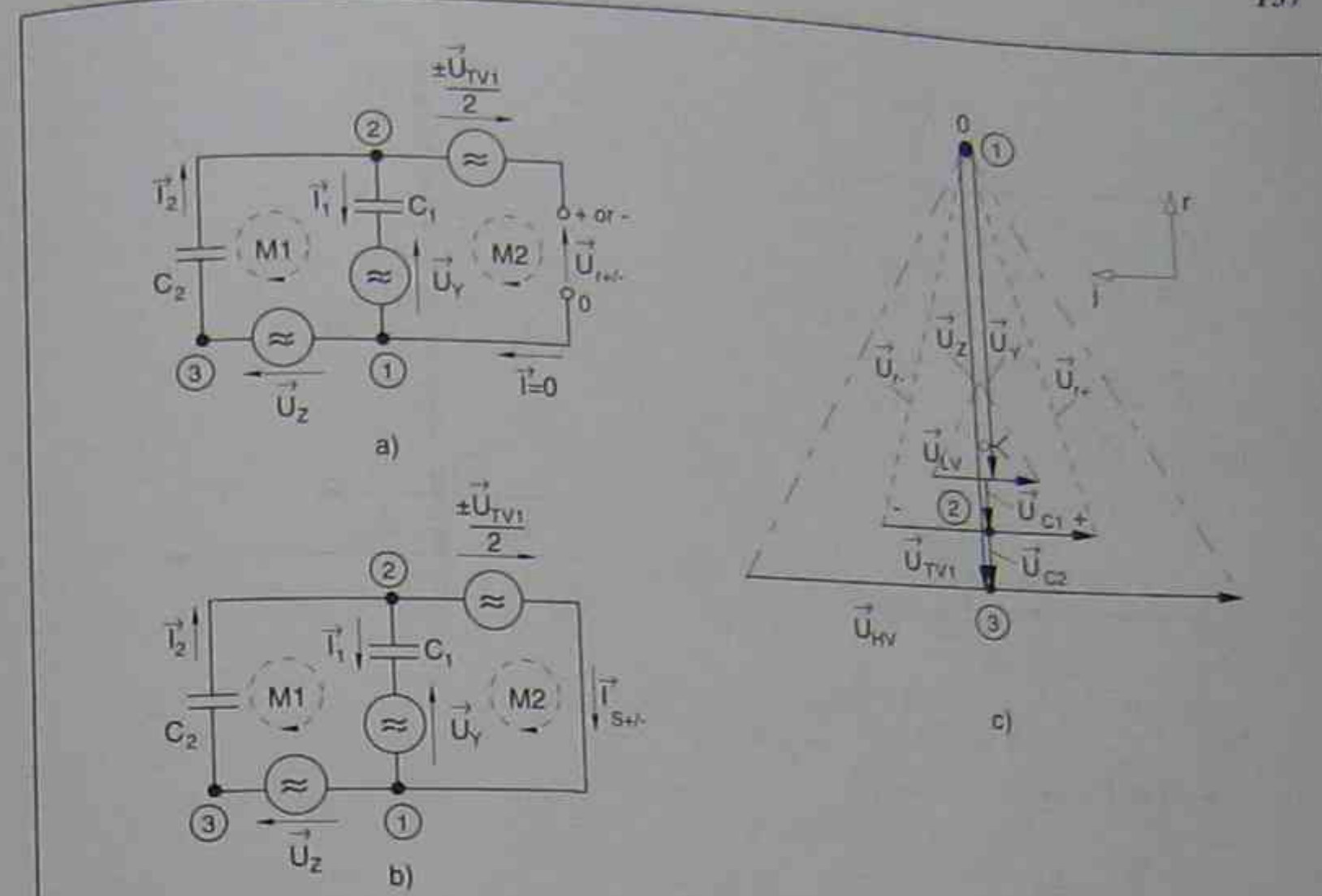
**Fig. 4.3-6:** OLTC (phase-shifting transformer) in mid-position with disconnected tap winding (TAP1) (**a:** equivalent network for calculation of the recovery voltage, **b:** equivalent network for calculation of the switched current, **c:** phasor diagram)

With equation 4.3_30 the absolute values of the recovery voltages can be calculated to:

$$|\bar{U}_{r+/-}| = \sqrt{\left( -\frac{U_1}{2\sqrt{3}} \left( \frac{2 \cdot C_1 + 3 \cdot C_2}{C_1 + C_2} \right) - \frac{U_2}{2\sqrt{3}} \left( \frac{C_1}{C_1 + C_2} \right) \right)^2 + \left( \frac{U_{T1}}{2} \right)^2} \qquad (4.3\_31)$$

Using the same relations as mentioned above the switched currents can be expressed as:

$$\bar{I}_{S+/-} = \frac{\bar{U}_1}{2\sqrt{3}} j \cdot \omega \cdot (2C_1 + 3C_2) + \frac{\bar{U}_2}{2\sqrt{3}} j \cdot \omega \cdot C_1 \pm \frac{\bar{U}_{T1}}{2} \omega \cdot (C_1 + C_2) \qquad (4.3\_32)$$

Herewith the absolute values of the switched currents become:

$$|\bar{I}_{S+/-}| = \omega \cdot \sqrt{\left( \frac{\bar{U}_{T1}}{2} (C_1 + C_2) \right)^2 + \left( \frac{\bar{U}_1}{2\sqrt{3}} (2C_1 + 3C_2) + \frac{\bar{U}_2}{2\sqrt{3}} C_1 \right)^2} \qquad (4.3\_33)$$

The stresses on the change-over selector contacts of tap winding 2 can be calculated acc. to Figs. 4.3-7 in the same way.
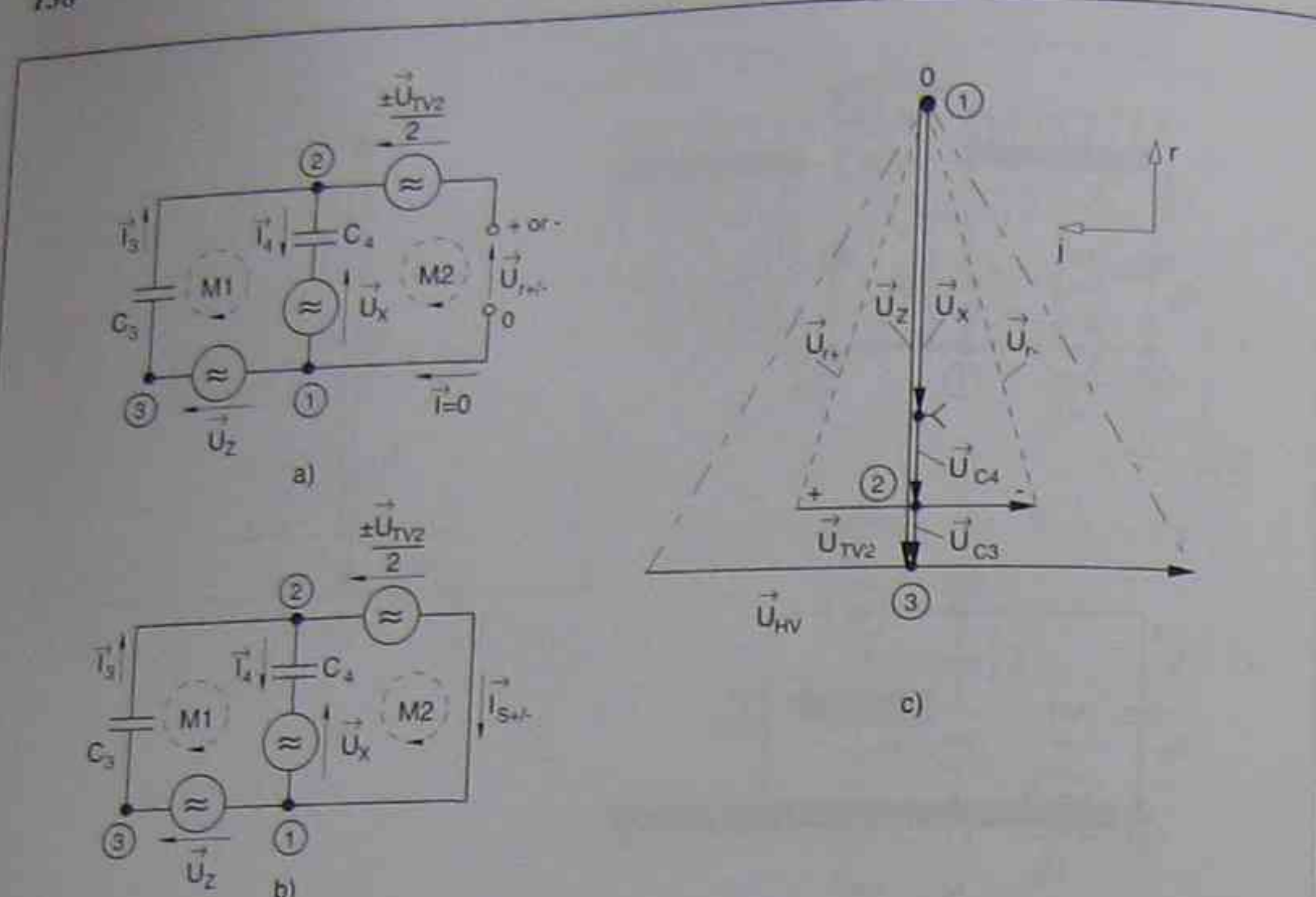
absolute values of the recovery voltages:

Fig. 4.3-7: OLTC (phase-shifting transformer) in mid-position with disconnected tap winding (TAP2) (a: equivalent network for calculation of the recovery voltage, b: equivalent network for calculation of the switched current, c: phasor diagram)

$$\left|\vec{U}_{r+/-}\right| = \sqrt{\left(-\frac{U_1}{2 \cdot \sqrt{3}}\left(\frac{2 \cdot C_4 + 3 \cdot C_3}{(C_3 + C_4)}\right)\right)^2 + \left(\frac{U_{T1}}{2}\right)^2} \qquad (4.3\_34)$$

absolute values of the switched currents:

$$\left|\vec{I}_{S+/-}\right| = \omega \cdot \sqrt{\left(\frac{\bar{U}_{T1}}{2}(C_3 + C_4)\right)^2 + \left(\frac{\bar{U}_1}{2\sqrt{3}}(2C_4 + 3C_3)\right)^2} \qquad (4.3\_35)$$

The phase angles between the recovery voltages and the switched currents are for both tap windings -90°.

*Example:*
(windings arrangement and nomenclature acc. to Figs. 4.3-5 to 4.3-7)

**Transformer data:**
675 MVA, 240 kV ± 40° (full load)/30 kV, 60 Hz, one core design

HV:   $U_1 = 240\,kV$
LV:   $U_2 = 30\,kV$
TV:   $U_T = 62,65\,kV$

capacities to the adjacent winding or potentials:
$C_1 = 1750\,pF$, $C_2 = 2540\,pF$, $C_3 = 3530\,pF$, $C_4 = 1700\,pF$

**TAP 1**

$$\left|\bar{U}_{r+/-}\right| = \sqrt{\left(\frac{240\,kV}{2 \cdot \sqrt{3}}\left(\frac{11120\,pF}{4290\,pF}\right) + \frac{30\,kV}{2 \cdot \sqrt{3}}\left(\frac{1750\,pF}{4290\,pF}\right)\right)^2 + \left(\frac{62.65\,kV}{2}\right)^2} = 185.78\,kV$$

$$\left|\bar{I}_{S+/-}\right| = 2\pi \cdot 60 \frac{1}{s} \cdot \sqrt{\left(\frac{62.65\,kV}{2}4290\,pF\right)^2 + \left(\frac{240\,kV}{2 \cdot \sqrt{3}}11120\,pF + \frac{30\,KV}{2 \cdot \sqrt{3}}1750\,pF\right)^2} = ..$$

$$\left|\bar{I}_{S+/-}\right| = 300.46\,mA$$

**TAP 2**

$$\left|\bar{U}_{r+/-}\right| = \sqrt{\left(\frac{240\,kV}{2 \cdot \sqrt{3}}\left(\frac{13990\,pF}{5230\,pF}\right)\right)^2 + \left(\frac{62.65\,kV}{2}\right)^2} = 187.95\,kV$$

$$\left|\bar{I}_{S+/-}\right| = 2\pi \cdot 60 \frac{1}{s} \cdot \sqrt{\left(\frac{62.65\,kV}{2}5230\,pF\right)^2 + \left(\frac{240\,kV}{2 \cdot \sqrt{3}}(13990\,pF)\right)^2} = 370.58\,mA$$

### 4.3.2.1.5 MODEL FOR THE CALCULATION OF THE RECOVERY VOLTAGES AND SWITCHED CURRENTS OF REVERSING CHANGE-OVER SELECTORS

In the previous four paragraphs it was demonstrated how to calculate the recovery voltages and switched currents by applying different equations derived from the corresponding equivalent electrical networks. When comparing these equivalent electrical networks in Figs. 4.3-2 through 4.3-7 it can be seen that the networks used for the calculation of the recovery voltages and switched currents are nearly identical, but the values of the individual components differ. Consequently it seems feasible to create a model which could be used for the calculation of all applications of OLTCs with reversing change-over selector. However, this model is only valid for two capacitances to the adjacent potentials and the lumped capacitors are connected to the middle of the tap winding.

Under these conditions the windings connection shown in Fig. 4.3-8a can be found and translated into the two equivalent electrical networks for the calculations of the recovery voltages (Fig. 4.3-8b) and the switched currents (Fig. 4.3-8c). From the windings connection it can be seen that the stresses on the "+" and "-" contacts only differ by the sign of $\frac{\bar{U}_{TV}}{2}$. These networks show small modifications compared with the networks used in the foregoing calculations to reach general validity.

The basic formulations for the calculation of the recovery voltages found with the equivalent electrical networks shown in Fig. 2.3-8b are:

from mesh 1 of the network:

$$\bar{U}_B - \bar{I}_A \cdot \frac{1}{j \cdot \omega \cdot C_A} - \bar{I}_B \cdot \frac{1}{j \cdot \omega \cdot C_B} = 0 \qquad (4.3\_36)$$

from mesh 2 of the network:

$$-\bar{U}_K + \bar{I}_B \cdot \frac{1}{j \cdot \omega \cdot C_B} \pm \frac{\bar{U}_{TV}}{2} = \bar{U}_{r+/-} \qquad (4.3\_37)$$

from the nodal equation at node ①:

$$\bar{I}_A - \bar{I}_B = \bar{I} \Rightarrow \bar{I}_A = \bar{I}_B \qquad (4.3\_38)$$

$\bar{U}_{r+/-}$ follows to:

$$\bar{U}_{r+/-} = \bar{U}_B \cdot \frac{C_A}{C_A + C_B} - \bar{U}_K \pm \frac{\bar{U}_{TV}}{2} \qquad (4.3\_39)$$

The calculation of the switched currents can be performed using the network shown in Fig. 4.3-8c with the use of the basic formulations:
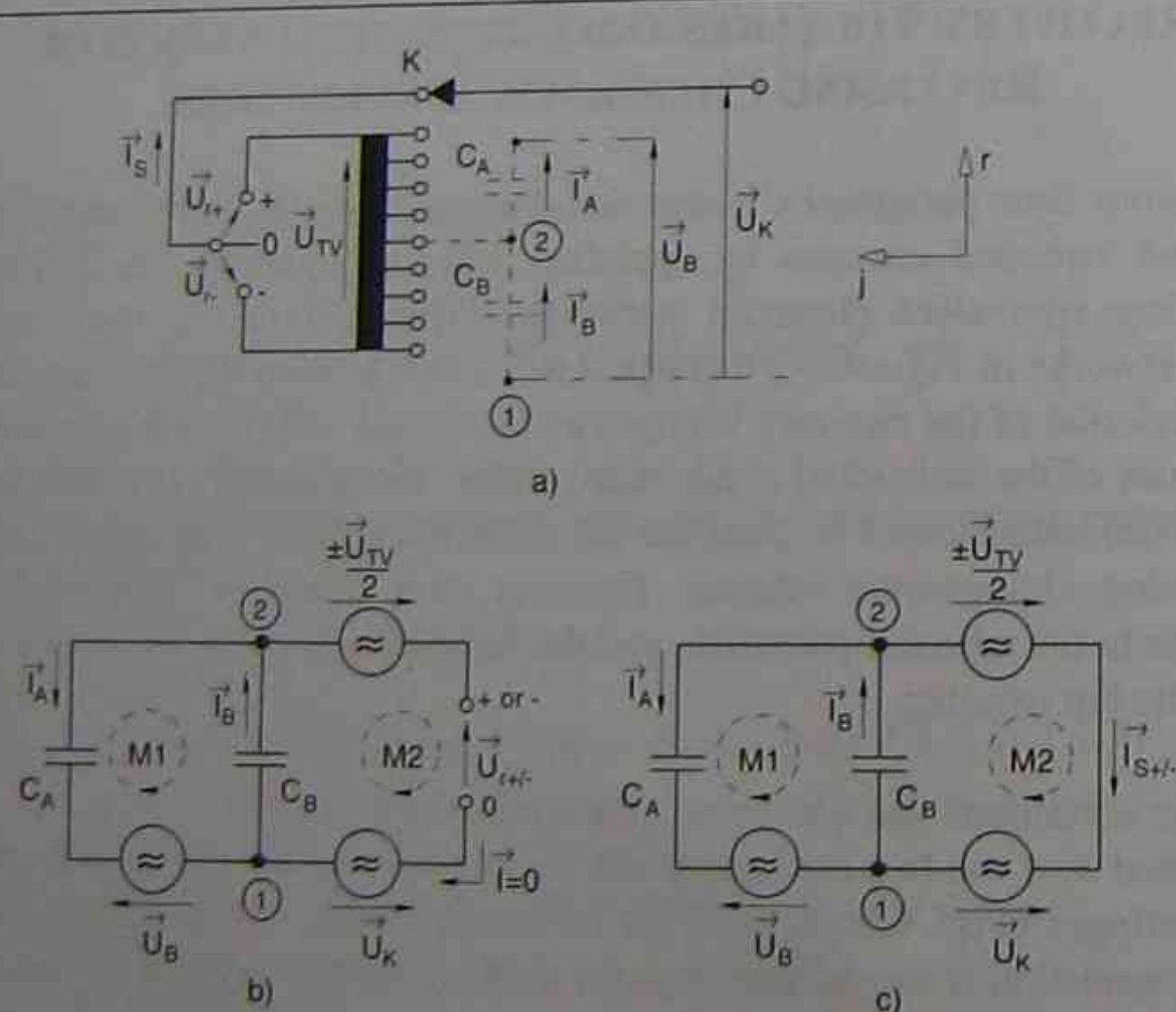


Fig. 4.3-8: Model for an OLTC in mid-position with disconnected tap winding (a: windings connection, b: equivalent network for calculation of the recovery voltage, c: equivalent network for calculation of the switched current)

from mesh 1 of the network:

$$\bar{U}_C - \bar{I}_A \cdot \frac{1}{j \cdot \omega \cdot C_A} - \bar{I}_B \cdot \frac{1}{j \cdot \omega \cdot C_B} = 0 \qquad (4.3\_40)$$

from mesh 2 of the network:

$$-\bar{U}_K + \bar{I}_B \cdot \frac{1}{j \cdot \omega \cdot C_B} \pm \frac{\bar{U}_{TV}}{2} = 0 \qquad (4.3\_41)$$

from the nodal equation at node ①:

$$\bar{I}_B - \bar{I}_A = \bar{I}_{S+/-} \Rightarrow \bar{I}_A = \bar{I}_B - \bar{I}_{S+/-} \qquad (4.3\_42)$$

$\bar{I}_{S+/-}$ follows to:

$$\bar{I}_{S+/-} = \bar{U}_K \cdot j \cdot \omega \cdot (C_A + C_B) - \bar{U}_B \cdot j \cdot \omega \cdot C_A \mp \frac{\bar{U}_{TV}}{2} \cdot j \cdot \omega \cdot (C_A + C_B) \qquad (4.3\_43)$$

The equations 4.3_39 and 4.3_43 can be used for every application that meets the conditions mentioned above. An important condition to reach the correct result is the exact determination of $\bar{U}_B$ and $\bar{U}_K$. These two phasors have to be expressed in their complex form.

For a better understanding how to use the two equations 4.3_39 and 4.3_43, the procedure shall be demonstrated here based on an application acc. to Figs. 4.3-3. The first step to be completed is the definition of node ① and the capacitors $C_A$ and $C_B$ (comp. Fig. 4.3-8a). For the example explained here the node ① is choosen as the grounded middle of the voltage triangle (neutral-end). With this definition $C_A$ has to be $C_1$ from Fig. 4.3-3b and $C_B$ has to be $C_2$. Now the voltage phasors $\bar{U}_B$ and $\bar{U}_K$ are fixed.

$\bar{U}_B$ starts at the neutral and ends where $C_1$ connects, this means in the middle of $\bar{U}_{HV}$. With the definition of the real and imaginary axis' in Figs. 4.3-3 follows:

$$\bar{U}_B = j \cdot \frac{U_{HV}}{2 \cdot \sqrt{3}} \qquad (4.3\_44)$$

$\bar{U}_K$ starts at the same point as $\bar{U}_B$ and it ends at the "K" contact which is connected to the edge of the triangle:

$$\bar{U}_K = -\frac{U_{HV}}{2} + j \cdot \frac{U_{HV}}{2 \cdot \sqrt{3}} \qquad (4.3\_45)$$

With the same conditions as agreed in 4.3.2.1.2 ($\bar{U}_{HV} = U_1$ and $\bar{U}_{TV} = U_T$) the recovery voltages (eq. 4.3_39) can be expressed as:

$$\bar{U}_{r+/-} = j\frac{U_1}{2\cdot\sqrt{3}}\cdot\frac{C_1}{C_1+C_2} - j\cdot\frac{U_1}{2\cdot\sqrt{3}} + \frac{U_1}{2} \pm \frac{\bar{U}_T}{2} \qquad (4.3\_46)$$

or converted to:

$$\bar{U}_{r+/-} = \frac{U_1}{2} \pm \frac{\bar{U}_T}{2} - j\cdot\frac{U_1}{2\cdot\sqrt{3}}\cdot\frac{C_2}{C_1+C_2} \qquad (4.3\_46a)$$

The switched currents follow under the same conditions and with some conversions to (eq. 4.3_43):

$$\bar{I}_{S+/-} = -\frac{U_1}{2\cdot\sqrt{3}}\cdot\omega\cdot C_2 - j\left(\frac{U_1 \pm U_T}{2}\right)\cdot\omega\cdot(C_1+C_2) \qquad (4.3\_47)$$

The equations 4.3_46a and 47 show the same result as the equations 4.3_15a and 18a.

The use of the above mentioned model for the calculation of the stresses during the reversing change-over selector operation is very simple. But the definitions needed for every calculation are of great importance and have to studied thoroughly.

## 4.3.2.2 REGULATION WITH COARSE CHANGE-OVER SELECTOR

### 4.3.2.1.1 NEUTRAL-END CONNECTION OF THE OLTC

Before the change-over selector operation takes place the tap selector is in position "K" and the change-over selector is in position "+" or "-". Figure 4.3-9 shows an example of a typical windings arrangement and the windings connection for a neutral-end regulation with coarse change-over selector and the OLTC in the mid-position.

The load current of the transformer does not flow through the regulating winding in this position. When the change-over selector is still closed a current flows through the change-over selector contacts "+" or "-" and the winding capacitances $C_1$ and $C_2$ due to the voltages $U_{CV}$ and $U_{TV}$. This capacitive current $I_{S+}$ or $I_{S-}$ has to be switched off during the change-over selector operation. The recovery voltage $U_{r+}$ or $U_{r-}$ is defined as the difference in potential between the change-over selector contacts "+" or "-" and the "0" contact when the contacts are open. In case of the coarse change-over selector, the potential of the common contact "0" which is connected to the tap winding floats. Whereas the potentials of the change-over selector contacts "+" and "-" are fixed by the connection to the coarse winding.

The winding capacities and the capacities to ground are represented in Fig. 4.3-9b as discrete equivalent capacitors, which are connected to the middle of the windings and fed by one half of the of the voltages $\bar{U}_{CV}$ and $\bar{U}_{TV}$. In the equivalent electrical
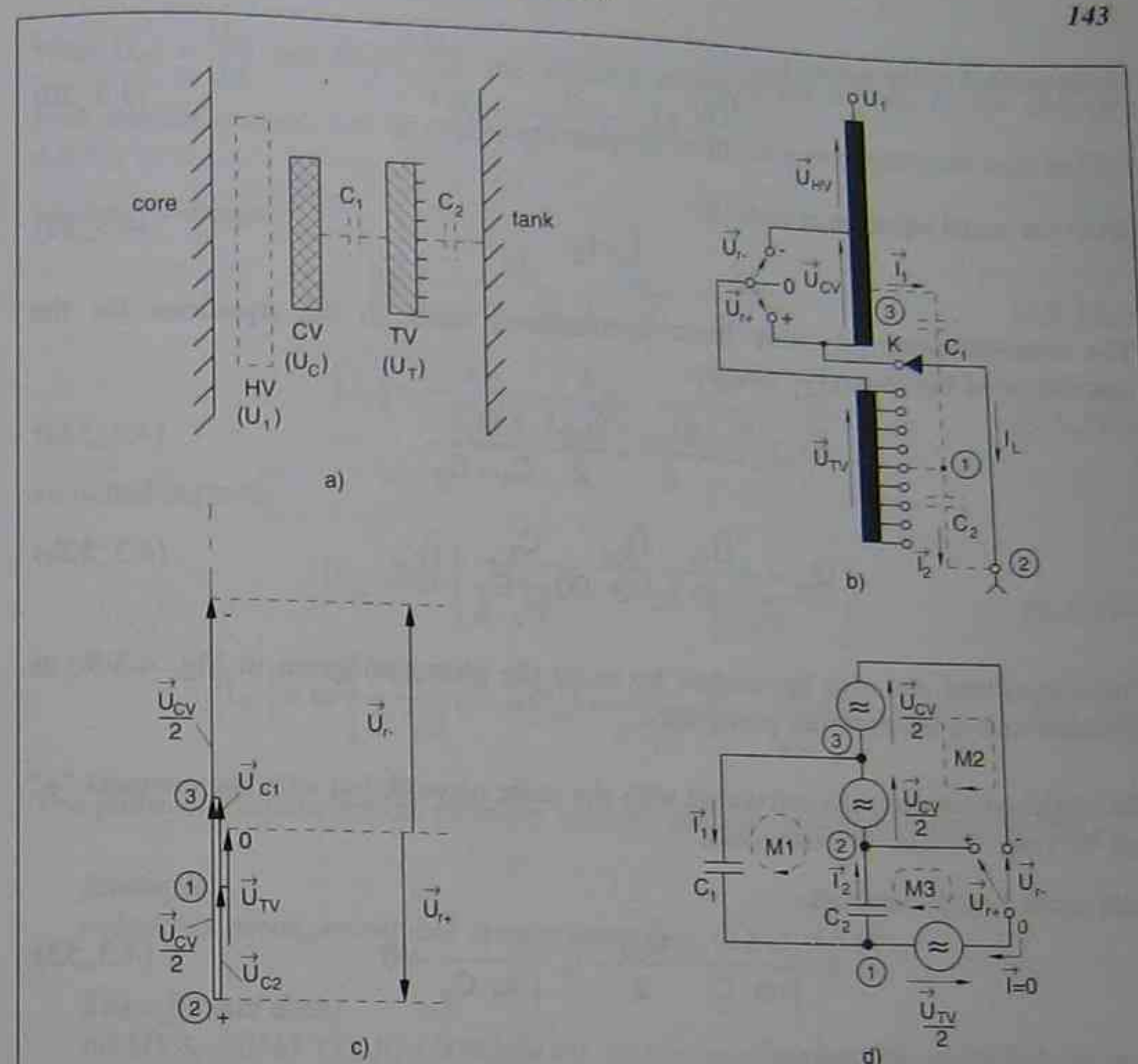
Fig. 4.3-9: OLTC (connected at the neutral-end) in mid-position with disconnected tap winding (a: windings arrangement, b: windings connection, c: phasor diagram, d: equivalent network for calculation of the recovery voltage)

network (4.3-9d) the voltages ($\frac{\bar{U}_{CV}}{2}$ and $\frac{\bar{U}_{TV}}{2}$) are represented by the equivalent voltage sources. This network serves for the calculation of the recovery voltages (change-over selector contacts are open).

Using the equivalent electrical network (Fig. 4.3-9d) the recovery voltages can be determined as follows:

from mesh 1 of the network:

$$-\bar{I}_1\cdot\frac{1}{j\cdot\omega\cdot C_1} - \frac{\bar{U}_{CV}}{2} - \bar{I}_2\cdot\frac{1}{j\cdot\omega\cdot C_2} = 0 \qquad (4.3\_48)$$

from mesh 2 of the network:

$$-\frac{\bar{U}_{TV}}{2} + \bar{I}_2\cdot\frac{1}{j\cdot\omega\cdot C_2} + \frac{\bar{U}_{CV}}{2} + \frac{\bar{U}_{CV}}{2} = \bar{U}_{r-} \qquad (4.3\_49)$$

from mesh 3 of the network:

$$-\frac{\bar{U}_{TV}}{2}+\bar{I}_2\cdot\frac{1}{j\cdot\omega\cdot C_2}=\bar{U}_{r+} \qquad (4.3\_50)$$

from the nodal equation at node ①:

$$\bar{I}_1=\bar{I}_2 \qquad (4.3\_51)$$

The transformation of these basic formulations leads to the equations for the calculation of the recovery voltages:

$$\bar{U}_{r+}=-\frac{\bar{U}_{TV}}{2}-\frac{\bar{U}_{CV}}{2}\cdot\frac{C_1}{C_1+C_2} \qquad (4.3\_52a)$$

$$\bar{U}_{r+}=-\frac{\bar{U}_{TV}}{2}-\frac{\bar{U}_{CV}}{2}\cdot\frac{C_1}{C_1+C_2}+\bar{U}_{CV} \qquad (4.3\_52b)$$

These equations can also be reached by using the phasor diagram in Fig. 4.3-9c as demonstrated in the previous paragraphs.

The switched currents are calculated with the same network but with the contacts "+" and "0" resp. "-" and "0" connected.

from mesh 1 of the network:

$$-\bar{I}_1\cdot\frac{1}{j\cdot\omega\cdot C_1}-\frac{\bar{U}_{CV}}{2}-\bar{I}_2\cdot\frac{1}{j\cdot\omega\cdot C_2}=0 \qquad (4.3\_53)$$

from mesh 2 of the network:

$$-\frac{\bar{U}_{TV}}{2}+\bar{I}_2\cdot\frac{1}{j\cdot\omega\cdot C_2}+\frac{\bar{U}_{CV}}{2}+\frac{\bar{U}_{CV}}{2}=0 \quad \text{for } \bar{I}_{s-} \qquad (4.3\_54)$$

from mesh 3 of the network:

$$-\frac{\bar{U}_{TV}}{2}+\bar{I}_2\cdot\frac{1}{j\cdot\omega\cdot C_2}=0 \quad \text{for } \bar{I}_{s+} \qquad (4.3\_55)$$

from the nodal equation at node ①:

$$\bar{I}_1=\bar{I}_2-\bar{I}_s \qquad (4.3\_56)$$

The equations for the calculation of the switched currents can be derived from these equations:

$$\bar{I}_{s+}=j\cdot\omega\cdot\left[\frac{\bar{U}_{TV}}{2}(C_1+C_2)+\frac{\bar{U}_{CV}}{2}\cdot C_1\right] \qquad (4.3\_57a)$$

$$\bar{I}_{s-}=j\cdot\omega\cdot\left[\frac{\bar{U}_{TV}}{2}\cdot(C_1+C_2)+\frac{\bar{U}_{CV}}{2}\cdot C_1-\bar{U}_{CV}\cdot(C_1+C_2)\right] \qquad (4.3\_57b)$$

With $\bar{U}_{CV}=\frac{U_C}{\sqrt{3}}$ and $\bar{U}_{TV}=\frac{U_T}{\sqrt{3}}$ the absolute values of the stresses on the change-over selector contacts can be expressed as (only valid for a configuration acc. to Fig. 4.3-9):

recovery voltages:

$$\left|\bar{U}_{r+}\right|=-\frac{U_C}{2\cdot\sqrt{3}}\cdot\frac{C_1}{C_1+C_2}-\frac{U_T}{2\cdot\sqrt{3}} \qquad (4.3\_58a)$$

$$\left|\bar{U}_{r-}\right|=-\frac{U_C}{2\cdot\sqrt{3}}\cdot\frac{C_1}{C_1+C_2}-\frac{U_T}{2\cdot\sqrt{3}}+\frac{U_C}{\sqrt{3}} \qquad (4.3\_58a)$$

switched currents:

$$\left|\bar{I}_{s+}\right|=\omega\cdot\left[\frac{U_T}{2\cdot\sqrt{3}}(C_1+C_2)+\frac{U_C}{2\cdot\sqrt{3}}\cdot C_1\right] \qquad (4.3\_59a)$$

$$\left|\bar{I}_{s-}\right|=\omega\cdot\left[\frac{U_T}{2\cdot\sqrt{3}}(C_1+C_2)+\frac{U_C}{2\cdot\sqrt{3}}\cdot C_1-\frac{U_C}{\sqrt{3}}(C_1+C_2)\right] \qquad (4.3\_59b)$$

The phase angle between the recovery voltages and the switched currents is -90°.

**Example:**
(windings arrangement and nomenclature acc. to Fig. 4.3-9)

**Transformer data:**
*60 MVA, 110 kV (1±10 1,00%)/24 kV, 50 Hz, regulation in the neutral-end*

HV: $U_1 = 99\,kV$
TV: $U_T = 110\,kV\cdot 0.1 = 11.0\,kV$
CV: $U_C = 110\,kV\cdot 0.1 = 11.0\,kV$

capacity to the adjacent winding: $\quad C_1 = 1750\,pF$
capacity to grounded parts: $\quad\quad C_2 = 350\,pF$

$$\left|\bar{U}_{r+}\right|=-\frac{11kV}{2\cdot\sqrt{3}}\cdot\left(\frac{1750pF}{1750pF+350pF}\right)-\frac{11kV}{2\cdot\sqrt{3}}=5.82kV$$

$$\left|\bar{U}_{r-}\right|=\frac{11kV}{2\cdot\sqrt{3}}\cdot\left(\frac{1750pF}{1750pF+350pF}\right)-\frac{30kV}{2\cdot\sqrt{3}}+\frac{11kV}{\sqrt{3}}=0.53kV$$

$$\left|\bar{I}_{s+}\right|=2\pi\cdot 50\frac{1}{s}\cdot\left(\frac{11kV}{2\cdot\sqrt{3}}(1750pF+350pF)+\frac{11kV}{2\cdot\sqrt{3}}1750pF\right)=3.84mA$$

$$\left|\bar{I}_{s-}\right|=2\pi\cdot 50\frac{1}{s}\cdot\left(\frac{11kV}{2\cdot\sqrt{3}}(2100pF)+\frac{11kV}{2\cdot\sqrt{3}}1750pF-\frac{11kV}{\sqrt{3}}(2100pF)\right)=0.35mA$$

## 4.3.2.2.2 DELTA CONNECTION OF THE OLTC

In the following example, the calculation of the recovery voltages and the switched currents is performed on an application with the OLTC located at the end of a delta winding. Figs. 4.3-9 shows an example for the calculation with the same windings arrangement as used in 4.3.2.2.1.

The equivalent electrical network shown in Fig. 4.3-10d is very similar to the network shown in Fig. 4.3-9d. The only difference is an additional equivalent voltage source $U_Y$ between nodes ① and ②. This additional voltage source represents the voltage difference between the grounded middle of the voltage triangle, where the capacitor $C_2$ is connected, and the contact "+" of the change-over selector (comp. 4.3.2.2.1: in case of a regulation at the neutral-end this voltage is zero).
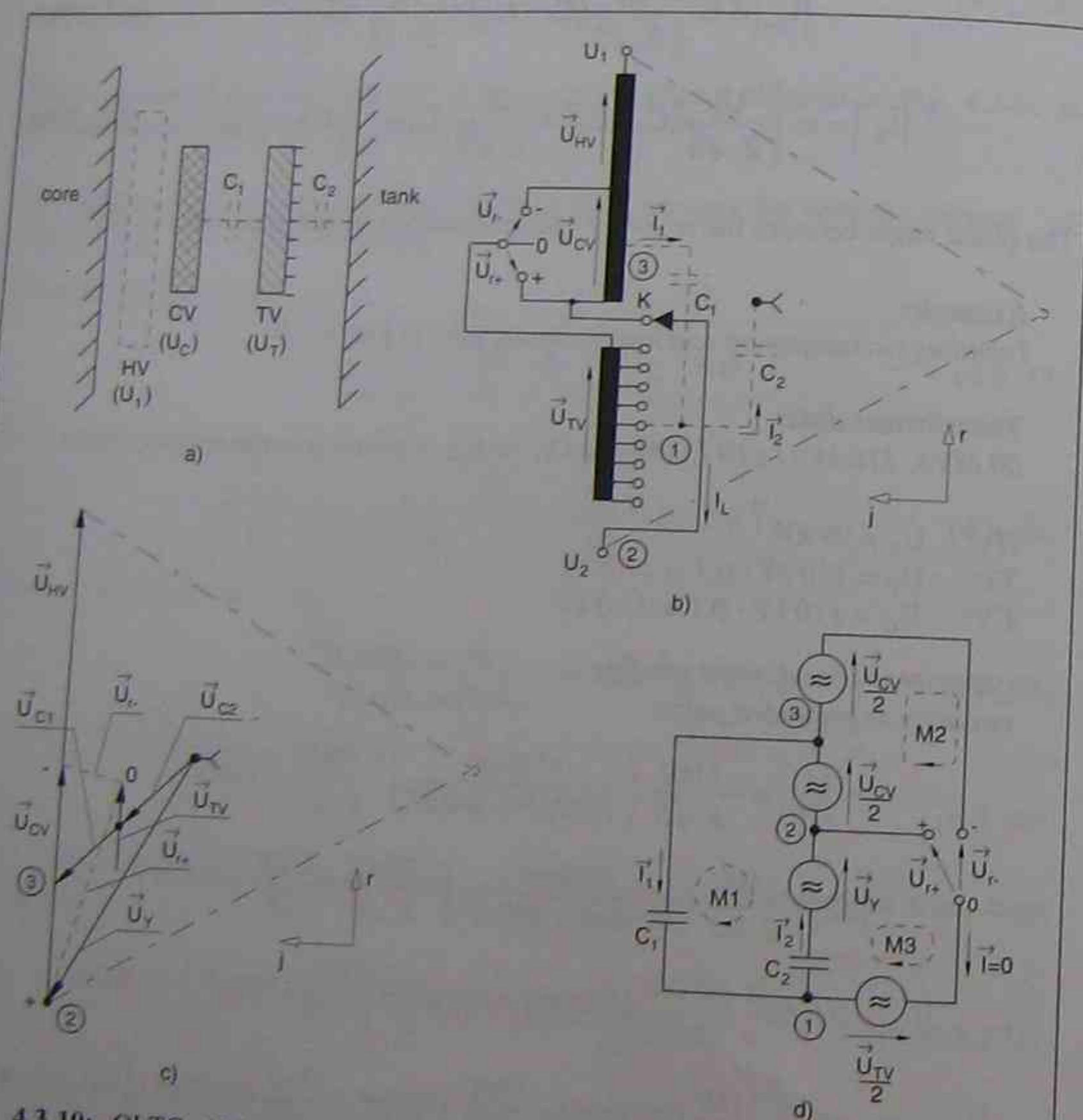


Fig. 4.3-10: OLTC (delta connected) in mid-position with disconnected tap winding
(a: windings arrangement, b: windings connection, c: phasor diagram, d: equivalent network for calculation of the recovery voltage)

The calculation of the recovery voltages can be performed in the same way as described under 4.3.2.2.1 but the basic formulations have to be changed (the additional voltage source).

Using this new basic formulations the equations for the calculation of the recovery voltage result to:

$$\bar{U}_{r+} = -\frac{\bar{U}_{TV}}{2} + \left(-\frac{\bar{U}_{CV}}{2} - \bar{U}_Y\right)\left(\frac{C_1}{C_1 + C_2}\right) + \bar{U}_Y \qquad (4.3\_60a)$$

$$\bar{U}_{r-} = -\frac{\bar{U}_{TV}}{2} + \left(-\frac{\bar{U}_{CV}}{2} - \bar{U}_Y\right)\left(\frac{C_1}{C_1 + C_2}\right) + \bar{U}_Y + \bar{U}_{CV} \qquad (4.3\_60b)$$

For the switched currents follows:

$$\bar{I}_{S+} = \left(\frac{\bar{U}_{TV}}{2} + \frac{\bar{U}_{CV}}{2}\right) \cdot j \cdot \omega \cdot C_1 + \left(\frac{\bar{U}_{TV}}{2} - \bar{U}_Y - \bar{U}_{CV}\right) \cdot j \cdot \omega \cdot C_2 \qquad (4.3\_61a)$$

$$\bar{I}_{S-} = \left(\frac{\bar{U}_{TV}}{2} + \frac{\bar{U}_{CV}}{2}\right) \cdot j \cdot \omega \cdot C_1 + \left(\frac{\bar{U}_{TV}}{2} - \bar{U}_Y - \bar{U}_{CV}\right) \cdot j \cdot \omega \cdot C_2 - \bar{U}_{CV} \cdot j \cdot \omega \cdot C_1 \qquad (4.3\_61b)$$

For the phasor $\bar{U}_Y$ (comp. Figs. 4.3-10b or c) with $\bar{U}_{HV} = U_1$, $\bar{U}_{TV} = U_T$ and $\bar{U}_{CV} = U_C$

follows: $\bar{U}_Y = -\dfrac{U_1 + U_C}{2} + j \cdot \dfrac{U_1 + U_C}{2 \cdot \sqrt{3}}$. With these definitions the stresses on the change-over selector contacts are calculated to (only valid for a configuration acc. to Fig. 4.3-10):

$$\left|\bar{U}_{r+}\right| = \sqrt{\left[\frac{U_1}{2}\left(\frac{C_1}{C_1 + C_2}\right) - \frac{U_1 + U_C - U_T}{2}\right]^2 + \left[\frac{U_1 + U_C}{2 \cdot \sqrt{3}}\left(1 - \frac{C_1}{C_1 + C_2}\right)\right]^2} \qquad (4.3\_62a)$$

$$\left|\bar{U}_{r-}\right| = \sqrt{\left[\frac{U_1}{2}\left(\frac{C_1}{C_1 + C_2}\right) - \frac{U_1 + U_C - U_T}{2} + U_C\right]^2 + \left[\frac{U_1 + U_C}{2 \cdot \sqrt{3}}\left(1 - \frac{C_1}{C_1 + C_2}\right)\right]^2} \qquad (4.3\_62b)$$

and

$$\left|\bar{I}_{S+}\right| = \omega \cdot \sqrt{\left[\frac{U_1 + U_C}{2 \cdot \sqrt{3}} \cdot C_2\right]^2 + \left[\frac{U_T + U_C}{2} \cdot C_1 + \frac{U_T + U_1 + U_C}{2} \cdot C_2\right]^2} \qquad (4.3\_63a)$$

$$\left|\bar{I}_{S-}\right| = \omega \cdot \sqrt{\left[\frac{U_1 + U_C}{2 \cdot \sqrt{3}} \cdot C_2\right]^2 + \left[\frac{U_T + U_C}{2} \cdot C_1 + \frac{U_T + U_1 + U_C}{2} \cdot C_2 - U_C \cdot (C_1 + C_2)\right]^2} \qquad (4.3\_63b)$$

The phase angle between the recovery voltages and the switched currents is -90°.

*Example:*
(windings arrangement and nomenclature acc. to Fig. 4.3-10)

*Transformer data:*
30 MVA, 110 kV (1±10 1,00%)/24 kV, 50 Hz, regulation at line end

HV:    $U_l = 99\,kV$
TV:    $U_T = 110\,kV \cdot 0.1 = 11\,kV$
CV:    $U_C = 110\,kV \cdot 0.1 = 11\,kV$

capacity to the adjacent winding:     $C_1 = 1950\,pF$
capacity to grounded parts:        $C_2 = 450\,pF$

$$\left|\bar{U}_{r+}\right| = \sqrt{\left[\frac{99kV}{2}\left(\frac{1950pF}{2400pF}\right) - \frac{121kV}{2}\right]^2 + \left[\frac{110kV}{2\cdot\sqrt{3}}\left(1 - \frac{1950pF}{2400pF}\right)\right]^2} = 21.14\,kV$$

$$\left|\bar{U}_{r-}\right| = \sqrt{\left[\frac{99kV}{2}\left(\frac{1950pF}{2400pF}\right) - \frac{121kV}{2} + 11kV\right]^2 + \left[\frac{110kV}{2\cdot\sqrt{3}}\left(1 - \frac{1950pF}{2400pF}\right)\right]^2} = 11.03\,kV$$

$$\left|\bar{I}_{s+}\right| = 2\pi\cdot50\frac{1}{s}\cdot\sqrt{\left[\frac{110kV}{2\cdot\sqrt{3}}450pF\right]^2 + \left[\frac{22kV}{2}1950pF + \frac{121kV}{2}450pF\right]^2} = 15.94\,mA$$

$$\left|\bar{I}_{s-}\right| = 2\pi\cdot50\frac{1}{s}\sqrt{\left[\frac{110kV}{2\cdot\sqrt{3}}450pF\right]^2 + \left[\frac{22kV}{2}1950pF + \frac{121kV}{2}450pF - 11kV\cdot2400pF\right]^2} =$$

$$\left|\bar{I}_{s-}\right| = 8.31\,mA$$

### 4.3.2.2.3 MODEL FOR THE CALCULATION OF THE RECOVERY VOLTAGES AND SWITCHED CURRENTS OF COARSE CHANGE-OVER SELECTORS

In the previous two paragraphs it was demonstrated how to calculate the recovery voltages and switched currents by applying different equations derived from the special equivalent electrical networks. The used equivalent electrical networks (Figs. 4.3-9 and 4.3-10) are very similar, but the values of the individual components differ. Therefore it is possible to create a model for the calculation of all applications of OLTCs with coarse change-over selector. However, this model is only valid for two capacitances to the adjacent potentials and the equivalent discrete capacitors connected in the middle of the tap winding.

Under these conditions the windings connection shown in Fig. 4.3-11a can be found. The equivalent electrical network for the calculations of the stresses on the change-over selector contacts is shown in Fig. 4.3-11b. These networks show small modifications compared to the networks used in the foregoing calculations to reach general validity.
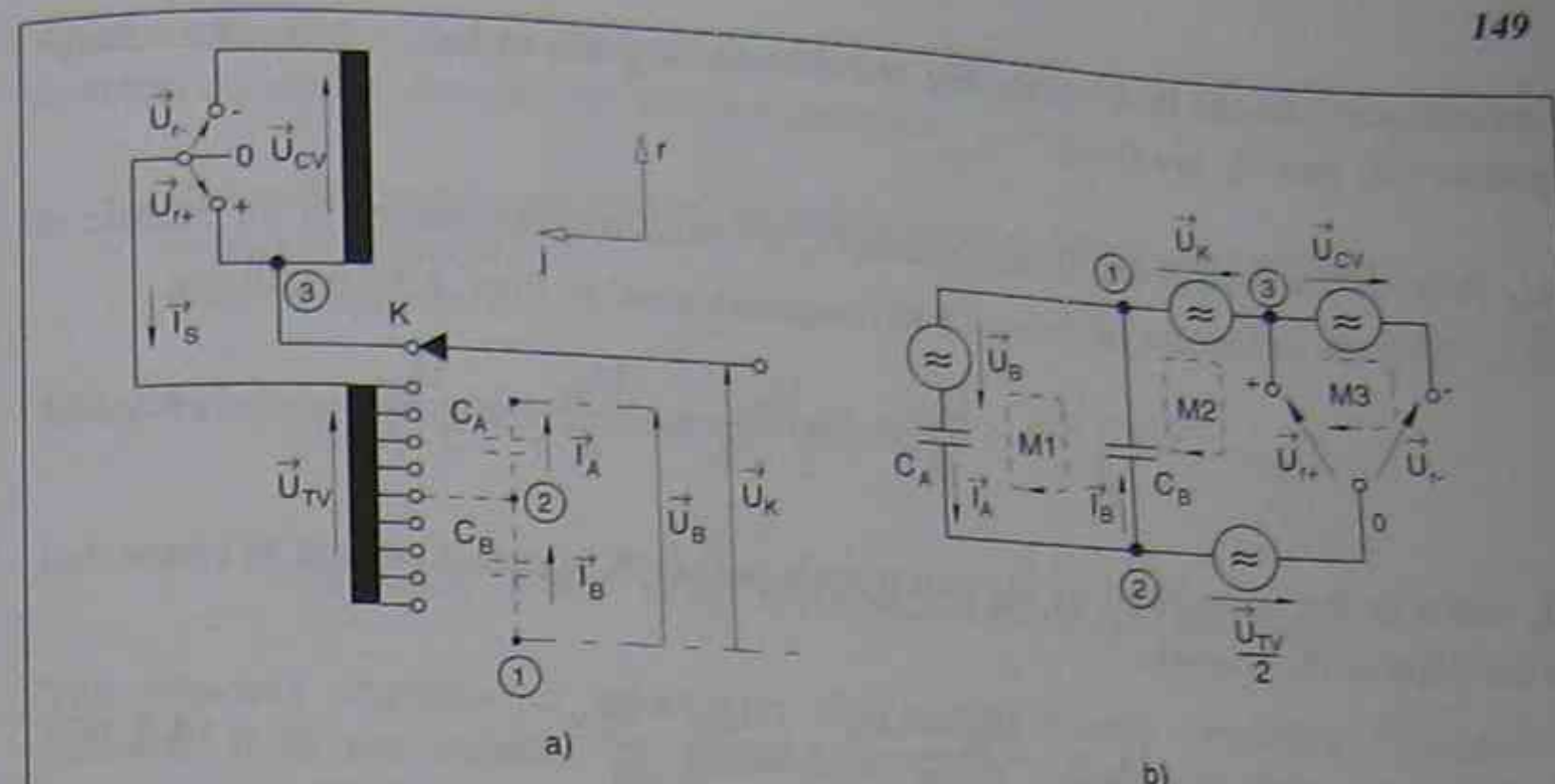
**Fig. 4.3-11:** Model for an OLTC in mid-position with disconnected tap winding (a: windings connection, b: equivalent electrical network)

With the transformation of the basic formulations of the meshes 1 to 3 and node ① (comp. 4.3.2.1.5) the recovery voltages can be found as:

$$\bar{U}_{r+} = \bar{U}_K - \frac{\bar{U}_{TV}}{2} - \bar{U}_B\cdot\left(\frac{C_A}{C_A + C_B}\right) \tag{4.3_64a}$$

$$\bar{U}_{r-} = \bar{U}_K - \frac{\bar{U}_{TV}}{2} - \bar{U}_B\cdot\left(\frac{C_A}{C_A + C_B}\right) + \bar{U}_{CV} = \bar{U}_{r+} + \bar{U}_{CV} \tag{4.3_64b}$$

and the switched currents as:

$$\bar{I}_{s+} = \bar{U}_B\cdot j\cdot\omega\cdot C_A + \left(\frac{\bar{U}_{TV}}{2} - \bar{U}_K\right)\cdot j\cdot\omega\cdot(C_A + C_B) \tag{4.3_65a}$$

$$\bar{I}_{s-} = \bar{U}_B\cdot j\cdot\omega\cdot C_A + \left(\frac{\bar{U}_{TV}}{2} - \bar{U}_K - \bar{U}_{CV}\right)\cdot j\cdot\omega\cdot(C_A + C_B) \tag{4.3_65b}$$

The equations 4.3_64a and b and 4.3_65a and b can be used for every application that meets the conditions mentioned above. An important condition to reach the correct result is the exact determination of $\bar{U}_B$ and $\bar{U}_K$. These two phasors have to be expressed in their complex form.

For a better understanding how to use the two equations 4.3_64a and b and 4.3_65a and b the procedure shall be demonstrated here based on an application acc. to Figs. 4.3-10. The first step to be completed is the definition of node ① and the capacitors $C_A$ and $C_B$ (comp. Fig. 4.3-10a). For the example explained here, the node ① is chosen as the grounded middle of the voltage triangle (neutral-end). With this

definition $C_A$ has to be $C_1$ from Fig. 4.3-10b and $C_B$ has to be $C_2$. Now the voltage phasors $\bar{U}_B$ and $\bar{U}_K$ are fixed.

$\bar{U}_B$ strats at the neutral and it ends where $C_1$ is connected, this means in the middle of $\bar{U}_{CV}$. With the definition of the real and imaginary axis' in Figs. 4.3-10 follows:

$$\bar{U}_B = -\frac{U_{HV} + U_{CV}}{2} + \frac{U_{CV}}{2} + j \cdot \frac{U_{HV}}{2 \cdot \sqrt{3}} = -\frac{U_{HV}}{2} + j \cdot \frac{U_{HV}}{2 \cdot \sqrt{3}} \qquad (4.3\_66)$$

$\bar{U}_K$ starts at the same point as $\bar{U}_B$ and it ends at the "K"-contact, which is connected to the edge of the triangle:

$$\bar{U}_K = -\frac{U_{HV} + U_{CV}}{2} + j \cdot \frac{U_{HV} + U_{CV}}{2 \cdot \sqrt{3}} \qquad (4.3\_67)$$

With the same conditions as agreed in 4.3.2.2.2 ($\bar{U}_{HV} = U_1$, $\bar{U}_{CV} = U_C$ and $\bar{U}_{TV} = U_T$) the recovery voltages (eq. 4.3_64a and b) can be expressed as:

$$\bar{U}_{r_+} = \frac{U_1}{2}\left(\frac{C_1}{C_1 + C_2}\right) - \frac{U_1 + U_C - U_T}{2} + j \cdot \frac{U_1 + U_C}{2 \cdot \sqrt{3}}\left(1 - \frac{C_1}{C_1 + C_2}\right) \qquad (4.3\_68a)$$

$$\bar{U}_{r_-} = \frac{U_1}{2}\left(\frac{C_1}{C_1 + C_2}\right) - \frac{U_1 + U_C - U_T}{2} + U_C + j \cdot \frac{U_1 + U_C}{2 \cdot \sqrt{3}}\left(1 - \frac{C_1}{C_1 + C_2}\right) \qquad (4.3\_68b)$$

and the switched currents (eq. 4.3_65a and b) as:

$$\bar{I}_{s_+} = \omega \cdot \left(\frac{U_1 + U_C}{2 \cdot \sqrt{3}} \cdot C_2\right) + j \cdot \omega \cdot \left(\frac{U_T + U_C}{2} \cdot C_1 + \frac{U_T + U_1 + U_C}{2} \cdot C_2\right) \qquad (4.3\_69a)$$

$$\bar{I}_{s_-} = \omega \cdot \left(\frac{U_1 + U_C}{2 \cdot \sqrt{3}} \cdot C_2\right) + j \cdot \omega \cdot \left(\frac{U_T + U_C}{2} \cdot C_1 + \frac{U_T + U_1 + U_C}{2} \cdot C_2 - U_C(C_1 + C_2)\right) \qquad (4.3\_69b)$$

## 4.3.3 METHODS TO OVERCOME THE RECOVERY VOLTAGE PROBLEM

In the foregoing chapter it was demonstrated how to determine the stresses on the change-over selctor contacts during the change-over selector operation. If these stresses exceed the admissible limits special precautions are necessary.

The admissible limits are defined by the OLTC manufacturer. The values of these limits depend on the design of the change-over selector (contact geometry, contact material, contact velocity) which determines its breaking capacity. Usually the limits of the recovery voltage are in the range of 15 kV to 40 kV and the capacitive currents are limited to a few hundred milliamps. A second factor which has to be considered is the amount of gas being generated. Today this becomes an important factor, because large power transformers are increasingly monitored by gas-in-oil analysis.

Three methods are used to decrease the stresses on the opening change-over selector contacts during the change-over selector operation:

- two-way change-over selector (double reversing change-over selector)
- capacitive control
- control resistors

In the following these three methods are described.

### 4.3.3.1 TWO-WAY CHANGE-OVER SELECTOR

The two-way change-over selector is also called double reversing change-over selector. It is not suitable for transformers with coarse and fine tap windings arrangement. With the two-way change-over selector the addition and subtraction of turns is possible and with this its function is comparable to the reversing change-over selector. However, its operation is different.

The addition and substraction of turns in case of the reversing change-over selector is effected by merely changing the beginning and end of the tap winding, while the two-way change-over selector changes the connections. The principle of operation of an OLTC with reversing change-over selector is shown in Figs. 4.3-12. The tap winding is connected to the main winding by the change-over selector either at the tip of the phasor $\bar{U}_{TV}$ or at the bottom. When the change-over selector is in the "+" position and the tap selector is on contact "1" the maximum number of turns is added (Fig. 4.3-12a). By changing the tap selector from contact "1" to "n" the number of added turns becomes smaller and on contact "K" no turns are added or subtracted. The load current does not flow through the change-over selector in this position allowing its loadfree movement from the "+" to the "-" position or vice versa. By changing the tap selector from the contact "K" to "1" and then to "n" with the change-over selector in position "-", the OLTC reaches its minus end-position (maximum number of substracted turns).

To reach one end-position coming from the other end-position the movable tap selector has to carry out two rotation cycles in the same direction (comp. Figs. 4.3-12).

The principle of operation of an OLTC with two-way change-over selector is shown in Figs. 4.3-13. The tap winding is connected to the main winding by the two-way change-over selector always at the tip of the phasor $\bar{U}_{TV}$. The change-over selector is in "+" position when the contacts A with D and C with B are connected. When the tap selector is on contact "1" the maximum number of turns is added (plus end-position). By changing the tap selector from contact "1" to contact "n" the number of added turns becomes smaller.
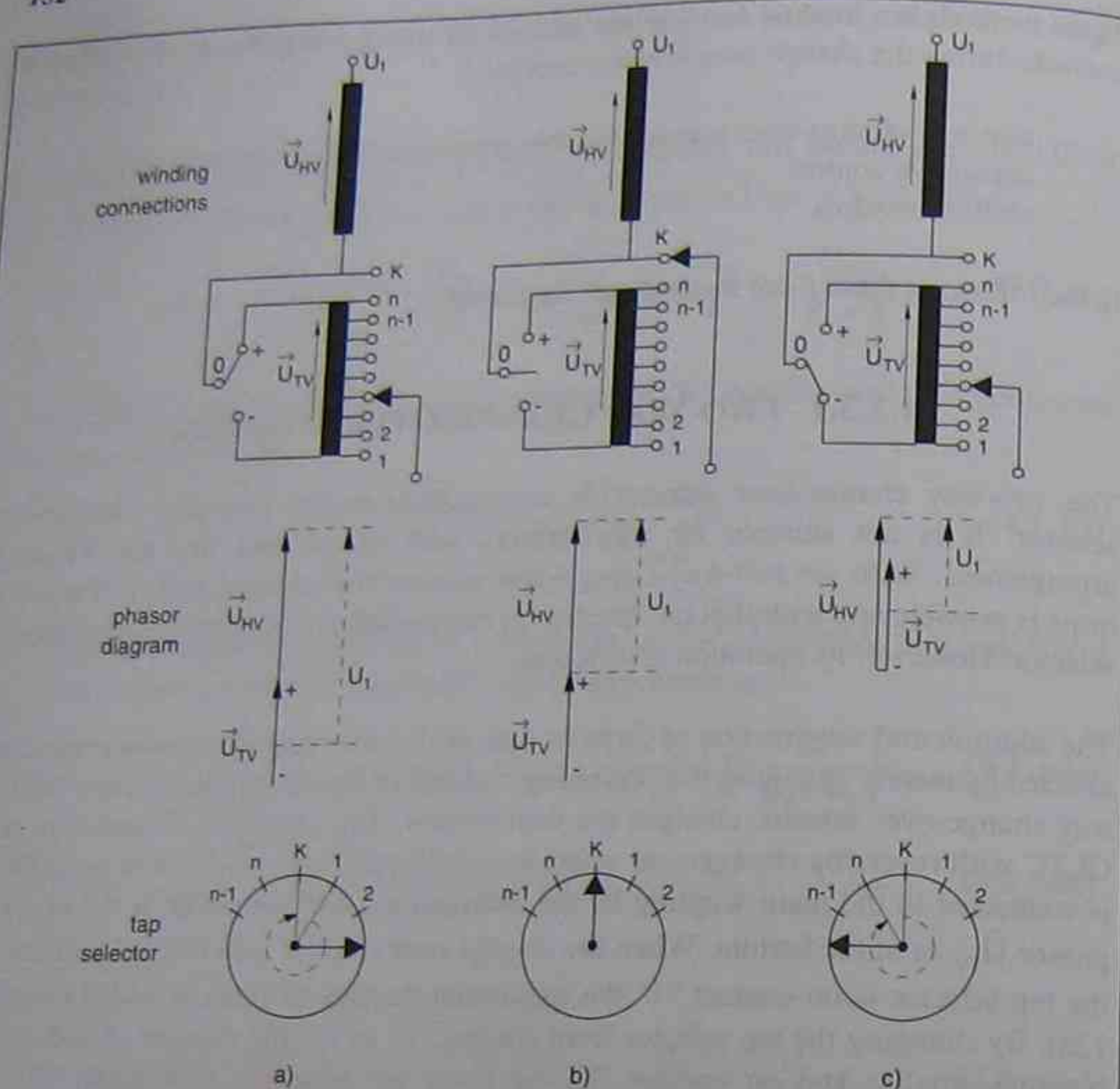
**Fig. 4.3-12:** Principle of operation of a reversing change-over selector from "+" to "-" (**a:** "+" position, **b:** mid-position, **c:** "-" position)

When the tap selector is on contact "K" no turns are added or subtracted. In this position the contacts A through D have the same potential, thus allowing a change-over selector with overlapping contacts. With this method the tap winding remains connected to the main winding during the change-over selector operation eliminating the recovery voltage problems.

The two-way change-over selector is fitted with two reversing contacts connected in parallel in the end-positions and actuated one after the other during the change-over selector operation to obtain contact overlapping.

By changing the tap selector from "K" to "n" and then to contact "1" the OLTC reaches its minus end-position (maximum number of subtracted turns). In contrast with the reversing change-over selector where the movable tap selector makes two rotations in the same direction to come from one end-position to the other, the motion of the tap selector of an OLTC with a two-way change-over selector has to be
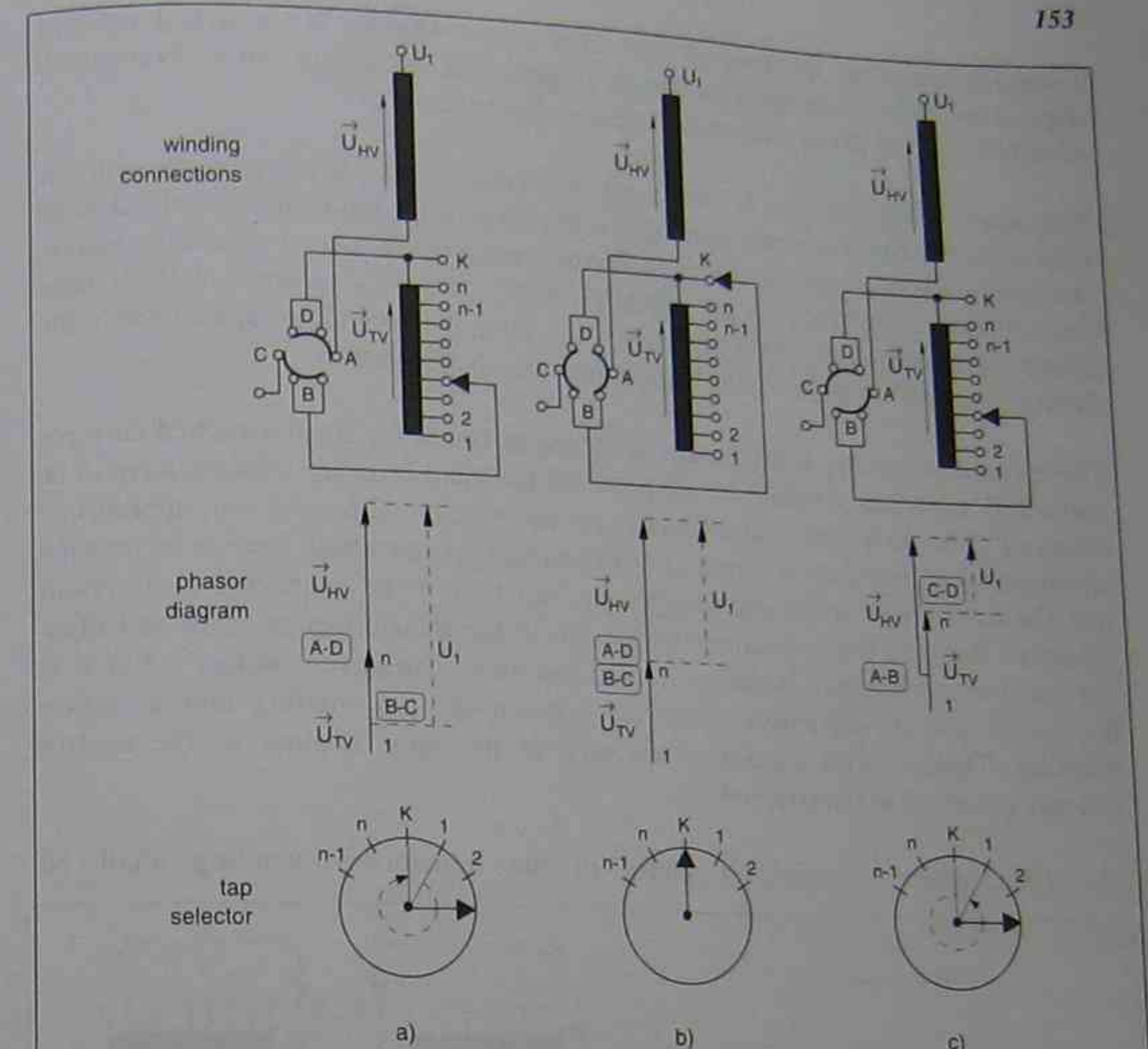
**Fig. 4.3-13:** Principle of operation of a two-way reversing change-over selector from "+" to "-" (**a:** "+" position, **b:** mid-position, **c:** "-" position)

reversed during the change-over selector operation. This change of motion needs a special gear unit.

According to Fig. 4.3-13b also in the mid-position of the OLTC the load current flows through the change-over selector and has to be commutated from one current path to the other one. Usually the two-way change-over selector is part of the tap selector and the current pathes are very short. With this the inductive loops are very small and the processes of commutation are not critical.

## 4.3.3.2 CAPACITIVE CONTROL

In chapter 4.3.2 it was shown that the stresses on the change-over selector contacts during change-over selector operation are determined decisively by the capacitances to the adjacent potentials and the potentials itself. In most of the cases the recovery

voltages depend on the ratio of the capacitances whereas the switched currents depend on the values of the capacitances. In general it can be said that to obtain small switched currents the sum of the capacitances has to be small.

The recovery voltages can be decreased by changing the capacitive ratio with the basic principle to get a strong capacitive connection of the tap winding to the desired potential of the common change over selector contact "0" in case of reversing change-over selector respectively to the potential of the "+" or "-" contact of the coarse change-over selector. A strong capacitive connection means a large capacitance to the desired potential compared to the capacitances to other potentials.

These two demands for a small sum of the capacitances for small switched currents and a high capacitance to the desired potential for small recovery voltages have to be balanced. The technical construction can be effected either by an appropriate arrangement of the relevant windings or by shielding plates which have to be inserted into the transformer windings arrangement and have to be connected to a certain potential. But with these measures the design of the transformer changes and often the transformers becomes larger in volume and more expensive. Another solution is the use of discrete capacitors connected between the tap winding and a certain potential. These control capacitors are used in the same manner as the control resistors described in paragraph 4.3.3.3.

The effectiveness of shielding plates in the transformer winding shall be
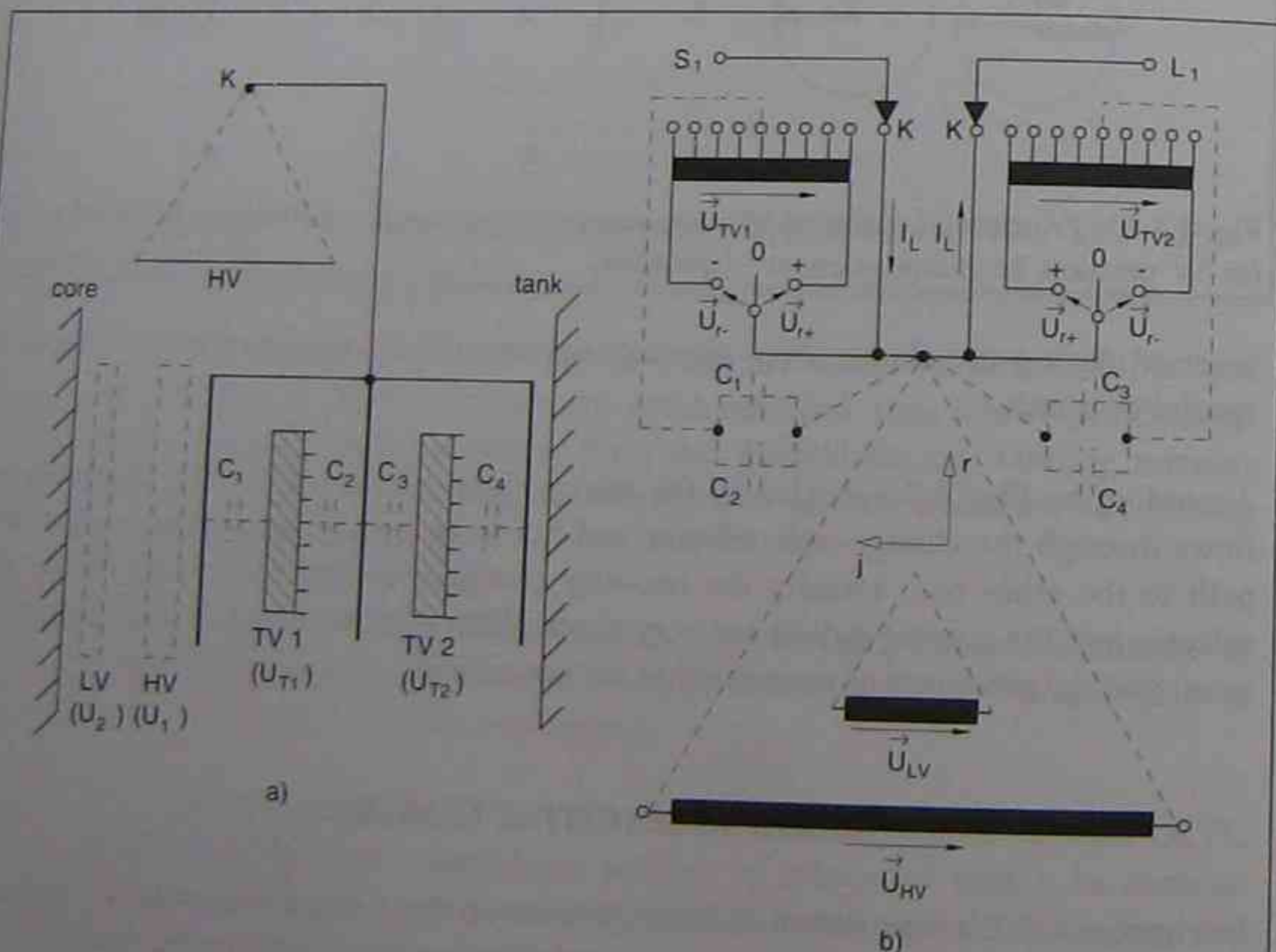


Fig. 4.3-14: OLTC (phase-shifting transformer) in mid-position with disconnected tap winding (a: windings arrangement with shields, b: windings connection)

demonstrated here for the example given in paragraph 4.3.1.2.4. By changing the windings arrangement shown in Fig. 4.3-5a and adding shields the stresses on the change-over selector contacts will decrease.

Fig. 4.3-14 shows the new arrangement. The winding is equipped with three shields which are connected to the relevant potential of the common change-over selector contact "0" or "K" respectively. This windings arrangement shows a very strong connection of the tap windings to the desired potential and is independent of the capacitance ratio because the capacities are in parallel. This produces the smallest possible recovery voltage which is half of the voltage of the tap windings.

$$\left|\bar{U}_{r+/-}\right| = \left|\frac{\bar{U}_{TV}}{2}\right| = \pm\frac{U_{T1}}{2} = \pm\frac{U_{T2}}{2}$$

The switched currents can be determiend to:

tap 1:
$$\left|\bar{I}_{S+/-}\right| = \pm\frac{U_{T1}}{2}\cdot\omega\cdot(C_1 + C_2)$$

tap 2:
$$\left|\bar{I}_{S+/-}\right| = \pm\frac{U_{T2}}{2}\cdot\omega\cdot(C_3 + C_4)$$

*Example:*
*Taking the example for the 675 MVA phase-shifting transformer in paragraph 4.3.2.1.4 with new values for the capacities the resulting stresses are:*

*capacities to the adjacent windings or potentials:*
$C_1 = 6000\,pF$, $C_2 = C_3 = 8000\,pF$, $C_4 = 5500\,pF$

**TAP 1**

$$\left|\bar{U}_{r+/-}\right| = \frac{62.65\,kV}{2} = 31.33\,kV$$

and

$$\left|\bar{I}_{S+/-}\right| = \frac{62.65\,kV}{2}\cdot 2\pi\cdot 60\frac{1}{s}\cdot(6000\,pF + 8000\,pF) = 165.33\,mA$$

**TAP 2**

$$\left|\bar{U}_{r+/-}\right| = \frac{62.65\,kV}{2} = 31.33\,kV$$

and

$$\left|\bar{I}_{S+/-}\right| = \frac{62.65\,kV}{2}\cdot 2\pi\cdot 60\frac{1}{s}\cdot(5500\,pF + 8000\,pF) = 159.42\,mA$$

A comparison of these values with the values calculated in 4.3.2.1.4 shows a large reduction of the recovery voltages and switched currents.

The capacitive control is rarely adopted as the only measure for the potential connection of the tap winding, but is applied in cases where the transformer design requires special measures for voltage control. The most frequent method of voltage control of the tap winding is the use of control resistors (see next paragraph).

A disadvantage of the capacitive control as the only measure used to control the stresses on the change-over selector contacts is that the phase angle between switched currents and recovery voltages remains at 90°. For the opening contacts this is the most difficult switching condition and this needs to be considered in case of high stresses.

### 4.3.3.3 CONTROL RESISTORS

Besides the capacitive control of the potential of the tap winding the during change-over selector operation the potential can also be controlled by the use of ohmic resistors. For this pupose fixed ohmic resistors, called tie-in resistors, with a high resistance (some ten to some hundred kΩ) are used. They are connected usually to the middle of the tap winding and the tap changer current take-off terminal as shown in Figs. 4.3-15 and 16. They are mounted to the tap selector and with this they are located in the transformer main tank. The lifetime of these resistors is very important, because they cannot be inspected during routine maintenance. The selection of the correct type of resistor has to be done very thoroughly. This measure for the potential connection of the tap winding has been carried out successfully for many years.

When the tie-in resistor is connected between the middle of the tap winding and the current take-off terminal, the operating voltage across the resistor depends on the tap position. It varies between zero when the tap changer is in the middle of the tap winding, and half the voltage of the tap winding when the tap changer is at the end of the tap winding. This has to be taken into account when dimensioning the tie-in resistor (thermally and with respect to the applied voltage).

The thermal stresses which affect the tie-in resistors have to be divided into two separate time intervals. The continous duty with the change-over selector closed is caused by the applied voltage. Since the tie-in resistors are connected to the middle of the tap-winding the thermal stress is given by:

$$P_{CD} = \frac{\left(\left|\vec{U}_{TV}\right|/2\right)^2}{R_P}$$

(4.3_70)

The short-time duty (approx. 1000 ms) with the change-over selector open is caused by the capacitive load current of the tap winding with the change-over selector closed and can be expressed as:

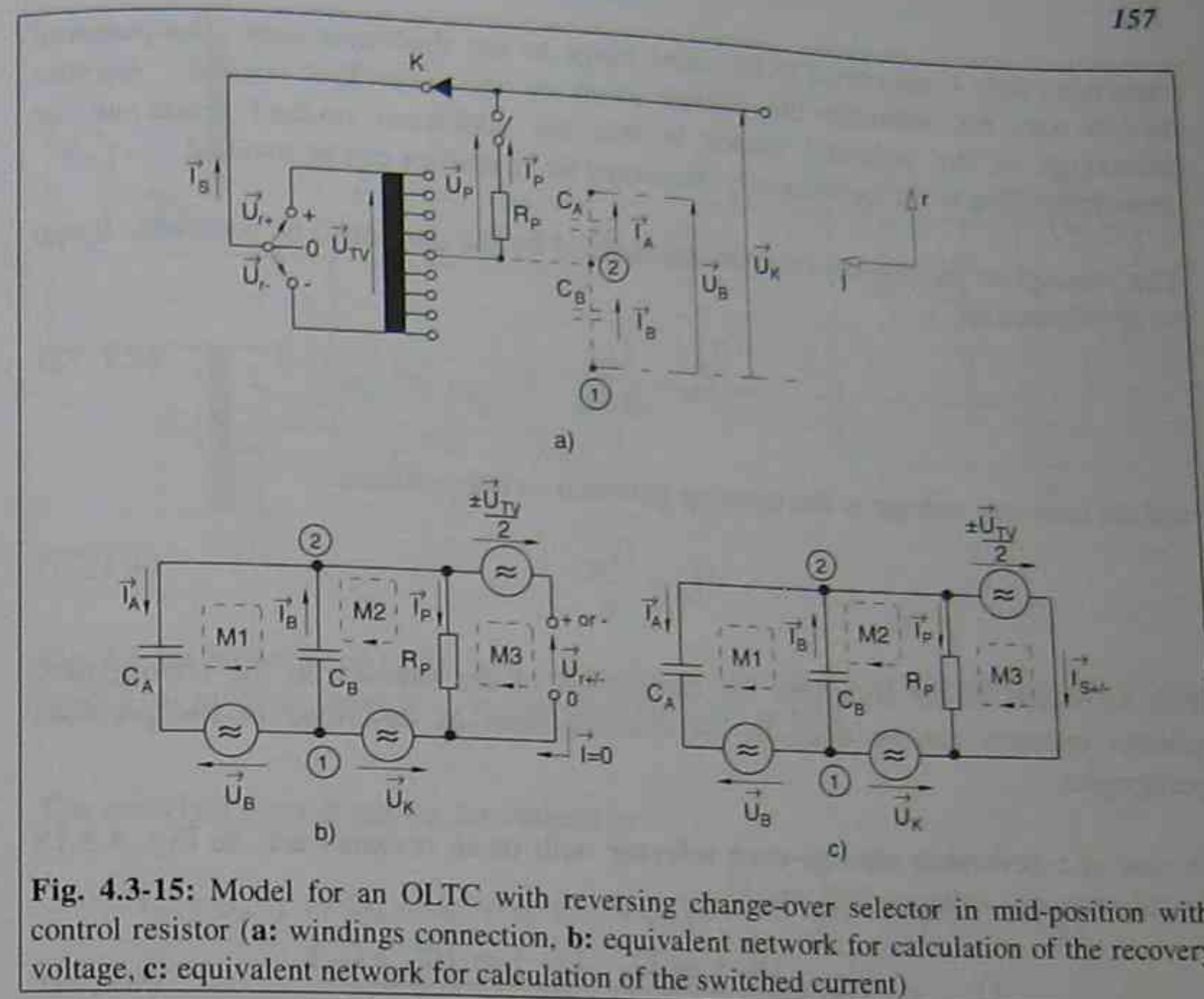$$P_{SD} = \left(\left|\vec{I}_S\right|\right)^2 \cdot R_P$$

(4.3_71)

**Fig. 4.3-15:** Model for an OLTC with reversing change-over selector in mid-position with control resistor (**a:** windings connection, **b:** equivalent network for calculation of the recovery voltage, **c:** equivalent network for calculation of the switched current)

The admissible limits for the thermal stress on the resistors depend on the surface stress of the resistor body and have to be indicated by the manufacturer. However, it can be stated that in case of commonly used resistors the limits for short-time duties are greater by the factor 2 to 4 to the limits for continous duty.

The size of the surface determines the possible heat exchange to the surrounding transformer oil. Consequently the admissible limits of thermal stress on the resistors can be increased by increasing the size of the surface. This can be accomplished by increasing the number of resistors.

In case of large regulating ranges the thermal (continous duty) and voltage stresses on the resistors increase. This makes it necessary to increase the number of tie-in resistors. The number of resistors can be increased by connecting them in series or in parallel or a combination of both. However, in such cases often it is more economic to use a potential switch.

The potential switch (comp. Figs. 4.3-15 and 16) is connected in series with the tie-in resistors and serves for the connection of the tie-in resistors shortly before the opening of the change-over selector, and for its disconnection shortly after the closing of the change-over selector. With this measure the admissible thermal stress limits, when the change-over selector is closed can be increased because the duration of the

continous duty is shortened to the same range as the short-time duty. The potential switch does not influence the voltage stress on the individual resistors. Another advantage of the potential switch is that the additional no-load losses in the transformer due to the permanently connected tie-in resistor can be avoided.

The stresses on the potential switch are defined by the current to be switched. It can be determined to:

$$\bar{I}_{SP} = \frac{\bar{U}_{TV}}{2 \cdot R_P} \qquad (4.3\_72)$$

and the recovery voltage at the opening potential switch contacts:

$$\bar{U}_{rP} = \frac{\bar{U}_{TV}}{2} \qquad (4.3\_73)$$

The derivation of the equations for calculation of the stresses on the change-over selector contacts can be done in the same manner as described in the previous paragraphs.

In case of a **reversing change-over selector** with tie-in resistors acc. to Fig. 4.3-15 for the recovery voltages follows:

$$\bar{U}_{r+/-} = \pm \frac{\bar{U}_{TV}}{2} + \frac{\bar{U}_B \cdot j \cdot \omega \cdot C_A - \bar{U}_K \cdot j \cdot \omega \cdot (C_A + C_B)}{\frac{1}{R_P} + j \cdot \omega \cdot (C_A + C_B)} \qquad (4.3\_74)$$

The switched currents can be determined to:

$$\bar{I}_{S+/-} = \pm \frac{\bar{U}_{TV}}{2}\left(\frac{1}{R_P} + j \cdot \omega \cdot (C_A + C_B)\right) + \bar{U}_K \cdot j \cdot \omega \cdot (C_A + C_B) - \bar{U}_B \cdot j \cdot \omega \cdot C_A$$

resp.

$$\bar{I}_{S+/-} = -\bar{U}_{r+/-} \cdot \left(\frac{1}{R_P} + j \cdot \omega \cdot (C_A + C_B)\right) \qquad (4.3\_75)$$

In case of a **coarse change-over selector** with tie-in resistors acc. to Fig. 4.3-16 for the recovery voltages follows:

$$\bar{U}_{r+} = \frac{\bar{U}_K \cdot j \cdot \omega \cdot (C_A + C_B) - \bar{U}_B \cdot j \cdot \omega \cdot C_A}{\frac{1}{R_P} + j \cdot \omega \cdot (C_A + C_B)} - \frac{\bar{U}_{TV}}{2} \qquad (4.3\_76a)$$

$$\bar{U}_{r-} = \frac{\bar{U}_K \cdot j \cdot \omega \cdot (C_A + C_B) - \bar{U}_B \cdot j \cdot \omega \cdot C_A}{\frac{1}{R_P} + j \cdot \omega \cdot (C_A + C_B)} - \frac{\bar{U}_{TV}}{2} + \bar{U}_{CV} \qquad (4.3\_76b)$$
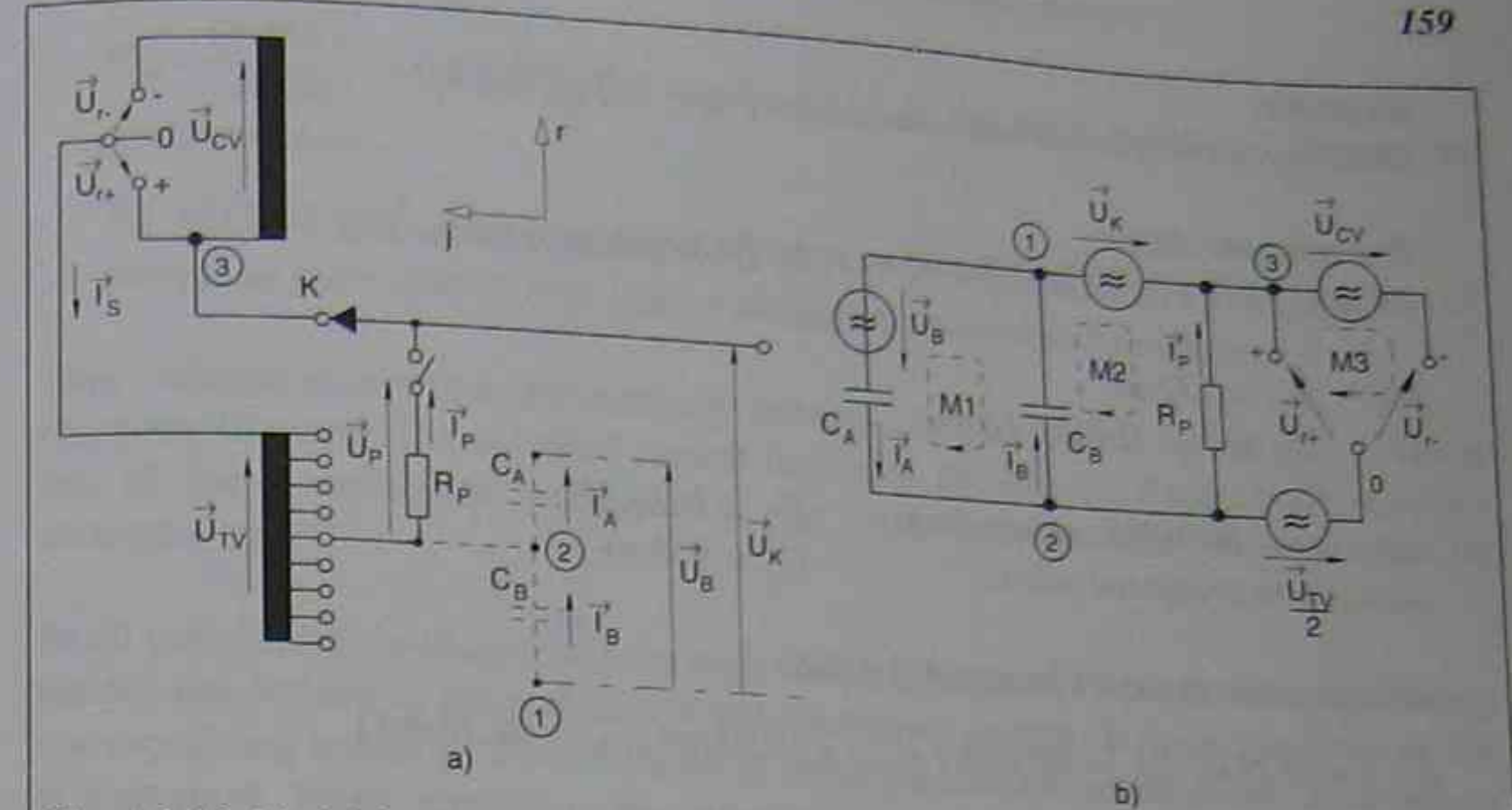
**Fig. 4.3-16:** Model for an OLTC with coarse change-over selector in mid-position with control resistor (**a**: windings connection, **b**: equivalent electrical network)

The switched current can be determined to:

$$\bar{I}_{S+} = \bar{U}_B \cdot j \cdot \omega \cdot C_A - \bar{U}_K \cdot j \cdot \omega \cdot (C_A + C_B) + \frac{\bar{U}_{TV}}{2}\left(\frac{1}{R_P} + j \cdot \omega \cdot (C_A + C_B)\right)$$

resp.

$$\bar{I}_{S+} = -\bar{U}_{r+} \cdot \left(\frac{1}{R_P} + j \cdot \omega \cdot (C_A + C_B)\right) \qquad (4.3\_77a)$$

$$\bar{I}_{S-} = \bar{U}_B \cdot j \cdot \omega \cdot C_A - \bar{U}_K \cdot j \cdot \omega \cdot (C_A + C_B) + \left(\frac{\bar{U}_{TV}}{2} - \bar{U}_{CV}\right)\left(\frac{1}{R_P} + j \cdot \omega \cdot (C_A + C_B)\right)$$

resp.

$$\bar{I}_{S-} = -\bar{U}_{r-} \cdot \left(\frac{1}{R_P} + j \cdot \omega \cdot (C_A + C_B)\right) \qquad (4.3\_77b)$$

When using the equations 4.3_74 to 4.3_77 it has to be taken into account that for economic reasons not every resistance value can be realized. Usually the resistors are taken from a standard series with discrete values acc. to IEC 63.

The use of the above mentioned models shall be demonstrated with the example given in 4.3.2.1.2 and 4.3.2.1.5.

*Example:*
(windings arrangement and nomenclature acc. to Fig. 4.3-3)

*Transformer data:*
*13 MVA, 132 kV (1±8·1,25%)/24 kV, 50 Hz regulation at line end*

HV:   $U_1 = 132\ kV$
TV:   $U_T = U_1 \cdot 0.1 = 13.2\ kV$

capacity to the adjacent winding:   $C_1 = 1810\ pF$
capacity to grounded parts:   $C_2 = 950\ pF$

*without tie-in resistors (comp. 4.3.2.1.2):*

$(|\bar{U}_{r+}| = 73.78kV, |\bar{U}_{r-}| = 60.83kV, |\bar{I}_{s+}| = 63.97mA, |\bar{I}_{s-}| = 52.75mA)$

*For this example the determination of the expressions for $\bar{U}_B$ and $\bar{U}_K$ were demonstrated in 4.3.2.1.5:*

from eq. 4.3_44:   $\bar{U}_B = j \cdot \dfrac{U_{HV}}{2 \cdot \sqrt{3}} = j \cdot \dfrac{U_1}{2 \cdot \sqrt{3}}$

from eq. 4.3_45:   $\bar{U}_K = -\dfrac{U_{HV}}{2} + j \cdot \dfrac{U_{HV}}{2 \cdot \sqrt{3}} = -\dfrac{U_1}{2} + j \cdot \dfrac{U_1}{2 \cdot \sqrt{3}}$

*with these expressions and $\bar{U}_{TV} = U_T$; $C_A = C_1$ and $C_B = C_2$ and separating into real and imaginary components eq. 4.3_74 becomes:*

$$\bar{U}_{r+/-} = \pm\frac{U_T}{2} + \frac{\dfrac{U_1}{2}\left(\dfrac{\omega \cdot C_2}{R_P \cdot \sqrt{3}} + \omega^2 \cdot (C_1 + C_2)^2\right) + j \cdot \dfrac{U_1}{2}\left(\dfrac{\omega \cdot (C_1 + C_2)}{R_P} - \dfrac{\omega^2 \cdot C_2 \cdot (C_1 + C_2)}{\sqrt{3}}\right)}{\left(\dfrac{1}{R_P}\right)^2 + \omega^2 \cdot (C_1 + C_2)^2}$$

$\bar{U}_{r+} = 13.28kV + j \cdot 14.41kV \Rightarrow |\bar{U}_{r+}| = 19.59kV$

$\bar{U}_{r-} = 0.08kV + j \cdot 14.41kV \Rightarrow |\bar{U}_{r-}| = 14.41kV$

with eq.4.3_75

$$\bar{I}_{s+/-} = \bar{U}_{r+/-} \cdot \left(\frac{1}{R_P} + j \cdot \omega \cdot (C_1 + C_2)\right)$$

$\bar{I}_{s+} = -34.93mA - j \cdot 62.98mA \Rightarrow |\bar{I}_{s+}| = 72.02mA$

$\bar{I}_{s-} = 12.19mA - j \cdot 51.54mA \Rightarrow |\bar{I}_{s-}| = 52.96mA$

*with eq. 4.3_70 and 4.3_71 the stresses on the tie-in resistors can be determined to:*

$P_{CD} = \dfrac{(6.6kV)^2}{280k\Omega} = 155.57W$ this means 31.11 W for each resistor (5 pieces) as continous duty

$P_{SD} = (72.02mA)^2 \cdot 280k\Omega = 1452.33W$ this means 290.47 W for each resistor (5 pieces) as short-time duty in case of the highest current to be switched.

This example shows that the recovery voltages can be reduced by the use of tie-in resistors. However, the switched current increases, because the fixed ohmic resistors are of lower resistance compared to the capacitances.. This is valid for all arrangements.

In all calculations in chapter 4.3 the high voltage phasor are defined in the real axis of the coordinate system. If these windings or the phasor corresponding windings are connected in delta the rotation sense of the three phases is important. When calculating the recovery voltages and switched currents with tie-in resistors different rotation senses can lead to different results. If the rotation sense of the delta connection is not specified, it is recommended to carry out the calculations also with the conjugate-complex form of the voltage phasors. With this procedure it will be ensured that the maximum possible values will be reached.

## 4.4 LEAKAGE INDUCTANCE OF COARSE/FINE TAP WINDINGS ARRANGEMENT

In case of coarse/fine tap windings arrangement there is one tap-change operation which is exceptional with respect to the phase shift between the step voltage and the circulating current. When carrying out the tap-change operation from the end of the fine tap winding to the end of the coarse tap winding and vice versa, the entire coarse and fine tap winding turns are effective between the selected and pre-selected taps (Fig. 4.4-1). This tap-changer position is called "critical mid-position" and results for the diverter switch circuit in a substantially higher leakage inductance than during all the operations within the fine tap winding, where only the leakage inductance of one tap section becomes effective /this being negligible).

This leakage inductance represents the short-circuit impedance of the coarse and the fine tap windings and can be determined either by calculation or by measurement. In Fig. 4.4-2 the test circuit for such a measurement is shown. The tap-changer must be in the "critical mid-position", i.e. the coarse change-over selector in the "-" position connecting contacts "0" and "-" and the fine tap selectors must have the positions "K" and "1". Now the short-circuit impedance of the coarse and fine tap winding can be determined by a simple voltage and current measurement.
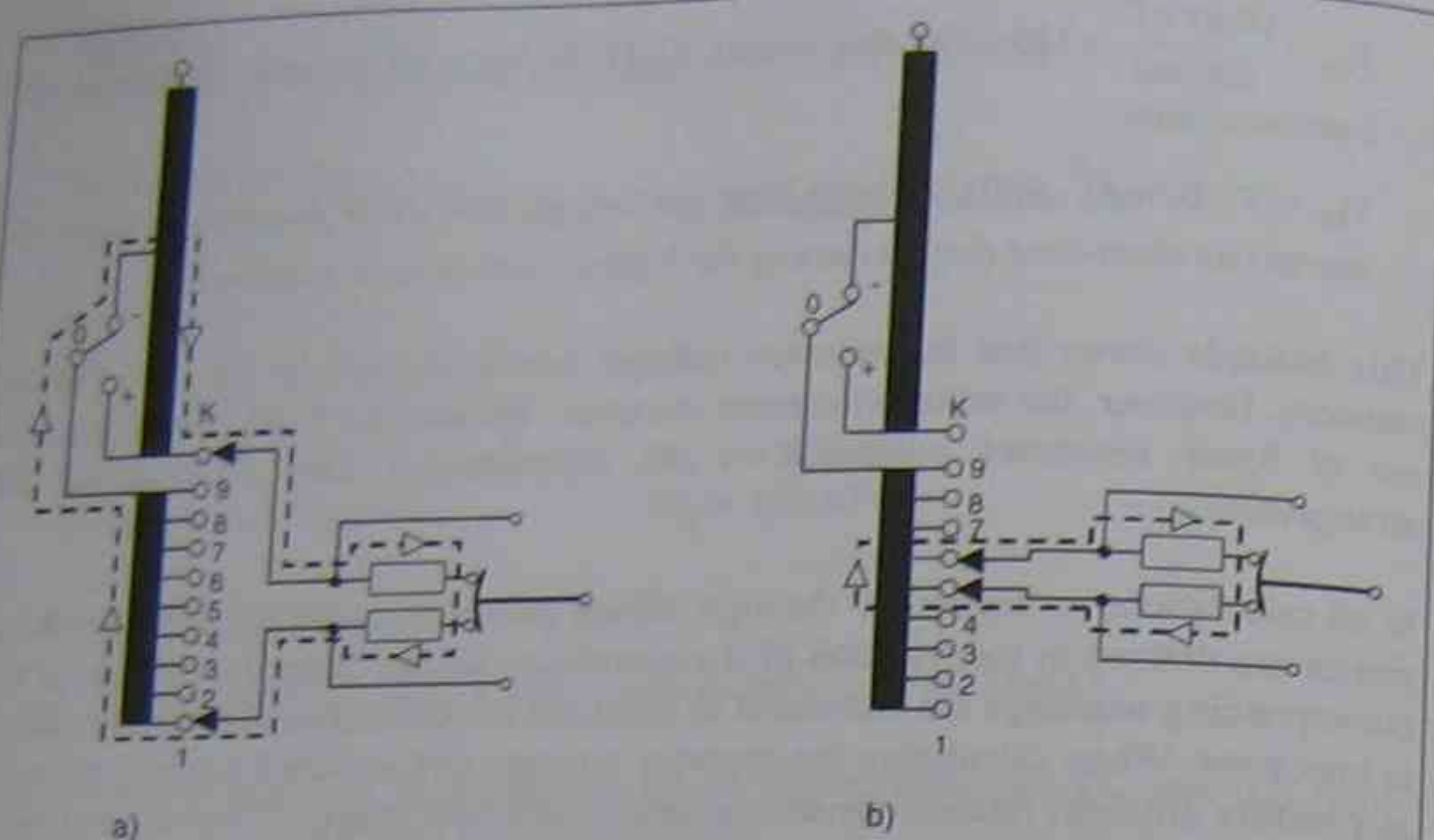
**Fig. 4.4-1:** Circulating current pathes of two different switching operations with diverter switch in the mid-position(a: switching operation from the end of the coarse tap winding to the end of the fine tap winding (or vice versa), b: switching operation within the fine tap winding)

In the following a diverter switch with a flag cycle mode of operation (compare 2.1.2.1) will be used to show the influence of the above mentioned effect. The operation from the end of the coarse tap winding (contact "K") to the end of the fine tap winding (contact "1") or vice versa shall be discussed in closer detail.

Besides the mode of operation of the diverter switch the resulting phase shift between switched current and recovery voltage also depends on the number of mid-positions of the tap selector (see paragraph 3.1). The differences will be explained lateron.
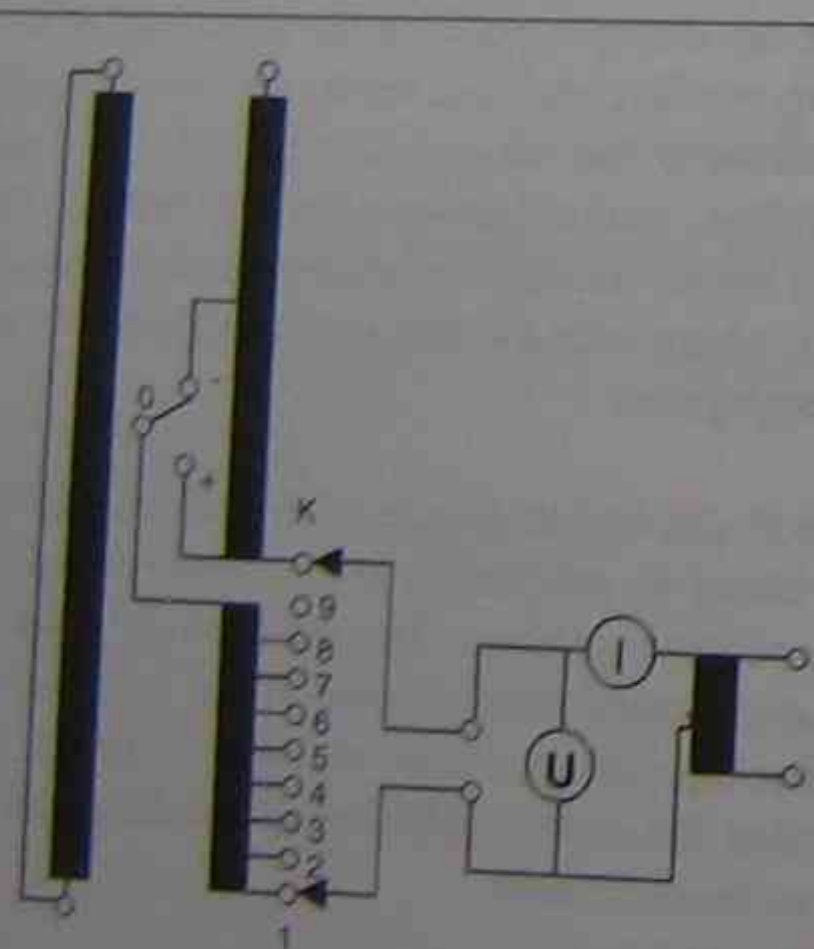


**Fig. 4.4-2:** Test circuit for the measurement of the leakage inductance in the "critical mid-position" of OLTC with coarse and fine tap windings

Following the operation order of the contacts in the diverter switch (see Table 2.1-1), first the main switching contact of the opening side breaks. Within this breaking operation the switched current and the recovery voltage are in phase as in any other tap-change operation. This was shown in paragraph 4.2.1.1.
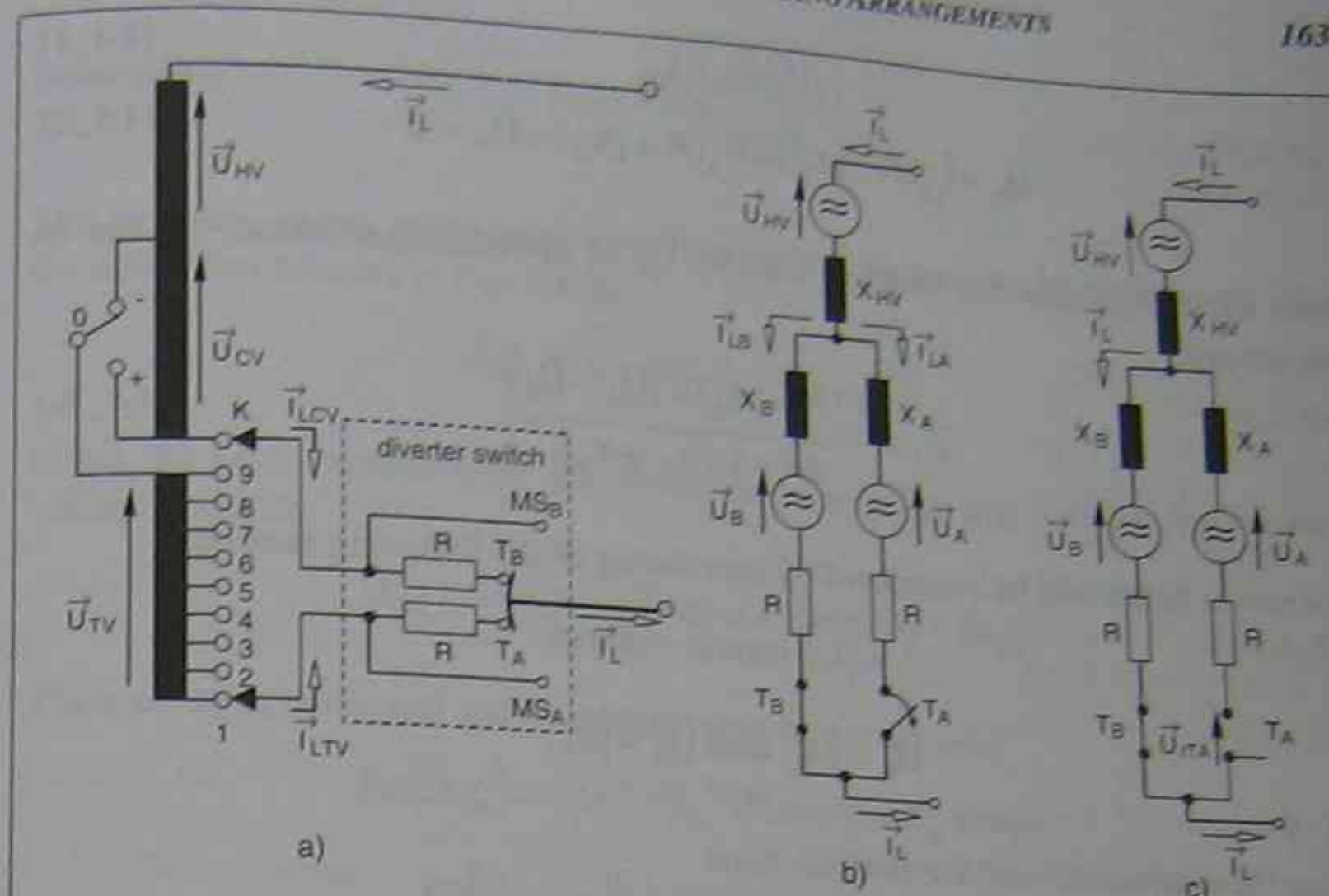
**Fig. 4.4-3:** Diverter switch operation (breaking at the transition contact) in the "critical mid-position"
**a:** circuit diagram
**b:** equivalent network for calculation of the switched current at the transition contact
**c:** equivalent network for calculation of the recovery voltage at the transition contact

After making of the transition contact of the closing side both transition resitors and both tap windings (coarse and fine) are effective. The through-current is split into two current pathes. The circuit diagram of this diverter switch position is given in Figure 4.4-3a for a tap selector with three mid-positions. The equivalent networks in Figures 4.4-3b and c show the moment of breaking of the transition contact $T_A$ of the opening side shortly before and after quenching of the arc in the current zero. The equivalent network in Fig. 4.4-3b is valid for the calculation of the switched current and the one in Fig. 4.4-3c is valid for the calculation of the recovery voltage. The equivalent networks can be used for both tap-changing directions. The used indices A and B describe only the opening and the closing side of the diverter switch.

The reactances $X_A$ and $X_B$ represent the leakage inductances of the coarse and the fine tap winding respectively. If the leakage inductance is measured with the above-mentioned method the most common way to get the single reactances is to divide the measured value by two.

The calculations below are valid for an operation from the end of the coarse tap winding (opening side of the diverter switch) to the end of the fine tap winding (closing side of the diverter switch).

The following two equations can be formulated from the equivalent network given in Figure 4.4-3b:

$$\bar{I}_L = \bar{I}_{LA} + \bar{I}_{LB} \qquad (4.4\_1)$$

$$\bar{U}_B - \bar{I}_{LB}(R + jX_B) + \bar{I}_{LA}(R + jX_A) - \bar{U}_A = 0 \qquad (4.4\_2)$$

From these equations the switched current $\bar{I}_{LA}$ at the transition contact $T_A$ can be determined:

$$\bar{I}_{LA} = \frac{\bar{I}_L(R + jX_B) + (\bar{U}_A - \bar{U}_B)}{2R + j \cdot (X_B + X_A)} \qquad (4.4\_3a)$$

The power factor will be considered by introducing of the following relations

$$\bar{I}_L = |\bar{I}_L| \cdot (\cos\varphi - j\sin\varphi)$$

$$\bar{U}_B = |\bar{U}_B| \text{ and } \bar{U}_A = |\bar{U}_A|$$

Using these equations and the simplification

$$(|\bar{U}_A| - |\bar{U}_B|) = |\bar{U}_\Delta|$$

the switched current $\bar{I}_{LA}$ becomes

$$\bar{I}_{LA} = \frac{\bar{I}_L(\cos\varphi - j\sin\varphi)(R + jX_B) + |\bar{U}_\Delta|}{2R + j \cdot (X_B + X_A)} \qquad (4.4\_3b)$$

The separation of the real and imaginary components of equation 4.4_3b leads to

$$Re(\bar{I}_{LA}) = \frac{|\bar{I}_L| \cdot ((2R^2 + X_B(X_B + X_A))\cos\varphi + R(X_B - X_A)\sin\varphi) + |\bar{U}_\Delta| 2R}{(2R)^2 + (X_B + X_A)^2}$$

$$(4.4\_4a)$$

$$Im(\bar{I}_{LA}) = \frac{|\bar{I}_L| \cdot (R(X_B - X_A)\cos\varphi - (X_B(X_B + X_A) + 2R^2)\sin\varphi) - |\bar{U}_\Delta|(X_B + X_A)}{(2R)^2 + (X_B + X_A)^2}$$

$$(4.4\_4b)$$

The absolute value and the phase angle related to the through-current $\bar{I}_L$ of the switched current $\bar{I}_{LA}$ at the transition contact can be expressed as

absolute value:
$$|\bar{I}_{LA}| = \sqrt{[Re(\bar{I}_{LA})]^2 + [Im(\bar{I}_{LA})]^2} \qquad (4.4\_5a)$$

phase angle:
$$\varphi_{ILA} = \arctg\frac{Im(\bar{I}_{LA})}{Re(\bar{I}_{LA})} \qquad (4.4\_5b)$$

The recovery voltage at the open transition resistor contact can be determined using the equivalent network in Fig. 4.4-3c.

$$\bar{U}_{rTA} = (\bar{U}_A - \bar{U}_B) - \bar{I}_L(R + jX_B) \qquad (4.4\_6a)$$

Using the same equations for the power factor and the step voltage, the recovery voltage becomes

$$\bar{U}_{rTA} = -|\bar{U}_\Delta| - |\bar{I}_L|(\cos\varphi - j\sin\varphi)(R + jX_B) \qquad (4.4\_6b)$$

The separation in the real and imaginary components delivers:

$$Re(\bar{U}_{rTA}) = -|\bar{U}_\Delta| - |\bar{I}_L| \cdot (R\cos\varphi + X_B\sin\varphi) \qquad (4.4\_7a)$$

$$Im(\bar{U}_{rTA}) = |\bar{I}_L| \cdot (R\sin\varphi - X_B\cos\varphi) \qquad (4.4\_7b)$$

Now the absolute value and the phase angle related to the through-current $\bar{I}_L$ of the recovery voltage $\bar{U}_{rTA}$ can be expressed as

absolute value:
$$|\bar{U}_{rTA}| = \sqrt{[Re(\bar{U}_{rTA})]^2 + [Im(\bar{U}_{rTA})]^2} \qquad (4.4\_8a)$$

phase angle:
$$\varphi_{UrTA} = \arctg\frac{Im(\bar{U}_{rTA})}{Re(\bar{U}_{rTA})} \qquad (4.4\_8b)$$

The phase shift between the switched current and the recovery voltage at the transition contact is the difference of the phase angles $\varphi_{ILA}$ and $\varphi_{UrTA}$

$$|\Delta\varphi_{IUTA}| = |\varphi_{ILA} - \varphi_{UrTA}| \qquad (4.4\_9)$$

The leakage inductances of the coarse and fine tap winding may be different. For equations 4.4_7 through 4.4_9 the worst case arises when the reactance $X_B$ is the larger one.

As mentioned above the phase shift depends on the number of mid-positions. The voltage difference $|\bar{U}_\Delta|$ differs with the number of mid-positions. In case of tap selectors with one mid-position the coarse tap winding is electrically one step longer as the fine tap winding (see Fig. 3.1-2).

$$(|\bar{U}_{CV}| - |\bar{U}_{TV}|) = |\bar{U}_\Delta| = |\bar{U}_S|$$

In case of tap selectors with three mid-positions (two dummy positions) the electrical length of the coarse and fine tap winding are equal (see Fig. 3.1-3).

$$\left(\left|\vec{U}_A\right| - \left|\vec{U}_B\right|\right) = \left|\vec{U}_\Delta\right| = 0$$

In Table 4.4-1 different breaking conditions (switched current $\vec{I}_{LA}$, recovery voltage $\vec{U}_{rTA}$, phase shift $\Delta\varphi_{IUTA}$) at the transition contact are listed. The given values are calculated for an example of a tap-change operation from the end of the fine tap winding to the end of the coarse tap winding with two different tap selector designs (one or three mid-positions). In addition the breaking conditions are given for a tap change operation within the fine tap winding. The calculations can be completed with the above given equations (with small modifications) or applying the equations 4.2_7 through 4.2_9 directly (with: $R_A = R_B = R$).

As described in paragraph 4.2.1 the quenching capability of a switching distance depends on the magnitude of the switched current and the instantaneous magnitude of the recovery voltage at the current zero. The breaking conditions of switching contacts can be evaluated with the theoretical value of the instantaneous power, which is defined as the product of the r.m.s. value of the switched current and the instantaneous value of the recovery voltage in the current zero:

$$P_{ITA} = \left|\vec{I}_{LA}\right| \cdot \left|\vec{U}_{rTA}\right| \cdot \sqrt{2} \cdot \sin(\Delta\varphi_{IUTA}) \qquad (4.4\_10)$$
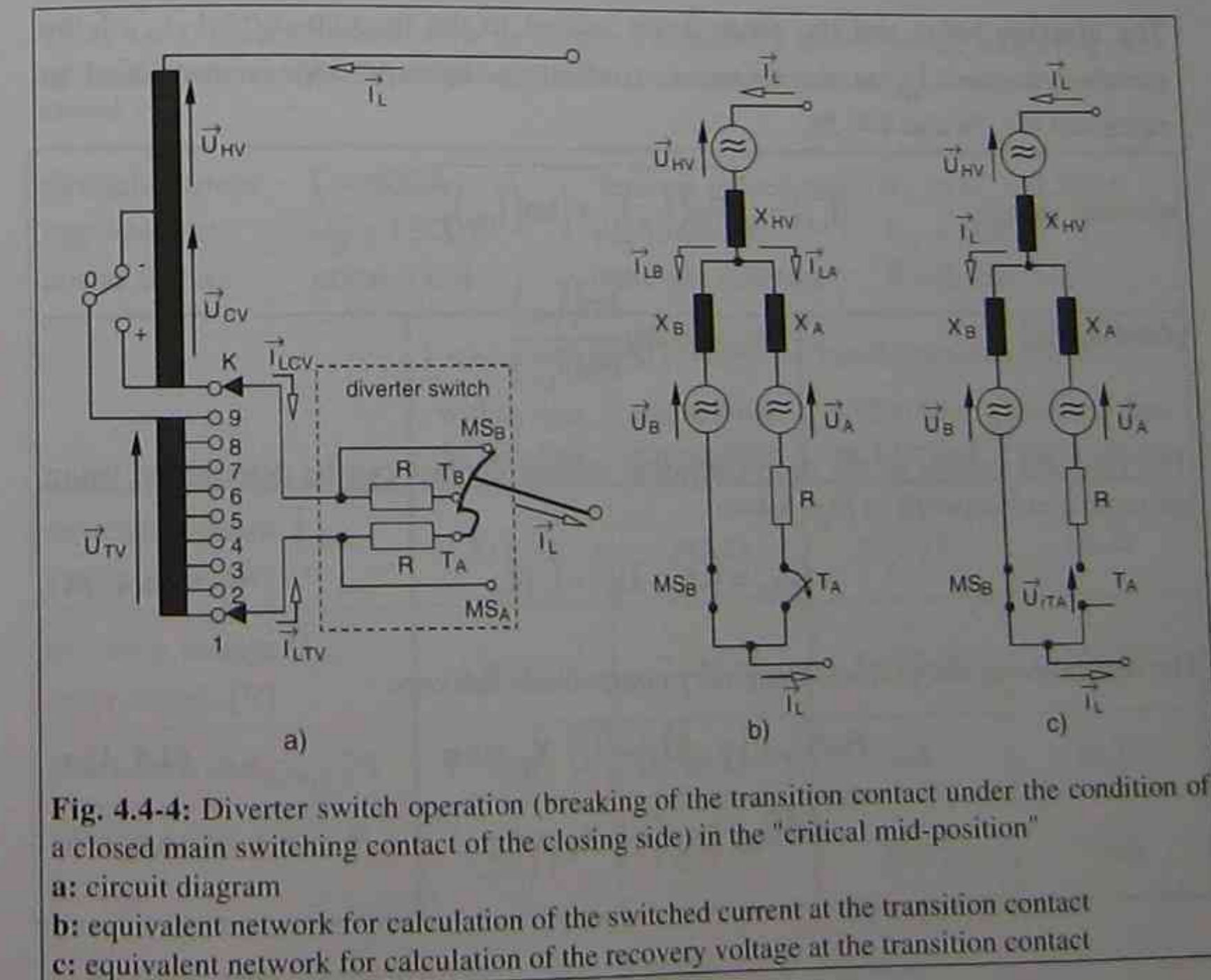
Table 4.4-1: Breaking conditions at the transition contact of a diverter switch with a flag cycle mode of operation

| through-current: | $I_L = 500\,A$ | "leakage inductance": | $X_A = X_B = 0.52\,\Omega$ | | |
|---|---|---|---|---|---|
| step voltage: | $U_S = 1,900\,V$ | step reactance: | $X_S = 50\,m\Omega$ | | |
| power factor: | $\cos\varphi = 0.8$ | transition resistors: | $R = 3.6\,\Omega$ | | |
| | | 1 mid-position ($\vec{U}_\Delta = \vec{U}_S$) | | 3 mid-positions ($\vec{U}_\Delta = 0$) | |
| | | within fine tap winding | coarse / fine tap winding | within fine tap winding | coarse / fine tap winding |
| switched current $\vec{I}_{LA}$ r.m.s. value, [A] | | 487.53 | 495.30 | 487.53 | 250.01 |
| recovery voltage $\vec{U}_{rTA}$ r.m.s. value, [V] | | 3,510.27 | 3,603.11 | 3,510.27 | 1,818.68 |
| phase shift $\left|\Delta\varphi_{IUTA}\right|$, [°] | | 0.4 | 8.22 | 0.4 | 8.22 |
| instantaneous power $P_{ITA}$ [kVA] | | 16.90 | 255.16 | 16.90 | 65.01 |

From Table 4.4-1 it can be seen that the breaking conditions are more severe in case of tap selectors with one mid-position. This is caused by the additional effective step voltage which drives the circulating current.

The diverter switch has to manage these breaking conditions. However, it is not a functional limit of the switch. If the diverter switch is not able to break the current (i.e. to quench the arc) at the transition contact in the first current zero after opening of the contacts, the arc will continue burning during the operation. In every following current zero there will be a trial to quench the arc. After 2 or 3 half cycles at the latest the main switching contact of the closing side closes changing the switching conditions. Often, the OLTC manufacturers assess the functional limit of the diverter switch in case of the tap-change operation from the end of the fine tap winding to the end of the coarse tap winding (and vice versa) by evaluating the breaking capability of the transition contact under the condition that the main switching contact of the closing side has closed.

However, these stresses do not cause danger to the diverter switch, although a higher switching gas production and a higher contact wear will occur. A short circuit is avoided, because the transition resistor of the opening side is still in the circuit and the transition resistors are able to carry current over a few half cycles.



Fig. 4.4-4: Diverter switch operation (breaking of the transition contact under the condition of a closed main switching contact of the closing side) in the "critical mid-position"
a: circuit diagram
b: equivalent network for calculation of the switched current at the transition contact
c: equivalent network for calculation of the recovery voltage at the transition contact

With the making of the main switching contact of the closing side the breaking conditions of the transition contact of the opening side change. In Fig. 4.4-4 the cicuit diagram of this diverter switch condition and the equivalent networks for the calculations of the switched current and the recovery voltage are shown.

Based on the following two equations

$$\bar{I}_L = \bar{I}_{LA} + \bar{I}_{LB} \qquad (4.4\_11)$$

$$\bar{U}_B - \bar{I}_{LB}\, jX_B + \bar{I}_{LA}(R + jX_A) - \bar{U}_A = 0 \qquad (4.4\_12)$$

the switched current can be separated into its real and imaginary components as follows (using the same operations and relations as shown in the above-mentioned calculation)

$$Re(\bar{I}_{LA}) = \frac{|\bar{I}_L| \cdot (X_B(X_B + X_A)\cos\varphi + RX_B\sin\varphi) + |\bar{U}_\Delta|R}{R^2 + (X_B + X_A)^2} \qquad (4.4\_13a)$$

$$Im(\bar{I}_{LA}) = \frac{|\bar{I}_L| \cdot (RX_B\cos\varphi - X_B(X_B + X_A)\sin\varphi) - |\bar{U}_\Delta|(X_B + X_A)}{R^2 + (X_B + X_A)^2} \qquad (4.4\_13b)$$

The absolute value and the phase angle related to the through-current $\bar{I}_L$ of the switched current $\bar{I}_{LA}$ at the transition contact can be expressed as mentioned in equations 4.4_5a and 4.4_5b.

absolute value:
$$|\bar{I}_{LA}| = \sqrt{\left[Re(\bar{I}_{LA})\right]^2 + \left[Im(\bar{I}_{LA})\right]^2}$$

phase angle:
$$\varphi_{ILA} = \text{arctg}\frac{Im(\bar{I}_{LA})}{Re(\bar{I}_{LA})}$$

The recovery voltage at the open transition resistor contact can be determined using the equivalent network in Fig. 4.4-4c.

$$\bar{U}_{rTA} = (\bar{U}_A - \bar{U}_B) - \bar{I}_L\, jX_B \qquad (4.4\_14)$$

The separation in the real and imaginary components delivers:

$$Re(\bar{U}_{rTA}) = -|\bar{U}_\Delta| - |\bar{I}_L| \cdot X_B\sin\varphi \qquad (4.4\_15a)$$

$$Im(\bar{U}_{rTA}) = -|\bar{I}_L| \cdot X_B\cos\varphi \qquad (4.4\_15b)$$

Now the absolute value and the phase angle related to the through-current $\bar{I}_L$ of the recovery voltage $\bar{U}_{rTA}$ can be expressed as in following equations 4.4_8a and 4.4_8b

absolute value:
$$|\bar{U}_{rTA}| = \sqrt{\left[Re(\bar{U}_{rTA})\right]^2 + \left[Im(\bar{U}_{rTA})\right]^2}$$

phase angle:
$$\varphi_{UrTA} = \text{arctg}\frac{Im(\bar{U}_{rTA})}{Re(\bar{U}_{rTA})}$$

The phase shift between the switched current and the recovery voltage at the transition contact is the difference of the phase angles $\varphi_{ILA}$ and $\varphi_{UrTA}$ as indicated in equation 4.4_9

$$|\Delta\varphi_{IUTA}| = |\varphi_{ILA} - \varphi_{UrTA}|$$

The breaking condition will be evaluated again using the instantaneous power as defined in equation 4.4_10. In Table 4.4-2 the breaking conditions at the transition contact for the same example used in Table 4.4-1 are listed, under the condition that the main switching contact of the closing side has closed. The breaking conditions within the fine tap winding can be calculated using the equations 4.4_13 a and b and 4.4_15 a with $X_A = 0$ and $X_B = X_S$.

Table 4.4-2: Breaking conditions at the transition contact of a diverter switch with a flag cycle mode of operation under the condition that the main switching contact of the closing side has closed

| through-current: $I_L = 500\,A$ | | "leakage inductance": $X_A = X_B = 0.52\,\Omega$ | | |
| step voltage: $U_S = 1,900\,V$ | | step reactance: $X_S = 50\,m\Omega$ | | |
| power factor: $\cos\varphi = 0.8$ | | transition resistors: $R = 3.6\,\Omega$ | | |

| | 1 mid-position ($\bar{U}_\Delta = \bar{U}_S$) | | 3 mid-positions ($\bar{U}_\Delta = 0$) | |
| --- | --- | --- | --- | --- |
| | within fine tap winding | coarse / fine tap winding | within fine tap winding | coarse / fine tap winding |
| switched current $\bar{I}_{LA}$ r.m.s. value, [A] | 531.92 | 551.48 | 531.92 | 69.38 |
| recovery voltage $\bar{U}_{rTA}$ r.m.s. value, [V] | 1,915.10 | 2,066.49 | 1,915.10 | 260.00 |
| phase shift $|\Delta\varphi_{IUTA}|$, [°] | 0.8 | 16.11 | 0.8 | 16.11 |
| instantaneous power $P_{iTA}$ [kVA] | 20.11 | 447.31 | 20.11 | 7.08 |

The comparison of Tables 4.4-1 and 4.4-2 makes the different breaking conditions evident. In case of the tap selector with three mid-positions the instantaneous power is smaller when the main switching contact of the closing side has made. For the tap selector with one mid-position the opposite is the case.

For a safe and reliable operation the OLTC has to control these breaking conditions. The functional limit is reached when the breaking stress under the condition that the main switching contact of the closing side has made exceeds the admissible values. This can be verified by the OLTC manufacturer provided the value of the leakage inductance for a given application is made available by the transformer maker.

Generally, the breaking stress at the transition contact increases with increasing leakage inductance and becomes dangerous when its value is in the range of the ohmic value of the transition resistors.

A rough estimation of the range of the leakage inductance can be performed based on the short-circuit impedance of the transformer. Taking for example a transformer with a regulating range of plus/minus 10% and a regulation with coarse and fine tap winding, both windings have roughly an electrical length of 10% of the rated voltage. The main winding of this transformer represents then 90% of the rated voltage.

In principle, the equivalent series impedance of a pair of windings or the short-circuit impedance $Z_k$ can be expressed with the impedance voltage drop $u_k$, the rated (throughput) power $S_r$ and the rated voltage U as:

$$Z_k = \frac{u_k}{100\%} \cdot \frac{U^2}{S_r} \qquad (4.4\_16)$$

In a transformer with a tapped winding, the value of the impedance voltage drop is referred to a particular tapping. For this rough estimation the principal tapping is assumed as the relevant tapping and corresponds to 100% of the rated voltage U. The equation 4.4_16 is not only valid for the entire winding, but also for a portion of it.

As shown above (see Fig. 4.4-1) in the critical mid-position the coarse and fine tap windings are connected in series in regards to the diverter switch's circulating current. The minimum leakage inductance of the coarse and fine tap winding $Z_{CF}$ can be calculated with equation 4.4_16 considering the electrical length of the series connection of the coarse and fine tap winding (the impedance $Z_{CF}$ is assumed to be purely inductive):

$$Z_{CF} = \frac{u_k}{100\%} \cdot \frac{\left(\frac{x}{100\%} \cdot U\right)^2}{S_r} = \frac{Z_k}{\left(\frac{x}{100\%}\right)^2} \qquad (4.4\_17)$$

In this equation $Z_{CF}$ is the value of the leakage inductance of the coarse and fine tap windings, $Z_k$ is the short-circuit impedance of the entire winding, $u_k$ the impedance voltage drop of the entire winding (in percent), x the regulating range (in percent), U the rated voltage of the winding and $S_r$ the rated (throughput) power.

When using this estimation it has to be considered that the real leakage inductance of the transformer can be considerably higher due to special transformer design features.

As an example, the leakage inductance of a 300 MVA; 220 kV ±10% transformer having an impedance voltage drop of 12 % can be estimated as follows (minimum value):

$$Z_{CF} = \frac{12\%}{100\%} \cdot \frac{\left(\frac{20\%}{100\%} \cdot 220kV\right)^2}{300MVA} = 0.77\Omega.$$

To conclude, with equation 4.4_17 it can be estimated, that a transformer with a high rated voltage and comparably small rated power has a large leakage impedance or inductance respectively.